

**MOLECULAR CHARACTERISATION OF THE PRO-APOPTOTIC  
MOLECULES APAF1 AND SMAC.**

Thesis submitted for the degree of  
Doctor of Philosophy  
at the University of Leicester

by

Darren Leslie Roberts BSc (York), MSc (Leicester)

MRC Toxicology Unit

University of Leicester

October 2001

UMI Number: U538567

All rights reserved

INFORMATION TO ALL USERS

The quality of this reproduction is dependent upon the quality of the copy submitted.

In the unlikely event that the author did not send a complete manuscript and there are missing pages, these will be noted. Also, if material had to be removed, a note will indicate the deletion.



UMI U538567

Published by ProQuest LLC 2013. Copyright in the Dissertation held by the Author.  
Microform Edition © ProQuest LLC.

All rights reserved. This work is protected against  
unauthorized copying under Title 17, United States Code.



ProQuest LLC  
789 East Eisenhower Parkway  
P.O. Box 1346  
Ann Arbor, MI 48106-1346

## **ABSTRACT**

### **Molecular Characterisation of the Pro-Apoptotic Molecules APAF1 and Smac by**

**Darren Leslie Roberts.**

Apoptosis is a key process involved in cell number regulation and a range of pathological disorders. It is a highly structured process that removes the cell from the body without damage to surrounding cells. The mitochondria has been shown to play a key role in apoptosis induced by a wide range of stimuli and can trigger the apoptotic pathway by release of apoptogenic factors. One of these factors is cytochrome *c*, a protein that normally functions in the electron transport chain but upon release it binds to the first mammalian homologue of CED-4, Apoptotic Protease Activating Factor 1 (APAF1) and induces the formation of a large caspase-activating complex. Another protein released from the mitochondria is Smac, a pro-apoptotic protein that functions by antagonising Inhibitor of Apoptosis Protein function. The data presented in this thesis demonstrated the existence of multiple splice forms of both APAF1 and Smac and investigated their roles in the apoptotic pathway. APAF1 forms the large molecular weight complex known as the apoptosome in 293 cells although epitope tagged APAF1 formed an incorrectly formed this complex in the absence of additional stimuli. APAF1 was also found to be cleaved by Caspase-3 during apoptosis and that the resulting 30 kDa fragment is associated with the inactive complex. Data also indicates that caspase-9 recruitment to the apoptosome occurs via interactions between both the CARD and the CED-4 homologous regions of APAF1. The pro-apoptotic protein Smac exists as several forms due to alternative splicing and one of these forms, Smac  $\beta$ , is pro-apoptotic even though it lacks the N-terminal Inhibitor of Apoptosis protein binding domain. Smac  $\beta$  is localised to the cell cortex and does not redistribute upon induction of apoptosis. These data demonstrate that Smac is able to induce apoptosis independently of Inhibitor of Apoptosis Protein binding. A polyclonal antibody to Smac / Smac  $\beta$  was also developed and characterised.

## **ACKNOWLEDGEMENTS**

I would like to thank my wife, Rachel, for her love and support during the preparation of this thesis, my Mam and Dad and my brother Garry, for encouraging me throughout my career and instilling in me curiosity about the world around me. I would also like to thank my supervisors, Marion and Gerry for their support and for pressuring me into doing “just one more thing”. For help during the entire project and particularly the immunocytochemistry my thanks go to Wendy Merrison. For their stimulating conversations and assistance at various times my thanks go Nick Harper, Shawn Bratton, Gail Walker and Mike Butterworth. To everyone else in the Department, past and present, who helped me during this time – thanks.

## TABLE OF CONTENTS

Abstract .....	2
Acknowledgements .....	3
Table of Contents .....	4
Table of Figures .....	10
Abbreviations .....	13
CHAPTER 1: Introduction.....	14
1.1 Introduction .....	15
1.2 Apoptosis in <i>Caenorhabditis elegans</i> . .....	16
1.2 Apoptotic pathways in humans .....	18
1.2.1 The Caspase Family .....	18
1.2.1 A The Caspase-1 Subfamily.....	20
1.2.1 B The Effector Caspases .....	21
1.2.1 C The Initiator Caspases .....	22
1.2.2 The Bcl-2 Family .....	23
1.2.2 A Anti-apoptotic Bcl-2 Family Members .....	24
1.2.2 B Pro-apoptotic Bcl-2 Family Members .....	26
1.2.3 APAF1 and Related Proteins .....	26
1.2.4 The Inhibitor of Apoptosis Proteins.....	31
1.2.5 IAP Binding Proteins .....	33
1.2.6 Extrinsic Apoptotic Signalling Pathways.....	34
1.2.7 Intrinsic Apoptosis Signalling Pathways .....	36
1.3 Summary .....	39
CHAPTER 2: Materials and Methods.....	40

2.1 Materials.....	41
2.1.2 Animals .....	42
2.2 Cell biology methods .....	42
2.2.1 Cell Culture .....	42
2.2.2 Transfection.....	42
2.2.2A Transfection using LipofectAMINE Reagent .....	42
2.2.2B Transfection using Fugene6™.....	43
2.2.3 Induction of Apoptosis.....	43
2.2.4 Assessment of Apoptosis .....	43
2.2.5 Immunocytochemistry and Confocal Microscopy .....	44
2.2.6 Development of a polyclonal antibody to Smac $\beta$ .....	44
2.3 Biochemical methods .....	46
2.3.1 Electrophoresis of DNA and proteins .....	46
2.3.1A Agarose gel electrophoresis of DNA .....	46
2.3.1B SDS-Polyacrylamide Gel Electrophoresis (SDS-PAGE) of proteins.....	46
2.3.2 Western blotting.....	48
2.3.3 Preparation of cellular lysates and fractions .....	50
2.3.3A Lysates for immunoprecipitation studies .....	50
2.3.3B Lysates for activation studies and FPLC .....	50
2.3.3C Sub-cellular fractionation .....	50
2.3.4 Fluorometric Assay .....	51
2.3.5 Gel filtration chromatography.....	52
2.3.6 Determination of protein concentration using the Bradford method .....	52
2.3.7 <i>In vitro</i> activation of caspases .....	53
2.4 Molecular biology methods.....	54

2.4.1 Bacterial culture and transformation .....	54
2.4.2 Plasmid DNA isolation .....	55
2.4.3 Production of recombinant proteins in bacteria .....	55
2.4.4 RNA isolation.....	56
2.4.5 RT-PCR.....	57
2.4.5A First-strand cDNA synthesis .....	57
2.4.5B Polymerase Chain Reaction.....	57
2.4.6 Cloning and subcloning.....	58
2.4.7 Library screening .....	59
2.4.7A Probe labelling.....	59
2.4.7B Hybridisation .....	59
2.4.8 Production of <sup>35</sup> S-labelled proteins .....	60
2.4.9 Immunoprecipitation and interaction studies .....	60
2.4.9A Immunoprecipitation .....	60
2.4.9B Interaction studies.....	61
CHAPTER 3: APAF1 exists as multiple forms .....	62
3.1. Introduction.....	63
3.2 Results .....	64
3.2.1 Database searching reveals alternatively spliced forms of APAF1 .....	64
3.2.2 RT-PCR of APAF1 .....	66
3.2.3 Identification of APAF1 genomic clones.....	69
3.2.4 Identification of splice sites in the APAF1 gene.....	71
3.2.5 Identification of multiple forms of the APAF1 protein .....	73
3.2.6 RT-PCR of additional APAF1 splice forms.....	73
3.3 Discussion .....	77

CHAPTER 4: Activation of caspases by dATP / cytochrome <i>c</i> and the role of the CED-4 region in caspase-9 binding.....	80
4.1 Introduction .....	81
4.2 Results .....	83
4.2.1 Effect of protein concentration on dATP / cytochrome <i>c</i> activation .....	83
4.2.2 Optimisation of dATP concentration for activation of 293 lysate .....	83
4.2.3 Cytochrome <i>c</i> /dATP activates caspase-3 and -7 in a lysate.....	86
4.2.4 Caspase -3 and -7 activity is maximal within 15 min .....	87
4.2.5 Caspase -3 and -7 activity is associated with a large molecular weight complex...87	
4.2.6 APAF1 and caspases are associated with a large molecular weight complex .....	88
4.2.7 Caspase-9 recruitment to APAF1 is enhanced by the CED-4 domain.....	90
4.2.8 The CARD / CED-4 region of APAF1 has higher affinity for caspase-9 than the CARD alone .....	92
4.2.9 Overexpression of the CARD / CED-4 is inhibitory to dATP / cytochrome <i>c</i> activation .....	93
4.2.10 Overexpression of the CARD / CED-4 region inhibits MG132 induced apoptosis .....	94
4.3 Discussion .....	96
CHAPTER 5: APAF1 activates caspases via the formation of an apoptosome and is itself a substrate for caspases. ....	99
5.1 Introduction .....	100
5.2 Results .....	101
5.2.1 Effect of induction of apoptosis on FLAG-tagged APAF1 .....	101
5.2.2 Effect of dATP and cytochrome <i>c</i> activation of 293 cell lysate on APAF1 .....	103
5.2.3 Effect of lysate activation on FLAG-APAF1 and T7-caspase-9 .....	105

5.2.4 Identification of the cleavage site in APAF1 .....	107
5.3 Discussion .....	111
CHAPTER 6: The identification and characterization of Smac $\beta$ , an alternatively spliced form of Smac.....	116
6.1 Introduction .....	117
6.2 Results .....	121
6.2.1 Identification of alternative splice forms of Smac .....	121
6.2.2 Smac $\beta$ localizes to the cortex of cells .....	124
6.2.3 Smac $\beta$ does not interact with IAPs in cells.....	126
6.2.4 Smac $\beta$ is N-terminally processed in cells .....	129
6.2.5 Smac $\beta$ potentiates apoptosis induced by various stimuli.....	131
6.2.6 N-terminal deletion mutants of Smac are pro-apoptotic .....	134
6.2.7 Smac but not Smac $\beta$ redistributes during apoptosis .....	134
6.2.8 Characterisation of anti- Smac $\beta$ antibody by Western blot analysis .....	137
6.2.9 Use of anti- Smac $\beta$ antibody for immuno-precipitation .....	137
6.2.10 Characterisation of Smac $\beta$ antibody in immuno-cytochemistry.....	139
6.3 Discussion .....	142
CHAPTER 7: Discussion.....	145
7.1 Discussion .....	146
7.1.1 APAF1.....	146
7.1.2 Smac and Smac $\beta$ .....	155
7.2 Concluding remarks .....	146
APPENDIX 1: Accession numbers of DNA sequences .....	158
APPENDIX 2: Primers used in this study.....	161
APPENDIX 3: Publications arising from this work .....	163

Bibliography.....180

## TABLE OF FIGURES

Figure 1.1 The basic apoptotic pathway in <i>C. elegans</i> .....	16
Table 1.1 Classification of the caspase family .....	19
Figure 1.2.2 Architecture of the Bcl-2 family of proteins.....	24
Figure 1.2.3 Domain structure of APAF1 .....	27
Figure 1.2.6 The Extrinsic Apoptotic Pathway .....	37
Figure 1.2.7 The Intrinsic Apoptosis Signalling Pathway .....	38
Table 2.1 Antibodies .....	41
Figure 2.1 Anti- Smac $\beta$ antibody production.....	45
Figure 2.2 Assembly of a transfer sandwich.....	49
Figure 3.1 Alternatively spliced forms of APAF1 .....	65
Figure 3.2 RT-PCR of APAF1.....	67-68
Figure 3.3 Identification and characterisation of APAF1 genomic clones .....	70-71
Figure 3.4 Identification of splice sites within genomic DNA .....	72
Figure 3.5 APAF1 exists as multiple forms at the protein level .....	73
Figure 3.6 Genomic organisation of APAF1 and RT-PCR analysis of splice forms.....	75-76
Figure 4.1 The effect of protein concentration on cytochrome <i>c</i> / dATP activation .....	84
Figure 4.2 Effect of dATP / MgCl <sub>2</sub> on lysate activation.....	85
Figure 4.3 Cytochrome <i>c</i> /dATP activation preferentially acts on caspases -3 and -7 .....	86
Figure 4.4 Time dependent activation of a cell lysate .....	87
Figure 4.5 Caspase-3 and -7 activity is attributable to a large molecular weight complex .	88
Figure 4.6 APAF1 and Caspase-9 associate in a high molecular weight complex.....	89
Figure 4.7 The CED-4 region of APAF1 enhances caspase-9 binding.....	91

Figure 4.8 The CARD / CED-4 region of APAF1 has higher affinity for caspase-9 than the CARD alone .....	92
Figure 4.9 Overexpression of the CARD / CED-4 region inhibits dATP / cytochrome <i>c</i> activation .....	94
Figure 4.10 Overexpression of the CARD / CED4 region delays MG132 induced apoptosis in 293 cells .....	95
Figure 5.1 APAF1 is cleaved during TRAIL –induced apoptosis in 293 cells.....	102
Figure 5.2 APAF1 can form an apoptosome in 293 cells .....	104
Figure 5.3 Epitope tagged APAF1 and caspase-9 form an apoptosome independently of dATP and cytochrome <i>c</i> .....	106
Figure 5.4 Identification of potential caspase cleavage sites within APAF1.....	108
Table 5.1 Predicted fragment sizes from potential caspase cleavage sites .....	108
Figure 5.5 D <sup>260</sup> but not D <sup>255</sup> is conserved between species.....	109
Figure 5.6 Caspase-3 cleaves APAF1 at D260 .....	110
Figure 6.1 Smac exists as multiple splice forms .....	122-123
Figure 6.2 Sub-cellular distribution of Smac and Smac $\beta$ .....	125
Figure 6.3 Sub-cellular fractionation of transfected cells .....	126
Figure 6.4 Smac $\beta$ does not interact with IAP family members .....	128
Figure 6.5 Smac and Smac $\beta$ exist as complexes of different molecular weight.....	130
Figure 6.6 Smac $\beta$ cannot bind XIAP <i>in vivo</i> due to N-terminal processing.....	132
Figure 6.7 Smac $\beta$ potentiates apoptosis.....	133
Figure 6.8 N-terminal deletions of Smac are pro-apoptotic.....	135
Figure 6.9 Smac but not Smac $\beta$ redistributes during apoptosis.....	136
Figure 6.10 Use of anti-Smac $\beta$ in Western blotting .....	138
Figure 6.11 Anti-Smac is suitable for immuno-precipitations.....	140

Figure 6.12 Anti-Smac is suitable for use in immuno-cytochemistry .....141

Figure 6.13 N-terminal truncation of Smac may disrupt the dimerization interface .....144

Figure 7.1 Model of the  $\beta$ -propeller structure assumed by WD40 repeats .....149

Figure 7.2 Opposing models for the binding of caspase-9 to APAF1 .....153

## ABBREVIATIONS

<b>CHAPS</b>	3-[(3-Cholamidopropyl)dimethylammonio]-1-propane sulfonate
<b>d</b>	days
<b>DD</b>	death domain
<b>DED</b>	death effector domain
<b>DEPC</b>	diethyl pyrocarbonate
<b>DISC</b>	death-induced signalling complex
<b>DMEM</b>	Dulbecco's modified eagles medium
<b>DMSO</b>	dimethylsulfoxide
<b>DNA</b>	deoxyribonucleic acid
<b>DTT</b>	dithiothreitol
<b>EDTA</b>	ethylenediaminetetraacetic acid
<b>FPLC</b>	Fast Protein Liquid Chromatography
<b>h</b>	hours
<b>HEPES</b>	N-[2-hydroxyethyl]piperazine-N'-[2-ethanesulfonic acid]
<b>(k)bp</b>	(kilo) base pair(s)
<b>(k)Da</b>	(kilo) Dalton(s)
<b>MDa</b>	megadaltons
<b>min</b>	minutes
<b>OD<sub>x</sub></b>	optical density at a wavelength of x nm
<b>PARP</b>	poly(ADP-ribose) polymerase
<b>PBS</b>	phosphate buffered saline
<b>PI</b>	propidium iodide
<b>PIPES</b>	piperazine-N,N' bis[2-ethanesulfonic acid]
<b>PMSF</b>	phenylmethylsulfonyl fluoride
<b>RNA</b>	ribonucleic acid
<b>Sec</b>	seconds
<b>TBS(T)-(M)</b>	tris buffered saline (with tween 20)-(and marvel)
<b>TEMED</b>	N,N,N',N' –tetramethylethylenediamine
<b>TNF(R)</b>	tumour necrosis factor (receptor)
<b>TRAIL</b>	TNF-related apoptosis inducing ligand
<b>Tween 20</b>	polyoxyethylenesorbitan monolaurate
<b>UTR</b>	untranslated region

**CHAPTER 1: INTRODUCTION**

## **1.1 INTRODUCTION**

During the development of multicellular organisms the number of cells is tightly regulated. Growth signals trigger cell division to increase cell number and cell death occurs to remove excess cells or those that have become damaged. As cells are filled with components such as enzymes and salts which may be harmful to the surrounding cells it is crucial for these cells to die in a tightly controlled manner. The uncontrolled death of a cell is characterized by leakage of intra-cellular components and is known as necrosis and is accompanied by inflammation of the surrounding area as the body attempts to “clean up” the leaked components. However each cell contains an intrinsic program which, when triggered, results in the cell committing suicide via a process known as apoptosis. Apoptosis results in the careful dismantling of the cell and the packaging of the cellular contents into discrete “apoptotic bodies” which can then be phagocytosed and the remains of the cell recycled. There are several characteristic hallmarks of apoptosis the first of which is the morphology of the cell. An apoptotic cell undergoes a ruffling of the plasma membrane that eventually develops into the characteristic “blebbing” and release of apoptotic bodies. The second key feature of an apoptotic cell is chromatin condensation and the degradation of genomic DNA. The DNA is initially cleaved into large 200 – 250 kB fragments, then into 30 – 50 kB fragments, which may represent chromatin loop and rosettes. The DNA is then cleaved into the characteristic DNA ladder of 180 bp internucleosomal fragments. Other features of apoptosis include changes in cell and organelle volume and exposure of proteins on the plasma membrane involved in recognition and phagocytosis of apoptotic cells.

## 1.2 APOPTOSIS IN *CAENORHABDITIS ELEGANS*.

Initial studies on apoptosis were performed in *Caenorhabditis elegans* where the development of each of the 1090 cells is known. Of these 1090 cells, 131 are known to die by apoptosis during development and analysis of mutants allowed the identification of several genes that regulate this process (Figure 1.1). By breeding *C. elegans* with several of these genes mutated it was possible to place them into a genetic pathway (Figure 1.1).

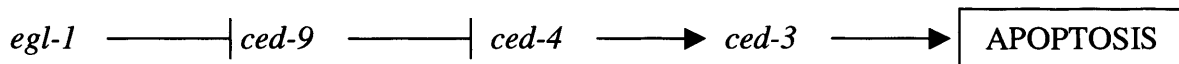


**Figure 1.1 The basic apoptotic pathway in *C. elegans***

Genetic analysis of *C. elegans* revealed three key genes that regulate the process of apoptosis. These were defined as *cell death defective* (*ced*) genes and later experiments identified *egg-laying defective -1* (*egl-1*) as a negative regulator of *ced-9*.

Of these genes the *cell death defective* (*ced*) genes were the first characterized and form the core of the pathway. *ced-3* was shown to be absolutely required for cell death and gain-of-function mutants identified it as the effector molecule in the pathway responsible for executing the signal. *ced-4* was found to activate *ced-3* and was in turn negatively regulated by *ced-9*. Later studies identified *egg-laying defective -1* (*egl-1*) as a negative regulator of *ced-9*. Analysis of the proteins encoded by these genes revealed that CED-3 was a cysteine protease with similarity to the mammalian Interleukin-1 beta converting enzyme (ICE). The CED-4 protein was unique but the CED-9 protein was found to be homologous to the mammalian protein BCL-2 that had previously been implicated in follicular lymphoma. The CED-4 protein is predicted to function by forming hexamers and inducing the activation of the CED-3 protease (Jaroszewski *et al.*, 2000). Within normal cells the CED-4 and CED-9

proteins are localized to the mitochondria but upon induction of apoptosis by activation of the CED-9 inhibitor EGL-1 the CED-4 protein translocates to the nucleus prior to the activation of CED-3 (Chen *et al.*, 2000a). This translocation may result in the activation of CED-4 either by separating the protein from its inhibitor CED-9 or by bringing it into proximity with CED-3. Several other proteins have been found to bind CED-4 and be involved in apoptosis. MAC-1 is an anti-apoptotic homologue of the *Drosophila* protein smallminded and is an AAA ATPase that forms large complexes with CED-4 and prevents activation of CED-3 (Wu *et al.*, 1999). The FEM-1 protein a Ca<sup>2+</sup>/calmodulin-dependent protein kinase phosphatase is a homologue of mammalian F1A $\alpha$  and is required for the male phenotype in *C. elegans*. FEM-1 has been shown to associate with CED-4 where cleavage by CED-3 releases a pro-apoptotic N-terminal fragment (Chan *et al.*, 2000; Tan *et al.*, 2001). Identification of these various proteins demonstrates that the CED-4 protein is a key point of regulation in the apoptotic pathway in *C. elegans*. CED-9 directly associates with CED-4 preventing the activation of the CED-3 protease possibly by competing for or masking the CED-3 binding site or CED-4 oligomerization domain. The association of CED-9 with CED-4 is itself regulated by the action of EGL-1 which disrupts this complex and allows CED-4 to associate with CED-3 and activate it (del Peso *et al.*, 2000). Many other genes have been identified in *C. elegans* that are involved in apoptosis such as the *ces-1* and *ces-2* genes, transcription factors involved in the expression of the *ced* genes, and *nuc-1*, involved in the phagocytosis of dying cells. There is also a group of CED-3 homologues, known as the caspase family, which act in a similar manner to CED-3 but do not absolutely require CED-4 for their function indicating their involvement in different apoptotic pathways which are still to be characterized (Shaham, 1998). As these are not directly related to this project they will not be discussed further here.

## 1.2 APOPTOTIC PATHWAYS IN HUMANS

In humans the basic apoptotic pathway can be triggered by two distinct mechanisms, extrinsic factors such as the death ligands and intrinsic factors such as stress. These two pathways both result in the death of the cell via similar mechanisms and in some cell types even cross over but will be dealt with separately here. All apoptotic pathways utilize a similar mechanism for the activation of the effector enzymes with adaptor molecules bringing initiator enzymes into close proximity to allow auto-activation (Salvesen & Dixit, 1999). This model is known as the induced proximity model of activation and is reliant upon the zymogen forms of the enzymes to possess activity, albeit at very low levels. As the cell has to respond to a wide range of stimuli and trigger the same execution step of the apoptotic pathway there is a great diversity of upstream proteins in these pathways but they all result in the activation of a relatively few effector proteins (Bossy-Wetzels & Green, 1999; Budihardjo *et al.*, 1999). Apoptosis is involved in a wide range of pathological and physiological situations including destruction of virally infected and or damaged cells, cells which are no longer receiving the correct trophic support and excess cells. Apoptosis can also result in pathological disorders such as autoimmune disease where cells are no longer recognized as “self” and are attacked by the immune system and triggered to undergo apoptosis. In stroke, incidental triggering of the apoptotic pathway in the surrounding neurons can cause more damage than the initial lesion.

### 1.2.1 The Caspase Family

The CED-3 protein has evolved into an entire family in humans, termed the caspase family. Caspases are cysteine proteases with an absolute requirement for aspartic acid in the P<sub>1</sub> position. The family currently contains at least 14 members which all share a conserved active site motif of QACXG (where X is G, Q or R). All family members are synthesized as inactive precursors (zymogens) that are activated by cleavage at aspartic acid residues to

yield an N-terminal pro-domain and large and small subunits. Although the size of the prodomain varies widely throughout the caspase family the large and small subunits are relatively consistent in size with the large subunit being 17 to 20 kDa and the small subunit being between 10 and 12 kDa. The crystal structure of two family members, caspase-1 (Interleukin-1 beta converting enzyme) and caspase-3 (CPP32) has been determined and this revealed that the active caspase is a heterotetramer of two large and two small subunits (Cohen, 1997). Activation of the caspases also results in the cleavage of various intracellular substrates that include other caspases and various structural proteins. The caspase family can be subdivided by phylogeny, length of prodomain and substrate preference (Table 1). Each of the families of caspases is dealt with individually below.

Caspase	Substrate preference	Prodomain	Substrates	Family
1	WEHD	Long	Pro-IL-1 $\beta$	Caspase-1
2	DEHD	Long		Initiator
3	DEVD	Short	PARP, Rb and many others	Effector
4	(W/L)EHD	Long	Caspase-1?	Caspase-1
5	(W/L)EHD	Long	?	Caspase-1
6	VEHD	Short	Lamins	Effector
7	DEVD	Short	Many, like caspase-3	Effector
8	LETD	Long	Caspase-3, BID	Initiator
9	LEHD	Long	Caspase-3, -7	Initiator
10	LETD	Long	Caspase-3	Initiator
11	(I/V/L/P) EHD	Long	Caspase-3, -1	Initiator
12	?	Long	?	Initiator
13	?	Long	?	?
14	?	Short	?	? Effector ?

**Table 1.1 Classification of the caspase family**

As virally infected cells are often targeted for removal by the induction of apoptosis by the immune system, viruses have evolved a range of anti-apoptotic strategies and these include caspase inhibitors. One of the main virally produced caspase inhibitors is cytokine response modifier A (crmA) produced by the cowpox virus (Deveraux *et al.*, 1999b). This protein is a

38 kDa serpin that demonstrates selectivity towards caspases -1, -4, -6 and -8. Another virally produced caspase inhibitor is p35, a gene product of the *Autographa californica* baculovirus that inhibits a similar but not identical group of caspases to crmA (caspases -1, -2, -3 and -4) (Zhou *et al.*, 1998). The IAP (Inhibitor of Apoptosis Protein) family was also originally identified in baculovirus but cellular homologues have since been identified and this class of caspase inhibitors will be discussed in detail later (see section 1.2.4).

### 1.2.1 A The Caspase-1 Subfamily

The caspase-1 subfamily of caspases appear to have the least involvement in apoptotic pathways with their main function being cytokine processing. Caspase-1 (Interleukin-1 Beta converting enzyme, ICE) was the first identified caspase and caspases were originally known as “ICE-like proteases” (Xue *et al.*, 1996). Caspase-1 is responsible for the maturation of pro-interleukin-1 beta by cleavage at Asp<sup>116</sup>. Caspase-1 over-expression induces apoptosis and caspase-1<sup>-/-</sup> mice have a slight defect in CD95 / Fas induced apoptosis in thymocytes (Kuida *et al.*, 1995). This may indicate that caspase-1 is involved in apoptosis although it may be readily substituted for by another caspase and therefore is not a main component of the apoptotic signalling pathways. Other members of the caspase-1 subfamily include caspases -4 and -5 which share very high homology with each other (77% identity) and with caspase-1 (55 and 50% identity respectively). Both can induce apoptosis upon over-expression although the presence of the prodomain was inhibitory in some studies, implying that the prodomain plays a regulatory role in these caspases. Physiological substrates have not yet been identified for these caspases but they may be involved in similar pathways to caspase-1. As no members of this subfamily have been demonstrated to play a major role in apoptosis they cannot be truly classified as either initiator or effector caspases despite all of them possessing a long prodomain that is characteristic of initiator caspases (Cohen, 1997).

### 1.2.1 B The Effector Caspases

These caspases are readily identifiable by the presence of a short prodomain and their involvement in a wide range of pathways. These caspases (-3, -7, and -6) are primarily responsible for dismantling of the cell during the execution phase of apoptosis. Caspase-3 was initially identified as a 32 kDa protease with homology to CED-3 and ICE, involved in apoptosis. The zymogen is activated by cleavage at an IETD site, between the large and small subunits, by various initiator caspases. This results in the formation of a p20 (the large) and a p12 (the small) subunit (Fernandes-Alnemri *et al.*, 1994). Autocatalytic processing then removes the short prodomain from the p20 to yield a p19 and then a p17 fragment by cleavage at NSVD and ESMD, respectively. Caspase-3 is thought to be the main effector caspase and has been shown to cleave a DNA repair enzyme, poly(ADP-ribose) polymerase (PARP), along with numerous other substrates within the cell. Caspase -3 and -7 share a similar substrate preference, both cleaving at D-X-X-D motifs within proteins (Cohen, 1997). Caspase-3<sup>-/-</sup> mice exhibit defects in a wide range of organs including the brain, eye and thymus primarily due to a lack of apoptosis and a decreased number of mice are born indicating embryonic lethality (Kuida *et al.*, 1996). This demonstrates the importance of caspase-3 and apoptosis in these developmental pathways. The phenotype of caspase-7<sup>-/-</sup> mice has not been reported and this may indicate that this knockout is entirely embryonic lethal. Both active caspase-3 and -7 are able to activate one another but neither induces apoptosis upon over expression demonstrating the requirement for an initiator caspase in their initial activation step (Duan *et al.*, 1996). Caspase-6 is activated by caspase-3 although, once activated, it is capable of activating caspase-3 and thereby establishing an amplification loop (Orth *et al.*, 1996). Caspase-6 cleaves the nuclear lamins and demonstrates a different substrate specificity to caspases -3 and -7 by recognizing VEID as its preferred cleavage site (Thornberry *et al.*, 2000).

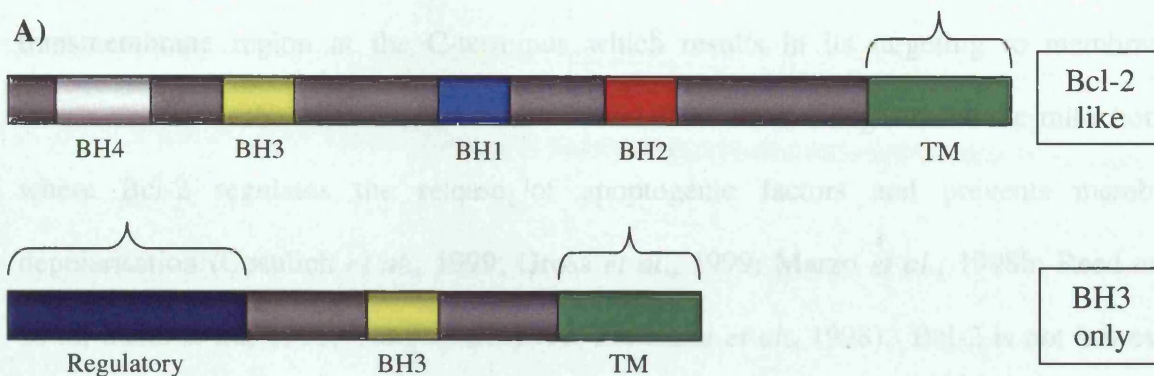
### 1.2.1 C The Initiator Caspases

The initiator caspases are characterized by the presence of a long prodomain and their involvement in the activation of effector caspases (Cohen, 1997). The main initiator caspases are caspases -2, -8, -9, -10 and -12, and of these caspases -2, -8 and probably -10 are involved in extrinsic (death-inducing ligand mediated) pathways and caspases -9 and -12 are involved in intrinsic (stress-mediated) pathways. Caspases -8 and -10 are very similar in structure and both contain two regions within the prodomain known as a death effector domain (DED) (Cohen, 1997). The DEDs are responsible for recruiting initiator caspases to a death induced signalling complex (DISC) via various adapter molecules. Only a single DED is utilized in this interaction and the role of the second is not understood. Caspase-2 is also recruited to a DISC via its own specific adapter but is different in structure to caspases -8 and -10. Within the prodomain of caspase-2 there is a caspase activation and recruitment domain (CARD) rather than a DED (Chou *et al.*, 1998; Fernandes-Alnemri *et al.*, 1995). Formation of a DISC results in the initiator caspases being brought into close proximity allowing autoactivation via cleavage between the small and large subunits. The active caspases are then able to remove their prodomains by proteolysis resulting in the release of an active enzyme into the cytosol. Caspase-2 is also localized to the golgi during apoptosis where it cleaves golgin-160 (Mancini *et al.*, 2000). Caspase-9 (Duan *et al.*, 1996; Srinivasula *et al.*, 1996) also contains a CARD in its prodomain and is activated following recruitment to a caspase-activating complex via autocatalytic processing between the large and small subunits. The caspase-9 activating complex is known as the “apoptosome” that is formed following mitochondrial damage (Cain *et al.*, 1999; Li *et al.*, 1997; Zou *et al.*, 1999). Damage or stress to the endoplasmic reticulum (ER) (Rao *et al.*, 2001) results in the activation of caspase-12 following its recruitment to Tumour Necrosis Factor Receptor – Associated Factor 2 (TRAF-2) (Yoneda *et al.*, 2001). As caspase-12 contains a CARD

domain but TRAF-2 does not this interaction is the first caspase activating non-homotypic interaction described.

### 1.2.2 The Bcl-2 Family

The first human homologue of CED-9 identified was the protein B-cell lymphoma-2 (Bcl-2). Bcl-2 is the founder member of a family of proteins that can be further subdivided into two groups based on function, the anti-apoptotic and pro-apoptotic Bcl-2 family members. One common feature which all Bcl-2 family members share is the presence of a BH (Bcl-2 homology) domain. Four of these domains are present in Bcl-2 (BH1 to BH4) and the sequence of each of these is different. Of these, the BH3 domain is found in both anti- and pro-apoptotic family members and in some pro-apoptotic family members is the only region of homology in the entire protein (Figure 1.2.2). Bcl-2 family members can act by forming either homo- or hetero- dimers, anti-apoptotic proteins thereby inhibiting the action of pro-apoptotic family members by dimerizing with them. Bcl-2 family members can also act by associating with the mitochondrial permeability transition pore of the cell (Harris & Thompson, 2000; Jacotot *et al.*, 2001; Tsujimoto & Shimizu, 2000; Vander Heiden *et al.*, 2001) and this association can influence the induction of apoptosis (Shimizu *et al.*, 2000a; Shimizu *et al.*, 1999; Shimizu *et al.*, 2000b). Viruses and bacteria have also exploited the anti-apoptotic role of Bcl-2 family members and often express homologues of the Bcl-2 family members or their binding partners to evade the immune system during infection of a host (Boya *et al.*, 2001; Hacker *et al.*, 1996; Huang *et al.*, 1997a). Bcl-2 family members have also been shown to be involved in cell cycle regulation with the phosphorylation state of Bcl-2 changing as the cell cycle progresses and various mutants causing cell cycle arrest (Huang *et al.*, 1997b; O'Reilly *et al.*, 1996) demonstrating that these proteins have functions other than their role in apoptosis that require further study.



B)

Name	Structure	Anti- or Pro- apoptotic
Bcl-2	Bcl-2 like	Anti-apoptotic
Bcl-x <sub>L</sub>	Bcl-2 like	Anti-apoptotic
Bcl-w	Bcl-2 like	Anti-apoptotic
A1	Bcl-2 like	Anti-apoptotic
Mcl-1	Bcl-2 like	Anti-apoptotic
BID	Bcl-2 like	Pro-apoptotic
Bax	Bcl-2 like	Pro-apoptotic
Bak	Bcl-2 like	Pro-apoptotic
Diva / Boo	Bcl-2 like	Pro-apoptotic
Bok	Bcl-2 like	Pro-apoptotic
Hrk	BH3 only	Pro-apoptotic
Bik	BH3 only	Pro-apoptotic
BNIP3	BH3 only	Pro-apoptotic
BNIP3L	BH3 only	Pro-apoptotic
Bad	BH3 only	Pro-apoptotic
Noxa	BH3 only	Pro-apoptotic
Bim	BH3 only	Pro-apoptotic

**Figure 1.2.2 Architecture of the Bcl-2 family of proteins**

The Bcl-2 family is composed of two types of protein, the Bcl-2 like and the BH3 only proteins with distinct domain structures (A). The Bcl-2 like group of proteins contains both pro- (BID, Bax, Bak, Diva / Boo, Bok) and anti- apoptotic (Bcl-2, Bcl-x<sub>L</sub>, Bcl-w, A1, Mcl-1) family members, whereas the BH3 only family members are all pro-apoptotic (Hrk, Bik, Bcl-XS, BNIP3, BNIP3L, Bad, Noxa, Bim) (B). The BH3 domain in the BH3 only proteins is also responsible for dimerization. Brackets indicate regions not found in all family members.

### 1.2.2 A Anti-apoptotic Bcl-2 Family Members

The *bcl-2* gene was first identified due to its location at the t(14;18) chromosomal translocation that occurs in follicular lymphomas. This translocation places the *bcl-2* gene

under control of the promoter of the JH segment of the immunoglobulin gene resulting in greatly elevated levels of Bcl-2 that, in turn, inhibits apoptosis. Bcl-2 possesses a transmembrane region at the C-terminus which results in its targeting to membranous structures within the cell. The main site of Bcl-2 action is thought to be the mitochondria where Bcl-2 regulates the release of apoptogenic factors and prevents membrane depolarisation (Cosulich *et al.*, 1999; Gross *et al.*, 1999; Marzo *et al.*, 1998b; Reed *et al.*, 1998; Susin *et al.*, 1996; Yang *et al.*, 1997; Zamzami *et al.*, 1998). Bcl-2 is not however a ubiquitous inhibitor of apoptosis and the ability of Bcl-2 to inhibit apoptosis varies with the stimulus. This differential inhibition of apoptotic pathways can reveal the presence of multiple pathways in a single cell type such as lymphoma cells in which extrinsic apoptosis induced by CD95 / Fas is not blocked by Bcl-2 but intrinsic apoptosis induced by  $\gamma$ -irradiation is inhibited (Strasser *et al.*, 1995). The regulation of Bcl-2 is at present unclear but it is clear that Bcl-2 can be phosphorylated by several kinases, including JNK (Deng *et al.*, 2001) and CDC2 (Furukawa *et al.*, 2000) and increased phosphorylation of Bcl-2 can induce its degradation via the proteasome (Breitschopf *et al.*, 2000). Bcl-2 may also be associated with the cellular cytoskeleton as treatment of cells with microtubule disrupting agents such as taxol result in increased phosphorylation of Bcl-2 (Fang *et al.*, 1998). Bcl-XL is another anti-apoptotic Bcl-2 family member that acts in a similar manner to Bcl-2 although the *bcl-x* gene can give rise to two distinct products, Bcl-XL and Bcl-XS, by alternative splicing. Bcl-XS is however pro-apoptotic allowing the cell to determine its own fate by the alternative splicing of a single gene. Bcl-XL may also play a role in oxidative phosphorylation (Dey & Moraes, 2000) allowing it to regulate apoptosis by means other than sequestering pro-apoptotic Bcl-2 homologues.

### 1.2.2 B Pro-apoptotic Bcl-2 Family Members

The pro-apoptotic Bcl-2 family members can also be characterized into two main types, the pro-apoptotic Bcl-2 homologues such as Bcl-x<sub>s</sub> and the larger family of BH3 domain only proteins that only share homology with the BH3 domain of Bcl-2 such as BID and Bax (Crompton, 2000; Luo *et al.*, 1998; Marzo *et al.*, 1998a; Pawlowski & Kraft, 2000; Shimizu & Tsujimoto, 2000). These proteins can act to induce apoptosis in two different ways: the first being utilized by the pro-apoptotic Bcl-2 homologues such as Bcl-x<sub>s</sub>. Bcl-x<sub>s</sub> forms dimers with anti-apoptotic Bcl-2 family members thereby preventing their action. The BH3 domain proteins act in a different manner to directly induce apoptosis by disruption of specific sites such as the mitochondria. The BH3 domain proteins achieve this in several ways, BID is cleaved by caspase-8 during TRAIL and CD95 / Fas induced apoptosis and then translocates to the mitochondria where it induces release of various apoptogenic factors and loss of mitochondrial membrane potential (Luo *et al.*, 1998; Yamada *et al.*, 1999). Upon translocation to the mitochondria truncated BID (tBID) induces the oligomerization and translocation of Bax to the mitochondrial membrane where it also can cause release of apoptogenic factors and membrane depolarisation (Eskes *et al.*, 2000). BID has recently been shown to have a role in lipid metabolism in the mitochondria and this may be its normal function in non-apoptotic cells which may help explain its targeting to the mitochondria and the resulting release of various proteins together with loss of mitochondrial membrane potential during apoptosis (Esposti *et al.*, 2001).

### 1.2.3 APAF1 and Related Proteins

The last of the human homologues of the core *C. elegans* apoptotic machinery identified was the human CED-4 homologue APAF1 (Apoptotic Protease Activating Factor -1). APAF1 was isolated by biochemical fractionation based upon its ability to activate caspase-3 in response to dATP and cytochrome *c* (Zou *et al.*, 1997). Previously activation of

caspase-3 in response to addition of cytochrome *c* and dATP to cellular lysates had been demonstrated (Liu *et al.*, 1996) and this was then used as a model for mitochondrial damage during apoptosis. APAF1 is a 135 kDa protein with a N-terminal CARD that is followed by 330 amino acids with high homology to CED-4. The C-terminal region of APAF1 contains 12 or 13 WD40 repeats and acts as a negative regulator of the N-terminal region of the molecule (Adrain *et al.*, 1999; Hu *et al.*, 1998b). Between the CED-4 and WD40 regions there is a region that is unique to APAF1 of unknown function (Figure 1.2.3). The CED-4 region of the protein contains the nucleotide binding site in the form of Walkers A and B boxes which are responsible for the binding of ATP and its hydrolysis (van der Biezen & Jones, 1998). This region, also referred to as a NB-ARC domain, has high homology with various plant resistance gene products (van der Biezen & Jones, 1998). These plant resistance gene products



**Figure 1.2.3 Domain structure of APAF1**

A schematic of the domain organisation of APAF1 showing the CARD (blue), Ced-4 (white) with the Walkers A and B boxes within it (green). The APAF1 unique domain is shown in black with the C-terminal WD40 repeats in yellow.

are involved in the plant hypersensitive response that involves cell death surrounding the point of infection. The CED-4 region and the APAF1 unique region C-terminal to it have both been implicated in the oligomerization of APAF1 (Hu *et al.*, 1998b; Srinivasula *et al.*, 1998) and the deletion of the WD40 repeats results in the formation of a constitutively active protein even in the absence of dATP and cytochrome *c* (Srinivasula *et al.*, 1998). The WD40 region may therefore be the binding site for cytochrome *c* with binding inducing a conformational switch by removing the inhibitory effect the WD40 region has upon the N-

terminus of the protein (Adrain *et al.*, 1999; Hu *et al.*, 1998b). The WD40 region was further implicated in cytochrome *c* binding by findings that showed the requirement of an additional WD40 repeat to be present for the binding of cytochrome *c* and the correct functioning of the protein (Benedict *et al.*, 2000). As WD40 (also known as Trp-Asp) repeats are commonly found to be involved in protein / protein interactions this region of APAF1 may have other, as yet unidentified, binding partners.

APAF1 homologues have been found in both *Drosophila* and Zebrafish (Inohara & Nunez, 2000; Rodriguez *et al.*, 1999a; Zhou *et al.*, 1999a) demonstrating conservation of this key molecule between species. Deletion of the *APAF1* gene in mice results in severe abnormalities in a range of tissues and a reduced incidence of birth indicating embryonic lethality (Cecconi *et al.*, 1998; Yoshida *et al.*, 1998). Abnormalities observed include craniofacial abnormalities due to lack of neuronal apoptosis, persistence of interdigital webs and abnormalities in the lens and retina (Cecconi *et al.*, 1998; Yoshida *et al.*, 1998), and the brain defects and craniofacial abnormalities also observed in caspase-9<sup>-/-</sup> (Hakem *et al.*, 1998; Kuida *et al.*, 1998) and caspase-3<sup>-/-</sup> mice (Kuida *et al.*, 1996). Some differences between these null mice suggest the existence of other parallel apoptotic pathways, for example both APAF1<sup>-/-</sup> and caspase-3<sup>-/-</sup> mice displayed altered eye development and yet caspase-9<sup>-/-</sup> mice did not. This suggests that APAF1 activates caspase-3 independently of caspase-9 during development of the eye. Cells from APAF1<sup>-/-</sup> mice are resistant to a wide range of apoptotic stimuli but both thymocytes and activated T lymphocytes were still found to be susceptible to CD95 / Fas mediated apoptosis demonstrating that APAF1 and therefore the mitochondria are not involved in this pathway in these cells (Cecconi *et al.*, 1998; Yoshida *et al.*, 1998). Those mice that do survive exhibit infertility in males indicating that APAF1-dependent apoptosis plays a role in spermatogenesis (Honarpour *et al.*, 2000). The fact that some mice do survive to adulthood and the differences between APAF1<sup>-/-</sup>, caspase-

$9^{-/-}$ , and caspase-3 $^{-/-}$  mice demonstrate the presence of other APAF1 homologues within the cell that are probably able to compensate for the loss of APAF1 and function in alternative pathways. The key role played by APAF1 in apoptosis is further demonstrated by the lack of apoptosis in cell lines and tumours which lack APAF1 protein or in cell lines where apoptosis is enhanced by the addition of exogenous APAF1 (Burgess *et al.*, 1999; Perkins *et al.*, 1998; Robles *et al.*, 1999; Shinoura *et al.*, 2000; Wolf *et al.*, 2001; Yamamoto *et al.*, 2000).

APAF1 forms a large molecular weight complex (~700 kDa) known as the apoptosome in cells induced to undergo apoptosis (Cain *et al.*, 1999; Zou *et al.*, 1999). Damage to the mitochondria induces release of cytochrome *c* from the intermembrane space into the surrounding cytosol. Cytochrome *c* then binds to APAF1 and, in the presence of dATP or ATP, induces APAF1 oligomerization and recruitment of caspase-9 (Cain *et al.*, 2000; Cain *et al.*, 1999; Hu *et al.*, 1999b; Jiang & Wang, 2000; Li *et al.*, 1997; Saleh *et al.*, 1999; Srinivasula *et al.*, 1998; Zou *et al.*, 1999). Caspase-9 is recruited to this complex via a CARD / CARD interaction and, once recruited, undergoes autoactivation (Saleh *et al.*, 1999; Srinivasula *et al.*, 1998; Zou *et al.*, 1999). This association between caspase-9 and APAF1 increases the activity of caspase-9 several fold by acting as a holoenzyme (Rodriguez & Lazebnik, 1999). This complex then recruits and activates effector caspases such as caspase-3. Incorrect folding or oligomerization of APAF1 results in the formation of a ~1.4 MDa apoptosome which is far more inefficient at activating effector caspases (Bratton *et al.*, 2001; Cain *et al.*, 2000).

The oligomerization of APAF1 is regulated in part by the heat shock protein family, in particular HSP70 and HSP90. HSP90 binds APAF1 in cells and prevents formation of the apoptosome and recruitment of caspase-9 (Pandey *et al.*, 2000b) whereas HSP70 binds to APAF1 in the apoptosome and blocks the recruitment of caspase-9 (Beere *et al.*, 2000; Saleh

*et al.*, 2000). HSP70 is reported to bind directly to the CARD of APAF1 thereby preventing the CARD / CARD association between APAF1 and caspase-9 (Saleh *et al.*, 2000). This association is dependent upon the ATPase domain of HSP70 (Beere *et al.*, 2000) although whether this is dependent upon the hydrolysis of ATP requires further investigation. Another protein that has been reported to regulate the function of APAF1 is NAC (NB-ARC and CARD containing protein): NAC is similar to APAF1 in structure, and contains CARD and NB-ARC domains with leucine rich repeats (LRRs) replacing the WD40 repeats of APAF1, and also contains a PYRIN domain. NAC acts to enhance the caspase activating properties of the apoptosome and is reported to associate with the ~1.4 MDa apoptosome to exert its function (Chu *et al.*, 2001) however this ~1.4 MDa complex has previously been reported to be the inactive form of the apoptosome (Cain *et al.*, 2000). NAC has also been identified by other groups as DEFCAP (Hlaing *et al.*, 2001), NALP1 and CARD7 (Fairbrother *et al.*, 2001; Hlaing *et al.*, 2001) who also describe its homology to APAF1 and ability to bind caspase-9. However, they also report a higher affinity for caspase-2 which has not been reported to be present in the apoptosome to date. NAC is therefore more likely to function in a different complex to activate caspase-2.

Several other proteins with a similar structure to APAF1 have been described: they all contain the NB-ARC domain but possess LRRs rather than the WD40 repeats found in APAF1. The first of these APAF1 homologues is NOD1 or CARD4 (Bertin *et al.*, 1999; Inohara *et al.*, 1999), which although able to bind caspase-9 is also able to activate the transcription factor NF- $\kappa$ B by binding and activating the kinase RICK. NOD1 / CARD4 is able to self associate and also binds to lipopolysaccharide (LPS) and may induce apoptosis or activate NF- $\kappa$ B in response to LPS in a manner similar to APAF1 activation of caspase-9 following cytochrome *c* release (Bertin *et al.*, 1999; Inohara *et al.*, 1999; Inohara *et al.*, 2001). NOD2 / CARD15 is also able to bind RICK and is similar in structure to NOD1 /

CARD14 except for the presence of two CARD domains (Inohara & Nunez, 2001; Ogura *et al.*, 2001b). NOD2 / CARD15 has been found mutated in both Crohn's disease and Blau syndrome (Cho, 2001; Hampe *et al.*, 2001; Hugot *et al.*, 2001; Miceli-Richard *et al.*, 2001; Ogura *et al.*, 2001a) providing a clinical reason for further research into the apoptotic pathways involving NOD2 / CARD15. The third and final protein with homology to APAF1 to date is Ipaf / CARD12 / CLAN (Damiano *et al.*, 2001; Geddes *et al.*, 2001; Poyet *et al.*, 2001), a protein with a CARD – NB-ARC – LRR domain structure. Ipaf / CARD12 / CLAN activates caspase-1 although it also binds NOD2, NAC and the other pro-apoptotic molecules Bcl-10 and Asc-1 (Damiano *et al.*, 2001; Geddes *et al.*, 2001; Poyet *et al.*, 2001) which would allow for signalling via apoptotic, inflammatory and NF- $\kappa$ B pathways.

#### 1.2.4 The Inhibitor of Apoptosis Proteins

Inhibitor of Apoptosis Proteins (IAPs) are a family of proteins initially identified in baculovirus that are also capable of regulating apoptosis. IAPs function by inhibition of active caspases and are characterised by the presence of Baculovirus Inhibitor of Apoptosis Repeat (BIR) domains (Deveraux & Reed, 1999; Eiben & Duckett, 1998). This family of proteins have diverse functions with those members containing multiple BIR domains functioning in apoptosis and those with only a single BIR domain having other functions. There are three multiple BIR domain proteins currently well characterised in humans, c-IAP-1 (cellular inhibitor of apoptosis -1), c-IAP-2 (cellular inhibitor of apoptosis -2), and XIAP (X-linked inhibitor of apoptosis) all of which contain three BIR domains. Both c-IAP-1 and c-IAP-2 contain a RING finger domain and a CARD domain and were isolated as components of the TNF receptor 2 DISC (Rothe *et al.*, 1995). Both proteins are responsible for inhibition of caspases in the DISC preventing any amplification of the apoptotic signal and activation of the transcription factor NF- $\kappa$ B (Chu *et al.*, 1997; Roy *et al.*, 1997; Wang *et al.*, 1998). Activation of NF- $\kappa$ B results in an increased level of both c-IAP-1 and c-IAP-2

providing an amplification loop for their action, i.e. as more protein is produced more NF- $\kappa$ B is activated thereby leading to increased protein production (Wang *et al.*, 1998). Both proteins act to inhibit caspases -3 and -7 and possibly caspase-9 (Deveraux *et al.*, 1998) but are unable to bind caspases -1, -6 and -8 (Roy *et al.*, 1997), thereby blocking the amplification step of the apoptotic signal rather than the initial activation of caspase-8. Although both of these proteins act as anti-apoptotic proteins cleavage by caspases results in the release of a pro-apoptotic fragment containing the RING finger domain from the C-terminus of c-IAP-1 (Clem *et al.*, 2001). This RING domain has been demonstrated to possess E3 ligase activity and promotes auto-ubiquitination and degradation of the protein via the proteasome (Suzuki *et al.*, 2001c; Yang *et al.*, 2000). The role of this ubiquitination step is not yet known although auto-ubiquitination would result in lower levels of IAPs and therefore promote apoptosis. However, if bound proteins were also ubiquitinated this would result in decreased caspase levels and possibly inhibition of apoptosis (Suzuki *et al.*, 2001c; Yang *et al.*, 2000). XIAP also contains a RING domain and is able to inhibit caspases (Deveraux *et al.*, 1997) but in contrast to c-IAP-1, cleavage of XIAP by caspases results in two anti-apoptotic fragments. Each of these fragments has specificities for different caspases thus allowing XIAP to act at two points in the pathway at once (Deveraux *et al.*, 1999a). The N-terminal fragment containing the BIR1 and BIR2 domains specifically inhibits caspases -3 and -7 whereas the C-terminal fragment containing the BIR3 and RING domains specifically inhibits caspase-9 (Deveraux *et al.*, 1999a). These interactions between the various caspases and XIAP have been modelled and these structures have revealed that it is not the actual BIR domains that interact with the caspases but rather the spacer regions between them (Riedl *et al.*, 2001; Suzuki *et al.*, 2001b). The inhibition of caspase-9 by XIAP is sufficient to block apoptosis demonstrating that inhibition of the downstream caspases -3 and -7 is a secondary function which probably comes into play in apoptotic

pathways not involving caspase-9 (Silke *et al.*, 2001). NAIP (Neuronal Apoptosis Inhibitor Protein) is another IAP that contains a nucleotide binding site and LRRs as well as the three BIR domains, but expression of this protein is limited to neuronal tissues and therefore will not be discussed further in this thesis (Deveraux & Reed, 1999; Eiben & Duckett, 1998; Liston *et al.*, 1996; Robertson *et al.*, 2000).

Other IAPs contain only a single BIR domain and have other functions other than suppression of apoptosis. These include survivin, which whilst suppressing apoptosis (Tamm *et al.*, 1998), is a poor inhibitor of caspases and instead is involved in cell division and the mitotic checkpoint (Li *et al.*, 1998; O'Connor *et al.*, 2000; Silke & Vaux, 2001). Another single BIR domain-containing IAP is BRUCE (BIR repeat containing ubiquitin-conjugating enzyme) that contains a single BIR domain and a ubiquitin-conjugating domain. This protein is also known as apollon and is involved in proteasomal degradation pathways (Chen *et al.*, 1999; Hauser *et al.*, 1998). In *Drosophila* three proteins, Reaper, Hid and Grim repress the action of IAPs and these will be discussed in detail in the next section.

### 1.2.5 IAP Binding Proteins

Studies in *Drosophila* identified three proteins that induced apoptosis by inhibition of IAP function, Reaper, Hid (Head involution defective) and Grim (Goyal *et al.*, 2000). These proteins share homology only in the N-terminal 10 to 15 amino acids of the protein later identified as the site of IAP interaction (Goyal *et al.*, 2000; Silke *et al.*, 2000). There are differences between the ability of these proteins to activate caspases, for example Reaper and Grim but not Hid can activate the *Drosophila* caspase DCP-1 in the retina (Song *et al.*, 2000). Reaper is not only able to induce apoptosis via inhibition of IAPs but can induce apoptosis by binding to Scythe (Thress *et al.*, 1998). This binding causes the release of a cytochrome *c* releasing activity normally sequestered by Scythe (Thress *et al.*, 1999a). Recently Scythe has been shown to interact with HSP70 and inhibits HSP70 protein folding

activity (Thress *et al.*, 2001) with Reaper repressing this function. As HSP70 has been shown to regulate the apoptosome this modulation of HSP70 activity by pro-apoptotic proteins may have an impact on apoptosome formation and activity. Although Reaper, Hid and Grim are functional in human cells (McCarthy & Dixit, 1998) until recently no human homologue was known. Smac (second mitochondrial-derived activator of caspases) and its murine homologue DIABLO (Direct IAP binding protein with low pI) have recently been described as homologues of Reaper, Hid and Grim (Du *et al.*, 2000; Verhagen *et al.*, 2000). Smac / DIABLO is a mitochondrial protein that possesses homology with Reaper, Hid and Grim in its N-terminal 15 amino acids of the mature form (Du *et al.*, 2000; Silke *et al.*, 2000; Verhagen *et al.*, 2000). This protein will be described in greater depth in later chapters (sections 6.1). Another *Drosophila* protein that has been reported to interact with IAPs and induce apoptosis is Doom (Harvey *et al.*, 1997). Doom does not contain any regions of homology with Reaper, Hid or Grim suggesting that it either interacts indirectly with the IAPs or it binds IAPs via a novel interaction motif. As no human homologues of Doom have been identified to date and it has been little studied in *Drosophila* this protein may represent a novel mechanism to regulate IAPs within the cell.

### 1.2.6 Extrinsic Apoptotic Signalling Pathways

The ability to signal a cell to undergo apoptosis without having to deliver a compound into the cell has always been an attractive prospect to researchers and as such the signalling of extrinsic apoptotic pathways is well studied. Numerous death receptors have been identified and these all are members of the tumour necrosis factor receptor (TNFR) superfamily that share a small intracellular domain known as the death domain (DD). Of these receptors the best studied is the CD95 / Fas receptor and this will be used as a model pathway from this point forward. Upon stimulation with a ligand or activating antibody the receptor trimerizes and recruits adapter proteins to the intracellular DD (Figure 1.2.6). In the

case of the Fas receptor this adapter is FADD (Fas Associated protein with Death Domain) that contains a N-terminal death effector domain (DED) and a C-terminal death domain (DD) (Bodmer *et al.*, 2000; Chinnaiyan *et al.*, 1996; Krammer, 1998; Krammer, 1999; Kuang *et al.*, 2000; Scaffidi *et al.*, 1999a; Schneider *et al.*, 1997; Sprick *et al.*, 2000; Wajant *et al.*, 1998; Walczak & Krammer, 2000). FADD in turn recruits caspase-8 to its DED via homotypic interactions with the two DEDs present in the prodomain of the caspase. This interaction allows the caspase-8 molecules to come into close proximity and auto-activate. This caspase-activating complex is known as the Death Induced Signalling Complex (DISC) (Kischkel *et al.*, 1995; Medema *et al.*, 1997; Scaffidi *et al.*, 1999b). This process can be regulated by cellular proteins known as FLIPs (Flice inhibitory proteins) that are homologous to caspase-8 but lack the active site cysteine thereby inhibiting caspase-8 activation (Krueger *et al.*, 2001; Scaffidi *et al.*, 1999c; Schneider & Tschopp, 2000; Thome *et al.*, 1997). Once caspase-8 is activated, it in turn activates effector caspases that cleave various intracellular substrates resulting in apoptosis. In cells with low levels of caspase-8 activation (type II cells) either due to low levels of caspase-8 or other signalling components, caspase-8 cleaves the Bcl-2 family protein BID (Scaffidi *et al.*, 1998; Scaffidi *et al.*, 1999d). This cleaved BID, tBID, then translocates to the mitochondria and initiates the intrinsic apoptotic pathway thereby amplifying the death receptor signal (Luo *et al.*, 1998). Bcl-2 and Bcl-X<sub>L</sub> can therefore only block the extrinsic pathway in type II cells by inhibiting the intrinsic apoptotic pathway. Other death receptors, such as the TNF receptors and TRAIL (TNF related apoptosis inducing ligand) receptors can also signal to survival factors such as NF- $\kappa$ B and do so in a similar way to that utilized for apoptotic signalling with the recruitment of adapter proteins and kinases to the receptor complex (Harper *et al.*, 2001; Herr *et al.*, 1999a; Herr *et al.*, 1999b; Hu *et al.*, 1999a; Lin *et al.*, 2000; Muhlenbeck *et al.*, 1998; Muhlenbeck *et al.*, 2000; Schulze-Osthoff *et al.*, 1998; Takeuchi *et al.*, 1996; Wallach

*et al.*, 1999; Ware *et al.*, 1996). Other extrinsic signals such as withdrawal of trophic support can induce apoptosis but these trigger the intrinsic apoptotic pathways by causing cellular stress.

### 1.2.7 Intrinsic Apoptosis Signalling Pathways

Many agents that induce apoptosis do so by inducing cellular stress and damage to subcellular compartments. Damage to the nucleus, mitochondria and ER are all known to induce apoptosis. Cancer chemotherapeutic agents such as etoposide damage nuclear DNA by inducing strand breaks and taxol disrupts the microtubules. Both of these cause the release of cytochrome *c* from the mitochondria and triggering of the intrinsic apoptotic signalling pathway. Also released from the mitochondria are AIF (Apoptosis Inducing Factor), responsible for the formation of the 50 kb DNA fragments during apoptosis (Granville *et al.*, 2001; Joza *et al.*, 2001; Lorenzo *et al.*, 1999) and endonuclease G, responsible for the formation of the internucleosomal 180 bp DNA fragments (Li *et al.*, 2001; Parrish *et al.*, 2001). Release of cytochrome *c* from the intermembrane space is negatively regulated by Bcl-2 and Bcl-X<sub>L</sub> (Cosulich *et al.*, 1999; Kim *et al.*, 1997; Yang *et al.*, 1997). Some pro-apoptotic Bcl-2 members such as tBID and Bax can induce cytochrome *c* release and upon release into the cytoplasm cytochrome *c* induces the formation of the apoptosome (Figure 1.2.7) as described earlier (Eskes *et al.*, 1998; Finucane *et al.*, 1999; Kluck *et al.*, 1999; Luo *et al.*, 1998; Pawlowski & Kraft, 2000; Shimizu & Tsujimoto, 2000). Apoptosome formation can be regulated at several points including cytochrome *c* release, cytochrome *c* binding to the apoptosome by HSP27 (Bruey *et al.*, 2000; Concannon *et al.*, 2001; Pandey *et al.*, 2000a), and IAP inhibition of caspase activation by Smac. Although Bcl-2 / Bcl-X<sub>L</sub> was initially thought to regulate APAF1 function in a manner similar to CED-4 regulation by CED-9 (Hu *et al.*, 1998a; Pan *et al.*, 1998) this has

since been disproved (Chipuk *et al.*, 2001; Conus *et al.*, 2000; Hausmann *et al.*, 2000; Moriishi *et al.*, 1999; Newmeyer *et al.*, 2000; Ruiz-Vela *et al.*, 2001). Fluctuations in the

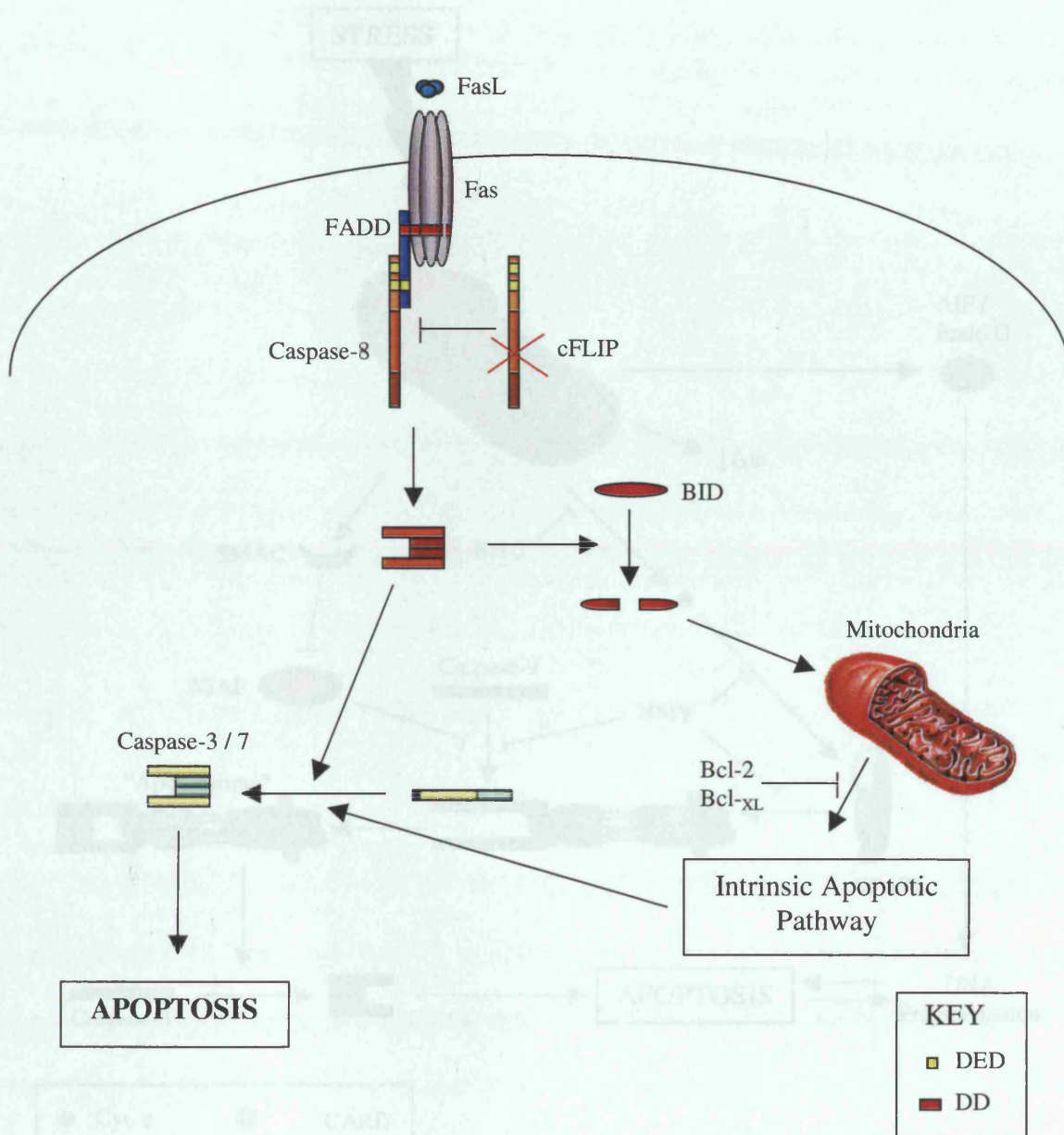


**Figure 1.2.6 The Extrinsic Apoptotic Pathway**

A model of extrinsically mediated apoptotic signalling. The CD95 / Fas signalling pathway has been used as a model of extrinsic apoptotic signalling. Trimerization of the receptor and recruitment of FADD and caspase-8 to the DISC results in activation of caspase-8. Depending upon levels of caspase-8 activation results in either the direct activation of the effector caspases -3 and -7 or the cleavage of BID. Cleaved BID triggers the intrinsic apoptotic pathway in type II cells by translocating to the mitochondria and causing cytochrome *c* release. Caspase-8 activation can be inhibited by recruitment of cFLIP to the DISC thereby preventing auto-activation of caspase-8. Bcl-2 and Bcl-XL can only exert an effect in type II cells by preventing the activation of the intrinsic apoptotic pathway.

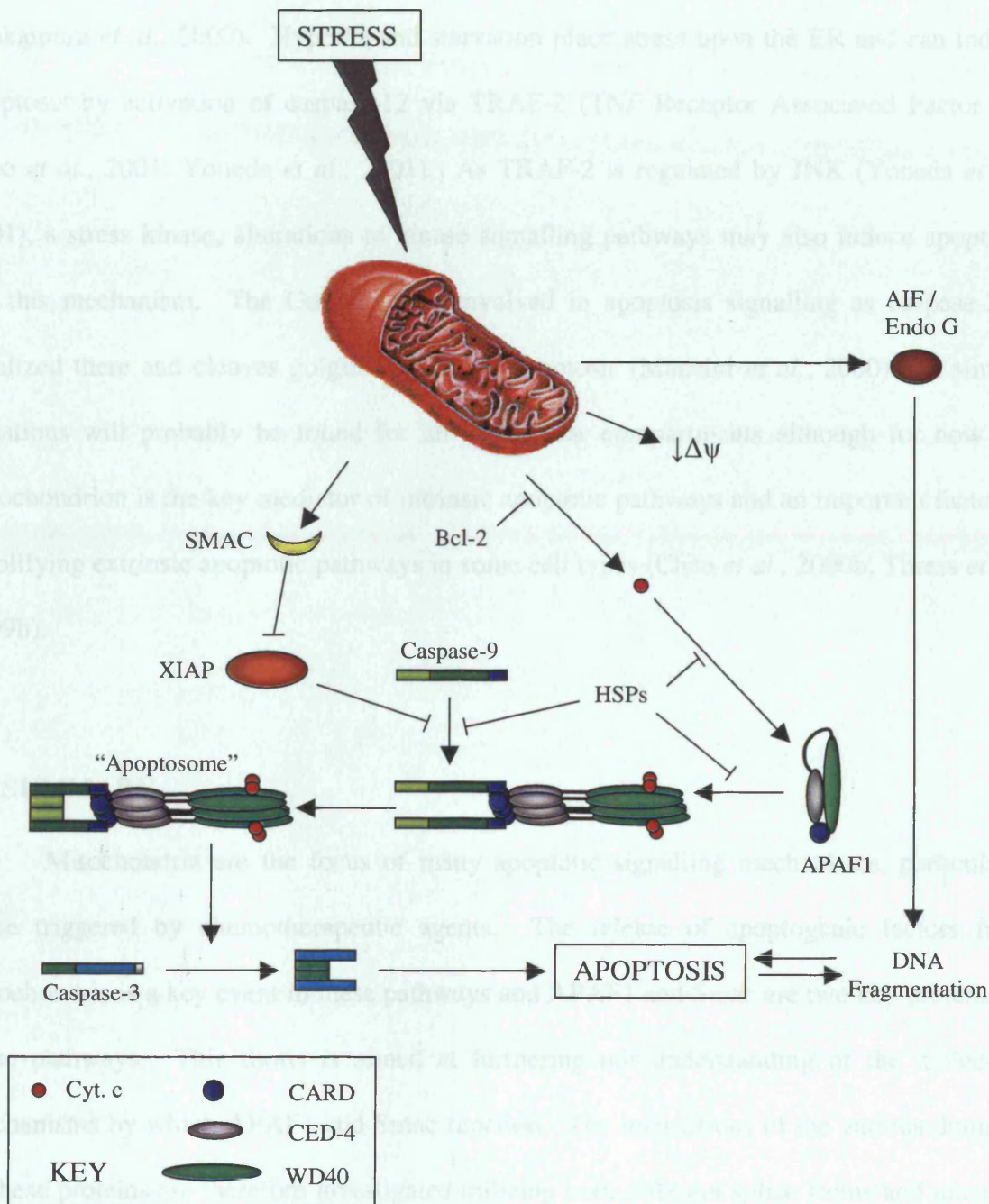


**Figure 1.2.7 The Intrinsic Apoptosis Signalling Pathway**

A schematic diagram of the intrinsic apoptosis signalling pathway via the mitochondria. Cellular damage induces cytochrome *c* (Cyt. *c*) release from the mitochondria inducing the formation of the apoptosome and activating caspases. Cytochrome *c* release is regulated by Bcl-2 and IAP inhibition of caspase activation is prevented by Smac released from the mitochondria. Heat shock proteins (HSPs) can also regulate the formation of the apoptosome by binding cytochrome *c* and blocking oligomerization and caspase-9 recruitment. AIF and endonuclease G (endo G) are also released from the mitochondria and are responsible for the characteristic degradation of DNA.

calcium stores within the cell such as the ER can also result in damage to the mitochondria (Nakamura *et al.*, 2000). Hypoxia and starvation place stress upon the ER and can induce apoptosis by activation of caspase-12 via TRAF-2 (TNF Receptor Associated Factor –2) (Rao *et al.*, 2001; Yoneda *et al.*, 2001). As TRAF-2 is regulated by JNK (Yoneda *et al.*, 2001), a stress kinase, alterations to kinase signalling pathways may also induce apoptosis via this mechanism. The Golgi is also involved in apoptosis signalling as caspase-2 is localized there and cleaves golgin-160 during apoptosis (Mancini *et al.*, 2000) and similar situations will probably be found for all subcellular compartments although for now the mitochondrion is the key mediator of intrinsic apoptotic pathways and an important factor in amplifying extrinsic apoptotic pathways in some cell types (Chen *et al.*, 2000b; Thress *et al.*, 1999b).

### 1.3 SUMMARY

Mitochondria are the focus of many apoptotic signalling mechanisms, particularly those triggered by chemotherapeutic agents. The release of apoptogenic factors from mitochondria is a key event in these pathways and APAF1 and Smac are two key proteins of these pathways. This thesis is aimed at furthering our understanding of the molecular mechanisms by which APAF1 and Smac function. The interactions of the various domains of these proteins are therefore investigated utilizing both different splice forms and mutants. These studies were aimed at identifying novel domains within these key proteins and determining the role each of these domains plays in the functioning of the protein. By improving our understanding of the interactions of these key proteins in various apoptotic pathways it may be possible to design therapeutic agents which act by disrupting or enhancing key interactions.

**CHAPTER 2: MATERIALS AND METHODS**

## 2.1 MATERIALS

Media and serum were purchased from Life Technologies (Paisley, Scotland). Benzyloxycarbonyl – Asp – Glu – Val – Asp – 7 – amino – 4 - trifluoromethylcoumarin (z-DEVD.AFC), benzyloxycarbonyl – Ile – Glu – Thr – Asp – 7 – amino – 4 - trifluoromethylcoumarin (z-IETD.AFC), benzyloxycarbonyl – Val – Glu – Ile – Asp – 7 – amino – 4 - trifluoromethylcoumarin (z-VEID.AFC), benzyloxycarbonyl – Leu – Leu – Val – Tyr – 7 – amino – 4 - trifluoromethylcoumarin (z-LLVY.AFC) and benzyloxycarbonyl – Val – Ala – Asp - fluoromethyl ketone (z-VAD.FMK) were from Enzyme Systems Inc. (Dublin, CA, USA). Carbobenzoxyl-leuciny-leuciny-leucinal (MG132) was from Calbiochem (Nottingham, UK). All other chemicals were from Sigma Chemical Co. (Poole, Dorset, UK) unless otherwise stated.

**Table 2.1 Antibodies**

Primary (dilution)	Secondary (dilution)	Origin of Primary
FLAG M5 (1:4500)	Goat anti-mouse HRP (1:2000)	Sigma, Poole, Dorset.
HSV (1:10000)	Goat anti-mouse HRP (1:2000)	Novagen, Nottingham.
T7 (1:10000)	Goat anti-mouse HRP (1:2000)	Novagen, Nottingham.
T7-HRP (1:5000)	N/A	Novagen, Nottingham.
c-IAP-1 (1:250)	Goat anti-rabbit HRP (1:2000)	R&D Systems, Abingdon, Oxon.
c-IAP-2 (1:500)	Goat anti-rabbit HRP (1:2000)	R&D Systems,
XIAP (1:250)	Goat anti-mouse HRP (1:2000)	Transduction Labs, Cowley, Oxford
APAF1 (1:1000)	Goat anti-rabbit HRP (1:2000)	Dr. X. Wang, University of Texas
Cytochrome c (1:1000)	Goat anti-mouse HRP (1:2000)	Pharmingen, San Diego, CA, USA
Smac (1:4000)	Goat anti-rabbit HRP (1:2000)	Darren Roberts

Secondary antibodies were as follows; Goat anti-rabbit HRP (DAKO, Denmark), Goat anti-mouse HRP (Sigma-Aldrich, Poole, Dorset, UK), Goat anti-mouse Alexa 488 (Molecular Probes, Eugene, OR, USA).

### 2.1.2 Animals

Rabbits were bred in the Clinical Sciences Department of the University of Leicester.

## 2.2 CELL BIOLOGY METHODS

### 2.2.1 Cell Culture

Human Embryonic Kidney 293 cells were obtained from the European Collection of Animal Cell Cultures and grown in high glucose DMEM supplemented with 10% FBS. MCF-7 Fas (MCF-7) human breast epithelial cells (a kind gift of Dr. M. Jaattela, Danish Cancer Society Research Center, Copenhagen, Denmark) were grown in RPMI 1640 supplemented with 10% FBS and 2mM Glutamax™. Both cell lines were routinely passaged every 3 to 4 days and cultured in an atmosphere of 5% CO<sub>2</sub> in air at 37°C.

### 2.2.2 Transfection

Cells were grown to a minimum of 50% confluency prior to transfection in either 6 or 12 well plates or 100mm dishes. Cells were then transfected using either LipofectAMINE (Life Technologies, Paisley, Scotland) or Fugene6™ (Roche Biochemicals, Indianapolis, USA) using 0.5µg (12 well plates), 0.5µg – 2µg (6 well plates) or 2µg – 4µg (100mm plates) DNA.

#### 2.2.2A Transfection using LipofectAMINE Reagent

Cells were transfected with LipofectAMINE as follows: media was replaced on the cells 2 h prior to transfection, DNA was diluted to 100µl in Optimem™ serum free medium (Life Technologies) and a separate master mix prepared of 3µl LipofectAMINE in 100µl Optimem™ (6 well plates) or 50µl LipofectAMINE in 400µl Optimem™ (100mm plates). The DNA and LipofectAMINE solutions were then mixed gently and incubated at room temperature for 30 min. Cells were then rinsed in Optimem™ and then 0.8ml Optimem™

was added to the transfection mixture and the diluted mixture added to the cells. The cells were then incubated at 37°C for 12 h after which time the transfection mixture was removed and complete media containing antibiotics (1U/ml Penicillin, 1µg/ml Streptomycin) was added and the cells incubated for a further 12 to 36 h.

### 2.2.2B Transfection using Fugene6™

5µl or 20µl Fugene6™ was added directly to 100µl or 400µl Optimem™ respectively, avoiding contact with the plastic of the tube and incubated for 5 minutes at room temperature after gentle mixing. The diluted Fugene6™ was then added drop-wise to a fresh tube containing 0.5µg to 4µg DNA and incubated at room temperature for 15 minutes. During this time the media on the cells was replaced with media containing antibiotics and then the transfection mixture was added drop-wise to the cells and mixed by swirling. Cells were then incubated for 24 to 48 h at 37°C prior to treatment or harvesting.

### 2.2.3 Induction of apoptosis

Apoptosis was induced in cells at 80 to 90% confluency by exposure to either 10µM etoposide, 0.1µM or 1µM MG132, 0.25 µg/ml (in MCF-7 cells) or 1 µg/ml (in 293 cells) TRAIL or 10ng/ml TNF-α (in the presence or absence of 1µM cycloheximide). Cells were treated for 6 h with the various stimuli at 37°C unless otherwise stated.

### 2.2.4 Assessment of Apoptosis

After treatment for the required time, cells that had been transfected with pRSC *lacZ* were washed twice in cold phosphate-buffered saline (PBS). Cells were then fixed in 0.25% glutaraldehyde in PBS at room temperature for 15 min. Cells were then washed twice in PBS to remove excess glutaraldehyde and then stained with X-gal staining solution (5mM K<sub>4</sub>Fe(CN)<sub>6</sub>, 5mM K<sub>3</sub>Fe(CN)<sub>6</sub>, 0.2mg/ml X-gal, 2mM MgCl<sub>2</sub>, in PBS) for 1 to 16 h at 37°C. The staining solution was then removed and the cells washed with PBS. Cells were then

manually counted and apoptosis was assessed based upon cell morphology as described in Duan *et al.* (1996). The amount of apoptosis was expressed as a percentage of apoptotic blue cells. Two individuals performed all counts on blinded samples.

### **2.2.5 Immunocytochemistry and Confocal Microscopy**

Cells were grown on coverslips and 24 h after transfection treated with various agents. After the required incubation time the cells were stained with 100nM MitoTracker™ Red CMXRos (Molecular Probes, Eugene, OR, USA) for 15 min at 37°C. Cells were then fixed in 3.8% Formaldehyde in PBS for 20 min at room temperature. Cells were then washed three times in PBS and permeabilized in 0.1% Triton X-100 in PBS and blocked overnight in 3% BSA in PBS at 4°C. Cells were then incubated with anti-HSV antibody (1:25000 in 3% BSA / PBS) for 3 h at room temperature. Cells were then washed three times with PBS prior to incubation with anti-mouse Alexa 488 (1:300 in 3% BSA / PBS) for 45 min at room temperature. Cells were then washed three times with PBS and the nuclei stained with 0.25µg/ml Hoechst 33258 for 20 min at room temperature. The coverslips were then mounted onto glass slides using Vectashield® (Vector Laboratories, Peterborough). Optical sections were then imaged on a Leica TCS-4D confocal imaging system using argon-krypton and UV lasers.

### **2.2.6 Development of a polyclonal antibody to Smac β**

In order to further investigate endogenous Smac and Smac β it was necessary to develop an antibody against Smac β. To enable the antibody to be used for a variety of different uses such as immuno-precipitation and immuno-cytochemistry as well as Western blotting it was necessary to produce an antibody that recognized multiple epitopes, i.e. a polyclonal antibody. Smac β was purified from bacteria by affinity chromatography on Ni-NTA beads and ion exchange chromatography on a Resource Q column. 1mg of Smac β protein was

then diluted with adjuvant (TitreMax Gold) and used to immunise two rabbits as described in Materials and Methods. Test bleeds were then taken from the animals and the serum tested by ELISA, and later, Western blotting. When the titre of the antibody was starting to drop, the animals were boosted with 0.5mg of protein without adjuvant (Fig. 2.1) and this regime was repeated until the serum obtained specifically recognised Smac and Smac  $\beta$  on a Western blot. Terminal bleeds were taken on day 174 and the sera stored for later use. IgG was purified from the sera (by W. Merrison) by affinity chromatography on a protein A column and this was then used in some of the experiments described later.

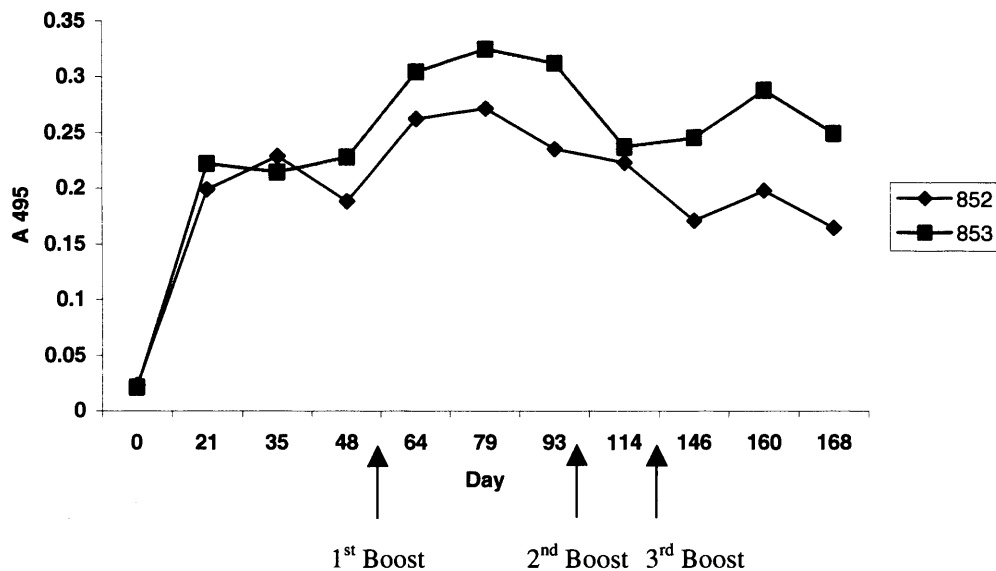


**Figure 2.1 Anti- Smac  $\beta$  antibody production**

Two rabbits (852 and 853) were injected with 1mg pure recombinant Smac  $\beta$  in 1ml 50% adjuvant on day 0. Test bleeds were taken on the days indicated and the sera tested by ELISA by Dr. X. M. Sun (MRC Toxicology Unit) at a 1:100 for reactivity to recombinant Smac  $\beta$ . Animals were boosted with 0.5mg antigen without adjuvant when the antibody titre started to drop (indicated by arrows).

## 2.3 BIOCHEMICAL METHODS

### 2.3.1 Electrophoresis of DNA and proteins

#### 2.3.1A Agarose gel electrophoresis of DNA

Purified plasmids or PCR products were analysed by agarose gel electrophoresis to determine both quantity and quality of the DNA before further use. Agarose gel electrophoresis was also utilised to separate DNA fragments prior to their purification. To prepare the agarose gel between 0.8 and 2 g of agarose (Life Technologies) was dissolved in 1xTAE (40mM Tris : Acetate pH 8.5, 2mM EDTA) and heated in a microwave until dissolved. The solution was then allowed to cool to ~60°C before the addition of 0.5µg / ml ethidium bromide and pouring into a casting tray. The comb(s) were then immediately inserted and any air bubbles removed. The gel was then left to set for approximately 20 min. The gel was then submerged in 1xTAE in a gel tank and the comb gently removed. 10x DNA loading buffer (0.5% (w/v) Orange G, 0.5% (w/v) Xylene cyanol, 25% (w/v) Ficoll 400, 20mM EDTA) was added to the sample to a final concentration of 1x and then the sample was loaded directly into the well. DNA ladders (1kB, 123bp and 100bp) obtained from Life Technologies, were used as molecular weight markers and approximately 1µg was run in each lane. The gel was run at 100V for approximately 30 min to 1 h or until the dye front reached approximately two thirds of the distance along the gel. The gel was then visualised using a UV transilluminator and photographed.

#### 2.3.1B SDS-Polyacrylamide Gel Electrophoresis (SDS-PAGE) of proteins

All gels were run using the MiniProtean II system from Bio-Rad (Hemel Hempstead, Herts., UK) and were assembled following the manufacturer's instructions. The glass plates were

cleaned with distilled water followed by ethanol prior to the gel casting. The appropriate percentage of resolving gel was then prepared as outlined below (all volumes are sufficient for 2 gels using 1.5mm spacers and combs):

	<b>% Resolving Gel</b>			
	<b>7%</b>	<b>10%</b>	<b>13%</b>	<b>15%</b>
30% Acrylamide (ml)	2.9	4.15	5.4	6.25
Resolving gel buffer (ml)	3.125	3.125	3.125	3.125
ddH <sub>2</sub> O (ml)	6.4	5.15	3.9	3.05

Acrylamide was purchased from National Diagnostics and the lower gel buffer (1.5M Tris-HCl, pH 8.8, 0.4% SDS) was filtered through a 0.45µm filter after preparation. The gel solution was then degassed for 10 min before pouring. Once degassed the gel polymerisation was initiated by the addition of 75µl 10% ammonium persulphate (APS) and 10µl TEMED and then approximately 7.25ml of the gel mixture was poured between each pair of glass plates. The gel solution was then gently overlaid with 70% ethanol to exclude air and provide a smooth interface with the stacking gel. The gel was then allowed to polymerise for 20 min at room temperature. During this time the stacking gel was prepared by mixing 1.35ml of 30% Acrylamide, 2.5ml 0.5M Tris-HCl, pH 6.8, 0.4% SDS and 6.1ml of deionised distilled (dd) H<sub>2</sub>O and degassed for 10 min. Once the resolving gel was polymerised the 70% ethanol was poured off and the gel surface washed with ddH<sub>2</sub>O. The surface was then dried by wicking off any excess water with a small piece of 3MM filter paper. The polymerisation of the stacking gel was then initiated by the addition of 50µl APS and 10µl TEMED and the gel solution was poured on top of the resolving gel and the combs inserted. The gel was then allowed to polymerise for 30 min.

Samples were prepared by resuspending  $\sim 0.5 \times 10^6$  cells, which had been previously washed with PBS to remove any excess serum and frozen until required, in 50 $\mu$ l of sample buffer (62.5mM Tris, pH 6.8, 15% glycerol, 2% SDS, 0.025g / 50ml bromophenol blue, 5% 2-mercaptoethanol (added fresh)). Protein samples were prepared in the same way with 15 $\mu$ g being equivalent to  $\sim 0.5 \times 10^6$  cells. Samples were then boiled for 5 min and then pulsed down prior to loading into the wells of the gel.

The gel was prepared for running by carefully removing the combs and then removing the gels from the casting stand and attaching them to the electrode assembly as per the manufacturer's instructions. This was then placed into the running tank and the central reservoir filled with electrode buffer (25mM Tris, 192mM glycine, 1% SDS). Sufficient electrode buffer was added to the running tank to cover the lower screws on the gel clamps and then the samples were loaded into the wells of the stacking gel. The gels were run at a constant current of 45mA and maximal voltage until the dye front reached the end of the gel.

### **2.3.2 Western blotting**

Samples were separated by SDS-PAGE as described in section 2.3.1. The gel was then removed from the glass plates and the stacking gel discarded. The resolving gel was then placed into transfer buffer (25mM Tris, pH 8.3, 192mM glycine, 20% (v/v) methanol) to allow equilibration and shrinkage to occur. A piece of Hybond C-extra supported nitrocellulose transfer membrane (Amersham, Bucks., UK) was cut to just larger than the gel and soaked in transfer buffer along with six pieces of Whatman 3MM filter paper of the same size. After approximately five minutes the transfer sandwich was set up as shown below (Figure 2.1) ensuring there were no air bubbles trapped between layers. The assembly was then placed into a transfer electrode assembly and placed along with a cooling pack into

a

## 2.2.3 Preparation of cellular lysates and fractions

## 2.2.3A. Lysates for immunoprecipitation studies

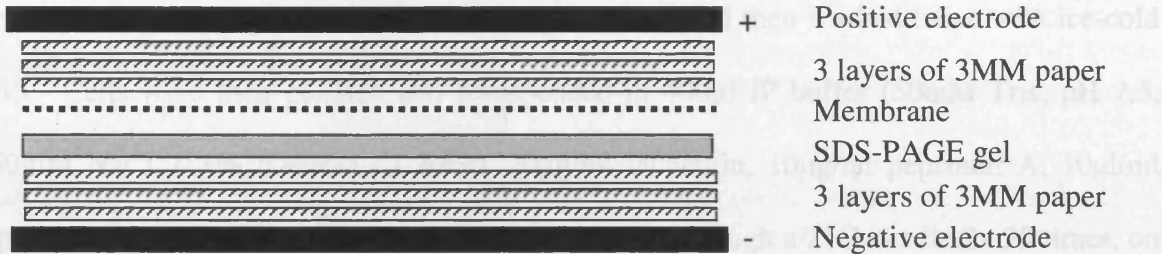


**Figure 2.2 Assembly of a transfer sandwich**

running tank filled with transfer buffer. The gel was then transferred at 30V overnight or 100V for 1 h. After transfer the transfer sandwich was disassembled and the membrane stained with Ponceau S to confirm equal loading and the absence of air bubbles. The stain was rinsed off with TBST (200mM Tris, pH 7.6, 1.37M NaCl, 0.1% Tween 20) and then non-specific protein binding blocked with TBST-M (TBST containing 5% non-fat dried milk (Marvel™)) for 1 h at room temperature. The blocking solution was discarded and the membrane then rinsed with TBST prior to incubation for 1 h in the required primary antibody diluted in TBST. The membrane was then washed as follows; 2x rinse in TBST-M, 1x 5 min in TBST-M, 1x rinse in TBST, 1x 5 min in TBST. The membrane was then incubated for 1 h in the appropriate horseradish – peroxidase (HRP) conjugated secondary antibody diluted in TBST. The wash steps were then repeated and then the membrane was washed in TBS (200mM Tris, pH 7.6, 1.37M NaCl). The immunocomplexes were then visualized using the ECL chemiluminescent detection kit (Amersham).

### 2.3.3 Preparation of cellular lysates and fractions

#### 2.3.3A Lysates for immunoprecipitation studies

Cells from a 100mm plate were harvested by scraping and then washed twice with ice-cold PBS. Cells were then pelleted and resuspended in 400µl IP buffer (50mM Tris, pH 7.5, 150mM NaCl, 0.1% IGEPAL- CA630, 20µg/ml leupeptin, 10µg/ml pepstatin A, 10µl/ml Aprotinin, 2mM PMSF). Cells were lysed by passing through a 21G needle 2x 20 times, on ice. Intact cells and nuclei were removed by centrifugation for 30 min at 14000rpm, 4°C in a Sigma benchtop centrifuge. The pellet was then discarded and the supernatant used in immunoprecipitation experiments or stored at -80°C until required.

#### 2.3.3B Lysates for activation studies and FPLC

To a pellet of  $1 \times 10^8$  cells that had been washed in PBS 160µl of PIPES buffer (50mM PIPES/KOH, pH 6.5, 2mM EDTA, 0.1% (w/v) CHAPS, 5mM dithiothreitol (DTT), 20µg/ml leupeptin, 10µg/ml pepstatin A, 10µl/ml Aprotinin, 2mM PMSF) was added. The cells were then frozen in liquid N<sub>2</sub> and thawed in a 37°C water bath three times. Cellular debris was removed by centrifugation at 14000rpm, 4°C for 30 min in a Sigma benchtop centrifuge. The supernatant was then retained and transferred to a TLA120.2 Beckman Ultracentrifuge rotor and centrifuged at 100,000xg for 45 min at 4°C in a Beckman Optima centrifuge. The supernatant was then stored at -80°C until required.

#### 2.3.3C Sub-cellular fractionation

Cells were harvested by trypsinisation and then allowed to recover for 10 min at 37°C in complete media. Cells were then pelleted and the cell pellet resuspended in 10 volumes of RSB buffer (10mM HEPES pH 7.9, 1.5mM MgCl<sub>2</sub>, 10mM KCl, 0.5mM DTT, 0.2mM

PMSF). The cells were then allowed to swell on ice for 10 min. The cell suspension was then transferred to a Dounce homogeniser and homogenised with 10 to 15 strokes of a B-type pestle. Eight volumes of 2.5x MS buffer (525mM Mannitol, 175mM sucrose, 12.5mM HEPES pH 7.35, 2.5mM EDTA) were added and mixed by inversion. The suspension was then brought to a total of 30 volumes with 1x MS buffer (210mM Mannitol, 70mM sucrose, 5mM HEPES pH 7.35, 1mM EDTA). The mix was then centrifuged at 1300xg for 5 min at 4°C. The nuclear pellet containing intact cells, nuclei and large membrane fragments was washed three times with RSB. The supernatant was then spun at 17000xg for 15 min at 4°C to pellet the mitochondria. The mitochondrial pellet was then washed three times with 1x MS buffer. The post-mitochondrial supernatant was spun at 100,000xg for 45 min at 4°C to pellet the microsomal fraction. The microsomal pellet was washed three times with 1x MS buffer. The post-microsomal supernatant was retained as S-100 lysate. All fractions were stored at -80°C until required.

#### 2.3.4 Fluorometric Assay

The activity of caspases in various cell lysates was measured using a continuous fluorometric assay as previously published (MacFarlane *et al.*, 1997). Use of the fluorogenic substrate z-DEVD.AFC allows the monitoring of caspase-3-like activity in a sample. z-DEVD.AFC mimics the cleavage site within PARP and cleavage releases the fluorogenic moiety AFC (7-amino-4-trifluoromethylcoumarin) that can be detected by a fluorimeter using the excitation wavelength of 400nm and emission wavelength of 505nm. Lysate was added to a well of a 96 well plate and 200µl of substrate diluted to 20µM in assay buffer (100mM HEPES, 10% (w/v) sucrose, 0.1% (w/v) CHAPS, 10mM DTT, pH 7.5) and assayed at 37°C using a Victor<sup>2</sup> fluorescent plate reader (Wallac) fitted with a thermostat. Routinely 15 to 100µg of protein was used in the assay and the readings taken over 5 min and specific activities were then

calculated. Standard curves for the concentration of the fluorogenic moiety were established and the  $x$  coefficient established for AFC fluorescence. The specific activity of a sample was calculated as follows:

$$\text{Activity (nmol/min)} = \frac{\text{fluorescence units / second}}{x \text{ coefficient}}$$

The activity was then corrected for volume ( $\times 0.2$ ), protein content and then converted to activity per minute ( $\times 60$ ) and converted to pmol/min ( $\times 1000$ ) to give a final activity reading of pmol/mg/min.

### **2.3.5 Gel filtration chromatography**

In order to separate protein complexes, cellular lysates were fractionated by FPLC using a HiPrep 16/60 S-300 Sephacryl high-resolution column (APAF1 studies) or a HiPrep 16/60 S-200 Sephacryl S-200 high-resolution column (Smac studies) (Amersham Pharmacia Biotech, Uppsala, Sweden) that separates proteins by gel filtration. The column was equilibrated in column buffer (20mM HEPES, 0.1% (w/v) CHAPS, 5mM DTT, 5% (w/v) sucrose, pH 7.0) (APAF1 studies) or IP buffer (Smac studies) prior to the application of the cellular lysate (1 to 10 mg) at a flow rate of 1ml / min. Fractions of 2ml were collected and analysed by Western blot for the presence of various proteins.

### **2.3.6 Determination of protein concentration using the Bradford method**

Protein concentrations were determined using the Bio-Rad protein assay reagent (Bio-Rad), which determines protein concentration using a modified Bradford method. Approximately 5 $\mu$ l of a sample to be measured was added to 1ml of assay reagent diluted to 20% with ddH<sub>2</sub>O and the OD<sub>595</sub> was measured. A standard curve was prepared using known

concentrations of a BSA standard (Bio-Rad) and used to determine the protein concentration in the samples.

### **2.3.7 *In vitro* activation of caspases**

In order to activate caspases within the cellular lysates the protein concentration was corrected to 10mg/ml with lysis buffer. Lysates were then incubated at 37°C in the presence of 2mM dATP, 2mM MgCl<sub>2</sub> and 0.25mg /ml horse heart cytochrome *c* for 10 to 60 min. To confirm activation of the caspases within the lysate, DEVDase activity within the lysate was measured using the fluorogenic assay described in section 2.3.4. Typically activation resulted in approximately a 150-fold increase in DEVDase activity.

## 2.4 MOLECULAR BIOLOGY METHODS

### 2.4.1 Bacterial culture and transformation

*Escherichia coli* strains DH5 $\alpha$  and BL21(DE3) were routinely grown and maintained on Luria agar (LA) with appropriate antibiotics for the maintenance of plasmids being carried. For liquid cultures Luria broth (LB) was routinely used and bacteria were grown at 37°C with shaking (200 to 300rpm). All constructs were stored as frozen stocks of DH5 $\alpha$  containing the plasmid in 15% glycerol / LB at -80°C. BL21(DE3) were routinely used for protein expression. Ampicillin was used at a final concentration of 100 $\mu$ g/ml in both LB and LA.

Competent bacteria were prepared as follows: an overnight 5ml culture of bacteria was used to inoculate 200ml of LB without antibiotics. This culture was grown to an OD<sub>550</sub> of 0.5 and then chilled on ice for 15 min. Bacteria were then pelleted by centrifugation at 4000rpm at 4°C for 15 min. Bacteria were then resuspended in 60ml RF1 buffer (100mM RbCl, 50mM MnCl<sub>2</sub>, 30mM K Acetate, 10mM CaCl<sub>2</sub>, 15% glycerol, pH 5.8) and incubated on ice for 30 min to 2 h. Bacteria were then pelleted as before and resuspended in 25ml RF2 buffer (10mM MOPS, 10mM RbCl<sub>2</sub>, 75mM CaCl<sub>2</sub>, 15% glycerol, pH 6.8). The competent bacteria were then aliquoted into 0.5ml aliquots and snap frozen in liquid N<sub>2</sub> and stored at -80°C.

Competent bacteria were transformed as follows; 100 $\mu$ l of bacteria were incubated with 1 to 20ng of plasmid DNA for 30 min on ice. The bacteria were then heat shocked at 42°C for 45 sec and then incubated on ice for 2 min. 900 $\mu$ l of SOC media (Life Technologies) was then added and the bacteria were allowed to recover for 1 h at 37°C with shaking. 200 $\mu$ l of the culture was then spread onto a LA plate containing selective antibiotics and incubated at 37°C overnight.

### **2.4.2 Plasmid DNA isolation**

Plasmid DNA was isolated from bacterial cultures using QIAGEN mini and maxi-prep kits (QIAGEN, Crawley, West Sussex, UK) as recommended by the manufacturer. Briefly a bacterial culture (1 to 5ml – mini, 50 to 100ml - maxi) was grown overnight and pelleted by centrifugation at 4000rpm, 4°C for 15 min. The bacteria were then lysed by the addition of an alkaline lysis buffer containing RNase and then proteins precipitated by addition of a precipitation buffer. The proteins and genomic DNA are then removed by centrifugation and the supernatant applied to a column. The plasmid DNA then binds to this column and is washed to remove bound proteins and contaminating RNA and genomic DNA. The DNA is then eluted and is either ready for use (mini) or is then precipitated with isopropanol and resuspended in the buffer of choice (maxi). Plasmid DNA was then quantified on a spectrophotometer (DNA/RNA calculator, Amersham Pharmacia) by absorbance at 260nm and the quality of the DNA determined by the ratio of absorbance at 260nm versus 280nm with a ratio of 1.8 being optimal. Plasmids were also quantified by agarose gel electrophoresis using a 1kB DNA ladder (Life Technologies) as a known quantity.

### **2.4.3 Production of recombinant proteins in bacteria**

BL21(DE3) cells were freshly transformed with a bacterial expression plasmid containing the protein of interest with a His<sub>6</sub>-tag to aid purification. A single colony was then picked and grown for 6 h in 5ml LB containing ampicillin (100µg/ml) or other selective antibiotic and the culture stored overnight at 4°C. The bacteria were then pelleted by centrifugation at 4000rpm for 15 min at room temperature and resuspended in fresh LB containing antibiotics and used to inoculate 400ml of LB containing antibiotics. This culture was then grown at 37°C with shaking until the OD<sub>550</sub> was 0.7. The culture was then incubated in the presence of 1mM IPTG for a further 3 h at 27° to 37°C depending upon the solubility of the protein

being expressed. The bacteria were then pelleted at 4000rpm for 15 min, washed with PBS and the pellet stored at  $-80^{\circ}\text{C}$  until ready for the purification of the protein. The bacteria were resuspended in 5ml of 20mM HEPES, pH 8.0, 0.1% CHAPS and then sonicated using a probe sonicator at maximum intensity for 10 cycles (15 sec on / 45 sec off per cycle). The debris was removed from the lysate by centrifugation at 12000rpm in a Beckman JA-17 rotor for 20 min at  $4^{\circ}\text{C}$ . 50 $\mu\text{l}$  of a 50% slurry of Ni-NTA agarose beads, washed in the lysis buffer were added to the clarified supernatant and incubated for 1 h at  $4^{\circ}\text{C}$  with gentle rotation on a daisy wheel. The Ni-NTA beads were then removed from the supernatant by centrifugation at 500xg at  $4^{\circ}\text{C}$  for 10 sec in a Sigma benchtop centrifuge. The supernatant then had a further 50 $\mu\text{l}$  of Ni-NTA beads added and the process was repeated. The beads were then washed four times in 1ml lysis buffer, containing 20mM imidazole, and then four times in buffer containing 100mM imidazole. Proteins were then either eluted from the beads with 150mM EDTA and stored at  $-80^{\circ}\text{C}$  or retained on the beads in PBS and stored at  $4^{\circ}\text{C}$ . SDS-PAGE and coomassie brilliant blue R-250 staining was used to assess the purity of the recombinant proteins.

#### **2.4.4 RNA isolation**

RNA was isolated from various cell lines and rat tissues using Tri-Reagent as recommended by the manufacturer. Essentially 5 to 10 x 10<sup>6</sup> cells or 50 to 100mg of snap-frozen rat tissue were added to 1ml of Tri-Reagent and either lysed by pipetting up and down (cells) or by using a Polytron homogeniser (tissue). The lysate was then allowed to stand for 5 min at room temperature to dissociate the nucleoprotein complexes. 200 $\mu\text{l}$  chloroform was then added and the sample was mixed vigorously for 15 sec but not vortexed. The sample was then incubated at room temperature for 15 min and then centrifuged at 12000xg for 15 min at  $4^{\circ}\text{C}$  in a Sigma benchtop centrifuge. The upper aqueous phase was then transferred to a

fresh tube and 500µl isopropanol were added to it and incubated at room temperature for 10 min. RNA was then pelleted by centrifugation at 12000xg for 10 min at 4°C. The pellet was then washed in 70% ethanol and re-pelleted at 7500xg for 5 min at room temperature. The pellet was then dried in a Speed-Vac for 2 - 3 min and then resuspended in 30µl DEPC-treated water. The RNA was then quantitated using a spectrophotometer and diluted to 100ng/µl with DEPC-treated water and stored at -80°C.

#### **2.4.5 RT-PCR**

Reverse transcription – polymerase chain reaction (RT-PCR) was used to analyse the expression of various apoptotic proteins at the RNA level and to clone novel cDNAs.

##### *2.4.5A First-strand cDNA synthesis*

Total RNA was reverse-transcribed using Expand™ Reverse Transcriptase (Roche Biochemicals) as described in the manufacturer's instructions. Basically the following reagents were added in the following order to a 0.2ml thin walled PCR tube; 1µg of total RNA, 50pmoles of Oligo(dT)<sub>15</sub> and ddH<sub>2</sub>O to 20µl. The RNA was then denatured for 10 min at 65°C and then immediately cooled on ice. To the reaction 4µl 5x reverse transcriptase buffer, 2µl 100mM DTT, 2µl of 10mM dATP, dCTP, dTTP and dGTP (Amersham Pharmacia), 0.5µl 40U/µl RNaseIn (Promega, Southampton, UK) and 1µl 50U/µl Reverse transcriptase were added. The reaction was then incubated for 60 min at 42°C and then transferred to ice to stop the reaction. The cDNA was then immediately used in the PCR reaction.

##### *2.4.5B Polymerase Chain Reaction*

PCR amplification of cDNA or DNA was performed using Pfu DNA polymerase (Stratagene, Amsterdam, The Netherlands) as recommended by the manufacturer. Basically

the reaction was prepared as follows; 10µl 10x buffer, 0.8µl 25mM dNTPs (dATP, dTTP, dGTP, dCTP), 100ng DNA template or 10µl of the RT reaction, 2.5µl of each 100ng/µl primer, 2µl Pfu DNA polymerase and ddH<sub>2</sub>O to 100µl. The reaction was then cycled using a Perkin Elmer GeneAmp 9700 as follows; 1 cycle of 94°C for 45 sec, 30 cycles of 94° 45 sec, Primer Tm -5°C (see appendix 2) 45 sec, 72°C for 2 min per 1kB of amplified target, followed by 1 cycle of 72°C for 10 min. The reaction was then stored at 4°C. The PCR products were analysed by agarose gel electrophoresis and purified by gel extraction using QIAQUICK gel extraction kit (Qiagen) as described in the manufacturer's instructions.

#### **2.4.6 Cloning and subcloning**

Various regions of APAF1 and Smac / Smac β were amplified by PCR or RT-PCR respectively and cloned into pFLAG-CMV2 (Sigma) or pTriEx-1 (Novagen, Nottingham, UK), respectively. The PCR products were gel-purified and then the purified products and empty vectors were digested with the appropriate restriction enzymes (Life Technologies) (*NotI* / *XhoI* for APAF1 and *BamHI* / *HinDIII* for Smac and Smac β) and re-purified by gel extraction. The insert and vector DNA was then combined in ratios of 1:1, 3:1 and 5:1 and ligated using T4 DNA ligase (Roche Biochemicals). 2µl of the ligation mix was then used to transform DH5α competent cells. Colonies were screened by PCR by growing the colony in ~1.5ml LB with antibiotics for 1 h and then pelleting the bacteria from ~1.4ml to use as a template and using vector- and insert-specific primers. All constructs were confirmed by DNA sequencing (PNAACL, CMHT, University of Leicester).

### 2.4.7 Library screening

The human genomic library RPC11 (Ioannou & de Jong, 1996) was obtained from the HGMP- resource centre as gridded filters.

#### 2.4.7A Probe labelling

A probe was prepared by random-prime labelling of a PCR product of the full-length coding sequence of APAF1 as follows: the PCR product was boiled for 5 min and then maintained at 37°C until required. To a screw-top micro-centrifuge tube, 4.8µl Water, 3µl OLB (see below), 0.6µl 10mg/ml BSA, 5µl PCR product, 1µl <sup>32</sup>P dCTP (3000 Ci/mmol, 10µCi/ml, Amersham), and 0.6µl Klenow fragment (1U/µl, Roche Biochemicals) were added and incubated at 37°C for 30 min. To this, 85µl stop solution (see below) was added and the solution mixed by pipetting.

OLB (oligo labelling buffer) was prepared as a 2:5:3 ratio of solution A (625µl 2M Tris-HCl, pH 8.0, 25µl 5M MgCl<sub>2</sub>, 350µl water, 18µl 2-mercaptoethanol, 5µl each of 100mM dATP, dTTP, dGTP), solution B (2M HEPES pH 6.6) and solution C (90 OD units/ml random hexamers, Pharmacia) and stored at -20°C. The stop solution is composed of 20mM NaCl, 20mM Tris-HCl, pH 7.5, 2mM EDTA, 0.25% SDS.

#### 2.4.7B Hybridisation

The filters were pre-washed in 1.5x SSPE (0.27M NaCl, 1.5mM sodium phosphate, pH 7.7, 1.5mM EDTA), 0.5% non-fat milk, 1% SDS, 6% polyethylene glycol 8000 for 1 h at 65°C in hybridisation tubes. The probe was then denatured by boiling for 10 min then rapidly cooled in ice water prior to addition to 20 ml of the pre-wash solution and added to the filters in a hybridisation chamber overnight at 65°C with gentle rocking. Filters were then rinsed for 10 min three times in 150ml 3x SSC (450mM NaCl, 45mM sodium citrate, pH 7.0), 0.1% SDS preheated to 65°C. The filters were then washed four times for 10 min in 0.5x SSC, 0.1%

SDS, 65°C. The filters were then drained and wrapped in Saran Wrap™ and exposed to film at –70°C for 2 d. Positive clones were then ordered from the HGMP-resource centre and the regions of interest PCR amplified and sequenced.

#### **2.4.8 Production of <sup>35</sup>S-labelled proteins**

<sup>35</sup>S-labelled proteins were produced using the Promega TNT coupled rabbit reticulocyte lysate kit and were used in interaction studies. Proteins produced in the TNT system were under the control of a T7 promoter in various vectors. To 25µl Rabbit Reticulocyte lysate 2µl TNT buffer, 1µl T7 RNA polymerase, 1µl RNasIn, 1µl amino acid mixture minus methionine, 2µl <sup>35</sup>S-methionine (NEN, Boston, MA, USA), 1µg plasmid DNA and water were added to a final volume of 50µl. This mixture was then incubated at 30°C for 90 min and then stored at 4°C until required. Production of radiolabelled protein was assessed by SDS-PAGE and autoradiography.

#### **2.4.9 Immunoprecipitation and interaction studies**

These studies utilised the existence of antibodies and the ability to produce recombinant or radiolabelled proteins to investigate protein – protein interactions.

##### *2.4.9A Immunoprecipitation*

A lysate was prepared from cells as described in section 2.3.3A and incubated with 30µl of either protein A or protein G sepharose (Amersham Pharmacia) for 8 h at 4°C with gentle rotation on a daisy wheel to remove non-specific protein binding to the matrix. The beads were then removed by centrifugation at 1000rpm for 10 sec and the supernatant transferred to a fresh tube. The lysate was then incubated with the antibody of choice for 1 h at 4°C on a daisy wheel prior to the addition of 20µl of a 50% slurry of protein G (mouse antibodies) or

protein A (rabbit antibodies)-sepharose washed in IP buffer. The lysate was then incubated overnight at 4°C on a daisy wheel. The beads were then precipitated by centrifugation at 1000rpm for 10 sec and the supernatant removed and stored at -80°C until required. The beads were washed four times with 1ml IP buffer and then resuspended in 30µl SDS-PAGE sample buffer and boiled. 15µl was then analysed by SDS-PAGE and Western blotting and compared to the supernatant.

#### *2.4.9B Interaction studies*

Beads with bound recombinant protein were washed in IP buffer and 10µl of radiolabelled protein was added in 1ml IP buffer. The reaction was then incubated at room temperature for 1 h with gentle agitation. The beads were then precipitated by centrifugation at 1000rpm for 10 sec and the supernatant stored for use as a control. The beads were then washed four times with 1ml IP buffer and resuspended in 30µl SDS-PAGE sample buffer and boiled. Samples of 15µl of the beads and 15µl of the supernatants diluted in 2x SDS-PAGE sample buffer were analysed by SDS-PAGE and visualised by autoradiography.

**CHAPTER 3: APAF1 EXISTS AS MULTIPLE FORMS**

### 3.1. INTRODUCTION

The *C. elegans* homologue of APAF1, CED4, can be alternatively spliced, with the insertion of 24 amino acids resulting in its conversion from a pro-apoptotic into an anti-apoptotic protein (Shaham & Horvitz, 1996). The resulting protein, CED4L, has been demonstrated to act in the same manner as CED9 indicating that CED4L is a functional protein and not simply a competitor of CED4 (Chaudhary *et al.*, 1998). Caspases are also frequently produced as multiple splice forms resulting in either pro- / anti- apoptotic proteins (i.e. caspase-9 (Seol & Billiar, 1999; Srinivasula *et al.*, 1999)) or multiple forms with no apparent difference in function (i.e. caspase-8 (Boldin *et al.*, 1996; Scaffidi *et al.*, 1997). The occurrence of splice forms in apoptotic signalling pathways is more common than is often perceived and the role of many of the splice forms is yet to be elucidated.

In this chapter, the apoptotic molecule APAF1 was analysed to determine if multiple splice forms existed and if these were present as both mRNA and protein within the cell. As APAF1 is the mammalian homologue of the *C. elegans* protein CED4, it was hypothesized that a similar splicing event to that in CED4 may convert APAF1 to an anti-apoptotic molecule. The APAF1 protein contains three other domains and insertions and / or deletions in any of the other domains could result in altered binding to other apoptosome components thereby altering the function of the protein. The alternative splicing of APAF1 could then represent a key regulatory step in apoptotic signalling. The experiments in this chapter were aimed at determining if alternative splicing of APAF1 occurred and which form, if any, was the major form within the cell. During the preparation of this work several groups published on alternative splice forms of APAF1, (Benedict *et al.*, 2000; Hahn *et al.*, 1999; Saleh *et al.*, 1999; Zou *et al.*, 1999), and these papers support the work in this study.

## 3.2 RESULTS

### 3.2.1 Database searching reveals alternatively spliced forms of APAF1

To identify splice variants and any possible homologues of APAF1 the cDNA sequence was used as a query in a BLASTN search of the GenBank databases. The search of the non-redundant database revealed a cDNA, KIAA0413 (accession # AB007873), which was identical to the APAF1 sequence but also contained an additional 132bp (Fig. 3.1 A). When translated this cDNA was found to encode an additional 44 amino acids in the WDR and these amino acids introduced an additional WD40 repeat into the protein, APAF1WD13 (Fig. 3.1 B). The GSS database was found to contain a single entry with homology to APAF1. This sequence, a BAC clone end sequence (accession # B70127), had 100% identity at the 3' end to a region of the WDR and was used to design primers for genomic library screening (see later). The search of the dbEST (human) database identified a transcript from a human foetal heart library that was identical to APAF1 but appeared to contain a region of low homology (EST 54430, accession # AA348012) (Fig. 3.1 A). Further searching of the dbEST database revealed the 3' sequence of the clone (EST 54429, accession # AA348011) that corresponded to the 3' UTR of APAF1. This clone was obtained from the HGMP resource centre and the sequence compared with that published. The size of the insert in the clone was also established by PCR and compared with that predicted from the published sequence. The sequencing data revealed that the region of low homology was in fact identical to APAF1 and was probably due to sequencing errors in the deposited sequence (Fig. 3.1 A). The insert size, however, did not match that predicted from the APAF1 sequence and indicated a deletion of approximately 1.5 Kb from the 3' untranslated region of the transcript. This deletion was confirmed by further sequencing (Fig. 3.1 A).

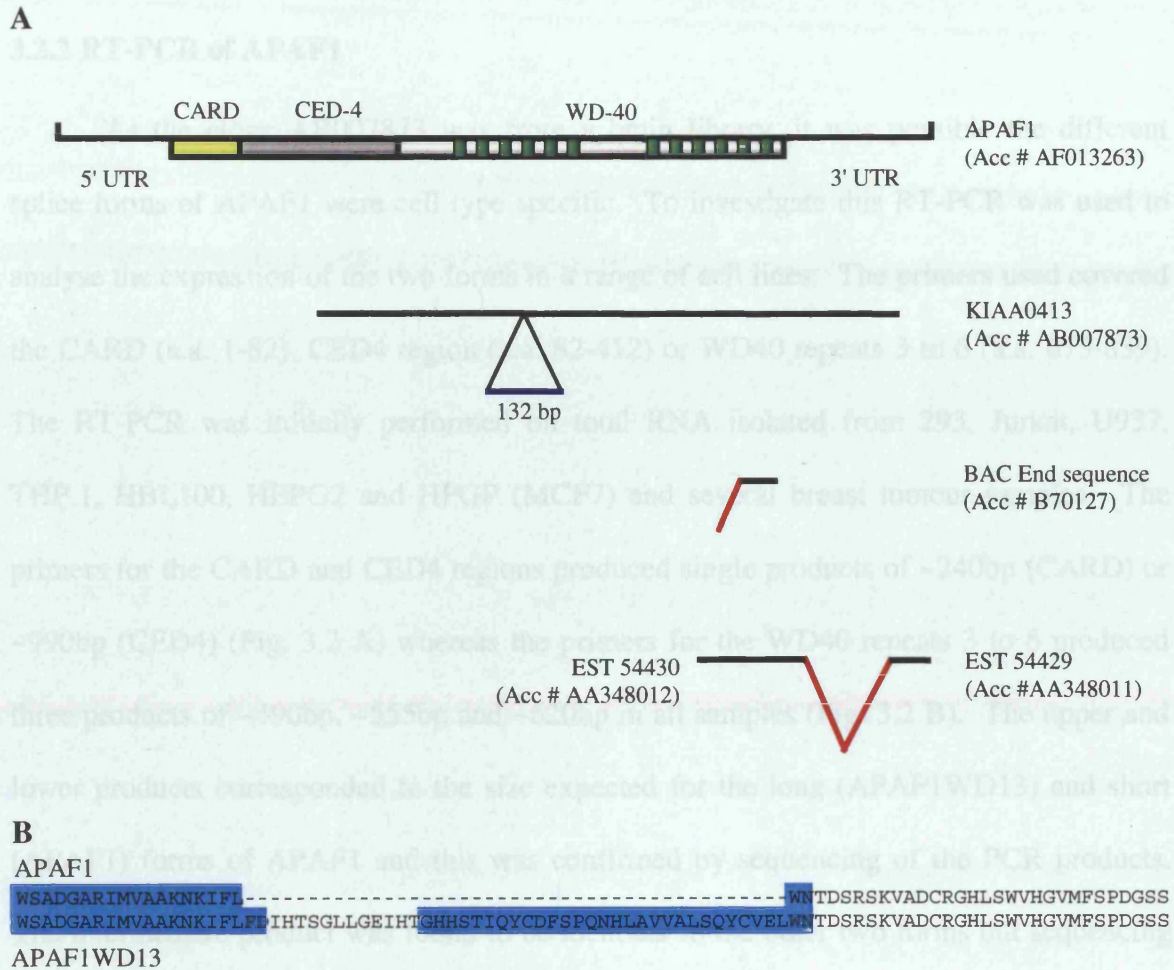


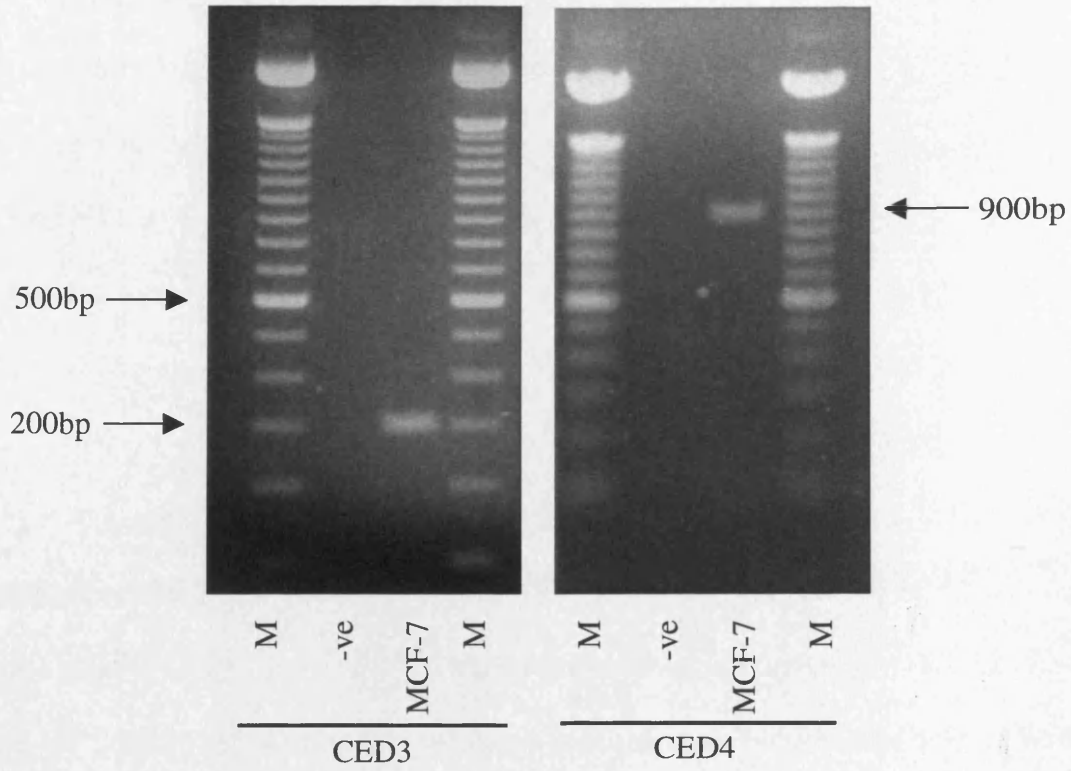
**Figure 3.1** Alternatively spliced forms of APAF1

Searches of the various databases using the BLAST programmes revealed several sequences related to APAF1 (A). The non-redundant database contained AB007873 that has an additional 132bp (indicated). The genome survey sites database contained a BAC end sequence, B70127, which was homologous to APAF1 at the 3' end. The EST from a human foetal heart library was found to have a deletion of 1.5kB within the 3' UTR. The published APAF1 cDNA is shown with the various domains indicated. The sequences are shown approximately to scale, non-homologous sequences are shown in red. The AB007873 sequence (APAF1WD13) was found to encode an additional 44 amino acids that introduced an additional WD40 repeat to the protein (B). WD40 repeats are shaded in blue.

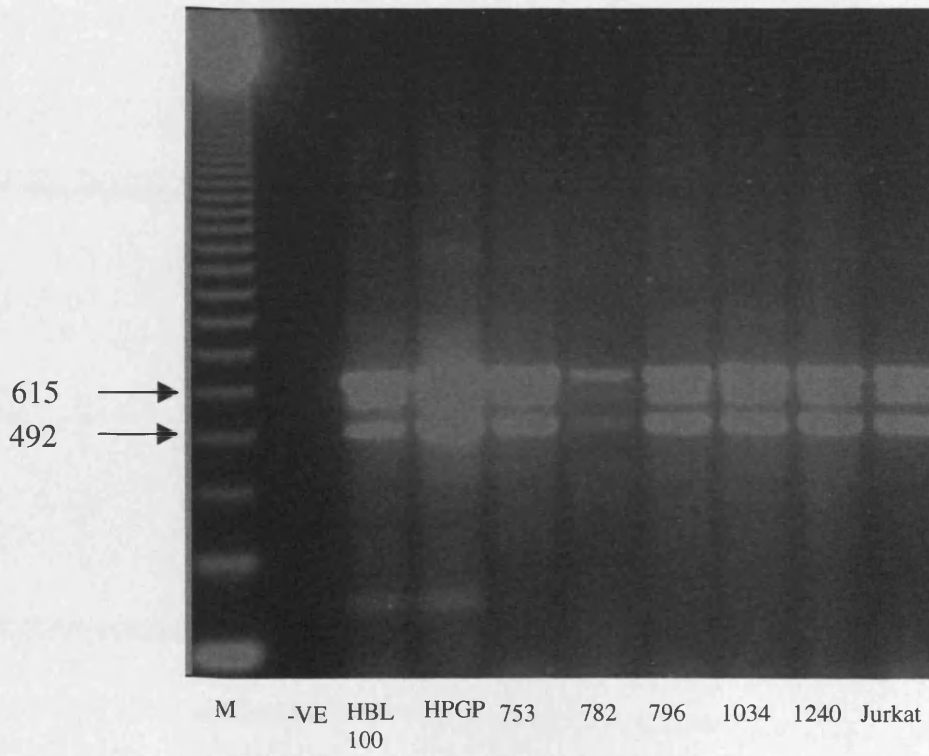
### 3.2.2 RT-PCR of APAF1

As the clone AB007873 was from a brain library, it was possible the different splice forms of APAF1 were cell type specific. To investigate this RT-PCR was used to analyse the expression of the two forms in a range of cell lines. The primers used covered the CARD (a.a. 1-82), CED4 region (a.a. 82-412) or WD40 repeats 3 to 6 (a.a. 675-839). The RT-PCR was initially performed on total RNA isolated from 293, Jurkat, U937, THP.1, HBL100, HEPG2 and HPGP (MCF7) and several breast tumour samples. The primers for the CARD and CED4 regions produced single products of ~240bp (CARD) or ~990bp (CED4) (Fig. 3.2 A) whereas the primers for the WD40 repeats 3 to 6 produced three products of ~490bp, ~555bp and ~620bp in all samples (Fig. 3.2 B). The upper and lower products corresponded to the size expected for the long (APAF1WD13) and short (APAF1) forms of APAF1 and this was confirmed by sequencing of the PCR products. The intermediate product was found to be identical to the other two forms but sequencing failed at the point at which the other two products diverged. From this, and the size of the product (exactly between the other two products), it was deduced that this product is a heterodimer of the other two PCR products (Fig. 3.2 C). To investigate the possibility that the presence of both forms is due to the transformed nature of the cell lines tested RT-PCR was performed on several freshly isolated rat tissues (brain, lung, liver, thymus, spleen, heart, kidney), human peripheral blood leukocytes, and several rat mammary tumour cell lines (NMU and DMBA). This revealed that both forms are present in all human samples tested whereas only APAF1WD13 is present in rat samples (Fig. 3.2 D).

**A**



**B**



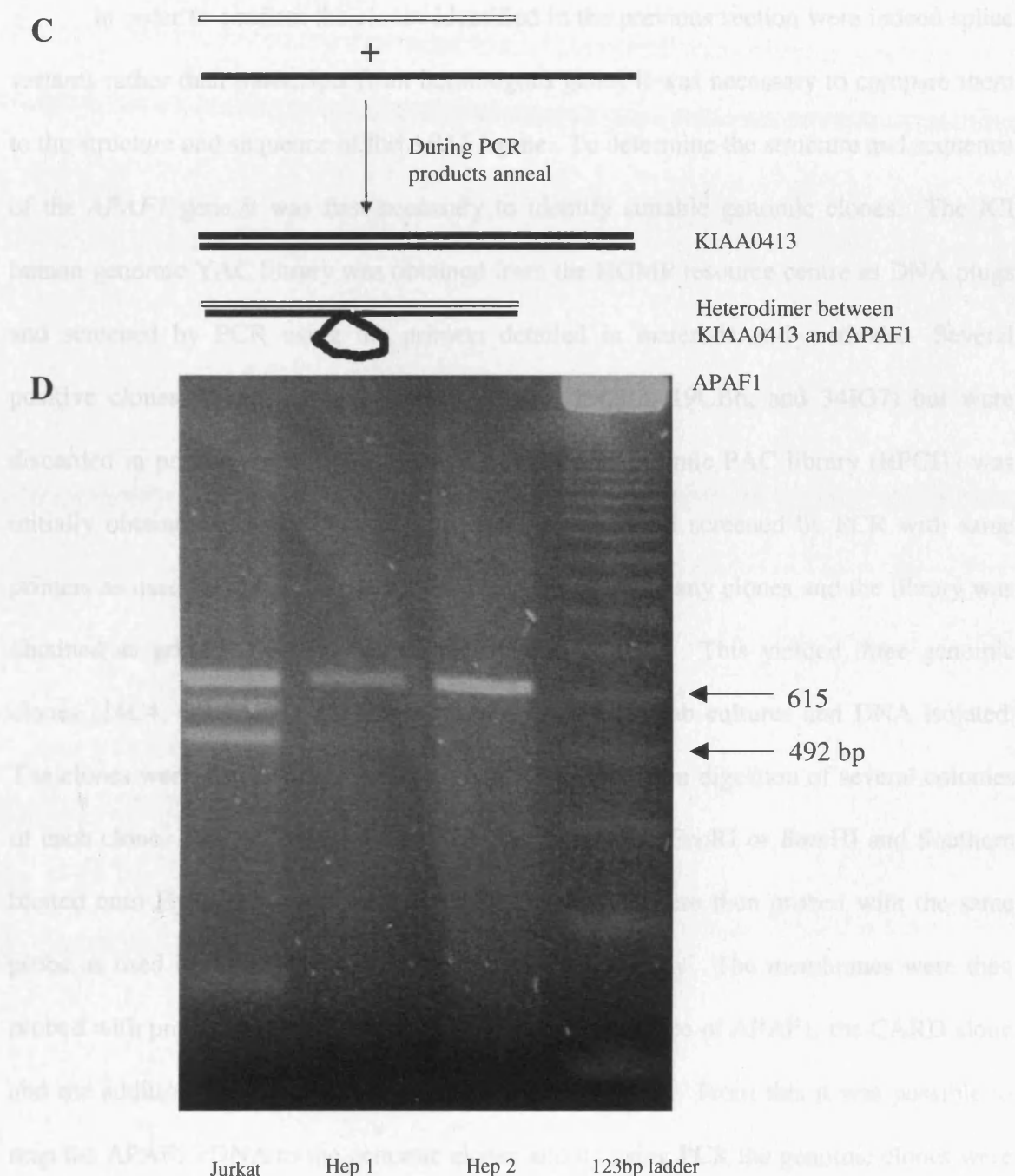
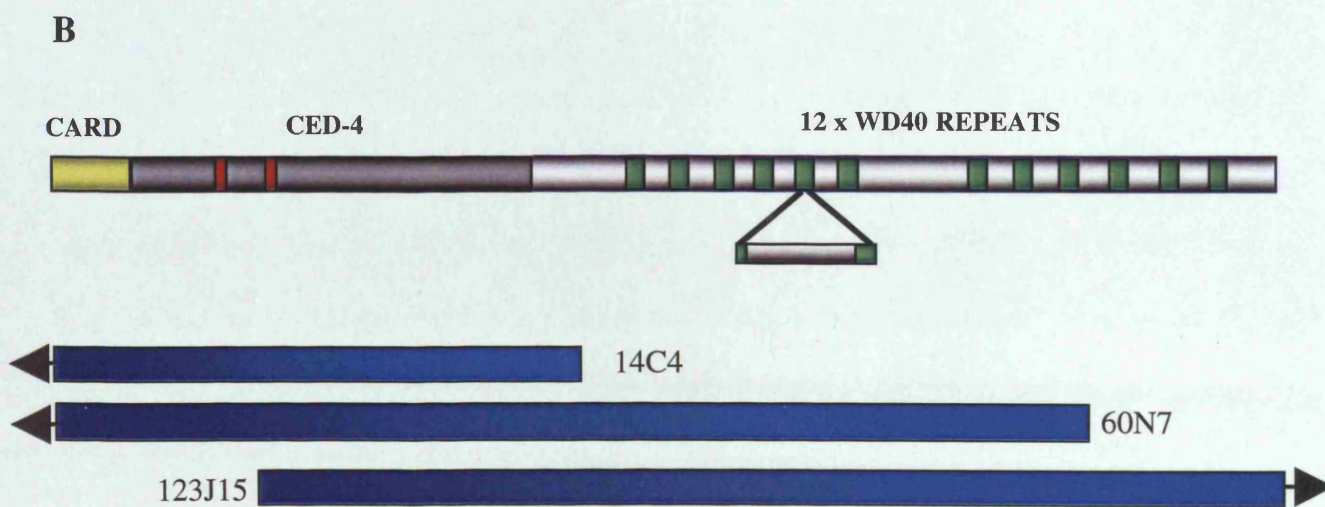
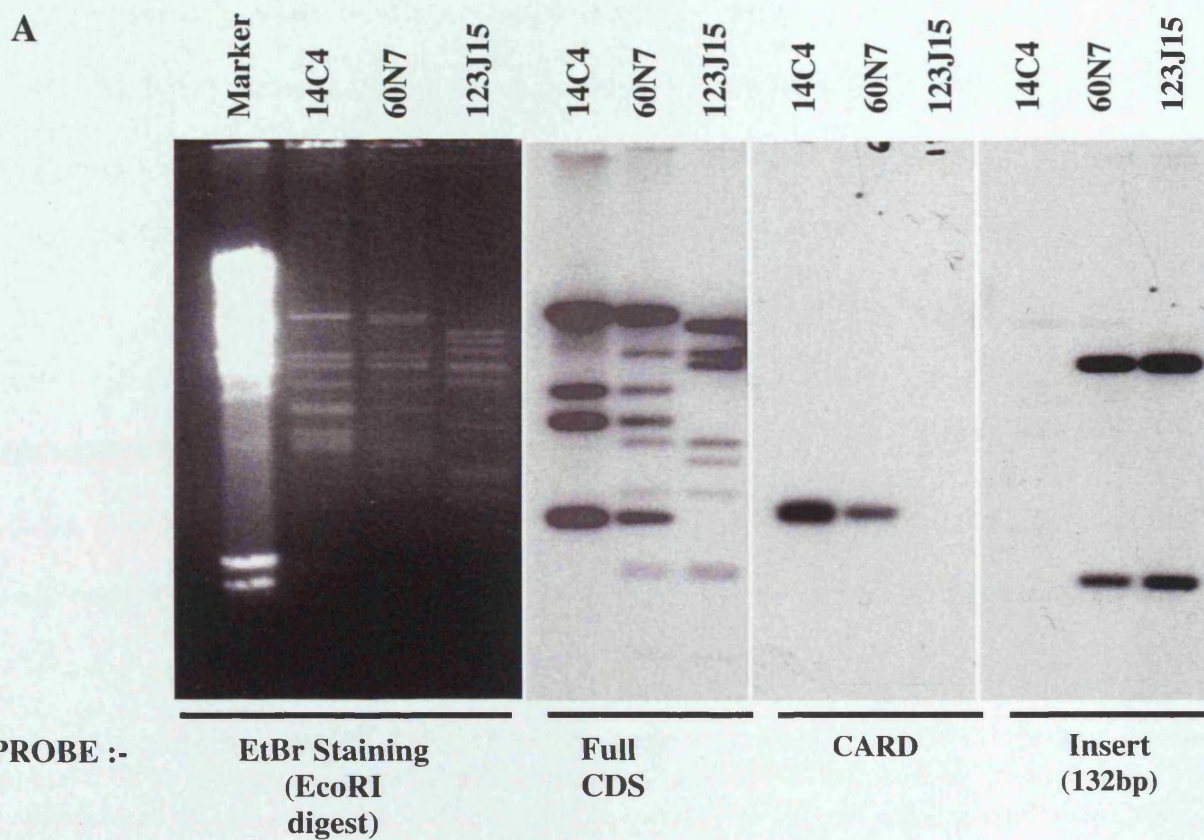


**Figure 3.2 RT-PCR of APAF1**

RT-PCR of the CARD and CED4 regions of APAF1 revealed no alternative splice forms in MCF-7 cells (A) (M= 100bp ladder) or any other cell line tested. However, the cells tested (HBL100, HPGP, Jurkat and the breast tumour samples 753, 782, 796, 1034, and 1240) were found to contain splicing differences in the WDR of APAF1 (B) (M= 123bp ladder). The RT-PCR of the WDR resulted in three products when visualised on an agarose gel with the intermediate product being a heterodimer of the other two products (C). To test if the presence of both splice forms of APAF1 was due to the transformed nature of the cells tested RT-PCR was performed on a range of primary rat tissues e.g. hepatocytes (D).

### 3.2.3 Identification of APAF1 genomic clones

In order to confirm the clones identified in the previous section were indeed splice variants rather than transcripts from homologous genes it was necessary to compare them to the structure and sequence of the *APAF1* gene. To determine the structure and sequence of the *APAF1* gene it was first necessary to identify suitable genomic clones. The ICI human genomic YAC library was obtained from the HGMP resource centre as DNA plugs and screened by PCR using the primers detailed in materials and methods. Several positive clones were identified (03HF6, 19IB3, 19CB3, 19CB6, and 34IG7) but were discarded in preference for PAC clones. The human genomic PAC library (RPC11) was initially obtained as glycerol stocks of bacterial pools and screened by PCR with same primers as used for the YAC library. This did not identify any clones and the library was obtained as gridded filters and screened by hybridisation. This yielded three genomic clones (14C4, 60N7 and 123J15) that were obtained as stab cultures and DNA isolated. The clones were tested for cross contamination by restriction digestion of several colonies of each clone. The clones were then digested with either *EcoRI* or *BamHI* and Southern blotted onto Hybond N membranes. These membranes were then probed with the same probe as used in the library screen to confirm their identity. The membranes were then probed with probes corresponding to the full coding sequence of APAF1, the CARD alone and the additional 132bp found in AB007873 (Fig. 3.3 A). From this it was possible to map the APAF1 cDNA to the genomic clones and by using PCR the genomic clones were found to cover approximately 6.1 Kb and covered the full coding region of the *APAF1* gene (Fig. 3.3 B). Database searches later revealed a fourth APAF1 clone from this library (373G19, Accession # AQ254952) but this was not used in this work.



## PCR results

TEMPLATE	PRIMERS	PRODUCT	
		Expected	Actual
14C4	CARD	279 bp	~300 bp
60N7	CARD	279 bp	~ 300 bp
123J15	CARD	279 bp	-
14C4	INSERT	n/a	-
60N7	INSERT	n/a	~6.1 kB
123J15	INSERT	n/a	~6.1 kB
14C4	WD40 (Genomic)	500 bp	-
60N7	WD40 (Genomic)	500 bp	500 bp
123J15	WD40 (Genomic)	500 bp	500 bp

**Figure 3.3 Identification and characterisation of APAF1 genomic clones**

In order to determine if the forms of APAF1 observed were true splice forms it was necessary to isolate a genomic clone of APAF1. Three PAC clones were identified as containing regions of the *APAF1* gene and Southern blotted to further characterise them. Blots of the three clones were probed with the full coding region of the APAF1 cDNA (full CDS) and then stripped and reprobed for the cDNA corresponding to the CARD and then the insert found in the WDR (A) (*Hin*DIII digest of Lambda DNA was used as a marker). These clones were then further characterised by PCR with primers for various regions and mapped to the cDNA (B). This also demonstrated that the *APAF1* gene is greater than 6.1 kB in size.

**3.2.4 Identification of splice sites in the APAF1 gene**

To confirm the APAF1 gene could give rise to the two splice forms proposed it was necessary to demonstrate the presence of a splice site at each end of the 132bp insert in the genomic DNA. As only the cDNA sequence was known, and the splice sites reside in the intron DNA, primers were designed to the proposed exon sequences and were used to sequence out from each end of the exons into the introns (Fig. 3.4 A) in both of the clones that contained the region of interest (60N7 and 123J15). The sequence of the exon / intron junctions was analysed using the “splice site prediction by neural network” and NetGene



### 3.2.5 Identification of multiple forms of the APAF1 protein

As translational regulation of APAF1 has been previously demonstrated (Coldwell *et al.*, 2000), the mRNA forms present may not reflect the forms present at the protein level. To address this concern whole cells were Western blotted using an anti-APAF1 antibody. This allowed both the level and form of APAF1 protein to be determined for the human Jurkat and THP•1 cell lines and the rat hepatoma cell line FAO (Fig. 3.5). To identify the correct bands on the western blot recombinant APAF1, APAF1WD13, and APAF1LWD13 (see later) were ran as markers. All cell lines tested were found to contain either APAF1WD13 or APAF1LWD13, which co-migrated under the conditions used, whereas only the human cell lines Jurkat and THP•1 contained APAF1, although at lower levels than APAF1WD13 (Fig. 3.5).

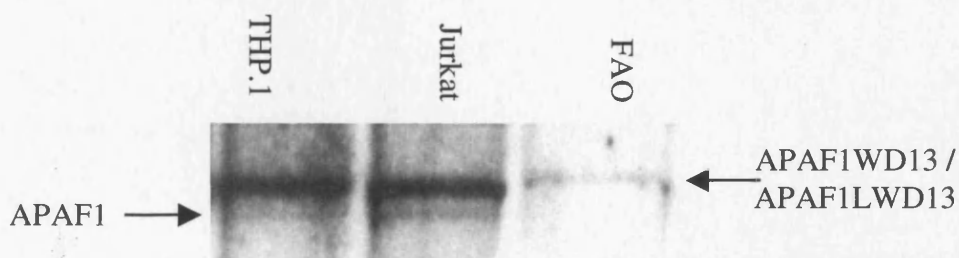


#### Figure 3.5 APAF1 exists as multiple forms at the protein level

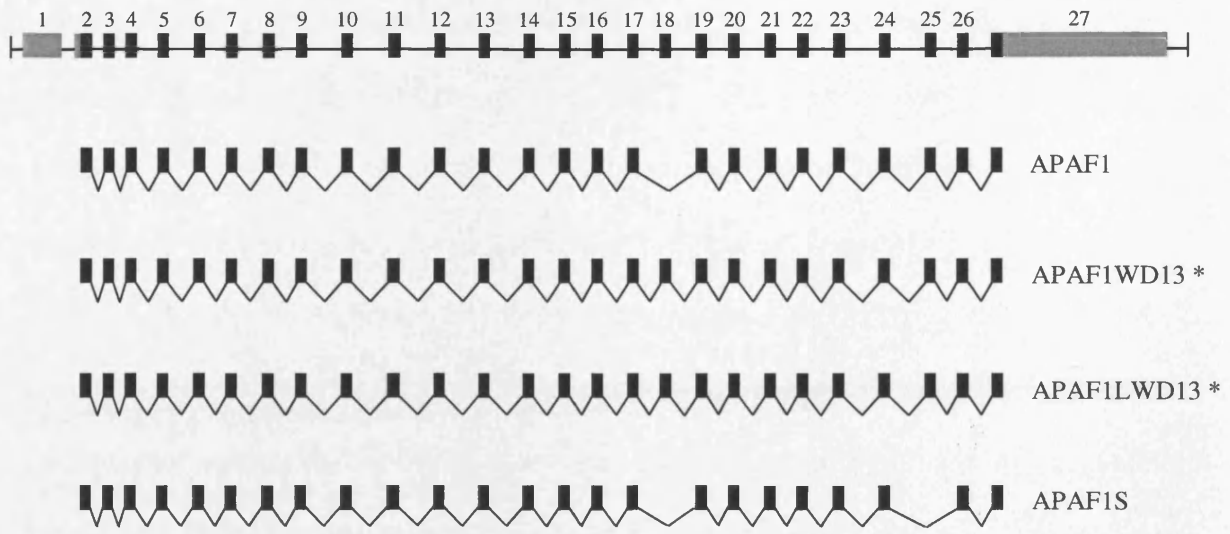
Whole cells were Western blotted and probed for APAF1. This revealed the presence of at least two forms of the protein in human cells (THP•1 and Jurkat) whereas only a single band was evident in the rat cells (FAO).

### 3.2.6 RT-PCR of additional APAF1 splice forms

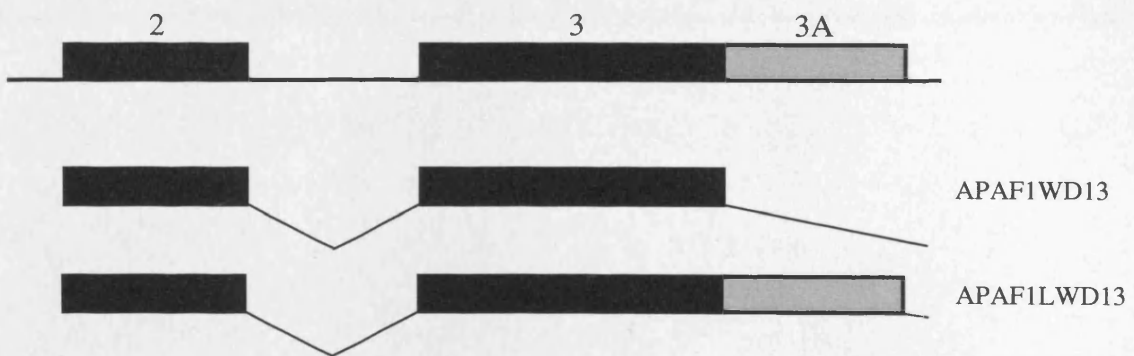
As stated previously during this study several groups reported the identification of several splice forms of APAF1, (Benedict *et al.*, 2000; Hahn *et al.*, 1999; Saleh *et al.*, 1999; Zou *et al.*, 1999). At the same time the intron / exon junction sequences of the *APAF1* gene were deposited in the GenBank database (see Appendix 1 for accession

numbers) and the structure of the gene has subsequently been reported (Bala *et al.*, 2000). The *APAF1* gene is composed of at least 27 exons and is localised at 12q23 (Bala *et al.*, 2000; Kim *et al.*, 1999) between the markers D12S1671 and D12S1082. The splice forms reported arise from the alternative splicing of exons 3, 18 and 25 (Fig. 3.6 A). The additional 33 bases between the CARD and the CED4 region arise from use of an alternative splice donor site in exon 3 (Fig. 3.6 B). In order to compare the published data with that already obtained the distribution of the splice forms of APAF1 was analysed by RT-PCR. Full length APAF1 was amplified from 293, Jurkat, THP•1 and FAO cells using long RT-PCR. The full-length cDNA was analysed by PCR for the presence or absence of exons 3, 18 and 25 (Fig. 3.6 C). All cell lines were found to contain APAF1LWD13, APAF1WD13 and APAF1S but only the human cell lines contained the APAF1 mRNA.

A



B



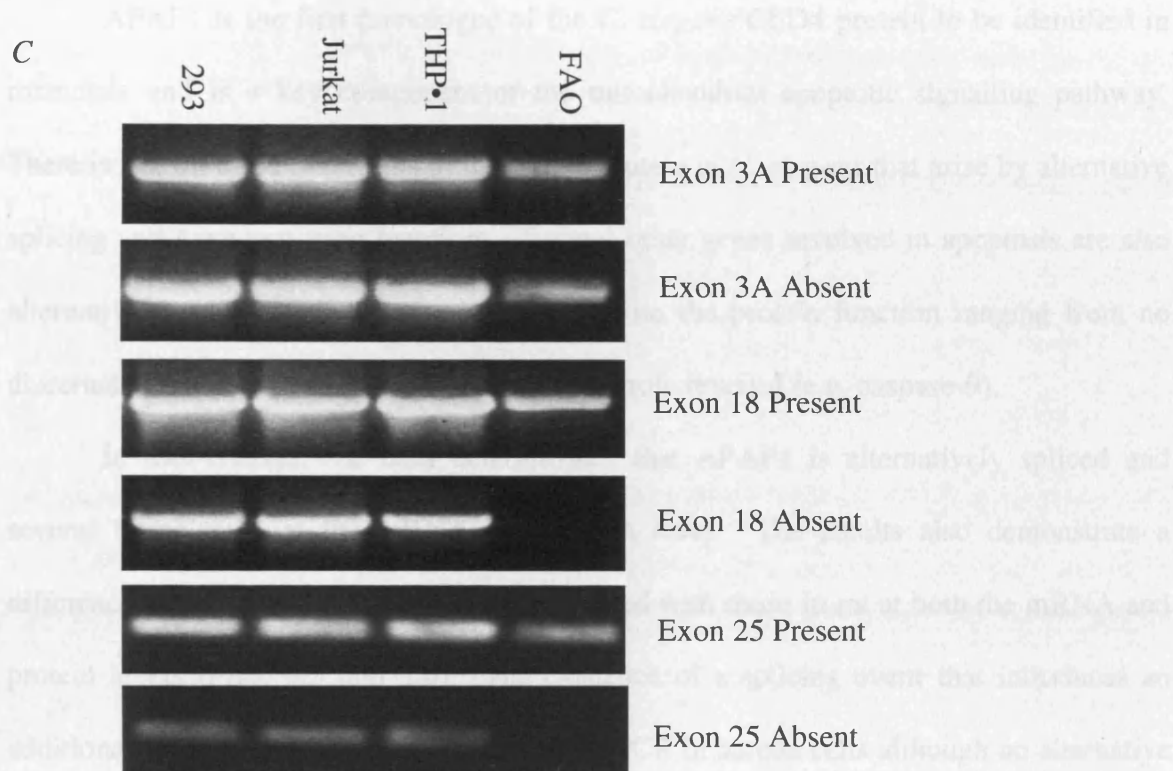


**Figure 3.6 Genomic organisation of APAF1 and RT-PCR analysis of splice forms**

The published genomic organisation of the *APAF1* gene showing the splicing events which give rise to the various published forms of APAF1 (A). APAF1WD13 and APAF1LWD13 differ only in 11 amino acids between the CARD and the CED4 that arises from the use of an alternative splice donor site in exon 3 (B). RT-PCR was used to analyse the distribution of these splice forms, full length APAF1 cDNA was produced and then used as a template in PCR reactions using primers specific for the presence or absence of the alternatively spliced exons (C). The primers used were designed to either anneal within the alternatively spliced exons (exon present) or to the 3' end of the upstream exon and the 5' end of the downstream exon (exon absent). Each primer pair utilized either the CED4 DS primer (exon 3A) or the WD40 DS primer (exons 18 and 25).

### 3.3 DISCUSSION

APAF1 is the first homologue of the *C. elegans* CED4 protein to be identified in mammals and is a key component of the mitochondrial apoptotic signalling pathway. There is known to be two forms of the CED4 protein in *C. elegans* that arise by alternative splicing and have opposing functions. Several other genes involved in apoptosis are also alternatively spliced and these varying effects on the protein function ranging from no discernable effect (e.g. caspase-8) to a complete role reversal (e.g. caspase-9).

In this chapter, the data demonstrates that APAF1 is alternatively spliced and several forms exist at the mRNA and protein level. The results also demonstrate a difference between the forms in human compared with those in rat at both the mRNA and protein levels (Figs. 3.5 and 3.6). The existence of a splicing event that introduces an additional WD40 repeat was confirmed by RT-PCR in human cells although no alternative forms of the CARD or the CED4 region were identified by this method (Fig. 3.2). Both forms of APAF1 were found in human cells and this was not due to the transformed nature of the cell lines whereas in rat only the AB007873 form was present (Fig. 3.2). In order to confirm that AB007873 is a true splice form of APAF1, rather than arising from a pseudogene, genomic clones of APAF1 have been isolated and characterised. The additional 132 bp found in AB007873 are flanked by splice donor and acceptor sites in the genomic clones indicating that the AB007873 form is formed by alternative splicing of the *APAF1* gene (Fig. 3.4).

As additional splice forms of APAF1 have been reported the existence of all known splice forms of APAF1 has been investigated by RT-PCR. This has revealed that all forms are present at the mRNA level in human cells, however alternative splicing of exons 18 and 25 does not occur in rat cells (Fig. 3.6). This difference in splicing of APAF1 mRNA suggests that exons 18 and 25 are essential for the correct function of APAF1 in rat. As

both of these exons encode segments of the WDR of APAF1, the alternative splicing may alter the binding of other proteins to APAF1 in the apoptosome. In order to investigate this the sequence of the rat *APAF1* gene must be elucidated and the presence of these regions as individual exons must be determined. As the longer forms of APAF1, APAF1WD13 and APAF1LWD13, were the major proteins present in human cells (Fig. 3.5) it follows that these have the greater role in the apoptotic pathway. Benedict *et al.* (2000) have reported that the presence of the additional WD40 repeat found in APAF1WD13 and APAF1LWD13 is responsible for the binding of cytochrome *c* and correct processing of caspase-9. The WDR has also been implicated in the regulation of APAF1 activity and has an inhibitory effect on the CARD and CED4 regions of the molecule (Adrain *et al.*, 1999; Hu *et al.*, 1998b). As the classical structure for WD-40 repeats is a  $\beta$ -propeller structure with multiple binding surfaces, alternative splicing which introduces an additional repeat (exon 18) or alters the spacing of the repeats (exon 25) may have significant effects on the structure and therefore the binding properties of the protein. The alternative splicing of these exons may effect the binding of the WDR to the CARD / CED4 region of the molecule, altering the efficiency of oligomerisation and caspase-9 activation or effect the binding of cytochrome *c* to this region. The evidence for the binding of cytochrome *c* to the WDR is, at present, indirect as deletion of the WDR results in a constitutively active protein with no requirement for cytochrome *c* and dATP (Srinivasula *et al.*, 1998). These results may however be misleading as the dATP binding site is formed by the Walkers A and B boxes in the CED4 region and although the site is still present the dATP requirement is lost. These and other results suggest the activity of APAF1 is dependent upon its conformation and a change in conformation upon binding of cytochrome *c* or hydrolysis of dATP / ATP results in the formation of the active apoptosome. The exact role of the

cytochrome *c* binding is still unclear but is probably transiently involved in stabilising the conformation of APAF1 during apoptosome formation.

It may be predicted that the differential cytochrome *c* binding efficiency of the various splice forms would be used in different cell types, with those with a low affinity for cytochrome *c* being found in cells with large numbers of mitochondria such as in muscle thereby preventing low levels of cytochrome *c* release from accidentally triggering the apoptotic pathway. This type of mechanism would prevent the cell from inadvertently undergoing apoptosis when mitochondria are repairable and only low levels of cytochrome *c* have been released but all forms are found in the cells tested which would negate this regulatory mechanism. A more likely explanation for the differential splicing resulting in different affinities for cytochrome *c* is that the cytochrome *c* binding site is modified to accept other molecules. This would allow the apoptosome to form in response to damage of other subcellular organelles such as the endoplasmic reticulum and the golgi.

The alternative splicing between the CARD and the CED4 regions (exon 3A) has an unclear function but as this splicing event has not been described in the absence of the alternative splicing of exon 18 it may simply act as a spacer region to allow the correct conformation of the CARD / CED4 and allow binding of the modified WDR.

**CHAPTER 4: ACTIVATION OF CASPASES BY dATP / CYTOCHROME C AND  
THE ROLE OF THE CED-4 REGION IN CASPASE-9 BINDING.**

## 4.1 INTRODUCTION

Release of cytochrome *c* from the mitochondria is thought to be a critical step in the induction of apoptosis resulting from stress or certain death receptors (Bratton *et al.*, 2000). The release of cytochrome *c* is regulated by the Bcl-2 family of proteins (Cosulich *et al.*, 1999) and, in some cell types, may involve the Permeability Transition Pore (PTP) which is thought to be responsible for the loss of mitochondrial membrane potential observed during apoptosis (Crompton, 1999). Once released cytochrome *c* binds to APAF1 in a 2:1 ratio and induces dATP binding to the Walkers A and B boxes of APAF1 (Jiang & Wang, 2000; Purring-Koch & McLendon, 2000; Zou *et al.*, 1997). ATP has been shown to be less effective than dATP in the activation of a cell lysate (Liu *et al.*, 1996) although which is utilised by APAF1 is still to be resolved. Interestingly it is the binding and not the hydrolysis of dATP that is responsible for apoptosome formation (Jiang & Wang, 2000) although hydrolysis of dATP may be required for the processing of the effector caspases (Li *et al.*, 1997). The presence of both cytochrome *c* and dATP then induces a conformation change in APAF1 resulting in its oligomerization (Li *et al.*, 1997; Srinivasula *et al.*, 1998). This conformation change in APAF1 removes the inhibitory action of the WDR on the CARD / CED4 region of the molecule and caspase-9 is then recruited to the complex via CARD / CARD interactions (Adrain *et al.*, 1999; Hu *et al.*, 1998b; Srinivasula *et al.*, 1998). As removal of the WDR results in constitutive activation of caspase-9 in the absence of cytochrome *c* and dATP the binding site of cytochrome *c* is proposed to be in the WDR (Purring-Koch & McLendon, 2000; Srinivasula *et al.*, 1998). The key event in the activation of caspases by APAF1 is the binding of caspase-9 to APAF1. The structure of the CARD domain of APAF1 has been modelled both alone and in complex with the CARD of caspase-9 and has been shown to assume a structure similar to that of the death effector domains

(Chou *et al.*, 1998; Day *et al.*, 1999; Qin *et al.*, 1999; Vaughn *et al.*, 1999; Zhou *et al.*, 1999b). The current model is that caspase-9 is recruited purely via a CARD / CARD interaction with APAF1 but the potential for additional interactions have not been investigated. In *C. elegans* CED-4 activates CED-3 by oligomerization in a manner similar to APAF1 (Jaroszewski *et al.*, 2000) but the interaction between CED-3 and CED-4 is not purely via N-terminal domains. CED-4 is also able to bind the protease domain of CED-3 through a region between the Walkers A and B boxes (Chaudhary *et al.*, 1998). As a homologous region exists in APAF1 similar interactions may take place.

Data presented in this chapter will demonstrate the optimisation of conditions for the activation of caspases by dATP and cytochrome *c* in a cellular lysate. The data will also demonstrate the role played by the CED-4 region of APAF1 in caspase-9 recruitment and that this region acts to enhance the binding of caspase-9.

## 4.2 RESULTS

### 4.2.1 Effect of protein concentration on dATP / cytochrome *c* activation

To confirm that cytochrome *c* and dATP were required to activate caspases in a cell lysate and to optimise the system for further studies a lysate was prepared from 293 cells. The protein concentration of the lysate was calculated using the Bradford method as described in Materials and Methods and then corrected to 10mg/ml with lysis buffer. To determine the optimal protein concentration for caspase activation as described previously (Liu *et al.*, 1996) the lysate was diluted to a range of concentrations with lysis buffer and activated by the addition of 0.25mg/ml cytochrome *c*, 2mM dATP and 2mM MgCl<sub>2</sub>. The lysate was activated for 1h at 37°C and then assayed for effector caspase activity using the substrate DEVD.AFC as described in Materials and Methods (Fig. 4.1). As expected a decrease in protein concentration resulted in a loss of activity with the lowest concentration of lysate that gave maximal activity being 5mg/ml.

### 4.2.2 Optimisation of dATP concentration for activation of 293 lysate

As earlier work by Dr. K. Cain had demonstrated that excess cytochrome *c* had no effect on the activation of the lysate whereas dATP concentrations could become inhibitory (personal communication) the dATP concentration used to activate the lysate was optimised. 293 cell lysate was prepared and adjusted to a concentration of 10mg/ml or 5mg/ml. The lysate was then activated for 1h at 37°C in the presence of 0.25mg/ml cytochrome *c*, and a range of concentrations of dATP and MgCl<sub>2</sub> (Fig. 4.2). The concentrations of dATP and MgCl<sub>2</sub> were maintained in a 1:1 ratio as MgCl<sub>2</sub> acts as a co-factor for the dATP. It was found that 0.2mM to 2mM dATP /MgCl<sub>2</sub> was optimal for the activation of both 10mg/ml and 5mg/ml lysates (Fig. 4.2 A.) whereas lower concentrations of dATP / MgCl<sub>2</sub> resulted in less activation.

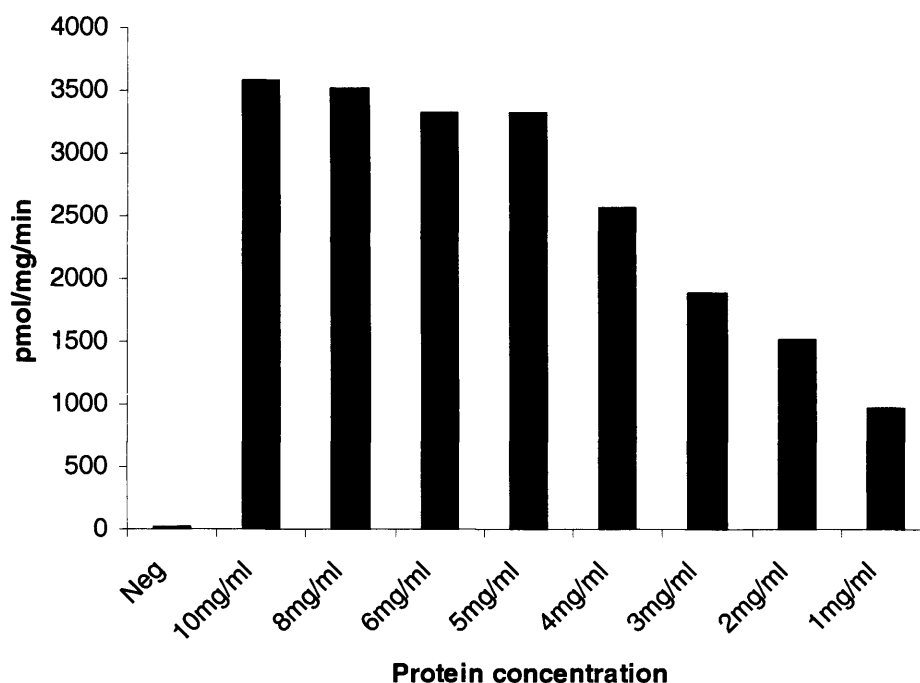


**Figure 4.1 The effect of protein concentration on cytochrome *c* / dATP activation**

Lysate was prepared from 293 cells and diluted to various protein concentrations with lysis buffer. The lysates were then incubated for 1h at 37°C in the presence of 0.25mg/ml cytochrome *c*, 2mM dATP and 2mM MgCl<sub>2</sub>. The effector caspase activity in the lysates was then assessed by fluorometric assay using the substrate DEVD.AFC (20µM) and activities calculated as pmol of released AFC per mg of protein in one minute (pmol/mg/min). The negative control (Neg) was incubated without added cytochrome *c*, dATP and MgCl<sub>2</sub>. Results are the mean of two experiments.

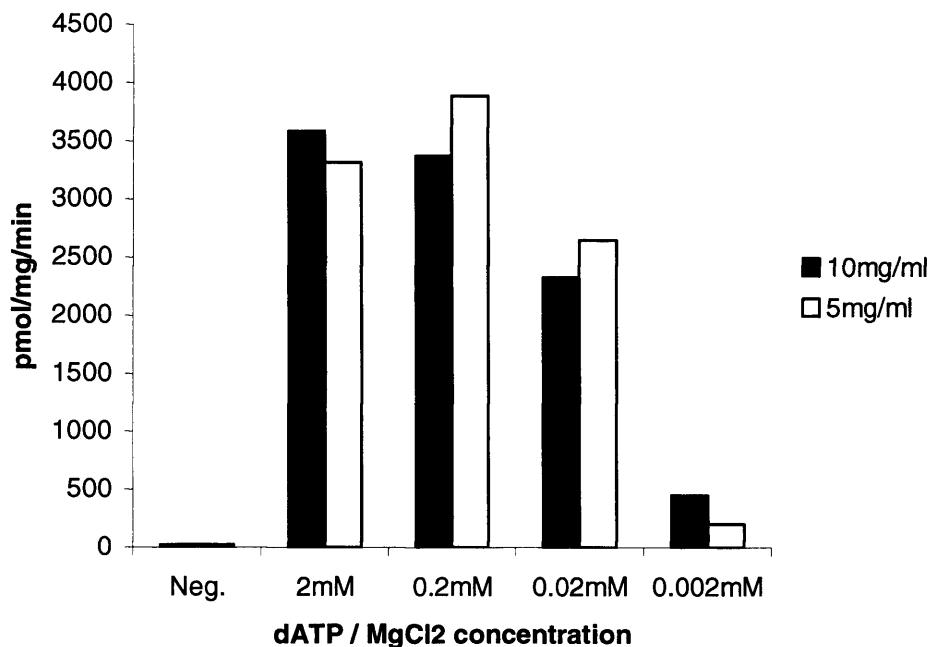


**Figure 4.2 Effect of dATP / MgCl<sub>2</sub> on lysate activation**

Lysate was prepared from 293 cells and corrected to a concentration of 10mg/ml or 5mg/ml. The lysates were then incubated with 0.25mg/ml cytochrome *c* and various concentrations of dATP / MgCl<sub>2</sub> for 1h at 37°C. The lysate was then assayed for DEVDase activity. The negative control was incubated without added cytochrome *c* / dATP / MgCl<sub>2</sub> and all values were the average of two independent experiments.

### 4.2.3 Cytochrome *c* /dATP activates caspase-3 and -7 in a lysate

In order to confirm that the cytochrome *c* /dATP activation was preferentially activating the effector caspases -3 and -7 the effect of activation on various other enzymatic activities was investigated. Lysate was prepared and activated as in the previous sections and then assayed for caspase-6 like activity with VEID.AFC, activity capable of activating caspase-3 (IETD.AFC) and proteasome activity (LLVY.AFC) along with caspase -3 / -7 activity (DEVD.AFC). These activities in control lysates incubated for 1h without any additions was then compared to the activities in lysates activated with cytochrome *c* /dATP for 1h and the fold-increase in activity calculated (Fig. 4.3). This demonstrated a ~140 fold increase in caspase -3 and -7 activity whereas the activity of the enzymes responsible for activating caspase-3 (IETDase) increased ~7 fold. The activity of caspase-6 increased ~8 fold after activation whereas the proteasome activity in the sample did not alter although these differences may reflect levels of protein in the lysate rather than the percentage of the enzymes which are activated.

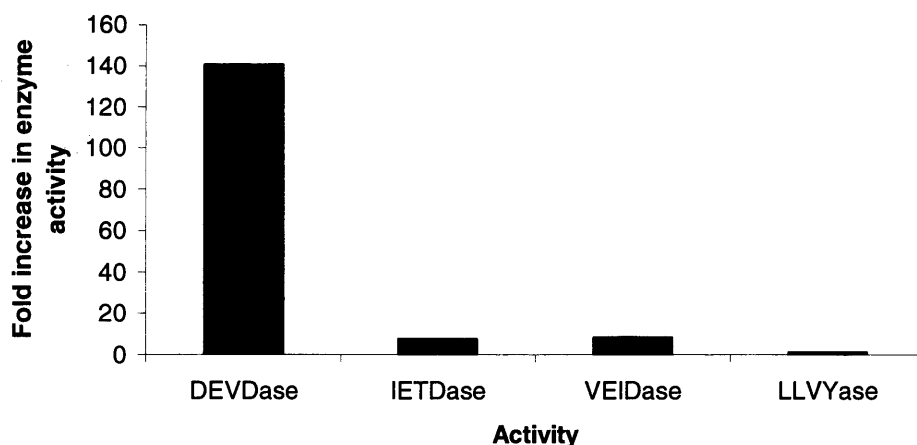


**Figure 4.3 Cytochrome *c* /dATP activation preferentially acts on caspases -3 and -7**

10mg /ml lysate prepared from 293 cells was activated with 0.25 mg/ml cytochrome *c* / 2mM dATP / 2mM MgCl<sub>2</sub> as described earlier and then various enzymatic activities measured and compared to levels found in non-activated lysate. Three classes of caspases were measured, caspases -3 and -7 (DEVDase), the caspases responsible for activating caspase-3 (IETDase), and the lamin cleaving caspase-6 (VEIDase). Proteasome activity was also measured (LLVYase). All substrates were at 20μM concentration in the assay.

#### 4.2.4 Caspase -3 and -7 activity is maximal within 15 min

293 cell lysates were activated for various times by incubation with cytochrome *c* / dATP and the activity of caspases -3 and -7 measured to determine the minimal incubation time required for maximal activation. Samples were assayed using the fluorogenic substrate DEVD.AFC at various times for up to 1 h incubation (Fig. 4.4). Maximal activity occurred within 15 min of activation and did not decrease at 1h.

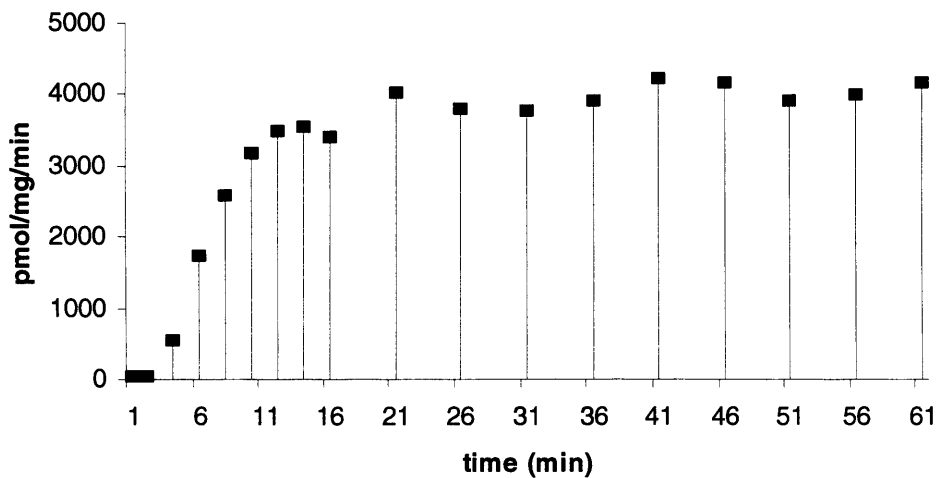


**Figure 4.4 Time dependent activation of a cell lysate**

A lysate was prepared from 293 cells and activated with cytochrome *c* / dATP. Samples were then removed at various time points and assayed for caspase -3 and -7 activity as described previously. All data is the mean of two independent experiments.

#### 4.2.5 Caspase -3 and -7 activity is associated with a large molecular weight complex

In order to confirm that the observed caspase activity was related to the apoptosome both activated and non-activated lysates were applied to a Sephacryl S-300 gel filtration column. The fractions collected were then assayed for caspase -3 and -7 activity using the fluorogenic substrate DEVD.AFC and activity calculated for each fraction (Fig. 4.5). This revealed that most of the caspase -3 and -7 activity eluted between fractions 3 and 6 (approximately 700 kDa) in the activated lysate with a broader peak of lower activity between fractions 9 and 13

(approximately 200 to 300 kDa). In some experiments a third peak of activity was evident in fractions 18 to 23 which was thought to correspond to the release of activated caspase -3 and -7 from the complex.

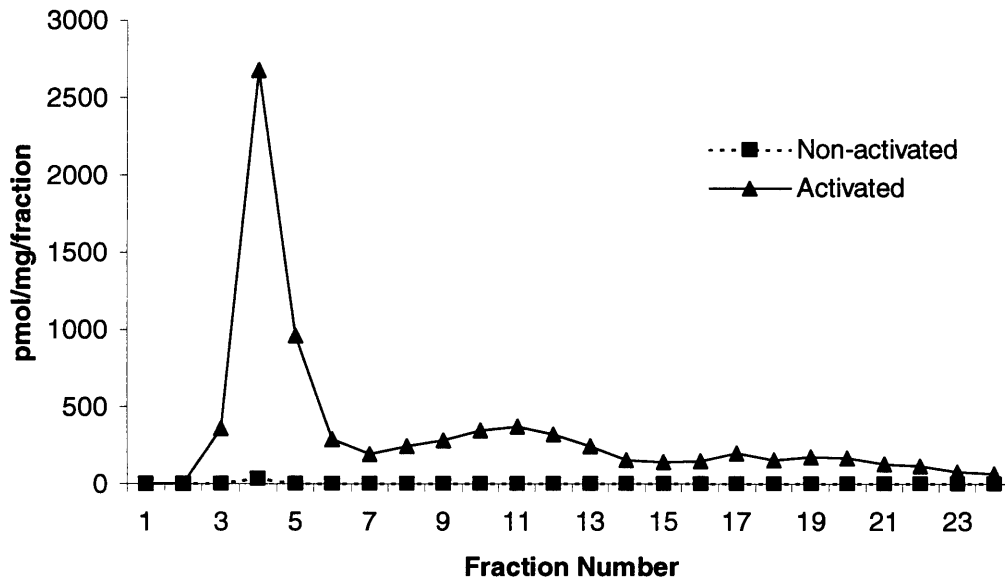


**Figure 4.5 Caspase-3 and -7 activity is attributable to a large molecular weight complex**  
 Non-activated and activated lysates were applied to a Sephacryl S300 gel filtration column and the resulting fractions assayed for caspase-3 and -7 activity. The majority of the activity was detected between fractions 3 and 6 indicating a molecular weight of ~700 kDa.

#### 4.2.6 APAF1 and caspases are associated with a large molecular weight complex

Activation of a cell lysate by dATP / cytochrome *c* resulted in a large molecular weight complex which possessed the majority of caspase-3 and -7 activity. To determine if this complex was the reported apoptosome composed of APAF1 and caspase-9 the fractions obtained from gel filtration of activated and non-activated lysates were Western blotted and probed for various apoptosome components (Fig. 4.6). APAF1, and caspases -9, -3 and -7 formed a large molecular weight complex of ~700 kDa (fractions 3 to 6) in activated lysate which corresponds to the fractions containing the peak of DEVDase activity (Fig. 4.5).

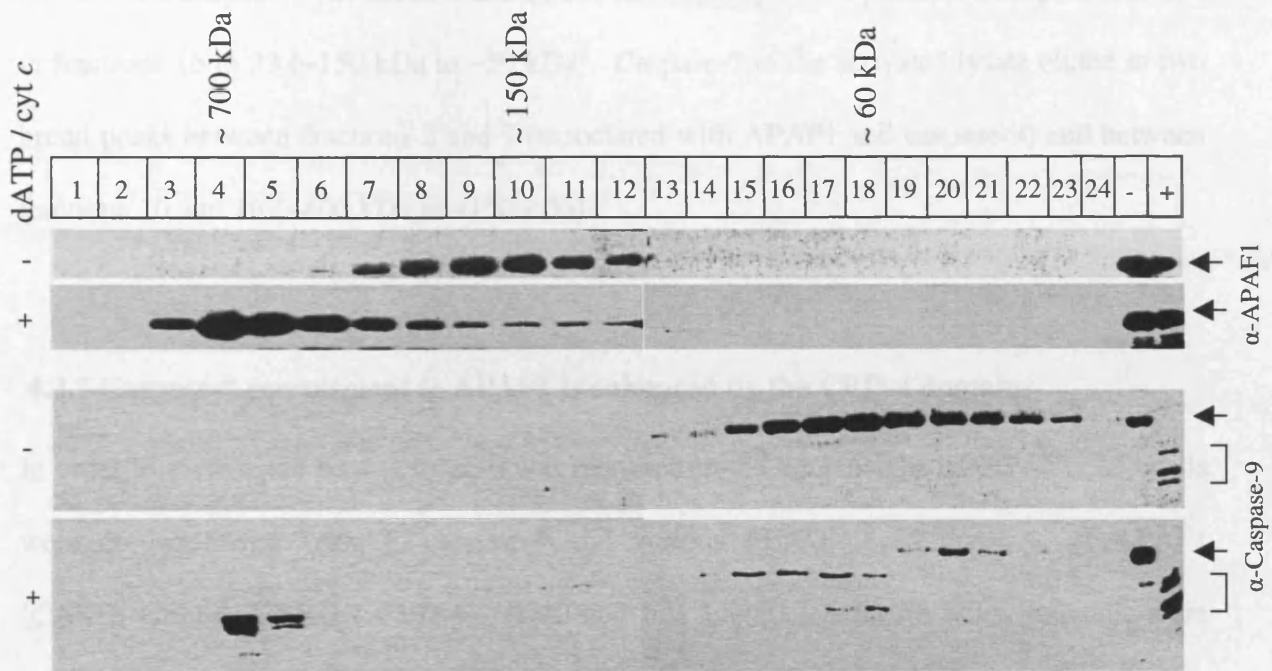


**Figure 4.6 APAF1 and caspase-9 associate in a large molecular weight complex**

Lysate prepared from 293 cells was incubated with (+) or without (-) dATP and cytochrome *c* prior to fractionation by gel filtration chromatography. The resulting fractions were then analyzed by Western blot for APAF1 and caspase-9. Pro-caspase-9 is indicated by arrows and processed subunits by brackets. Un-activated (-) and activated (+) lysate before fractionation was ran as a marker for processed caspase-9 on the blots. The positions of molecular weight standards on the Sephacryl S-300 column are also shown.

APAF1 was found in a broad peak of between ~200 and ~600 kDa (Fractions 6 to 12) in non-activated lysate, however in an activated lysate the majority of APAF1 eluted in fractions 3 to 6 indicating a molecular weight of ~700 kDa (see Cain *et al.*, 1999 for calibration of the column). Caspase-9 was predominantly in its zymogen form in the non-activated lysate eluting between fractions 14 and 23 indicating that it was not associated with APAF1 (fractions 6 to 12). Upon activation of the lysate caspase-9 was processed to its subunits that eluted in fractions 4 and 5 indicating that they were associated with APAF1 (fractions 3 to 6), some zymogen was still present as “free” caspase-9 in fractions 20 and 21. Caspases -3 and -7 demonstrated a similar distribution to that of caspase-9 in non-activated lysates however in activated lysates some processed caspase-3 was found in complex with

APAF1 and caspase-9 (fractions 4 and 5) but the majority of the processed caspase-3 eluted in fractions 16 to 23 (~150 kDa to ~50 kDa). Caspase-7 in the activated lysate eluted in two broad peaks between fractions 3 and 7 (associated with APAF1 and caspase-9) and between fractions 10 and 16 (~400 kDa to ~150 kDa).

#### **4.2.7 Caspase-9 recruitment to APAF1 is enhanced by the CED-4 domain**

In order to investigate how caspase-9 was recruited to the apoptosome by APAF1, 293 cells were co-transfected with T7-caspase-9 and various FLAG-tagged domains of APAF1 (CARD, CED-4, CARD / CED-4, WD40 and full length). After 48 hours the cells were harvested and lysates prepared. Samples of the lysates were analysed to confirm equal expression levels of the constructs and then the domains of APAF1 were immunoprecipitated from the lysate using an anti-FLAG M5 antibody. The immunoprecipitated complexes were then Western blotted and probed with anti-T7 HRP to detect the presence of epitope tagged caspase-9 (Figure 4.7). The presence of the CED-4 region of APAF1 resulted in the highest binding of T7-caspase-9 (lanes 4 and 6) although interaction was observed between all of the domains of APAF1 and caspase-9. The overexpression of the WD40 region resulted in the removal of the prodomain of caspase-9 (Figure 4.7 marked \*) and overexposure of the blot revealed that this also occurred upon overexpression of full length APAF1.

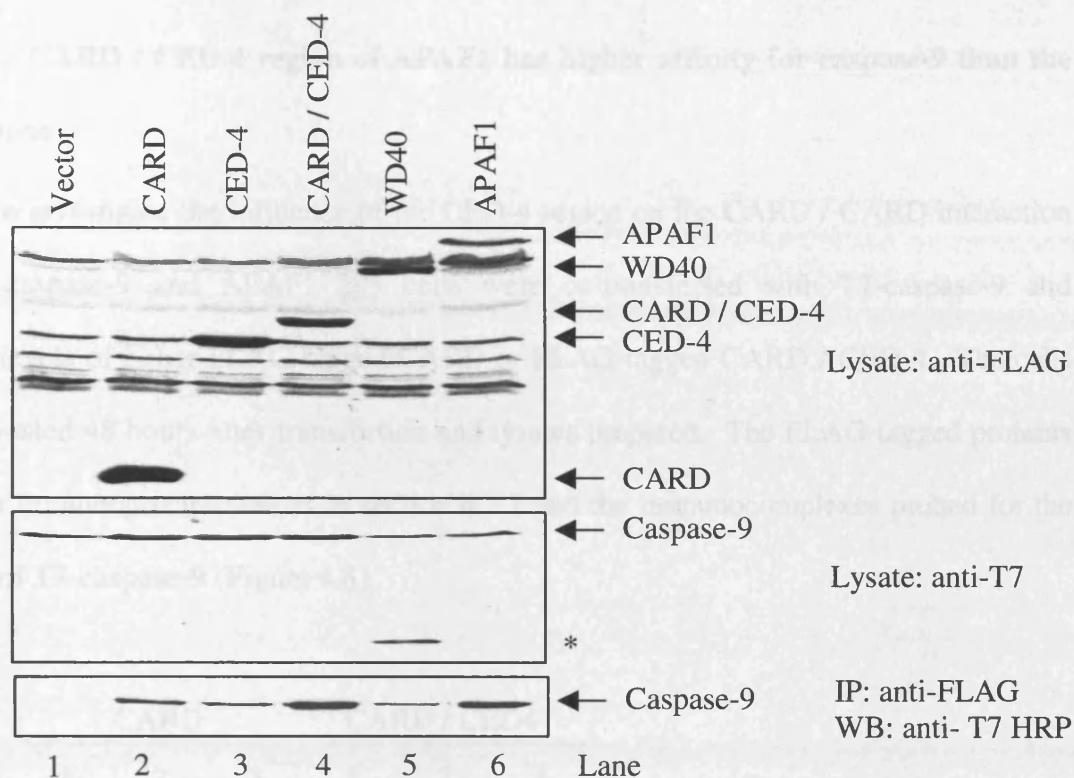


#### Figure 4.7 The CED-4 region of APAF1 enhances caspase-9 binding

293 cells were transiently co-transfected with the constructs for FLAG-tagged domains of APAF1 and T7-tagged caspase-9 and a lysate prepared after 48 hours expression. The domains of APAF1 were then immunoprecipitated from the lysate using anti-FLAG M5 antibody and the immunoprecipitates were probed with anti-T7 HRP conjugate. T7 caspase-9 was found to co-immunoprecipitate with all of the domains of APAF1 but strongest with those containing both the CARD and CED4 regions (lanes 4 and 6). The overexpression of the WD40 domain resulted in some processing of caspase-9 in the lysate (\*).

binding of T7-caspase-9 (lanes 4 and 6) although interaction was observed between all of the domains of APAF1 and caspase-9. The overexpression of the WD40 region resulted in the removal of the prodomain of caspase-9 (Figure 4.7 marked \*) and overexposure of the blot revealed that this also occurred upon overexpression of full length APAF1.

### 4.2.8 The CARD / CED-4 region of APAF1 has higher affinity for caspase-9 than the CARD alone

In order to investigate the influence of the CED-4 region on the CARD / CARD interaction between caspase-9 and APAF1 293 cells were co-transfected with T7-caspase-9 and different levels of either FLAG-tagged CARD or FLAG-tagged CARD / CED-4. The cells were harvested 48 hours after transfection and lysates prepared. The FLAG-tagged proteins were then immunoprecipitated as in section 4.2.7 and the immunocomplexes probed for the presence of T7-caspase-9 (Figure 4.8).

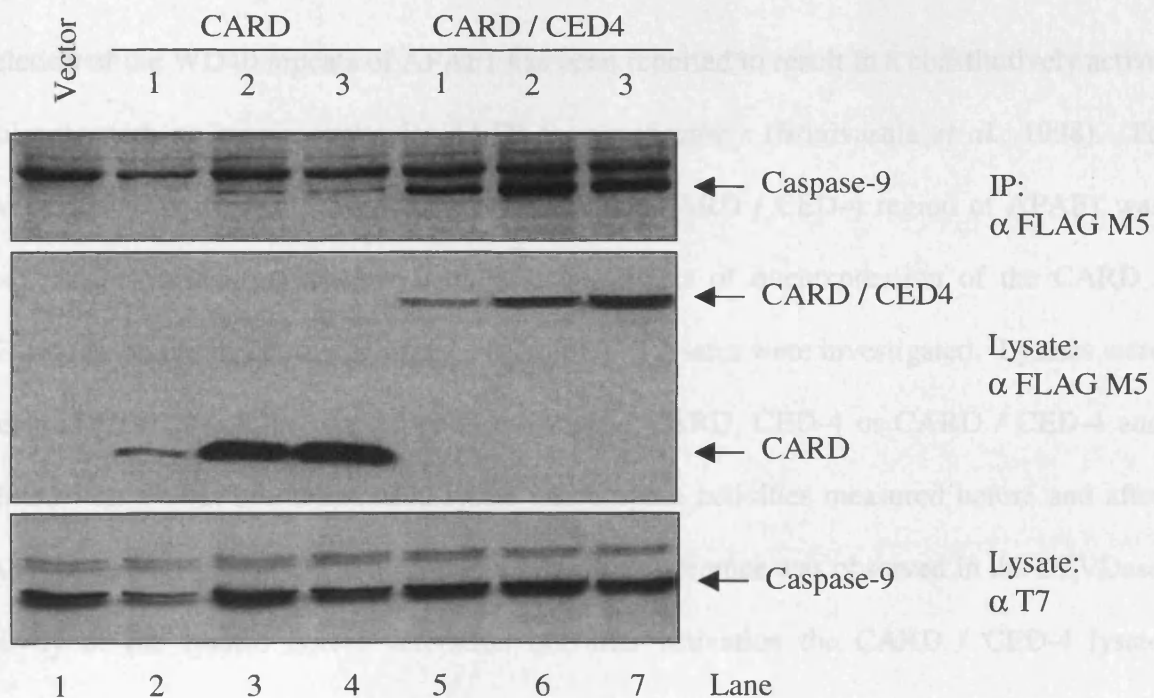


**Figure 4.8 The CARD / CED-4 region of APAF1 has higher affinity for caspase-9 than the CARD alone**

293 cells were transiently co-transfected with the constructs for FLAG-tagged CARD or CARD / CED4 domains of APAF1 and T7-tagged caspase-9 and a lysate prepared after 48 hours expression. The domains of APAF1 were then immunoprecipitated from the lysate using the anti-FLAG M5 antibody and the immunoprecipitates were probed with anti-T7 HRP conjugate. T7 caspase-9 was found to co-immunoprecipitate far more efficiently with the CARD / CED4 region than the CARD domain alone (compare lanes 2 and 5).

This revealed that the CARD / CED-4 region had a higher affinity for caspase-9 than the CARD alone as when the two regions were expressed to the same level far more caspase-9 was detected associated with the CARD / CED-4 region than with the CARD (Figure 4.8 compare lanes 2 and 5). This demonstrated that the CED-4 region either had a direct interaction with caspase-9 or it enhanced the CARD / CARD interaction between APAF1 and caspase-9.

#### **4.2.9 Overexpression of the CARD / CED-4 is inhibitory to dATP / cytochrome *c* activation**

Deletion of the WD40 repeats of APAF1 has been reported to result in a constitutively active molecule with no requirements for dATP or cytochrome *c* (Srinivasula *et al.*, 1998). To investigate if the high affinity for caspase-9 of the CARD / CED-4 region of APAF1 was associated with this constitutive activation the effects of overexpression of the CARD / CED-4 region on dATP / cytochrome *c* activation of lysates were investigated. Lysates were prepared from 293 cells expressing FLAG-tagged CARD, CED-4 or CARD / CED-4 and diluted 1 in 4 with non-transfected lysate and caspase activities measured before and after dATP / cytochrome *c* activation (Figure 4.9A). No difference was observed in the DEVDase activity of the lysates before activation but after activation the CARD / CED-4 lysate exhibited lower levels of activity. At extended times the levels of activity in all lysates were equal (Figure 4.9B).

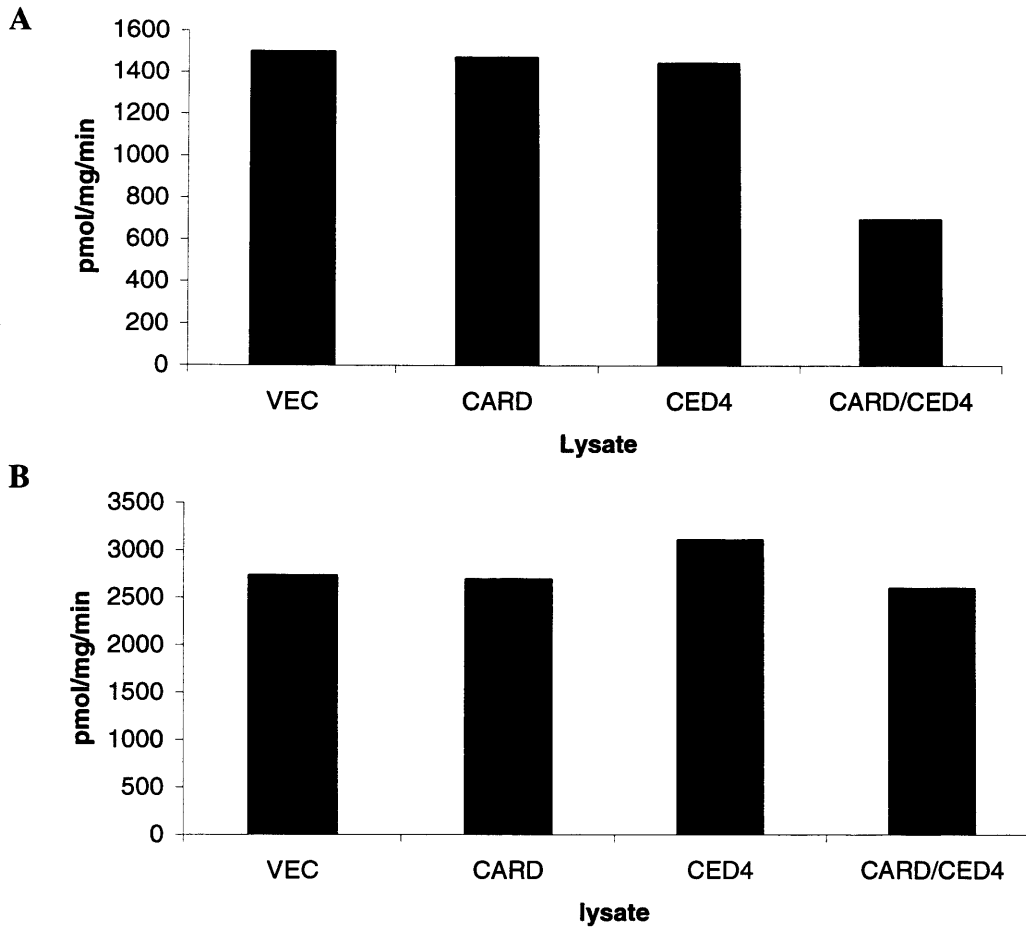


**Figure 4.9 Overexpression of the CARD / CED-4 region inhibits dATP / cytochrome *c* activation**

Lysates were prepared from 293 cells transiently transfected with CARD, CED4 or CARD / CED4 and then diluted 1 in 4 with non-transfected 293 cell lysates. The mixed lysates were then activated with dATP and cytochrome *c* and the activity towards DEVD.AFC was then measured after 10 minutes (A) and 30 minutes (B). The expression of the CARD / CED4 domain resulted in an approximately 50% reduction in activity at 10 minutes but the activities were approximately equal at 30 minutes. Equal expression of the various domains was confirmed by western blotting. Results are the mean of two independent experiments with triplicate samples.

#### 4.2.10 Overexpression of the CARD / CED-4 region inhibits MG132 induced apoptosis

To determine if the inhibitory effect of the CARD / CED-4 was physiologically relevant 293 cells were co-transfected with pRSC *lacZ* (¼ of the total DNA) and FLAG-tagged CARD or

CARD / CED-4 and after 48 hours induced to undergo apoptosis. After 30, 60 and 120 minutes treatment with 1 $\mu$ M MG132, a proteasomal inhibitor, the cells were fixed and stained. The extent of apoptosis was then assessed by morphology and expressed as a percentage of blue (transfected) cells. The CARD transfected cells underwent apoptosis in a time dependent manner in a similar manner to empty vector transfected cells (Figure 4.10) whereas the CARD / CED-4 transfected cells showed lower levels of apoptosis at both 30 and 60 minutes but at 120 minutes had similar levels to those seen in CARD and empty vector transfected cells.

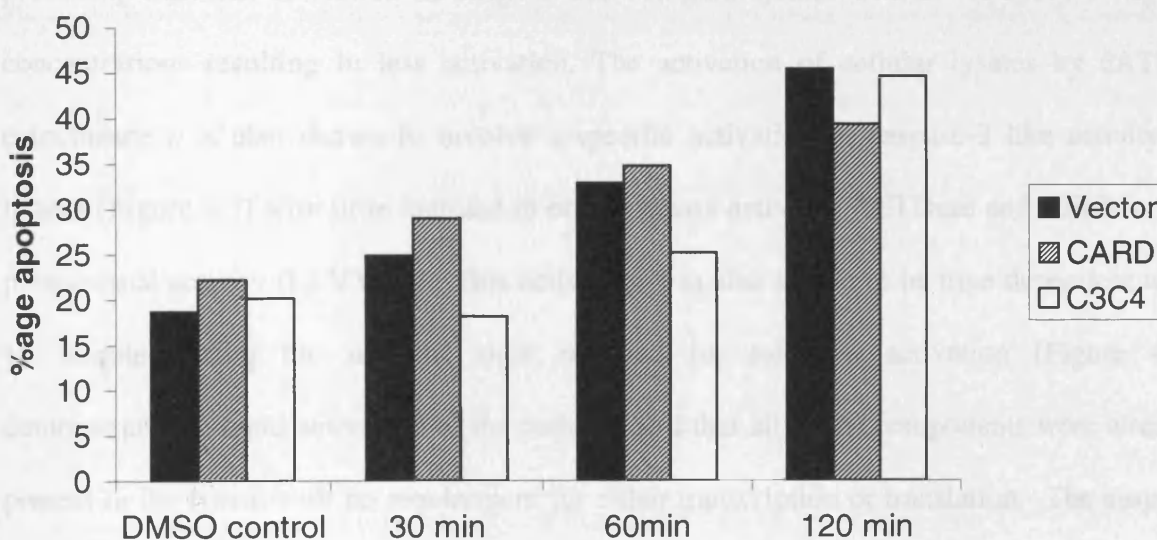


**Figure 4.10 Overexpression of the CARD / CED4 region delays MG132 induced apoptosis in 293 cells**

293 cells were transfected with pRSC *lacZ* and either empty vector, pFLAG-CARD or pFLAG-CARD / CED-4. After 48 hours the cells were treated with 1 $\mu$ M MG132 and then fixed and stained at various times. Apoptosis was determined by morphology and expressed as a percentage of blue cells. Results are the mean of two independent experiments performed in triplicate.

### **4.3 DISCUSSION**

The data presented in this chapter demonstrates the role of the CED-4 region in caspase-9 recruitment and the optimisation of activation of cellular lysates by dATP and cytochrome *c*. This data demonstrates that 293 cell lysates must be at a minimum of 5mg/ml for maximal activation (Figure 4.1) and activation is dependent upon protein concentration. This confirms the requirement for protein / protein interactions in the initiation of caspase activation with the components being too dilute at low protein concentrations to associate and activate caspases. The data also demonstrates that protein concentration alters the dATP / MgCl<sub>2</sub> requirement for activation (Figure 4.2) with 0.2mM to 2mM dATP / MgCl<sub>2</sub> producing maximal activation in 5mg/ml and 10mg/ml lysates with lower dATP / MgCl<sub>2</sub> concentrations resulting in less activation. The activation of cellular lysates by dATP / cytochrome *c* is also shown to involve a specific activation of caspase-3 like activity in lysates (Figure 4.3) with little increase in other caspase activities (IETDase and VEIDase) or proteasomal activity (LLVYase). This activation was also shown to be time dependent with 15 minutes being the minimal time required for maximal activation (Figure 4.4) demonstrating a rapid activation of the pathway and that all of the components were already present in the lysate with no requirement for either transcription or translation. The caspase activity was found to be associated with a large (~700 kDa) molecular weight complex as has been previously been reported for the apoptosome (Figures 4.5 and 4.6). An interesting point is that the vast majority of the caspase-3 like activity detected is associated with this large molecular weight complex although at most 50% of the caspases -3 and -7 are seen to be associated with this complex (see chapter 5). This would indicate that caspases -3 and -7 demonstrate maximal activity whilst associated with the apoptosome. In order to investigate the recruitment of the initiator caspase, caspase-9 to APAF1 co-immunoprecipitation of epitope tagged proteins was investigated. Caspase-9 was found to associate with all of the

domains of APAF1 but had a greater affinity for those which contained the CARD / CED-4 region (Figure 4.7). The association of caspase-9 with the WD40 region may be due to oligomerization with endogenous APAF1 as the construct also contains the APAF1 unique region (amino acids 413 – 530) which has previously been reported to be required for oligomerization (Srinivasula *et al.*, 1998) also the prodomain of caspase-9 is removed in this situation and this usually requires cleavage at an aspartic acid residue by a caspase. Further experiments in the presence of the pan-caspase inhibitor z-VAD.FMK would determine if the cleavage is caspase dependent. Caspase-9 was also shown to associate with the CED-4 domain of APAF1 supporting the hypothesis that APAF1 can also associate with caspase-9 via interactions between the protease domain of caspase-9 and the CED-4 region of APAF1 as has been demonstrated for CED-4 and CED-3 in *C. elegans* (Chaudhary *et al.*, 1998). Further experiments using various levels of CARD and CARD / CED-4 expressed in cells demonstrated that the CARD / CED-4 region had a far higher affinity for caspase-9 than the CARD alone (Figure 4.8). As the CARD / CED-4 construct did not possess the region required for oligomerization (Srinivasula *et al.*, 1998) this enhanced binding of caspase-9 is not due to oligomerization with endogenous APAF1. The effect of the CARD / CED4 region on dATP / cytochrome *c* was investigated as the removal of the WD40 region may have resulted in a constitutively active protein (Adrain *et al.*, 1999; Hu *et al.*, 1998b; Srinivasula *et al.*, 1998). The overexpression of the CARD / CED-4 was found to be inhibitory (Figure 4.9) demonstrating that although the protein is able to bind caspase-9 a region between amino acids 412 and 530 is required for the formation of a constitutively active form of APAF1. The inhibitory effect of the CARD / CED-4 was found to be only temporary with activity being equivalent to that in non-transfected lysate at later times due to the ability of caspases to activate other caspases allowing amplification of the apoptotic signal. The CARD / CED-4 region was also found to delay apoptosis induced by the

proteasome inhibitor MG132 (Figure 4.10) demonstrating that this region is able to out-compete the endogenous apoptosome for caspase-9 during apoptosis. By investigating this role of the CED-4 region of APAF1 on caspase-9 binding further it may be possible to improve our understanding of apoptosome formation and structure. This data also demonstrates that molecules designed to mimic or disrupt the interaction between the CARD / CED-4 region and caspase-9 may be of greater therapeutic value than those which mimicked or disrupted only the CARD / CARD interaction.

**CHAPTER 5: APAF1 ACTIVATES CASPASES VIA THE FORMATION OF AN  
APOPTOSOME AND IS ITSELF A SUBSTRATE FOR CASPASES.**

## 5.1 INTRODUCTION

APAF1 is a 135 kDa protein and, as demonstrated in the previous chapter exists as multiple splice forms at both the mRNA and protein levels in the cell. The N-terminal 80 amino acids of APAF1 represent the CARD (Caspase Activation and Recruitment Domain), which is responsible for the recruitment of caspase-9 to the apoptosome. The apoptosome itself is a complex of ~700 kDa which forms in response to a range of apoptotic stimuli (Cain *et al.*, 1999) although the complex can incorrectly form in which case the inactive complex is approximately twice the size at ~1.4 MDa (Cain *et al.*, 2000). The ~1.4 MDa complex is often seen whilst utilizing a recombinant system and several novel proteins have been reported to be associated with this larger complex (Chu *et al.*, 2001; Hlaing *et al.*, 2001).

In this chapter the formation of a large molecular weight complex by APAF1 will be investigated. Data demonstrating that APAF1 is cleaved by caspase-3 during apoptosis will be presented along with data to show that the ~1.4 MDa complex has the resulting p30 fragment of APAF1 associated with it. The formation and characterization of an apoptosome by over-expressed epitope tagged proteins will also be described.

## 5.2 RESULTS

### 5.2.1 Effect of induction of apoptosis on FLAG-tagged APAF1

Several proteins involved in apoptosis are activated, or in the case of anti-apoptotic proteins, inactivated during apoptosis. Both pro- and anti-apoptotic members of the Bcl-2 family are regulated in this way such as activation of pro-apoptotic BID (Luo *et al.*, 1998) and inactivation of anti-apoptotic Bcl-X<sub>L</sub> (Basañez *et al.*, 2001; Clem *et al.*, 1998) by caspase cleavage. Other proteins such as IAP family members are regulated by proteolytic processing (Clem *et al.*, 2001; Deveraux *et al.*, 1999a; Johnson *et al.*, 2000) as are the caspases themselves (Cohen, 1997). It was hypothesized that APAF1 may be regulated in a similar manner during induction of the apoptotic program. To investigate this 293 cells were transfected with FLAG-tagged APAF1 and apoptosis was induced by addition of the apoptosis-inducing ligand TRAIL to the culture media 48 h after transfection in the presence or absence of the pan caspase inhibitor z-VAD.FMK (20µM). Cells were then harvested 14 h later and analyzed by Western blot with an anti-FLAG monoclonal antibody (Figure 5.1A) which revealed a z-VAD.FMK inhibitable loss of full length APAF1 (arrow). To confirm that the observed loss of full length APAF1 was due to a specific cleavage rather than non-specific degradation via the proteasome samples were taken at various time points and analyzed by Western blot which revealed specific cleavage products of ~85 kDa and ~30 kDa (Figure 5.1B, lower two arrows, lanes 6 to 11). The immuno-reactive bands were not visible in empty vector transfected cells (lanes 1 and 2) and their formation was partially inhibited by pre-treatment with z-VAD.FMK (lane 8) indicating that these bands arise from FLAG-APAF1 following caspase activation.

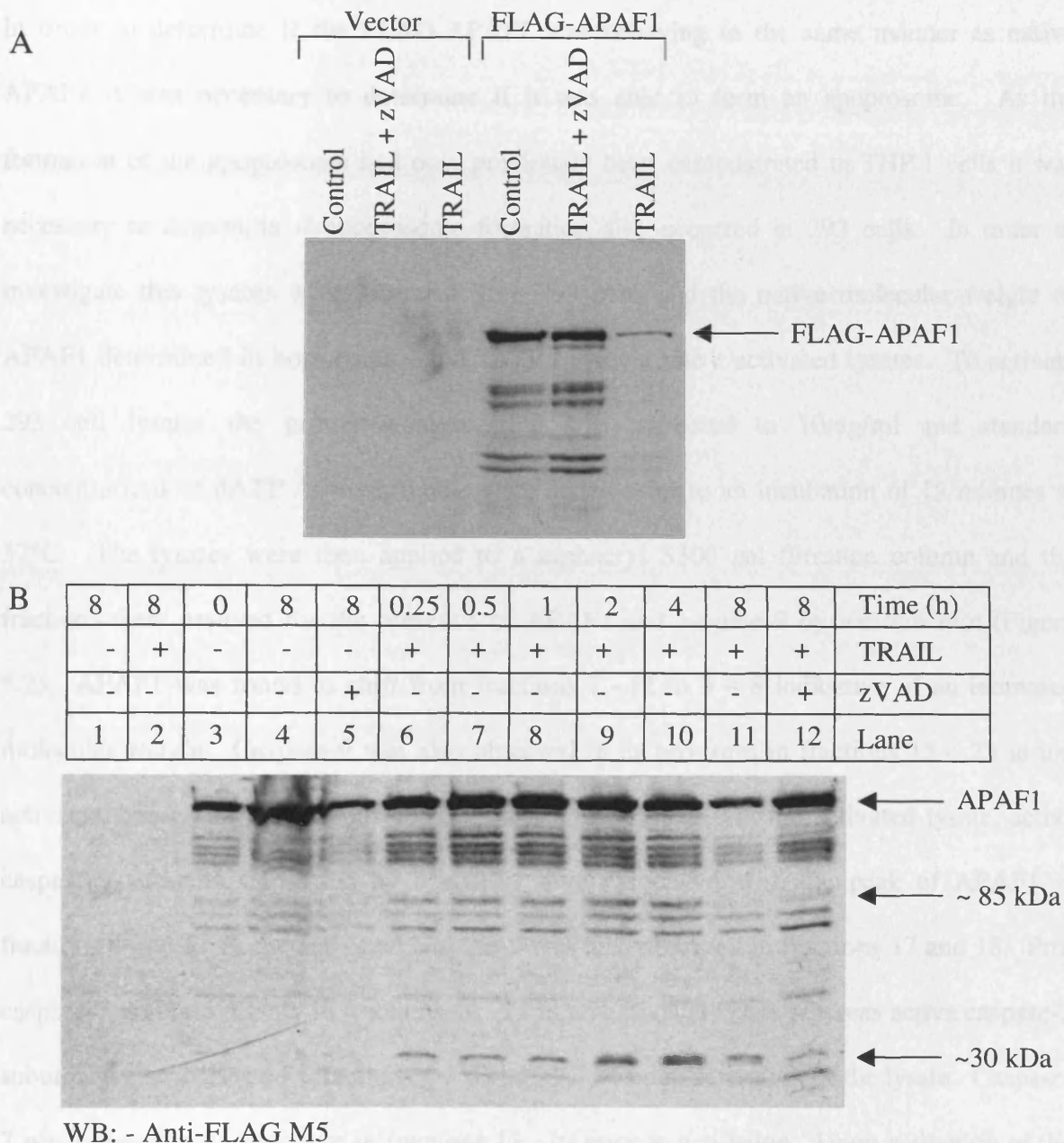


**Figure 5.1** APAF1 is cleaved during TRAIL –induced apoptosis in 293 cells.

293 cells were transfected with either empty vector or pFLAG-CMV2 APAF1 and after 48 h incubated in the presence or absence of 20 $\mu$ M zVAD.FMK for 1h. Apoptosis was then induced by addition of TRAIL. Cells were then harvested and the status of APAF1 analyzed by Western blot using an anti-FLAG monoclonal antibody. Overnight incubation with TRAIL resulted in a z-VAD.FMK inhibitable loss of APAF1 (A). Further analysis showed this loss was time-dependent and revealed the formation of fragments of ~ 85 and 30kDa over time (B).

### 5.2.2 Effect of dATP and cytochrome *c* activation of 293 cell lysate on APAF1

In order to determine if the FLAG-APAF1 was behaving in the same manner as native APAF1 it was necessary to determine if it was able to form an apoptosome. As the formation of the apoptosome had only previously been demonstrated in THP.1 cells it was necessary to determine if apoptosome formation also occurred in 293 cells. In order to investigate this lysates were prepared from 293 cells and the native molecular weight of APAF1 determined in both control and dATP / cytochrome *c* activated lysates. To activate 293 cell lysates the protein concentration was corrected to 10mg/ml and standard concentrations of dATP / cytochrome *c* were added prior to an incubation of 15 minutes at 37°C. The lysates were then applied to a sephacryl S300 gel filtration column and the fractions were assayed for the presence of APAF1 and caspase-9 by western blot (Figure 5.2). APAF1 was found to shift from fractions 7 –12 to 3 – 8 indicative of an increased molecular weight. Caspase-9 was also observed in its pro-form in fractions 15 – 23 in un-activated lysate and in fractions 19 – 21 in activated lysate. In the activated lysate, active caspase-9 subunits (indicated by brackets) were associated with the peak of APAF1 in fractions 4 and 5. Some activated caspase-9 was also observed in fractions 17 and 18. Pro-caspase-3 is found mainly in fractions 14 –23 in un-activated lysate whereas active caspase-3 subunits were observed in fractions 4 – 6 and 11 – 24 upon activation of the lysate. Caspase-7 was present in its pro-form in fractions 13 –19 prior to activation. Upon activation of the lysate, the active subunits of caspase-7 were found throughout the fractions but had two main peaks in fractions 3 – 6 and 11 – 16.

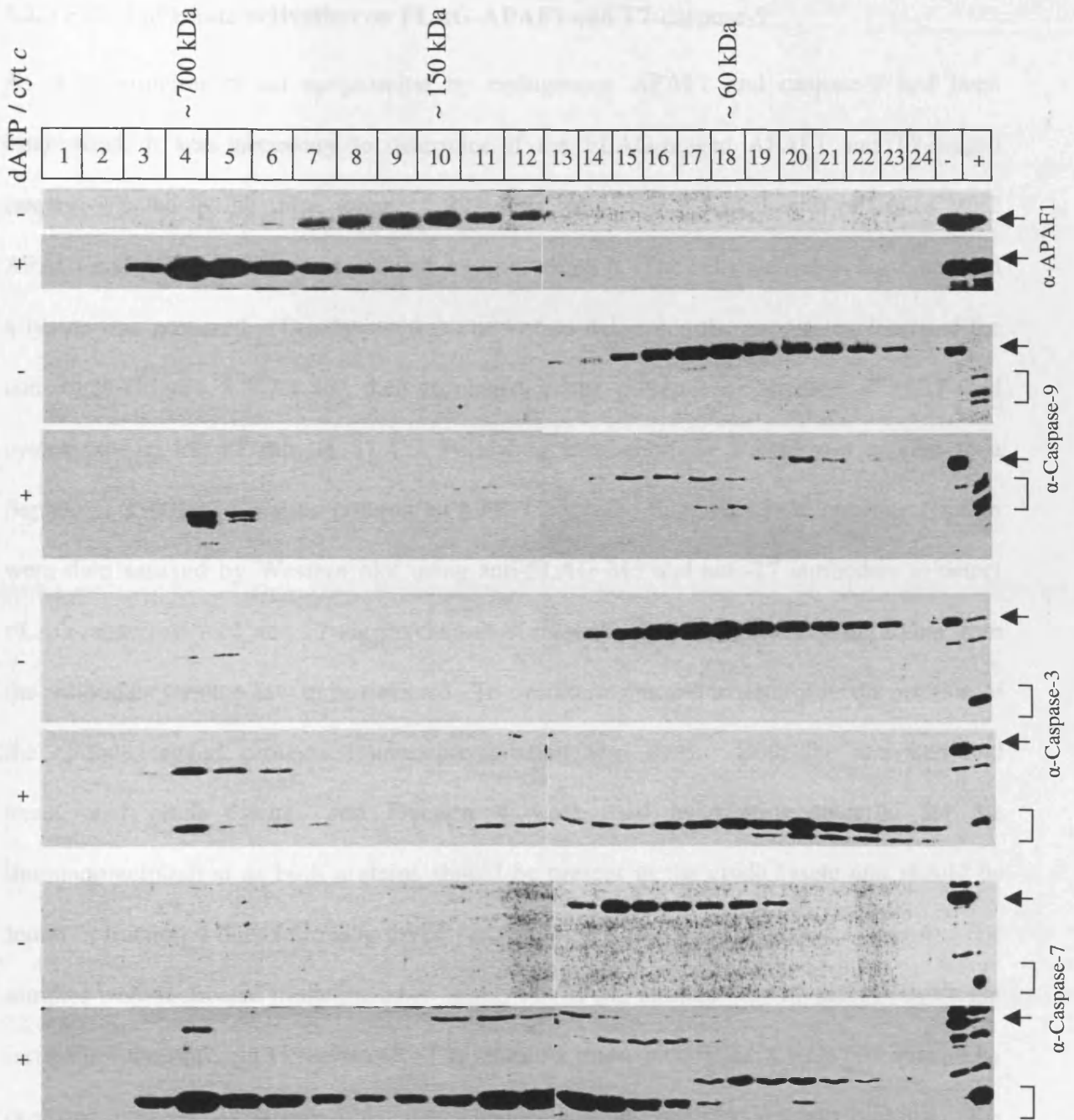


**Figure 5.2 APAF1 can form an apoptosome in 293 cells**

Lysate prepared from 293 cells was incubated with (+) or without (-) dATP and cytochrome *c* prior to fractionation by gel filtration chromatography. The resulting fractions were then analyzed by Western blot for APAF1 and caspases -9, -3 and -7. Pro-caspases are indicated by arrows and processed subunits by brackets. Un-activated (-) and activated (+) lysate before fractionation was ran as a marker for processed caspases on the blots. The positions of molecular weight standards on the Sephacryl S-300 column are also shown.

### 5.2.3 Effect of lysate activation on FLAG-APAF1 and T7-caspase-9

As the formation of an apoptosome by endogenous APAF1 and caspase-9 had been established, it was necessary to determine if the FLAG-tagged APAF1 and T7-tagged caspase-9 acted in the same manner. 293 cells were co-transfected with pFLAG-CMV2 APAF1 and pcDNA3 T7 caspase-9 and cultured for 48 h. The cells were then harvested and a lysate was prepared. This lysate was checked to determine the expression levels of the constructs (Figure 5.3 A) and then incubated in the presence or absence of dATP and cytochrome *c* for 15 min at 37°C. Following incubation the lysate was applied to a Sephacryl S300 gel filtration column on a FPLC system. Samples of the resulting fraction were then assayed by Western blot using anti-FLAG M5 and anti-T7 antibodies to detect FLAG-tagged APAF1 and T7-tagged caspase-9, respectively. Unfortunately, the signal from the antibodies was too low to be detected. To overcome this and to determine the position of the epitope tagged proteins immunoprecipitation was used. Both the activated and unactivated crude lysates and Fraction 4 were used as starting material for the immunoprecipitation as both proteins should be present in the crude lysate and should be found in fraction 4 only following dATP / cytochrome *c* activation (Figure 5.2, lane 4). The samples were incubated in the presence of anti-FLAG M5 antibody for 1 h prior to overnight incubation with protein G sepharose. The resulting immunocomplexes were precipitated by centrifugation and both the supernatants and pellets analyzed by Western blotting. T7-caspase-9 and FLAG-APAF1 were co-immunoprecipitated from both crude lysate and fraction 4 irrespective of the activation state of the lysate (Figure 5.3 B). This indicates that the epitope tagged proteins did not require additional dATP and cytochrome *c* to associate and form a complex of similar molecular weight to the apoptosome (~ 700 kDa).

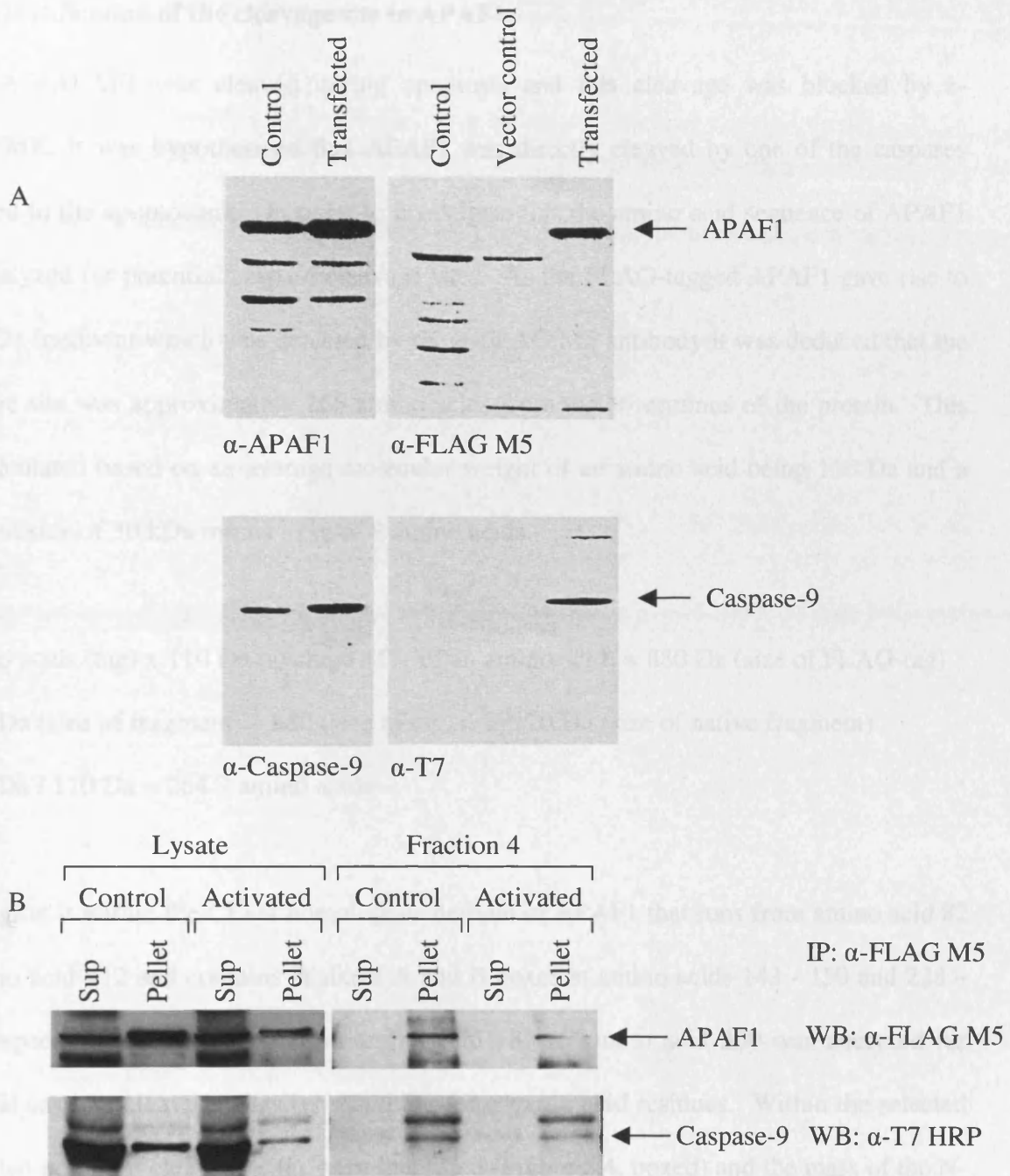


**Figure 5.3 Epitope tagged APAF1 and caspase-9 form an apoptosome independently of dATP and cytochrome *c***

293 cells were co-transfected with FLAG-tagged APAF1 and T7-tagged caspase-9 and lysates prepared and the expression levels compared with the endogenous proteins (A). The lysate was then incubated in the presence (activated) or absence (control) of dATP and cytochrome *c* and fractionated by gel filtration on an S300 column. FLAG-tagged APAF1 was immunoprecipitated from the crude lysate and fraction 4 of both activated and control lysates. Both the supernatant and pellet were then Western blotted for both FLAG-APAF1 and T7-caspase-9 (B).

#### 5.2.4 Identification of the cleavage site in APAF1

As FLAG-APAF1 was cleaved during apoptosis and this cleavage was blocked by z-VAD.FMK, it was hypothesized that APAF1 was directly cleaved by one of the caspases recruited to the apoptosome. In order to investigate this the amino acid sequence of APAF1 was analyzed for potential caspase cleavage sites. As the FLAG-tagged APAF1 gave rise to a 30 kDa fragment which was detected by the  $\alpha$ -FLAG M5 antibody it was deduced that the cleavage site was approximately 265 amino acids from the N-terminus of the protein. This was calculated based on an average molecular weight of an amino acid being 110 Da and a fragment size of 30 kDa minus a tag of 8 amino acids.

8 amino acids (tag) x 110 Da (average MW of an amino acid) = 880 Da (size of FLAG-tag)

30000 Da (size of fragment) – 880 (size of tag) = 29120 Da (size of native fragment)

29120 Da / 110 Da = 264.7 amino acids

This region is within the CED4 homologous domain of APAF1 that runs from amino acid 82 to amino acid 412 and contains Walkers A and B boxes at amino acids 143 - 150 and 228 – 232, respectively. The region from amino acid 181 to amino acid 300 was analyzed for potential caspase cleavage sites by searching for aspartic acid residues. Within the selected region ten potential cleavage sites were identified (Figure 5.4, boxed) and the mass of the N-terminal fragments that would be liberated by cleavage at these residues calculated using the Compute pI/Mw tool ([http://ca.expasy.org/tools/pi\\_tool.html](http://ca.expasy.org/tools/pi_tool.html)) at the ExpASY Molecular Biology server (<http://www.expasy.ch>). Of the fragments only 2, TTRD and SVTD, had a predicted molecular weight in the correct range (Table 5.1).

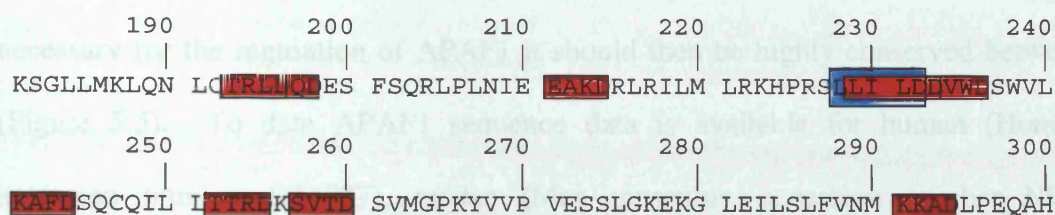


**Figure 5.4 Identification of potential caspase cleavage sites within APAF1**

The sequence of amino acids 181 to 300 in human APAF1 containing the Walker's B box (Blue) was searched for the presence of potential caspase cleavage sites. The sites were determined by the presence of aspartic acid residues (boxed in red). These sites were then evaluated by predicted fragment sizes and the known sequence specificity of various caspases.

Amino Acid Residue	Site	Molecular weight
196	TRLD	21730.26
198	LDQD	21858.39
214	EAKD	23831.52
232	LILD	26057.34
233	ILDD	26172.42
236	DVWD	26572.86
244	KAFD	27519.96
255	TTRD	28779.40
260	SVTD	29309.98
294	KKAD	32986.37

**Table 5.1 Predicted fragment sizes from potential caspase cleavage sites**

The N-terminal fragment size resulting from cleavage of APAF1 at each of the potential caspase cleavage sites was calculated using the Calculate pI / Mw tool on the ExPASy Molecular Biology Server. Of these two were found to yield a fragment of a size close to that observed in cells (~30 kDa).

In order to determine which of these two sites was the correct cleavage site the amino acid sequence of APAF1 from various species was aligned because if the cleavage site was necessary for the regulation of APAF1 it should then be highly conserved between species (Figure 5.5). To date APAF1 sequence data is available for human (*Homo sapiens*, accession number O14727), mouse (*Mus musculus*, accession number NP\_033814), *Drosophila melanogaster* (known as DARK, HAC1, or ARK, accession number AAD45988) and zebrafish (*Danio rerio*, accession number AAF67189). Although both sites contained three conserved residues only D<sup>260</sup> was conserved between species, and based on the conservation of this site, the caspase cleavage site was proposed to be SVTD in human APAF1 (Figure 5.5).

Homo sapiens	K	A	F	D	S	Q	C	Q	I	L	L	T	T	R	D	K	S	V	T	D	S	V
Mus musculus	K	A	F	D	S	Q	C	Q	I	L	L	T	T	R	D	K	S	V	T	D	S	V
Drosophila melanogaster	N	A	F	N	L	S	C	K	I	L	L	T	T	R	F	K	Q	V	T	D	F	L
Danio rerio	R	S	F	D	I	Q	C	R	V	L	L	T	T	R	N	R	A	L	T	D	S	V
															↑							↑
															255							260

**Figure 5.5 D<sup>260</sup> but not D<sup>255</sup> is conserved between species**

The amino acid sequences of APAF1 from *Homo sapiens*, *Mus musculus*, *Drosophila melanogaster* and *Danio rerio* were aligned using the CLUSTAL program. Conserved residues (boxed in red) in the region 241 to 263 containing the two possible caspase cleavage sites is shown. All numbering is given based on the human (*Homo sapiens*) sequence.

Based upon data produced by Dr. S. Bratton within the laboratory it was predicted that APAF1 was cleaved by caspase-3 within cells (Bratton *et al.*, 2001). In order to investigate this further D<sup>260</sup> was mutated to an alanine to produce a non-cleavable mutant form of APAF1 encoding amino acids 1-530. This was then used to produce either <sup>35</sup>S labeled wild type APAF1-530 or mutant APAF1-530 D→A protein in the Promega TNT system. The <sup>35</sup>S labeled protein was then treated with recombinant caspase-3 and the resulting fragments

separated by SDS-PAGE (Figure 5.6). This revealed that mutation of D<sup>260</sup>→A completely inhibited the action of caspase-3 upon APAF1-530 (lanes 6 to 8).

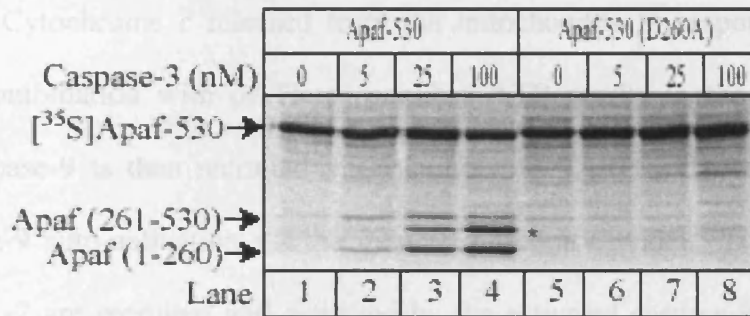


**Figure 5.6 Caspase-3 cleaves APAF1 at D260**

<sup>35</sup>S labeled APAF1-530 and APAF1-530 D<sup>260</sup>→A were incubated with various concentrations of recombinant caspase-3 and the resulting fragments separated by SDS-PAGE and visualized by autoradiography. The two halves of APAF1-530 are indicated. The C-terminal fragment of APAF1-530 was further cleaved to a smaller product (\*) at higher caspase-3 concentrations as demonstrated by the loss of APaf 261-530 at these concentrations.

Further studies upon the p30 fragment of APAF1 were undertaken by Dr. S. Bratton within the laboratory and these revealed that this fragment specifically associates with the ~1.4 MDa complex formed by APAF1. He also demonstrated that this complex is formed due to the inappropriate oligomerization of APAF1 and the caspase cleavage site is accessible in this complex whereas it is normally inaccessible in the ~700 kDa active apoptosome.

### 5.3 Discussion

It has previously been reported that APAF1 activates caspases in a cytochrome *c* and dATP dependent manner via the formation of a macromolecular complex known as the apoptosome. Cytochrome *c* released from the mitochondria in response to an apoptotic stimulus in combination with dATP or possibly ATP results in the oligomerization of APAF1. Caspase-9 is then recruited via a homotypic CARD / CARD interaction which allows caspase-9 auto-activation via the induced proximity model. To this complex both caspase-3 and -7 are recruited and activated by the activated caspase-9. Active caspase-3 and -7 are then released and cleave various cellular proteins, which results in apoptosis. These active caspases are also responsible for an amplification loop involving the mitochondria by both disrupting the mitochondrial membrane and by activating caspase-8, which then activates the pro-apoptotic Bcl-2 family member BID. Both of these mechanisms result in the further release of cytochrome *c* from the mitochondria thereby triggering further apoptosome formation. The apoptosome is ~700 kDa in size and occasionally can form into a larger inactive complex of ~1.4 MDa.

The data in this chapter demonstrates that during apoptosis APAF1 is degraded by caspase activity (Figure 5.1) and whilst endogenous APAF1 and caspase-9 can form an apoptosome, overexpression of epitope tagged forms of APAF1 and caspase-9 can associate even in the absence of cytochrome *c* and dATP (Figures 5.2 and 5.3). The caspase cleavage site within APAF1 is also identified as SVTD<sup>260</sup> by computer analysis and mutation studies (Figures 5.4, 5.5, 5.6 and Table 5.1). Further work by Dr. S. Bratton revealed that the p30 fragment of APAF1 is present preferentially in the inactive ~1.4 MDa apoptosome and it is formed due to APAF1 assuming the incorrect conformation within this complex.

The cleavage of APAF1 by caspase-3 in the ~1.4 MDa apoptosome gives some important clues to the structure of the protein. The CED4 homologous region of APAF1 has been

reported to form a structure similar to the protein kinase Ras (Cardozo & Abagyan, 1998) and the D2 domain of N-ethylmaleimide-Sensitive Fusion Protein and the delta subunit of clamp loader of DNA polymerase III (Jaroszewski *et al.*, 2000). These structures can be used to predict the accessibility of the caspase cleavage site and trypsin cleavage sites within the CED-4 homologous region of APAF1. The accessible cleavage sites can then be used to predict fragment sizes and these can be compared with those generated experimentally using both the ~700 kDa and ~1.4 MDa complexes of APAF1. This data will aid in determining both the accuracy of the models and the regions involved in protein / protein interactions. When the CED-4 region of APAF1 is modeled onto the structures of the D2 domain of N-ethylmaleimide-Sensitive Fusion Protein and the delta subunit of clamp loader of DNA polymerase III (Jaroszewski *et al.*, 2000) the caspase cleavage site is located on the surface of the molecule. In this model, the D260 cleavage site in APAF1 would be accessible. As only the APAF1 found in the ~1.4 MDa complex is cleaved by caspase-3 this model probably predicts the structure of the incorrectly oligomerized APAF1 rather than the APAF1 in the ~700 kDa complex. The other alternative is that in the ~700 kDa complex a protein binds to this surface of APAF1 and masks the caspase cleavage site.

The effect that cleavage of APAF1 has on either APAF1 or the ~1.4 MDa complex is still unclear. Whether APAF1 has assumed the incorrect conformation and been cleaved by caspase-3 before or after formation of the ~1.4MDa complex and whether caspase cleavage of APAF1 is required for the formation of the ~1.4MDa complex is still to be addressed. Further investigation is therefore required to determine if the large ~1.4 MDa complex is still formed in cells which only express a non-cleavable form of APAF1 as complex formation would demonstrate that cleavage of APAF1 occurs after the formation of the complex and the formation is independent of the cleavage. Other groups have recently described the cleavage of APAF1 by caspases during apoptosis. Reimertz *et al.* (J. Neuro. 2001) report a

loss of full length APAF1 in response to  $\text{Ca}^{2+}$  in a neuroblastoma cell line and propose this as an anti-apoptotic mechanism of  $\text{Ca}^{2+}$ . It is not possible to say if this is the same degradation observed during this study as no degradation products of APAF1 were detected in their study, although they do demonstrate that loss of APAF1 is independent of calpains. The study by Lauber *et. al.* reports the formation of an ~84 kDa fragment of APAF1 resulting from cleavage within the CARD at LEKD<sup>19</sup> and at another unidentified site within the WD40 region of APAF1. This fragment was found to form oligomers in the absence of cytochrome *c* and dATP, presumably due to the disruption of the WD40 repeats. As the second cleavage is within the CARD of APAF1 it was proposed that the function of this cleavage event was to release active caspases from the apoptosome. As only caspase-9 is associated with APAF1 via the CARD domain and requires this association with APAF1 for its activity the proposed function of releasing active caspases is called into question. Furthermore, APAF1 should be in complex with caspase-9 when this cleavage event takes place and this association may mask the cleavage site within the CARD of APAF1.

The observed interaction between FLAG-tagged APAF1 and T7-tagged caspase-9 shows that although these molecules demonstrate an interaction they cannot be used for further studies on the apoptosome. The aim of using epitope tagged proteins was to enable immunoprecipitation of the apoptosome as an initial purification step. This would have allowed purification without exposing the complex to varying salt concentrations and other such changes in conditions associated with column chromatography. This would allow the retention of loosely associated proteins and facilitate their purification and identification. There are several possible explanations for the observed interaction between the overexpressed tagged versions of these proteins, the main being that increasing the levels of these proteins may “force” the proteins together in a non-physiological manner. As the levels of both proteins are already high in 293 cells when compared with other cell types this

may seem likely but neither protein was expressed to a maximal level with only a two fold increase of the overall protein levels observed by Western blot. A second explanation would be that the epitope tags used in this study resulted in the incorrect folding of the proteins. This seems unlikely because although both tags are on the N-terminus of APAF1 and caspase-9 they do still allow the CARD / CARD interaction between APAF1 and caspase-9. Another reason may be that the incorrect splice form of APAF1 was used in these experiments and that use of one of the other isoforms, most likely either APAF1LWD13 or APAF1WD13, would result in correct formation of the apoptosome. The function of these forms is, however, coming into question as some studies have demonstrated that cells lacking these longer splice forms are still able to undergo apoptosis in response to cytochrome *c* release (Fu *et al.*, 2001; Walke & Morgan, 2000). This does not however address the issue of how oligomerization of endogenously expressed APAF1 isoforms is regulated within the cell. If APAF1 formed an apoptosome simply because it lacked the additional amino acids found in the other splice forms why does the endogenous APAF1 not continually cause apoptosis? One possible reason is the existence of unidentified co-factors that regulate the formation of the apoptosome and may regulate the conformation of APAF1 itself. A possible candidate for this role is the heat shock family of proteins that have been shown to be involved in apoptosis and the formation of the apoptosome (Beere *et al.*, 2000; Bruey *et al.*, 2000; Li *et al.*, 2000; Pandey *et al.*, 2000a; Pandey *et al.*, 2000b; Saleh *et al.*, 2000). HSP70 has been shown to act by preventing the recruitment and therefore activation of caspases within the apoptosome (Beere *et al.*, 2000) and this is achieved by the binding of HSP70 to the CARD of APAF1 (Saleh *et al.*, 2000). This interaction would prevent the observed interaction between APAF1 and caspase-9.

In summary, this data demonstrates that 293 cells are able to form an apoptosome and activate caspases as has been reported previously for other cell types. The data also

demonstrate that APAF1 is cleaved during apoptosis and the preferential caspase cleavage site is now identified. Additional data from Dr. S. Bratton also demonstrated that the resulting fragments of APAF1 are associated with the inactive ~1.4 MDa complex and that caspase cleavage probably results from the incorrect folding of APAF1. The data also demonstrates that epitope tagged proteins can form an apoptosome in the absence of cytochrome *c* and dATP and due to this these proteins were not suitable for use in further apoptosome formation studies.

Part of the data presented in this chapter has been published (Bratton *et al.*, 2001).

**CHAPTER 6: THE IDENTIFICATION AND CHARACTERIZATION OF SMAC  $\beta$ ,  
AN ALTERNATIVELY SPLICED FORM OF SMAC.**

## 6.1 INTRODUCTION

The Inhibitor of Apoptosis family of proteins, also known as the IAPs, were originally identified in baculovirus where they function to prevent the infected host cell from undergoing apoptosis. The IAP family broadly falls into two groups of proteins: those with a single BIR domain and those with multiple (in humans three) BIR domains (Deveraux *et al.*, 1999b; Richter *et al.*, 2001). The best studied IAP containing only a single BIR domain is Survivin, which is involved in mitosis and although its overexpression can delay apoptosis, Survivin is relatively poor at inhibiting caspases (Deveraux & Reed, 1999). There are currently five other IAPs in humans of which only one, BRUCE, contains a single BIR domain. BRUCE also contains an ubiquitin-conjugating domain implicating it in the proteasome pathway for protein degradation but it is not yet known if it is able to suppress apoptosis (Hauser *et al.*, 1998). The NAIP (Neuronal Apoptosis Inhibitor) protein contains three BIR domains and as the name suggests its expression is restricted to neuronal tissue (Liston *et al.*, 1996). Originally identified in the TNF-receptor DISC (Rothe *et al.*, 1995), both c-IAP-1 and c-IAP-2 can inhibit caspases -3, -7 and -9 (Deveraux *et al.*, 1998; Roy *et al.*, 1997). The final member of the human IAP family, XIAP, is encoded by a gene on the X chromosome. XIAP has also been shown to inhibit the activity of caspases -3, -7 and -9 (Deveraux *et al.*, 1998; Deveraux *et al.*, 1997) and is cleaved by caspases during apoptosis resulting in two fragments with differing affinities for caspases. The BIR1 - BIR2 containing fragment is specific for caspases -3 and -7 whereas the BIR3 - RING fragment is specific for caspase -9 (Deveraux *et al.*, 1999a). Whether the cleavage of XIAP is functional or a consequence of binding active caspases remains to be demonstrated.

IAPs act downstream of Bcl-2 and cytochrome *c* release in the mitochondrial pathway at the level of caspase activation by the apoptosome (Duckett *et al.*, 1998).

Several IAPs have also been reported to possess E3 ubiquitin ligase activity, which is dependent upon the presence of a normal RING domain (Huang *et al.*, 2000; Yang *et al.*, 2000). This activity results in auto-degradation and the degradation of any bound proteins, i.e. caspases, and could be either pro- or anti-apoptotic. Auto-degradation would result in a decreased level of IAPs, reducing the potential for caspase inhibition thereby promoting apoptosis. The degradation of bound caspases would result in loss of caspases from the cell and therefore would act in an anti-apoptotic manner. Whether both of these mechanisms function in cells is yet to be fully investigated and may help explain the function of proteasome inhibitors as anti-cancer drugs.

In *Drosophila*, three pro-apoptotic proteins REAPER, HID (Head Involution Defective) and GRIM, have been shown to bind IAPs thereby preventing their inhibitory action on caspases (Goyal *et al.*, 2000; Lisi *et al.*, 2000; McCarthy & Dixit, 1998; Vucic *et al.*, 1997; Vucic *et al.*, 1998). The IAP binding site resides in the N-terminal ten to fifteen amino acids of all three proteins although this region demonstrates only low homology between the proteins.

REAPER is the best studied of these proteins and its transcription is regulated by *Drosophila* p53 (Steller, 2000). In addition to IAP binding, REAPER is also known to bind to the *Xenopus* protein Scythe that causes cytochrome *c* release resulting in apoptosis (Thress *et al.*, 1999a). REAPER has also been shown to require co-expression of HID in the midline cells of the CNS in *Drosophila* where it acts in a co-operative fashion with HID (Zhou *et al.*, 1997) and GRIM (Wing *et al.*, 1998) to induce apoptosis. The ability of REAPER to act co-operatively with GRIM or HID in midline cells is not dependent upon the N-terminal IAP binding domain as deletion mutants of REAPER lacking the N-terminus induce higher levels of apoptosis than wild-type REAPER. This however seems to be a cell type specific effect as the same mutants, when co-expressed with GRIM or

HID in the adult eye of *Drosophila* was less effective than wild-type REAPER (Wing *et al.*, 1998).

GRIM may also act independently of IAPs as apoptosis induced by overexpression of GRIM was not inhibited by overexpression of the *Drosophila* IAP homologue, DIAP-2 (Wing *et al.*, 1998). GRIM appears to possess a second IAP binding site as IAP binding and pro-apoptotic activity are both retained when the N-terminal 14 amino acids are removed (Vucic *et al.*, 1998). The N-termini of REAPER and GRIM have also been shown to act on potassium channels inhibiting their activation possibly inducing apoptosis by a third mechanism (Hay, 2000). This inhibitory function is independent of IAP binding and therefore may be another pro-apoptotic mechanism of these proteins. REAPER, HID and GRIM may signal in part via the *Drosophila* homologue of APAF1, DARK, as absence of DARK results in reduced apoptosis induced by overexpression of REAPER, HID and GRIM (Rodriguez *et al.*, 1999b) although whether or not this pathway is dependent on IAPs remains to be seen. The function of REAPER, HID and GRIM is conserved in mammalian cells as they induce apoptosis when overexpressed in cell lines although until recently no mammalian homologue was identified (McCarthy & Dixit, 1998).

Two groups have recently identified Smac (Second Mitochondrial Activator of Caspases) (Du *et al.*, 2000) / DIABLO (direct IAP binding protein with low pI) (Verhagen *et al.*, 2000) proposed to be a mammalian homologue of Reaper, HID and Grim. Smac binds to a number of different IAPs and is localized to mitochondria (Du *et al.*, 2000). Smac is synthesized as a 293 amino acid precursor that is targeted to mitochondria by the N-terminal 55 amino acids that form a classical mitochondrial targeting sequence (MTS). Once in the mitochondria, the MTS is removed and the mature protein is then released during apoptosis along with cytochrome *c* (Du *et al.*, 2000). The mature protein is then

able to bind XIAP, and other IAPs, resulting in the displacement of caspase -9 and thereby allows caspase activation by the apoptosome (Ekert *et al.*, 2001). The binding site of IAPs in Smac has recently mapped to the N-terminus of the mature protein (Chai *et al.*, 2000; Srinivasula *et al.*, 2000) and contains some homology to the N-termini of REAPER, HID and GRIM (Silke *et al.*, 2000). Overexpression of Smac / DIABLO also potentiated apoptosis induced by several different stimuli (Du *et al.*, 2000; Ekert *et al.*, 2001; Srinivasula *et al.*, 2000). This however restricts Smac to the mitochondrial pathway and recently a second splice form, Smac-S, was identified which resides in the cytoplasm (Srinivasula *et al.*, 2000) that is also described in this chapter.

In this chapter, the second splice form of Smac, Smac-S, and two further putative splice forms identified by database searching are described. As two further short forms of Smac are identified, Smac-S is referred to as Smac  $\beta$  from here on. Smac  $\beta$  and deletion mutants of Smac were characterised and found to potentiate apoptosis induced by a range of stimuli. This demonstrates that IAP binding is not essential for the pro-apoptotic function of Smac. Production and characterisation of a polyclonal antibody to Smac  $\beta$  is also described in this chapter.

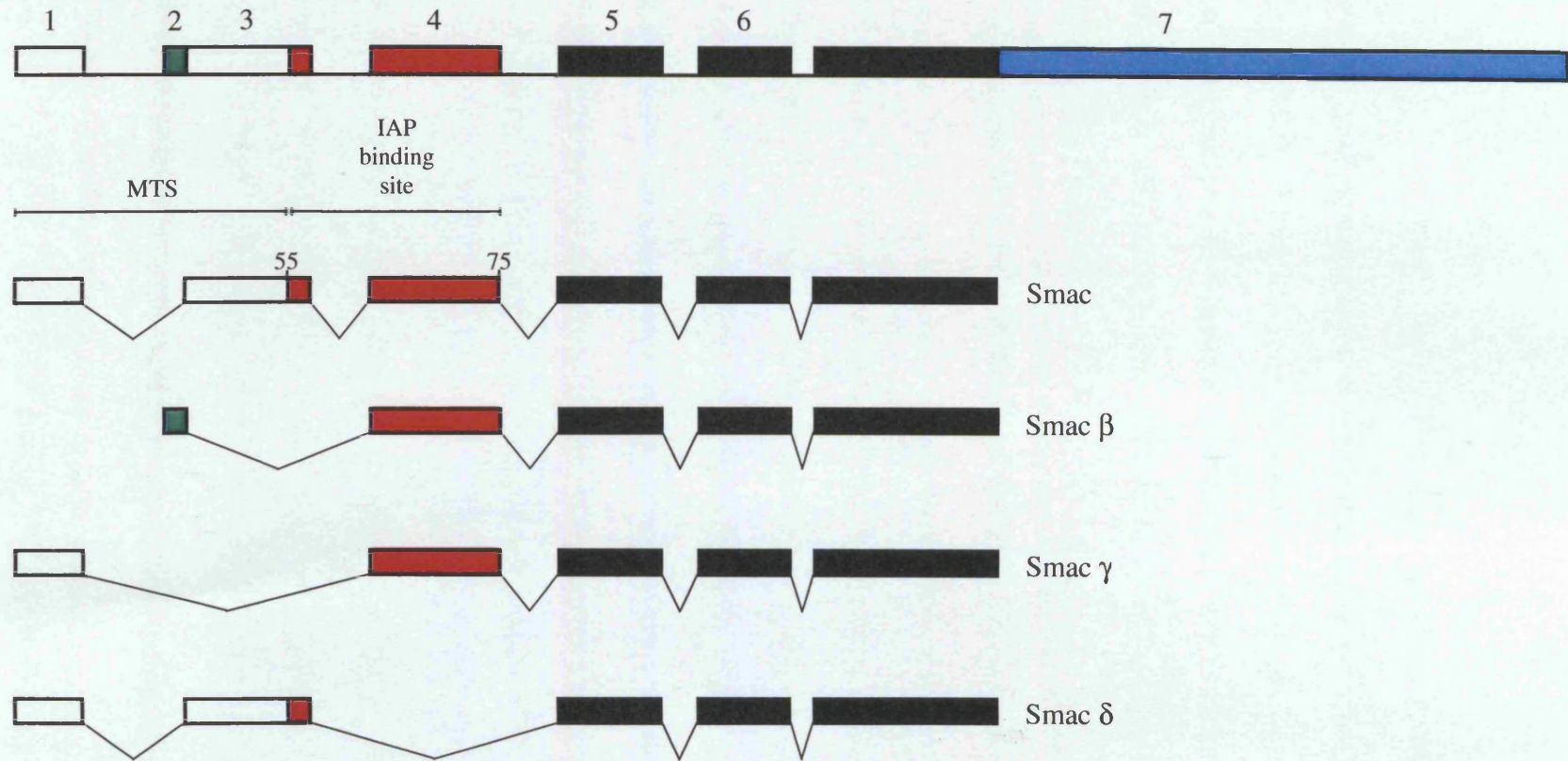
## 6.2 RESULTS

### 6.2.1 Identification of alternative splice forms of Smac

To identify any alternative splice forms or homologues of Smac the GenBank databases were searched using the Smac protein sequence and the TBLASTN programme. Searches of human ESTs revealed several ESTs corresponding to the published sequence and several that appeared to be alternatively spliced forms (Fig. 6.1 A). The first of these splice forms (e.g. accession number AA156765), referred to as Smac  $\beta$ , had an alternative 5' end. Other sequences identified contained deletions in either the MTS (Smac  $\gamma$ ) or the N-terminus of the mature protein (Smac  $\delta$ ) (Fig. 6.1 A). Further searches of the non-redundant database revealed a full-length cDNA (accession number AK001399) for Smac  $\beta$  containing an open reading frame of 186 amino acids with an alternative N-terminus (Fig. 6.1 B). In order to confirm the identity of these sequences as splice forms a search of the HTGS database was performed, this revealed a genomic sequence (accession number NT\_009438) with homology to all of the sequences. This indicated that the *Smac* gene is composed of seven exons and all identified sequences are in fact splice variants (Fig. 6.1 A).

To examine expression of both Smac and Smac  $\beta$  in cells primers were designed to amplify both full-length coding sequences. Total RNA from different cell lines was then used as a template for RT-PCR using both primer pairs (Fig. 6.1 C). This demonstrated that both Smac and Smac  $\beta$  were expressed in the cell lines tested with low levels of possibly either Smac  $\gamma$  or Smac  $\delta$  evident below the Smac RT-PCR product. It is not possible to distinguish between these alternatively spliced forms, as the products would co-migrate on

A



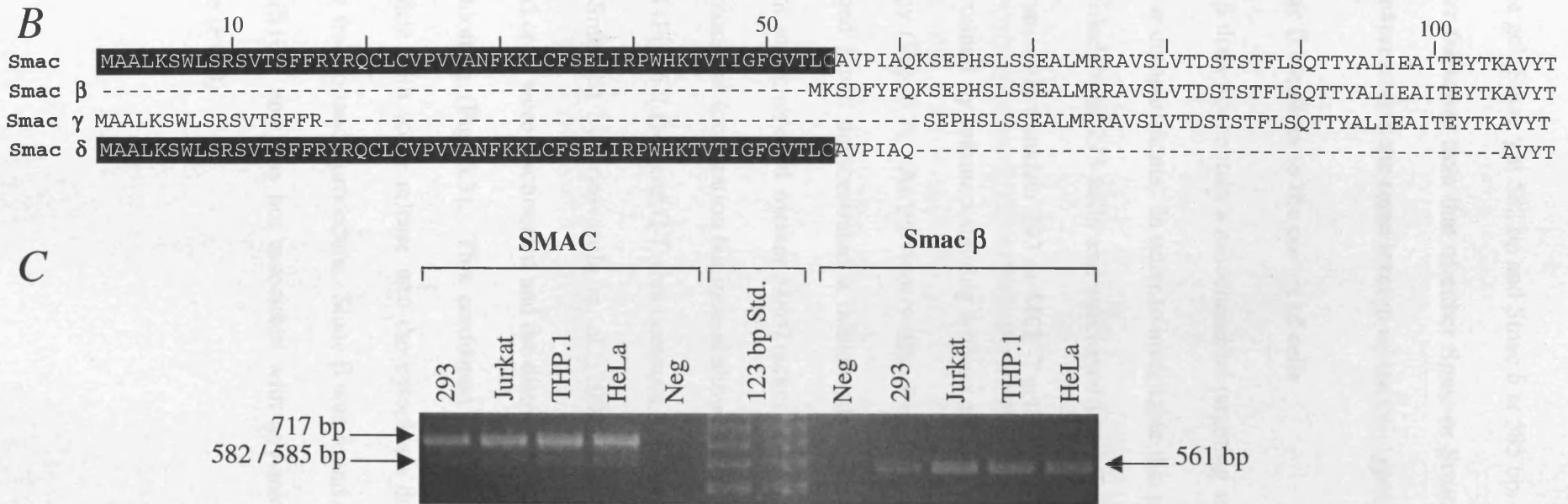


**Figure 6.1 Smac exists as multiple splice forms**

A schematic representation of the *Smac* gene (A) showing the genomic structure (upper) and the various splice forms identified by database searching. The IAP binding site is shown in red, the mitochondrial targeting sequence (MTS) is shown as an open box and the alternative N-terminus in green. The non-coding 3' UTR is also within exon 7 (blue). (B) Alignment of *Smac* splice forms showing the predicted amino acids sequence (the MTS is boxed). (C) RT-PCR analysis of various cell lines using *Smac* and *Smac*  $\beta$  specific primers. The expected sizes for the various splice forms are indicated, *Smac* 717 bp, *Smac*  $\beta$  561 bp, *Smac*  $\gamma$  and *Smac*  $\delta$  582 / 585 bp.

an agarose gel, Smac  $\gamma$  at 582 bp and Smac  $\delta$  at 585 bp. The abundance of these two forms is however far lower than that of either Smac or Smac  $\beta$ . All splice forms of Smac are, however expressed to the same level in all the cell types tested.

### 6.2.2 Smac $\beta$ localizes to the cortex of cells

As Smac  $\beta$  does not contain a mitochondrial targeting sequence, it may be targeted to other sub-cellular compartments. In order to investigate this possibility Smac and Smac  $\beta$  cDNA was amplified from 293 cells and subcloned into pTriEx-1. These constructs were then used to transiently transfect 293 or MCF-7 cells. The localization of Smac / Smac  $\beta$  was then determined by immuno-staining with an anti-HSV antibody and analysis by confocal microscopy (Fig. 6.2). As previously described for endogenous Smac (Du *et al.*, 2000), HSV tagged Smac demonstrated a mitochondrial distribution by co-localizing with the fluorescent mitochondrial marker MitoTracker™ (Fig. 6.2 A-C). Smac  $\beta$  did not show any mitochondrial localization but instead showed a distinct distribution towards the cortex of the cell (Fig. 6.2 D-F and G-I) that contrasts with the cytosolic distribution described for Smac-S (Smac  $\beta$ ) by Srinivasula *et. al.* (2000). In order to confirm this distribution, transfected cells were fractionated and the distribution of Smac and Smac  $\beta$  determined by Western blotting (Fig. 6.3). This confirmed that Smac was primarily localized to the mitochondria with some release into the cytoplasm due to damage to the mitochondria during the fractionation procedure. Smac  $\beta$  was found only in the cytoplasmic fraction of the cells (S100) and was not associated with any microsomal structures or the plasma membrane (P100).

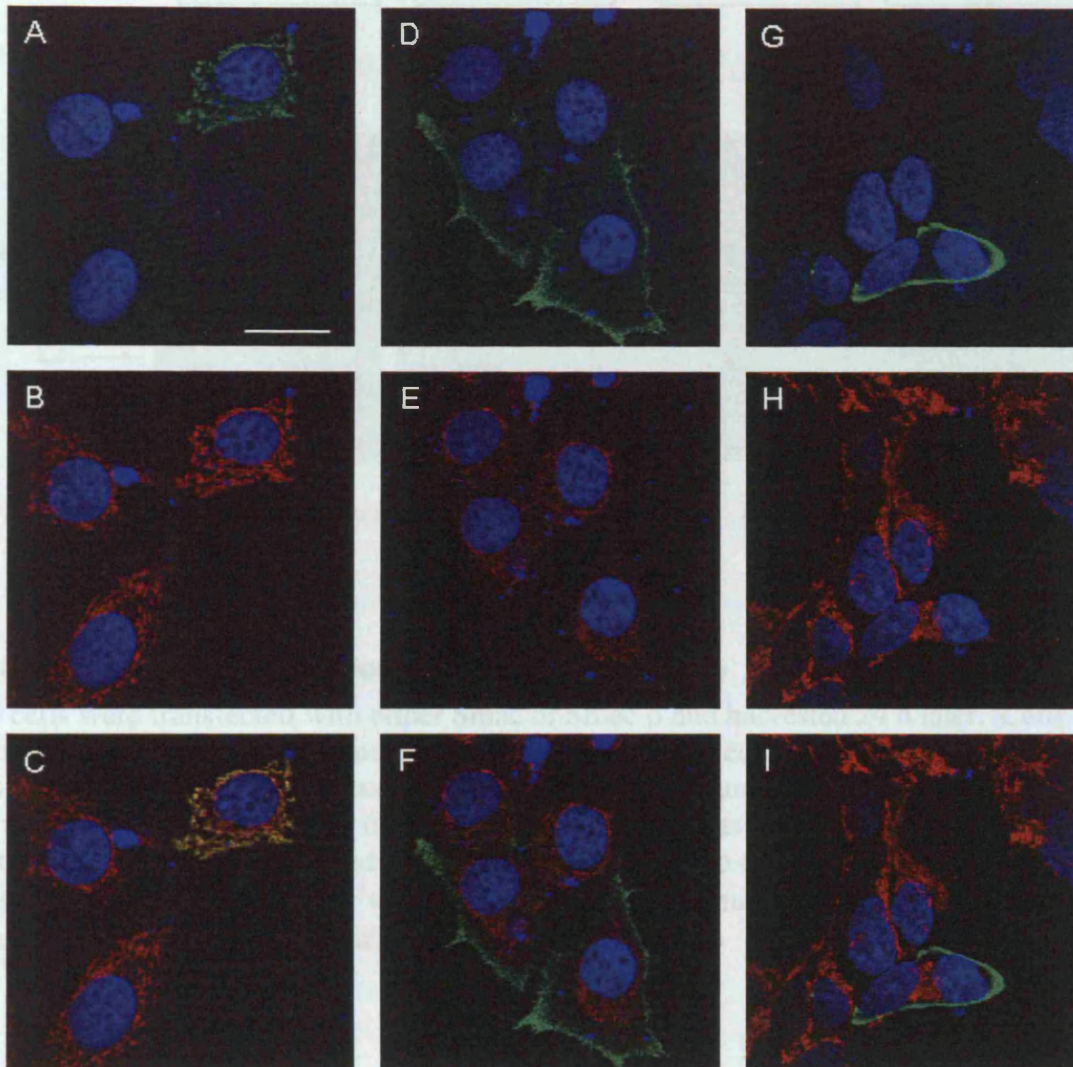


**Figure 6.2 Sub-cellular distribution of Smac and Smac  $\beta$**

Smac (A-C) or Smac  $\beta$  (D-I) were transiently transfected into MCF-7 (A-F) or 293 (G-I) cells and after 24 h cells were fixed and stained. Cells expressing the HSV tagged proteins were stained green (Alexa 488). MitoTracker™ red CMXRos was used to stain mitochondria (B-C, E-F and H-I). Hoechst 33258 was used to label cell nuclei (A-I). Smac co-localized with mitochondria but not Smac  $\beta$  (C vs. F and I). Bar, 10  $\mu$ m.

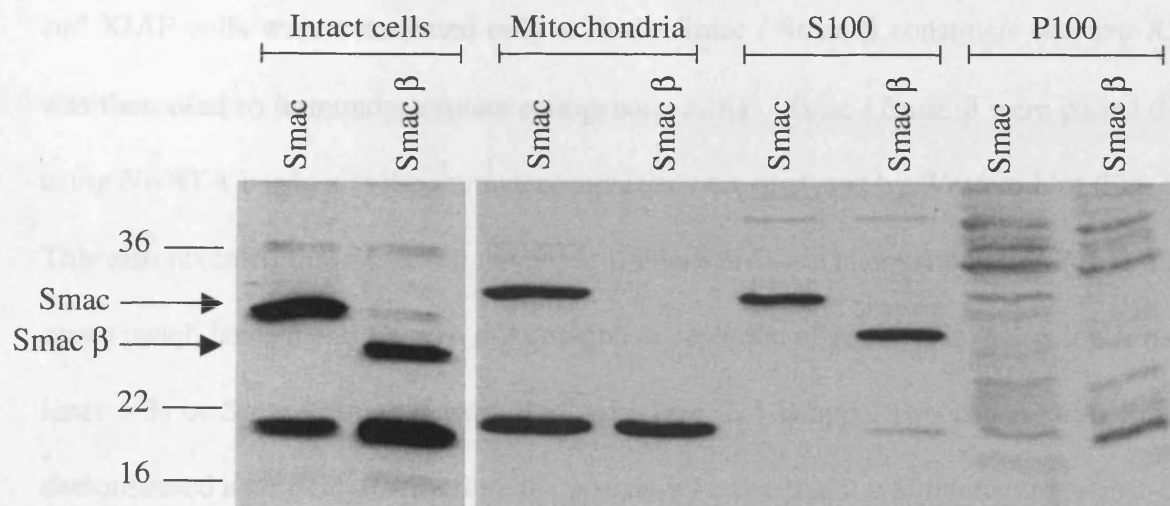


**Figure 6.3 Sub-cellular fractionation of transfected cells**

293 cells were transfected with either Smac or Smac  $\beta$  and harvested 24 h later. Cells were then fractionated and crude nuclei and intact cells removed. The remaining supernatant was then fractionated into Mitochondria, S100 (cytosol) and membranous structures such as microsomes and plasma membrane (microsomes) as described in Materials and Methods. Intact cells were used as a positive control and to confirm equal expression. The Western blot was then probed with anti-HSV to detect Smac or Smac  $\beta$  (arrows). Equal protein (20 $\mu$ g) was loaded in each lane.

### 6.2.3 Smac $\beta$ does not interact with IAPs in cells

As Smac  $\beta$  lacks only the first five amino acids of mature Smac, its ability to bind IAP family members was investigated by co-immunoprecipitation studies. 293 cells were co-transfected with pTriEx-1, pTriEx-Smac or pTriEx-Smac  $\beta$  and pcDNA3 hILP (XIAP) and after 24 hours cell lysates were prepared. The lysates were then immunoprecipitated with either XIAP or Smac / Smac  $\beta$  using anti-Flag antibody or Ni-NTA beads, respectively. The immunoprecipitated complexes were then analysed by Western blotting. It was found that Smac but not Smac  $\beta$  associated with the overexpressed XIAP (data not shown). To

exclude the possibility that overexpression alone was causing an interaction between Smac and XIAP cells were transfected only with the Smac / Smac  $\beta$  constructs and anti-XIAP was then used to immunoprecipitate endogenous XIAP. Smac / Smac  $\beta$  were pulled down using Ni-NTA beads and the immunocomplexes were analysed by Western blot (Fig. 6.4). This also revealed that Smac but not Smac  $\beta$  interacted with endogenous XIAP (Fig. 6.4 A upper panel, lanes 5 and 6) even after complete depletion of XIAP (Fig. 6.4 A lower panel, lanes 1-3) or Smac / Smac  $\beta$  from the lysate (Fig. 6.4 B upper two panels). As Smac  $\beta$  demonstrated a cortical distribution, the possibility arose that it was interacting with c-IAP-1 or c-IAP-2, which are recruited to the TNF-R DISC. To address this possibility the Western blots of immunoprecipitated Smac / Smac  $\beta$  were reprobbed for c-IAP-1 and c-IAP-2 (Fig. 6.4 B lower two panels, lanes 5 and 6). This revealed that neither Smac nor Smac  $\beta$  interacted with endogenous c-IAP-1 or c-IAP-2 when immunoprecipitated from whole cells. This is in contradiction with previously reported *in vitro* results (Chai *et al.*, 2000; Du *et al.*, 2000; Srinivasula *et al.*, 2000). Both Smac and Smac  $\beta$  were shown to be at similar levels in the lysate by Western blotting (Fig. 6.4 C). To confirm that Smac  $\beta$  did not interact with XIAP, c-IAP-1 or c-IAP-2 a lysate was prepared from transfected 293 cells. The lysate was then applied to a Sephacryl S200 gel filtration column and the elution position of the IAPs and Smac / Smac  $\beta$  determined by Western blotting (Fig. 6.5). This confirmed that Smac  $\beta$  (fractions 6 to 16) did not interact with XIAP, c-IAP-1 or c-IAP-2 (fractions 3 to 9) as they eluted at different positions from the column. Interestingly Smac eluted in fractions 3 to 10 but the peak of protein was in fractions 7 to 10 where very little of the IAPs eluted. Both the IAPs and Smac eluted at a larger molecular weight than predicted for the monomeric proteins. Smac is reported to form a dimer which runs at ~100 kDa due to its structure whereas c-IAP-1 and c-IAP-2

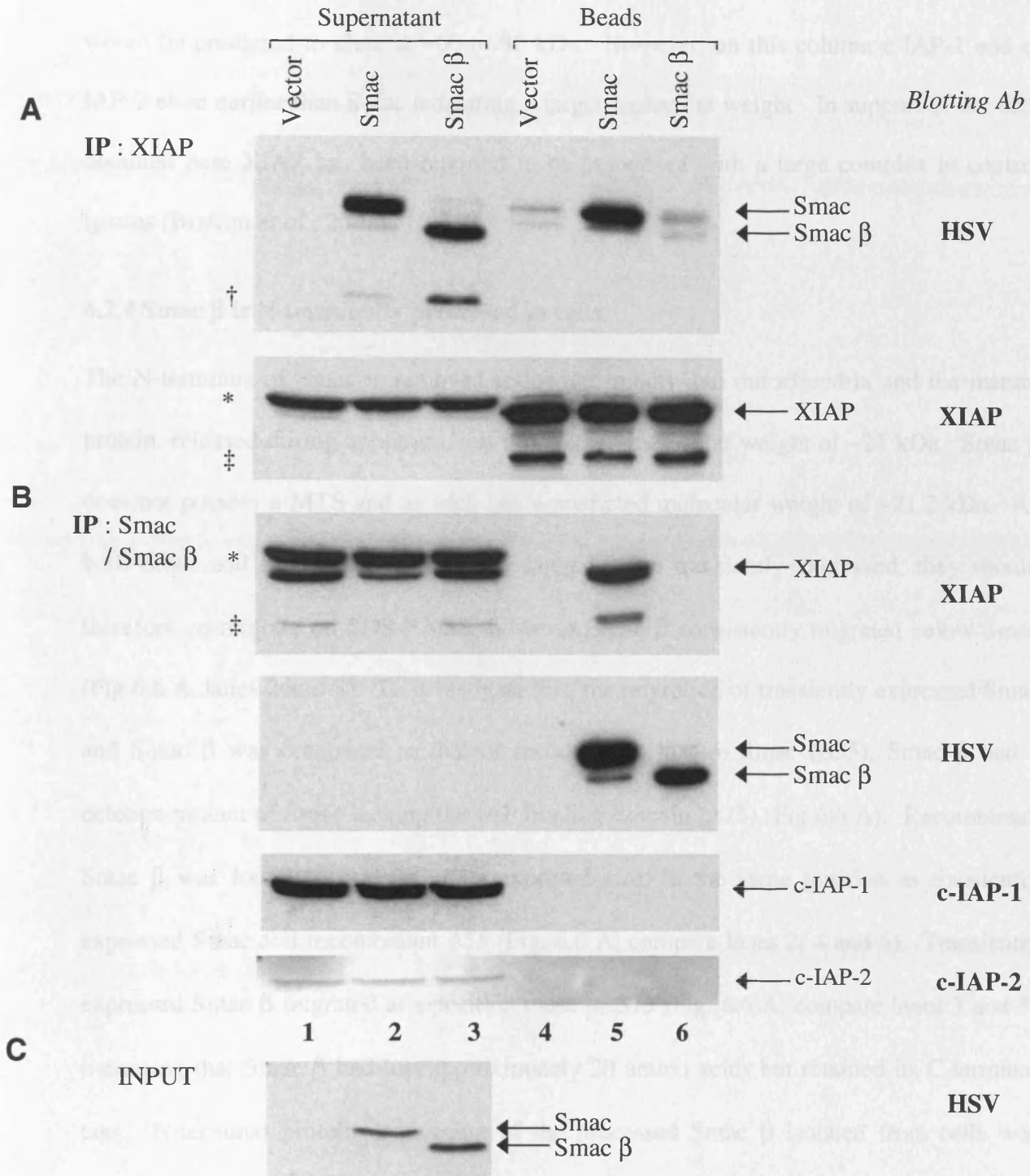


**Figure 6.4 Smac  $\beta$  does not interact with IAP family members**

(A) Endogenous XIAP was immunoprecipitated and the supernatant and pellet examined for Smac / Smac  $\beta$  using the HSV Ab (upper panel) or for XIAP (lower panel). (B) Ni-NTA beads were used to precipitate His<sub>6</sub> tagged Smac and Smac  $\beta$  and were probed for XIAP (upper panel) or Smac and Smac  $\beta$  (middle panel). The blots were reprobed for c-IAP-1 or c-IAP-2 (lower panels). (C) Expression levels of Smac and Smac  $\beta$  were measured in the transfected cell lysates confirming equal input. Non-specific bands detected by the anti-XIAP Ab (\*), and the heavy chain of the immunoprecipitation antibody (‡) are indicated. Occasionally an alternative start site in the Smac and Smac  $\beta$  constructs gave rise to a product (marked †), which did not interact with IAPs.

would be predicted to elute at ~60 to 80 kDa. However, on this column c-IAP-1 and c-IAP-2 elute earlier than Smac indicating a larger molecular weight. In support of the data obtained here XIAP has been reported to be associated with a large complex in control lysates (Bratton *et al.*, 2001).

#### 6.2.4 Smac $\beta$ is N-terminally processed in cells

The N-terminus of Smac is removed following import into mitochondria and the mature protein, released during apoptosis, has a predicted molecular weight of ~21 kDa. Smac  $\beta$  does not possess a MTS and as such has a predicted molecular weight of ~21.2 kDa. As both Smac and Smac  $\beta$  are identically tagged when transiently expressed, they should therefore co-migrate on SDS-PAGE, however Smac  $\beta$  consistently migrated below Smac (Fig 6.6 A, lanes 2 and 3). To investigate this, the migration of transiently expressed Smac and Smac  $\beta$  was compared to that of recombinant mature Smac ( $\Delta 55$ ), Smac  $\beta$  and a deletion mutant of Smac lacking the IAP binding domain ( $\Delta 75$ ) (Fig 6.6 A). Recombinant Smac  $\beta$  was found to migrate at its expected size, in the same position as transiently expressed Smac and recombinant  $\Delta 55$  (Fig. 6.6 A, compare lanes 2, 4 and 6). Transiently expressed Smac  $\beta$  migrated at a position close to  $\Delta 75$  (Fig. 6.6 A, compare lanes 3 and 5) indicating that Smac  $\beta$  had lost approximately 20 amino acids but retained its C-terminal tags. N-terminal protein sequencing of the processed Smac  $\beta$  isolated from cells was attempted but the protein was N-terminally blocked. In order to confirm that all IAP binding occurs via the N-terminal 15 amino acids of Smac, recombinant proteins were used to assess the binding of IAPs to either full length Smac  $\beta$  or Smac  $\Delta 75$  in an *in vitro* binding assay. Smac  $\Delta 75$  was unable to bind XIAP, c-IAP-1 or c-IAP-2 whereas recombinant Smac  $\beta$  was able to bind all three IAPs (Fig. 6.6 B, compare lanes 3 and 4).

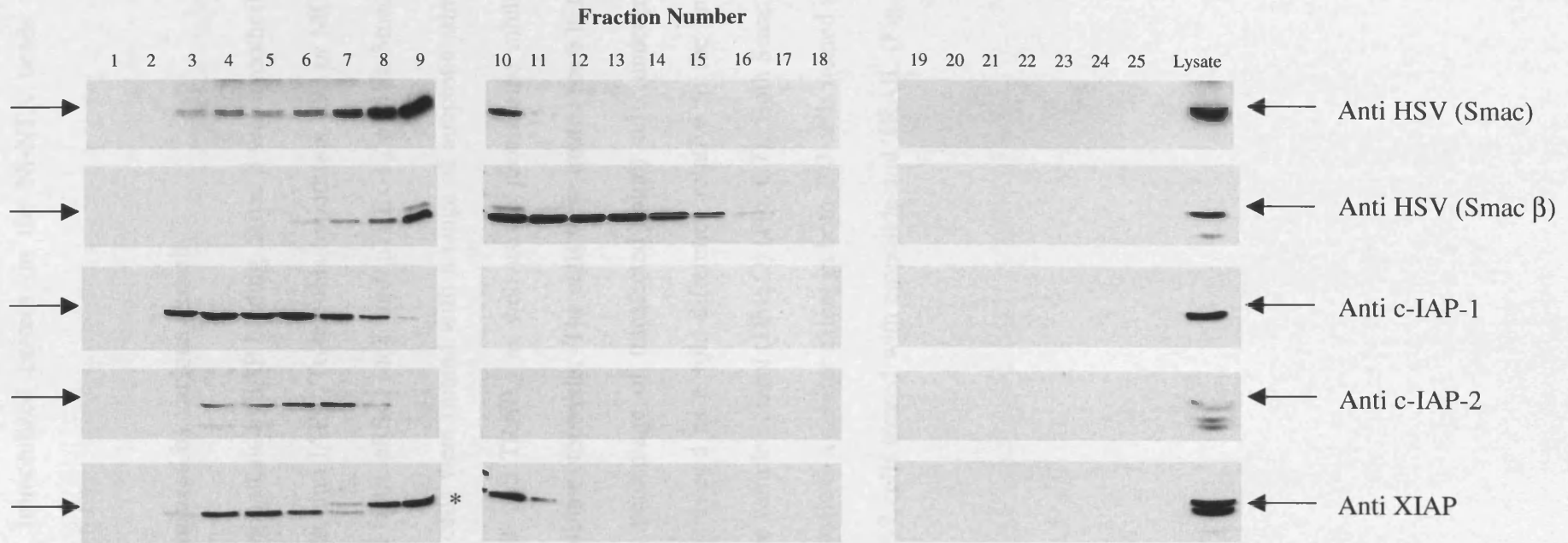


**Figure 6.5 Smac and Smac  $\beta$  exist as complexes of different molecular weight**

Lysates were prepared from cells transfected with Smac or Smac  $\beta$ . Lysates were then subjected to gel filtration on a sephacryl S200 column and the eluted proteins analysed by Western blotting for Smac, Smac  $\beta$ , c-IAP-1, c-IAP-2 or XIAP. Whole lysate was used as a positive control on the Western blots. A non-specific protein was detected by the anti-XIAP antibody (\*) which eluted at a lower molecular weight.

The presence of equal amounts of immobilized protein on the Ni-NTA beads was confirmed by Western blotting (Fig. 6.6 C).

### 6.2.5 Smac $\beta$ potentiates apoptosis induced by various stimuli

As Smac was proposed to potentiate apoptosis by IAP binding, Smac  $\beta$  was hypothesized to be anti-apoptotic as it was unable to bind IAPs. To test this hypothesis, 293 or MCF-7 cells were transiently co-transfected with pRSC *lacZ* and pTriEx-1, pTriEx-Smac or pTriEx-Smac  $\beta$ . After 24 hours the cells were treated with a range of apoptotic stimuli, including death receptor stimuli (TNF and TRAIL) as well as the proteasome inhibitor MG-132 and the topoisomerase II inhibitor etoposide. The cells were treated for 6 h, then fixed and stained with X-gal. The percentage of transfected (blue) cells undergoing apoptosis was then calculated and expressed as a fold-difference relative to the empty vector transfected cells treated with the vehicle control (DMSO) (Fig. 6.7). Both Smac and Smac  $\beta$  caused a potentiation of apoptosis to a similar extent in both 293 cells treated with all five stimuli (Fig. 6.7 A) and MCF-7 cells treated with etoposide and TRAIL (Fig. 6.7 B).

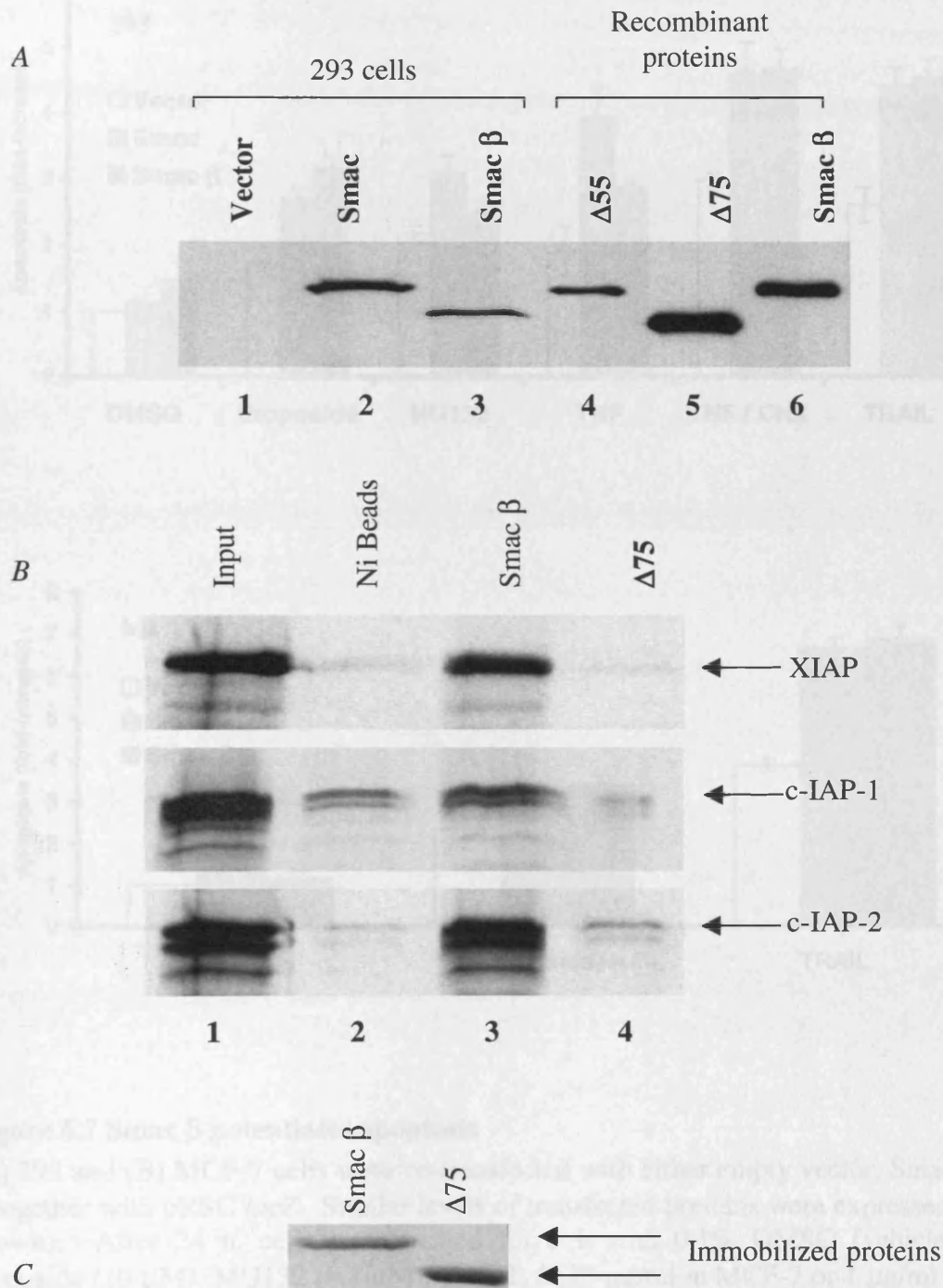


**Figure 6.6 Smac  $\beta$  cannot bind XIAP *in vivo* due to N-terminal processing.**

(A) 293 cells were transfected with vector alone, Smac or Smac  $\beta$  and harvested at 24 h (lanes 1-3). The migration on SDS gels of Smac and Smac  $\beta$  was then compared with recombinant Smac  $\Delta 55$ , Smac  $\Delta 75$  and Smac  $\beta$  (lanes 4-6). (B)  $^{35}\text{S}$  IAPs were incubated with beads alone, recombinant Smac  $\beta$  or Smac  $\Delta 75$  bound to Ni-NTA beads, washed and analysed by autoradiography. (C) Input control showing the beads bound to Smac  $\beta$  or Smac  $\Delta 75$ .

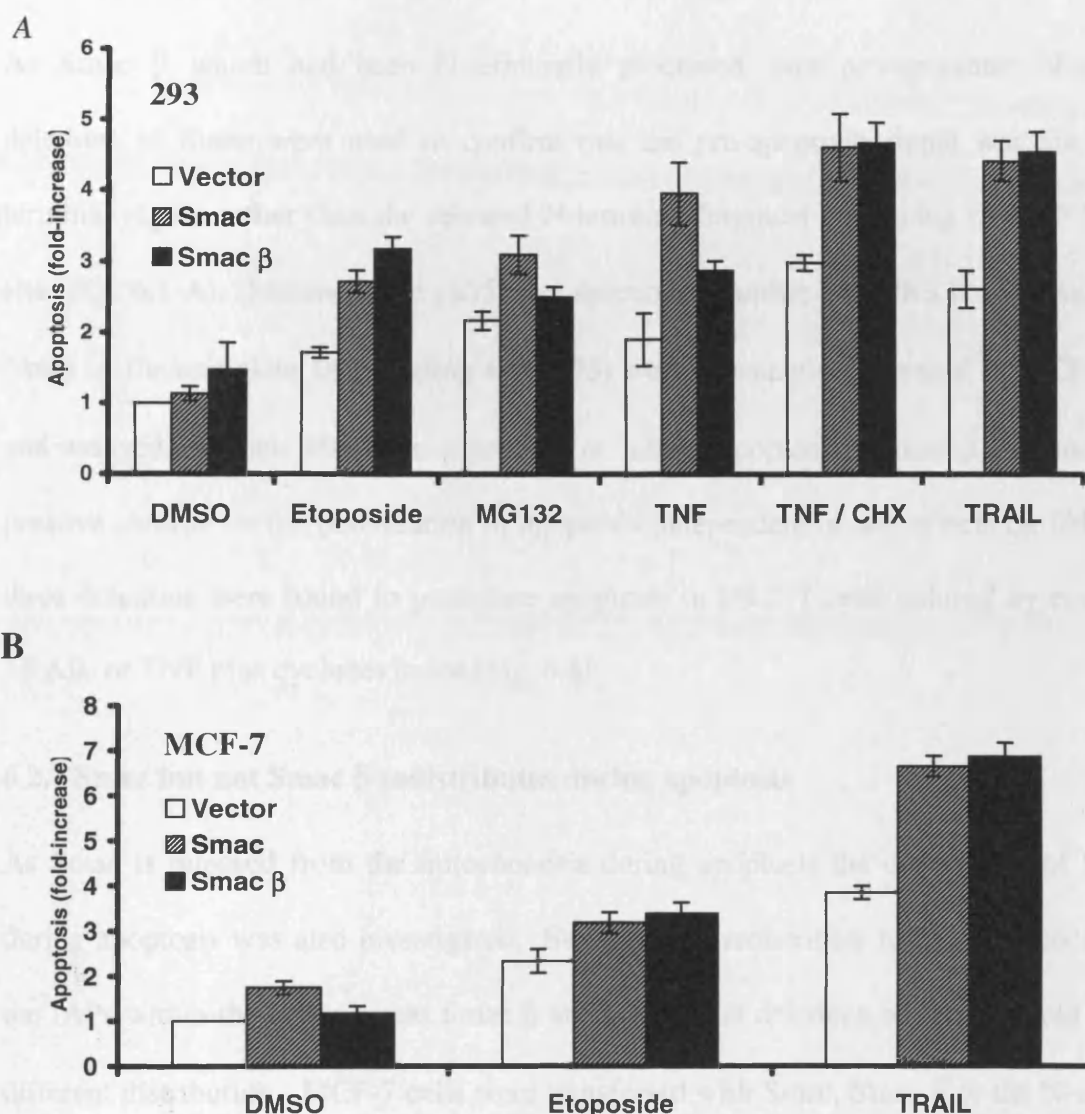


**Figure 6.7 Smac β potentiates apoptosis**

(A) 293 and (B) MCF-7 cells were co-transfected with either empty vector, Smac or Smac β together with pRSC *lacZ*. Similar levels of transfected proteins were expressed (data not shown). After 24 h, cells were treated for 6 h with 0.1% DMSO (vehicle control), etoposide (10 μM), MG132 (0.1 μM), TRAIL (0.25 μg/ml in MCF-7 or 1 μg/ml 293 cells) or TNF (10 ng/ml) in the presence or absence of cycloheximide (1 μM). Cells were then fixed and stained with X-gal. Apoptosis was assessed by morphological analysis and expressed as a percentage of transfected (blue) cells. The extent of apoptosis represents the fold-increase increase over DMSO-treated cells transfected with empty vector. The bars represent the Mean ± S.E. of three independent experiments performed in triplicate (n=3). In all experiments, the potentiation of apoptosis by Smac and Smac β was significantly different (p<0.05) from the vector controls as assessed by single factor ANOVA.

### 6.2.6 N-terminal deletion mutants of Smac are pro-apoptotic

As Smac  $\beta$  which had been N-terminally processed, was pro-apoptotic, N-terminal deletions of Smac were used to confirm that the pro-apoptotic signal was via the C-terminal region rather than the released N-terminal fragment containing the IAP binding site (Fig. 6.1 A). Mature Smac ( $\Delta 55$ ) and deletions of either the BIR3 binding site alone ( $\Delta 60$ ) or the complete IAP binding site ( $\Delta 75$ ) were transiently expressed in MCF-7 cells and assayed for their ability to potentiate or inhibit apoptosis. Smac  $\beta$  was used as a positive control for the potentiation of apoptosis independent of any effects on IAPs. All three deletions were found to potentiate apoptosis in MCF-7 cells induced by etoposide, TRAIL or TNF plus cycloheximide (Fig. 6.8).

### 6.2.7 Smac but not Smac $\beta$ redistributes during apoptosis

As Smac is released from the mitochondria during apoptosis the distribution of Smac  $\beta$  during apoptosis was also investigated. Smac should redistribute to the same location as the IAPs within the cell whereas Smac  $\beta$  and N-terminal deletions of Smac should show a different distribution. MCF-7 cells were transfected with Smac, Smac  $\beta$  or the N-terminal deletions of Smac and stained with anti- HSV 24 h after transfection (Fig. 6.9). Both Smac- and Smac  $\beta$ - transfected cells were treated with either etoposide or TRAIL for 3 h to induce apoptosis before staining. Smac redistributed from the mitochondria (Fig. 6.9 A) to the cytosol and in some apoptotic cells redistributed to the cell periphery (Fig. 6.9 B and C) in a manner similar to Smac  $\beta$ . Smac  $\beta$  did not redistribute from the cell cortex but displayed a more punctate staining in this region of some cells (Fig. 6.9 D to F). Deletion mutants of Smac were localized to the cell cortex (Fig. 6.9 G to I) similar to Smac released during apoptosis and Smac  $\beta$ .

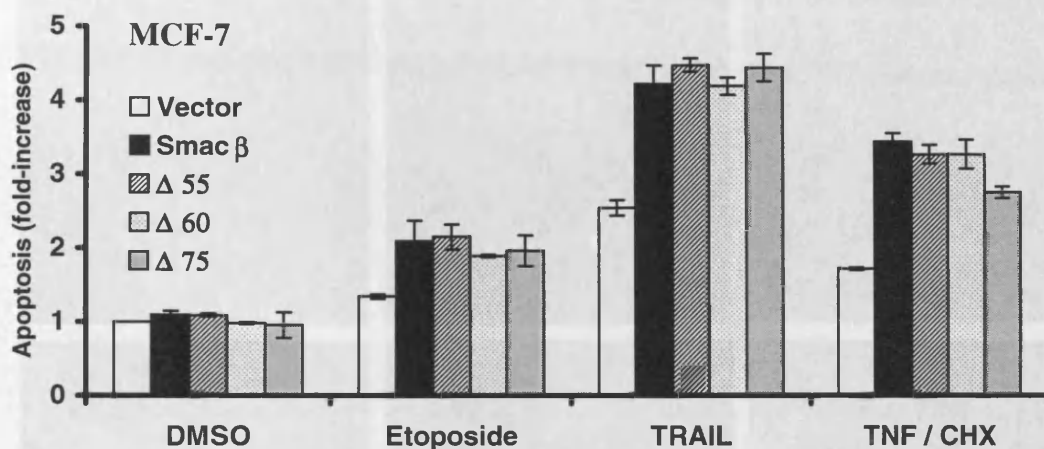


**Figure 6.8 N-terminal deletions of Smac are pro-apoptotic**

MCF-7 cells were co-transfected with either empty vector, Smac  $\beta$  or N-terminal deletions of Smac together with pRSC *lacZ*. Similar levels of transfected proteins were expressed (data not shown). After 24 h, cells were treated for 6 h with 0.1% DMSO (vehicle control), etoposide (10  $\mu$ M), TRAIL (0.25  $\mu$ g/ml) or TNF (10 ng/ml) in the presence of cycloheximide (1  $\mu$ M). Apoptosis was assessed as described earlier for full length Smac and Smac  $\beta$ . The bars represent the Mean  $\pm$  S.E. of three independent experiments performed in triplicate (n=3). All experiments demonstrated a significant ( $p < 0.05$ ) potentiation of apoptosis by Smac  $\beta$  and the deletion mutants as assessed by single factor ANOVA.

**Figure 6.9 Smac but not Smac  $\beta$  redistributes during apoptosis**

MCF-7 cells were transfected with Smac (A to C), Smac  $\beta$  (D to F) or deletion mutants of Smac (G to I). Cells were then treated with 0.25  $\mu$ g/ml TRAIL (B and E) or 10 ng/ml etoposide (C and F) for 3 hours and stained with anti-PSY (green), MitoTracker™ (red) and Hoechst 33258 (blue). Smac redistributed from the nucleus (A) to the periphery of the cell during late stages (B and C - arrows) of apoptosis. Smac  $\beta$  was found at the cell cortex in normal (D) and did not redistribute to apoptotic cells (E and F - arrows). N-terminal deletions of Smac ( $\Delta 55$  - G,  $\Delta 60$  - H, and  $\Delta 75$  - I) were localized to the cell cortex.

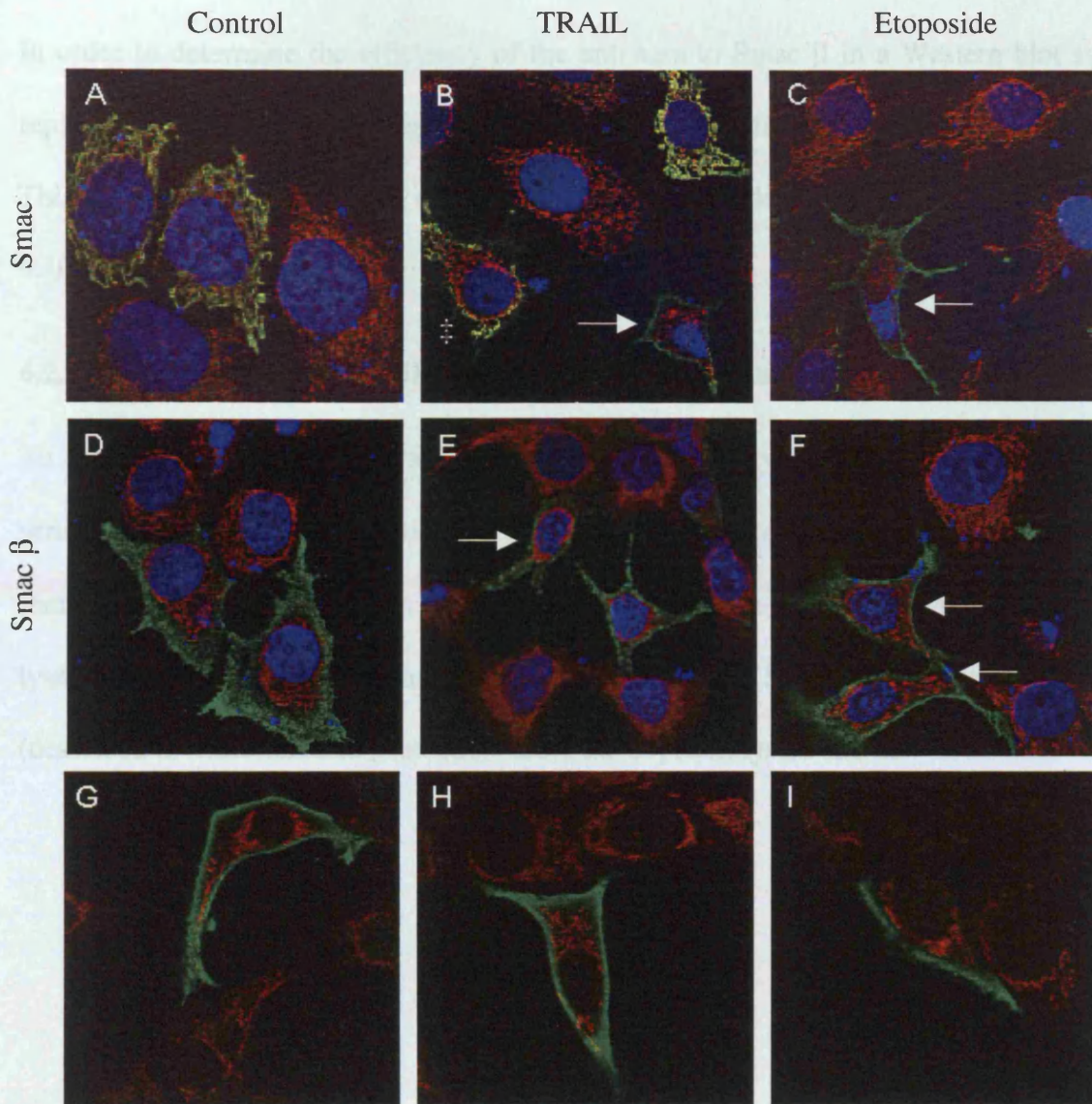


**Figure 6.9 Smac but not Smac  $\beta$  redistributes during apoptosis**

MCF-7 cells were transfected with Smac (A to C), Smac  $\beta$  (D to F) or deletion mutants of Smac (G to I). Cells were then treated with 0.25 $\mu$ g/ml TRAIL (B and E) or 10 $\mu$ M etoposide (C and F) for 3 hours and stained with anti- HSV (green), MitoTracker<sup>TM</sup> (red) and Hoechst 33258 (blue). Smac redistributed from the mitochondria (A) to the periphery of the cell during late stages (B and C -arrows) and early stages (B - ‡) of apoptosis. Smac  $\beta$  was found at the cell cortex in normal (D) and did not redistribute in apoptotic cells (E and F - arrows). N-terminal deletions of Smac ( $\Delta$ 55 - G,  $\Delta$ 60 - H, and  $\Delta$ 75 - I) were localized to the cell cortex.

### **6.2.8 Characterisation of anti- Smac $\beta$ antibody by Western blot analysis**

In order to determine the efficiency of the anti-sera to Smac  $\beta$  in a Western blot system replicate membranes were prepared and probed with different dilutions of the anti-sera. This then allowed the optimal dilution of antibody to be determined for each animal (Fig. 6.10).

### **6.2.9 Use of anti- Smac $\beta$ antibody for immuno-precipitation**

To confirm the antibody was able to recognize the tertiary structure of Smac / Smac  $\beta$  a series of test immunoprecipitations were performed. Lysates were prepared from 293 cells transfected with empty vector, Smac or Smac  $\beta$  and non-transfected MCF-7 cells. The lysates were immunoprecipitated with either XIAP or Smac using standard methods (described in Materials and Methods). Both the depleted lysate and the

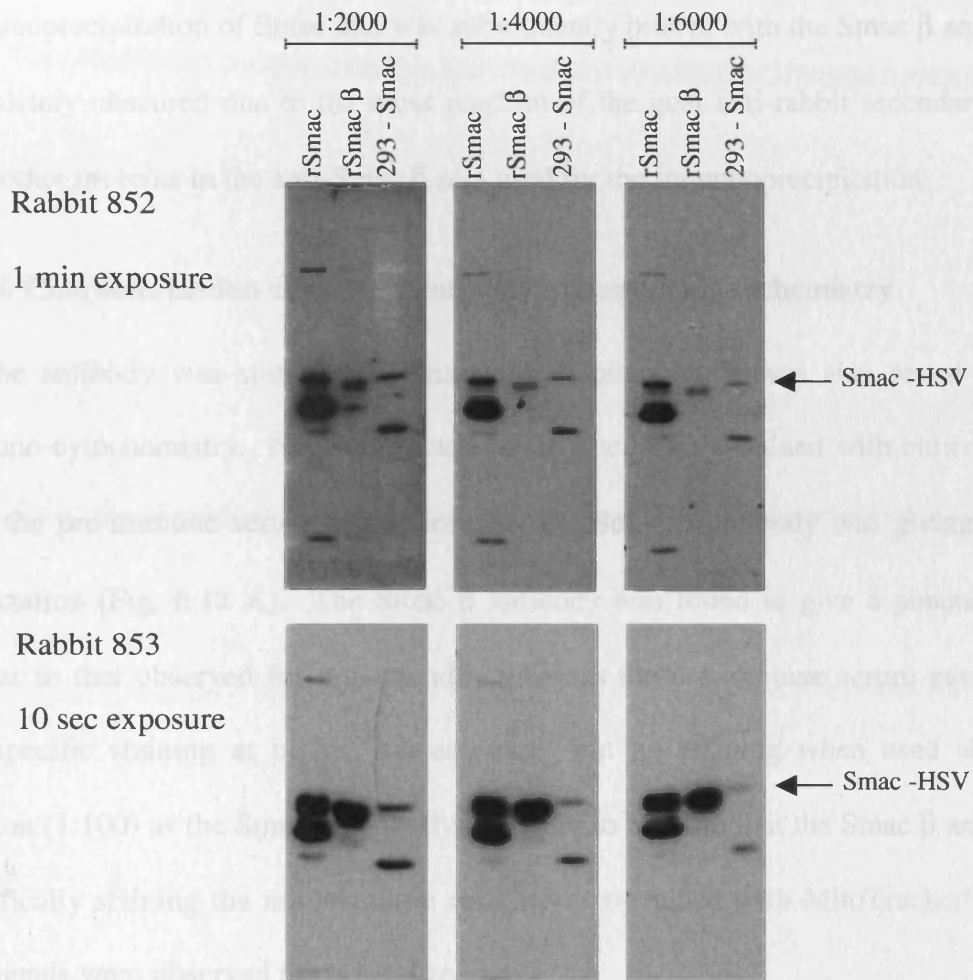


**Figure 6.10 Use of anti-Smac  $\beta$  in Western blotting**

Serum from either rabbit 852 (upper panel) or 853 (lower panel) was diluted 1:2000, 1:4000, or 1:6000 and used to probe identical Western blots. This demonstrated that the antibody recognised recombinant Smac and recombinant Smac  $\beta$  as well as HSV-tagged Smac expressed in 293 cells (arrow). Serum from rabbit 853 gave a significantly stronger signal requiring only a 10 second exposure of the film compared with than that from rabbit 852 (1 minute).

immunoprecipitated complexes were then probed for XIAP (Fig. 6.11) or Smac. The immunoprecipitation of Smac that was subsequently probed with the Smac  $\beta$  antibody was completely obscured due to the cross reaction of the goat anti-rabbit secondary antibody with other proteins in the anti-Smac  $\beta$  sera used for the immunoprecipitation.

#### **6.2.10 Characterisation of Smac $\beta$ antibody in immuno-cytochemistry**

As the antibody was suitable for immuno-precipitations, it was also tested for use in immuno-cytochemistry. Non-transfected MCF-7 cells were stained with either anti-Smac  $\beta$  or the pre-immune serum to confirm that the Smac  $\beta$  antibody was giving a specific localization (Fig. 6.12 A). The Smac  $\beta$  antibody was found to give a punctate staining similar to that observed for mitochondria whereas the pre-immune serum gave a diffuse non-specific staining at higher concentrations but no staining when used at the same dilution (1:100) as the Smac  $\beta$  antibody. In order to confirm that the Smac  $\beta$  antibody was specifically staining the mitochondria cells were co-stained with MitoTracker™ Red and the signals were observed to co-localize.

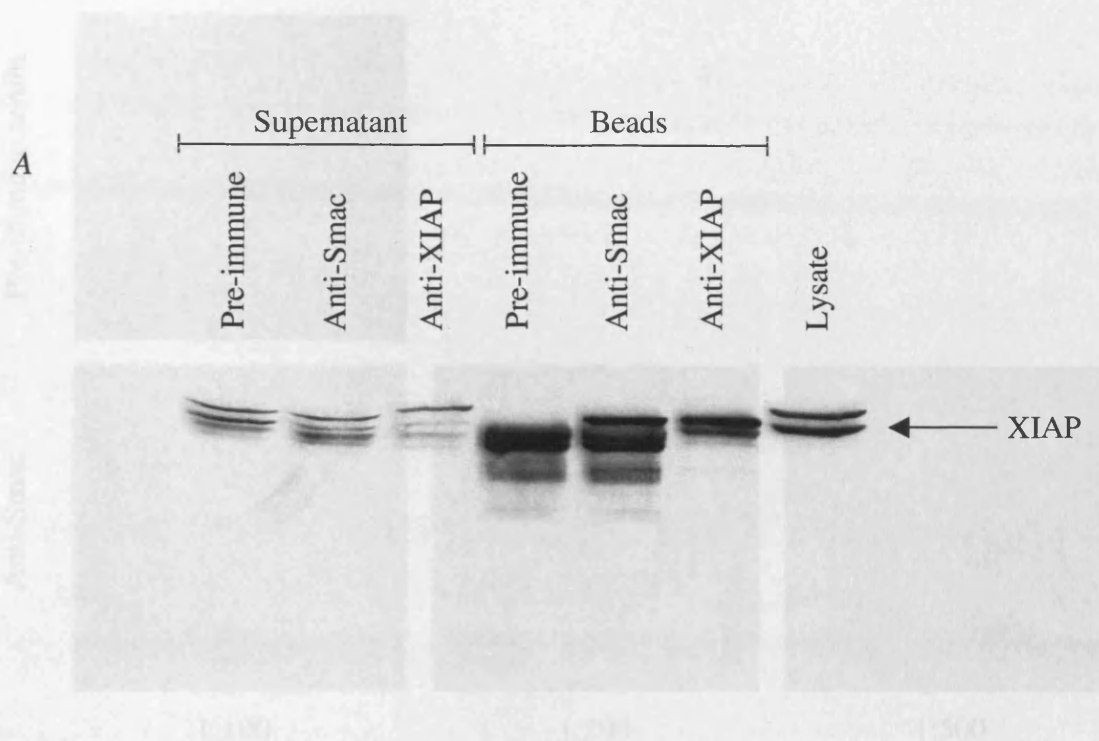


**Figure 6.11 Anti-Smac is suitable for immuno-precipitations**

Lysate was prepared from non-transfected MCF-7 cells and immuno-precipitations performed with pre-immune serum, anti-Smac serum and anti-XIAP. Immuno-precipitated proteins were then probed for XIAP (A).

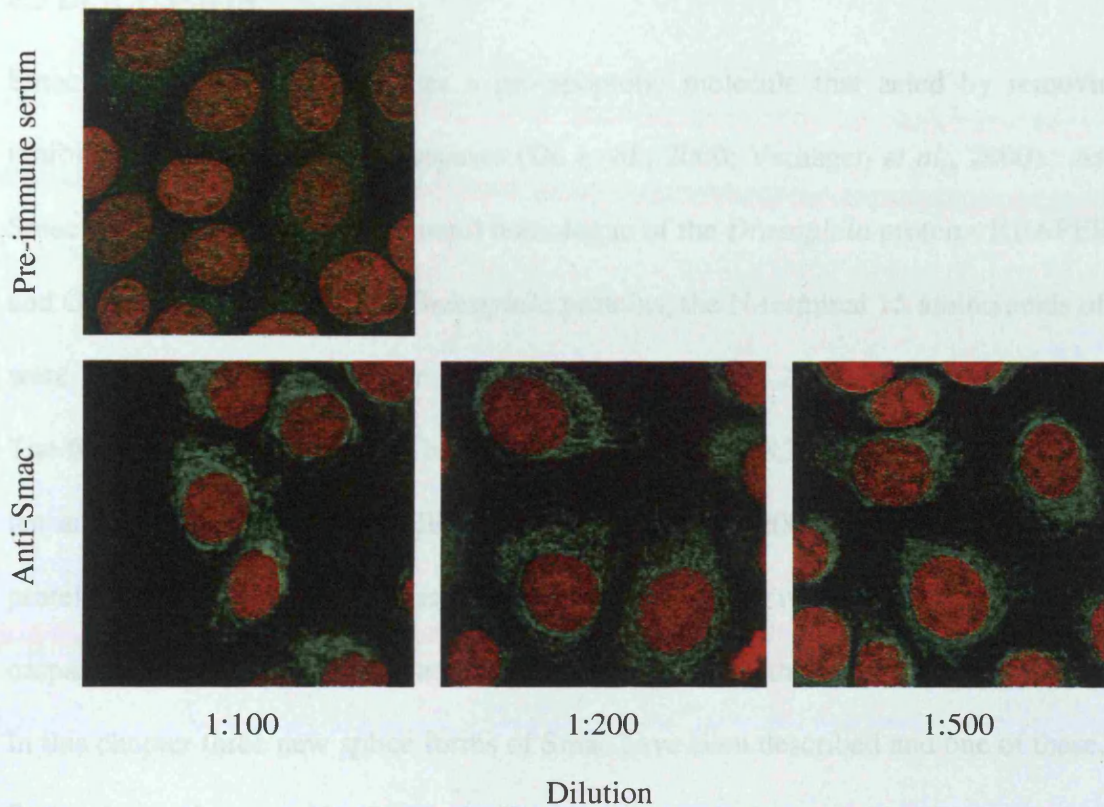


**Figure 6.12 Anti-Smac is suitable for use in immuno-cytochemistry**

MCF-7 cells were stained with either pre-immune serum or anti-Smac  $\beta$  from rabbit 853 and the nuclei counter stained with propidium iodide. Pre-immune serum did not give any staining at the same dilution (1:100) giving mitochondrial staining with the anti-Smac serum.

### 6.3 DISCUSSION

Smac was recently described as a pro-apoptotic molecule that acted by removing the inhibitory action of IAPs on caspases (Du *et al.*, 2000; Verhagen *et al.*, 2000). As such, Smac was thought to be a functional homologue of the *Drosophila* proteins REAPER, HID and GRIM. As with the three *Drosophila* proteins, the N-terminal 15 amino acids of Smac were found to be necessary for IAP binding (Chai *et al.*, 2000; Srinivasula *et al.*, 2000). The first five amino acids have been shown to bind the BIR3 domain of XIAP and the next ten amino acids bind to the BIR2 domain (Chai *et al.*, 2000). Smac is a mitochondrial protein released during apoptosis and as XIAP is primarily responsible for the inhibition of caspases -9 and -3 it is likely that Smac acts at the level of the apoptosome.

In this chapter three new splice forms of Smac have been described and one of these, Smac  $\beta$ , has been shown to be N-terminally processed which results in the loss of the IAP binding domain. Processed Smac  $\beta$  is localized to the cell cortex and does not redistribute during apoptosis whereas Smac is released from the mitochondria and redistributed to the cell cortex. Both the processed form of Smac  $\beta$  and N-terminal deletions of Smac were also demonstrated to potentiate apoptosis induced by a wide range of stimuli. This data indicates that Smac does not require XIAP binding for its pro-apoptotic activity. The development of a polyclonal Smac  $\beta$  antibody suitable for Western blotting, immunoprecipitation and immuno-cytochemistry is also described.

The alternative splicing of Smac could potentially result in drastic alterations in either its distribution or function. Smac  $\beta$ , which lacks the MTS and the first five amino acids of the IAP binding site, has been shown to be localized to the cell cortex and to be pro-apoptotic but unable to bind IAPs due to N-terminal processing. Smac  $\gamma$  lacks exons 2 and 3 and as such has a truncated MTS and IAP binding site that may result in a difference in distribution and IAP binding properties. Smac  $\delta$  lacks exon 4 which contains the BIR2

binding domain, this would result in a mitochondrial protein which would have a reduced IAP binding efficiency.

Smac  $\beta$  appears to be localized to the cell cortex based on both confocal microscopy and cell fractionation studies. This distribution did not alter during apoptosis induced by both death receptor and chemical stimuli, which indicates that Smac  $\beta$  exerts its pro-apoptotic function in the region of the cell cortex. As N-terminal truncations of Smac were pro-apoptotic and localized to the cell cortex, it is likely that Smac plays a pro-apoptotic role in the cortex. Identification of other Smac binding proteins could provide clues as to the function of Smac and Smac  $\beta$  in the cell cortex.

Smac exists as a dimer in cells and runs at approximately 100 kDa due to its conformation based on its X-ray crystal structure (Chai *et al.*, 2000). Gel filtration has revealed that Smac  $\beta$  elutes at a smaller size than Smac and both proteins elute over a wide range of sizes. Smac probably elutes over a wide range of sizes, as Smac dimers will also bind to XIAP thereby increasing the size of the complex. Smac  $\beta$  however elutes at the predicted size of the Smac dimer and as well as associated with smaller complexes. This could indicate that Smac  $\beta$  exists as a monomer and in complex with other proteins. The N-terminal cleavage of Smac  $\beta$  may disrupt the dimerization interface resulting in Smac  $\beta$  being unable to form dimers (Fig. 6.13). If Smac  $\beta$  was demonstrated to exist as a monomer rather than as a dimer this would indicate that dimerization is required for IAP binding but not for the pro-apoptotic activity of this molecule.

The data presented in this chapter also demonstrates that the affinity of Smac for XIAP is far greater than for c-IAP-1 or c-IAP-2 in a cellular context. This may be due to differential localization of the IAPs within the cell but due to the poor availability of antibodies suitable for immunocytochemistry this hypothesis has not been investigated.

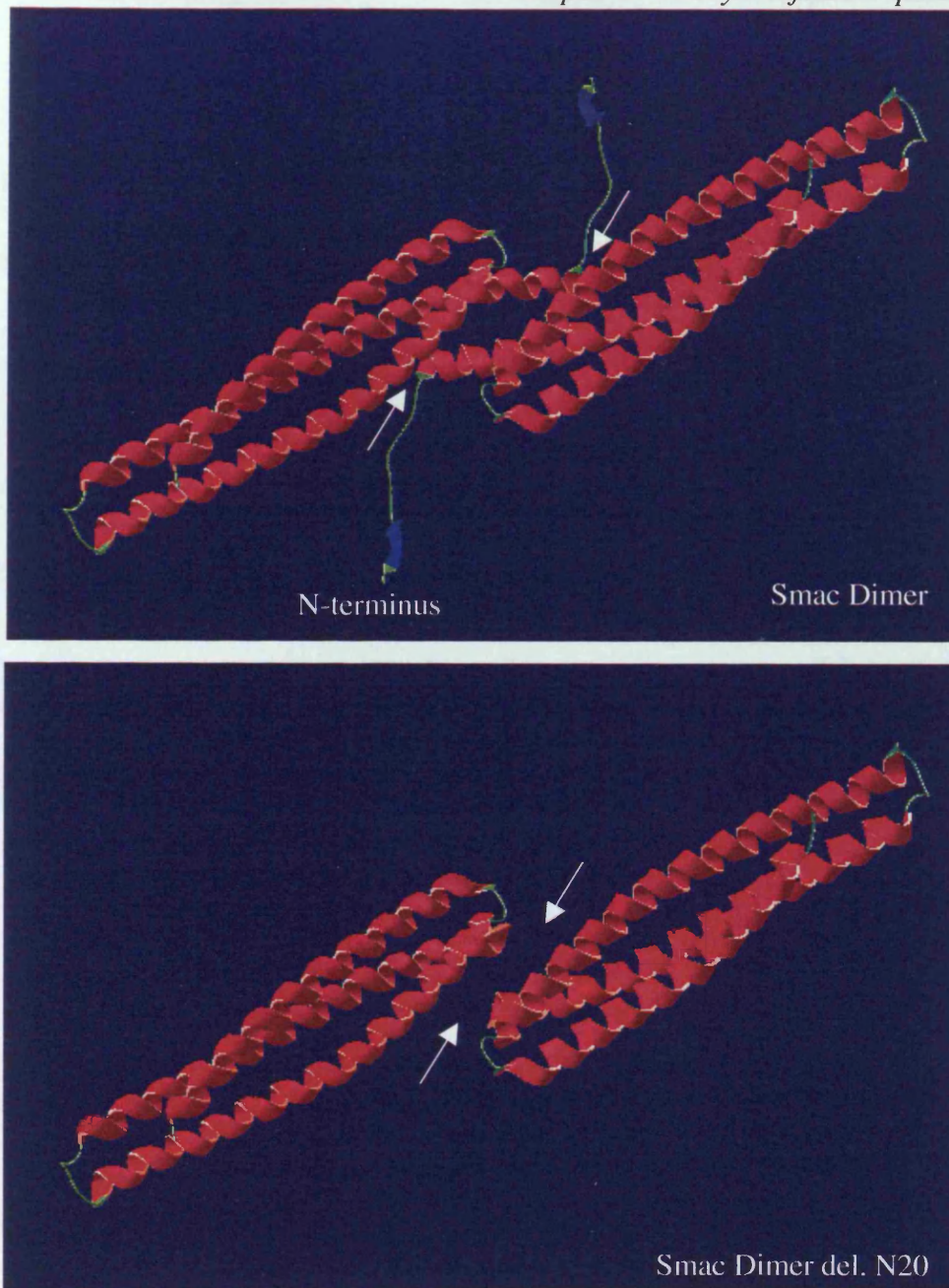


**Figure 6.13 N-terminal truncation of Smac may disrupt the dimerization interface**

Structure of a Smac dimer (upper panel) and the effect of deletion of the N-terminal 20 amino acids (lower panel). The dimerization interface is indicated by arrows and the N-terminus of the full-length mature protein is labelled. Structures modified from the PDB 1G73 using the DeepView program.

In summary the data demonstrates that Smac does not require XIAP binding to exert its pro-apoptotic effect and therefore can act in an IAP independent manner. Data presented in this chapter has been published (Roberts *et al.*, 2001).

**CHAPTER 7: DISCUSSION**

## 7.1 DISCUSSION

The data presented in the previous chapters is aimed at clarifying the role played by two of the key mediators of apoptosis induced by cancer chemotherapeutic agents in humans, APAF1 and Smac. By dissecting the mechanisms by which these proteins, and others like them, act within the cell the various mechanisms by which they are regulated become apparent and the molecular framework in which they operate is more clearly understood. This may then be used in the design of therapeutic approaches to treat disorders in which the apoptotic pathway has become disrupted. As alternative splicing is one of the major mechanisms whereby a cell alters the function of endogenous proteins, examining the alternatively spliced forms of such key molecules can help in the identification of important regulatory domains and binding sites within these proteins.

### 7.1.1 APAF1

Apoptotic-Protease-Activating-Factor 1 (APAF1) was the first CED-4 homologue identified in humans and as alternative splicing of CED-4 alters its function from a pro-apoptotic protein to an anti-apoptotic one (Chaudhary *et al.*, 1998) an investigation to determine if APAF1 was also alternatively spliced was undertaken. By analysing sequences within the GenBank database several sequences of interest were identified and it became apparent that several splice variants of APAF1 existed. One of these sequences (Acc # AA348011 and Acc # AA348012) involved the loss of approximately 1.5 kB within the 3' UTR of the APAF1 mRNA. The significance of this loss is unclear but this splicing event may have an impact upon the translation of the mRNA as both the 5' UTR and the 3' UTR are involved in the formation of the translational machinery. Alternatively, this splicing event may simply be a polymorphism within the population. Identification of a

second splicing event within the WD40 region of APAF1 was also found using database searching and revealed a cDNA containing an additional 132 bp that resulted in the insertion of an additional 44 amino acids with no effect on the reading frame (Acc # AB007873). Analysis of this splice variant revealed that it introduced an additional WD40 repeat in APAF1. This was achieved by splitting an existing repeat and by introducing a new C-terminus and a new N-terminus to the remainder of the original repeat. RT-PCR demonstrated that these two forms were not tissue-specific, nor were they due to the transformed nature of the cells initially tested and it was also demonstrated that only the long form (APAF1WD13) existed in the rat. RT-PCR also indicated that no splicing events occurred within the CARD or CED-4 regions of APAF1. By identifying genomic clones of APAF1 this cDNA was identified as a true splice form that arises from alternative splicing of exon 18 in humans, although this splicing event does not occur in rat. During this time several other groups reported the existence of APAF1 splice forms (Benedict *et al.*, 2000; Hahn *et al.*, 1999; Saleh *et al.*, 1999; Zou *et al.*, 1999) and further RT-PCR analysis confirmed the alternative splicing of exon 3A in both human and rat tissue with alternative splicing of exon 25 only evident in human samples. The presence of both APAF1 and APAF1WD13 / APAF1LWD13 at the protein level in human cells and only APAF1WD13 / APAF1LWD13 in rat cells was confirmed by western blotting. As only the APAF1 forms that contain exons 18 and 25 are found to be expressed in rat cells the alternative splicing of exon 3A probably arose earlier in evolution than the splicing of these two exons. Therefore the alternative splicing of exon 3A is probably of more functional significance than the other splicing events. As the exon 3A splicing event introduces 11 amino acids between the CARD and CED-4 regions of APAF1, spacing between these two crucial domains may influence their function. Introduction of these additional amino acids may also result in altered binding of the WD40 region to this region

either by enhancing or reducing its inhibitory effect. Addition of these few amino acids may also affect the structure of the dATP binding region thereby altering its function. The alternative splicing of the WD40 region and the introduction of an additional repeat may result in altered cytochrome *c* binding (Benedict *et al.*, 2000). As WD40 repeats often form  $\beta$ -propeller structures in other proteins, such as the G $\beta$  proteins (Garcia-Higuera *et al.*, 1996; Smith *et al.*, 1999) (Figure 7.1 A) it is possible that they assume a similar structure in APAF1. The  $\beta$  propeller structure is composed of seven WD40 repeats in the G $\beta$  proteins, therefore the WD40 repeats in APAF1 could form a single large propeller with 12 blades or two propellers with six blades each. The formation of two propellers is the more likely of the two options due to the spacing between the repeats. If they were to form a single propeller the spacing between the repeats would have to be approximately equal to allow the repeats to assume the correct conformation. In APAF1 the WD40 repeats are in two clusters of six repeats with a relatively large gap between the clusters. This would allow the two groups of repeats to form independent propellers with the gap between the clusters acting as a linker between the two. The introduction of an additional repeat into the N-terminal group of repeats would result in the formation of a seven-bladed propeller followed by a six-bladed propeller. As each propeller has three binding surfaces, top, bottom and side of the cylindrical structure (Figure 7.1A), having two differently sized propellers would alter the binding of proteins to the sides of these propellers (Figure 7.1B). If the two propellers were of equal size they would be able to align with each other and present a broader binding surface on the side of the structure. Having two differently sized propellers alters the topology of the structure around the circumference without significantly altering the top and bottom binding surfaces. As the introduction of an additional WD40 repeat has an effect on

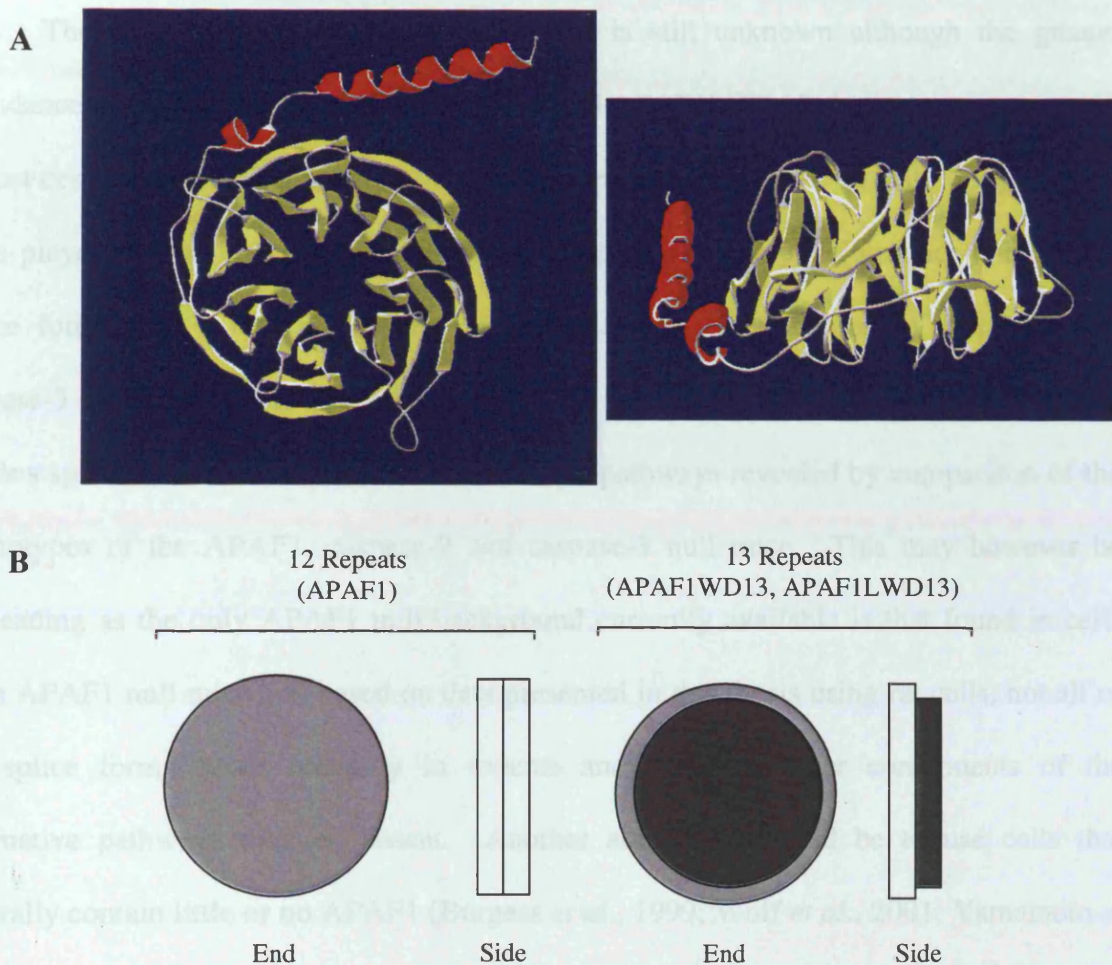


**Figure 7.1 Model of the  $\beta$ -propeller structure assumed by WD40 repeats**

The WD40 repeat protein G $\beta$  has been found to assume a  $\beta$ -propeller structure with each of the seven repeats forming a blade of the propeller (A - yellow). Views are shown from the top (left) and side (right). The WD40 repeats of APAF1 may form two propellers and the insertion of an additional WD40 repeat would alter the binding surfaces where these two propellers interact (B).

cytochrome *c* binding the site of interaction may involve residues on the circumference of both propellers. This alteration in structure may also affect the binding of the WD40 region to the CARD / CED-4 portion of the protein. This is less likely, as the larger binding surfaces would be unaffected by this change in structure and it would require great

flexibility of the protein in order to allow binding of the CARD / CED-4 region to the outer edge of the propellers.

The roles played by these splice forms is still unknown although the greater abundance of the longer forms (APAF1WD13 and APAF1LWD13) indicates that these are almost certainly more important in the apoptotic pathway. In order to truly determine the roles played by the various splice forms it would be necessary to introduce each of the splice forms into a null background and then assess the activation of caspase-9 and caspase-3 in response to various stimuli. This would help to determine which of the various splice forms are involved in the different pathways revealed by comparison of the phenotypes of the APAF1, caspase-9 and caspase-3 null mice. This may however be misleading as the only APAF1 null background currently available is that found in cells from APAF1 null mice and based on data presented in this thesis using rat cells, not all of the splice forms occur naturally in rodents and therefore other components of the alternative pathways may be absent. Another alternative would be to use cells that naturally contain little or no APAF1 (Burgess *et al.*, 1999; Wolf *et al.*, 2001; Yamamoto *et al.*, 2000), although as many of these are tumour cells they all are likely to have down-regulated other components of the apoptotic pathway in addition to APAF1.

APAF1 forms an apoptosome in 293 cells and during apoptosis APAF1 itself is cleaved by caspases. The purpose of caspase-mediated cleavage of APAF1 at SVTD<sup>260</sup> is unclear and may merely be a “bystander” effect of caspase activation. Although cleavage of APAF1 appeared to occur primarily in the inactive ~1.4 MDa apoptosome this is probably only because the cleavage site is available in this complex. However, the cleavage of APAF1 in the ~1.4MDa apoptosome and not in the ~700 kDa apoptosome does give some clues as to the relative structure of APAF1 in these two complexes. The caspase cleavage site in APAF1 is located within the CED-4 region. This region may be

involved in APAF1 oligomerization (Hu *et al.*, 1999b; Srinivasula *et al.*, 1998) and molecular modelling has predicted that CED-4 oligomerizes into hexamers in order to activate CED-3. Therefore as the CED-4 region of APAF1 is predicted to form a similar structure (Jaroszewski *et al.*, 2000) APAF1 would be predicted to form hexamers in order to activate caspase-9. In this model, the caspase cleavage site would therefore be buried within the correctly formed complex and the caspases would then not be able to access it. This combined with the reported lack of caspase-activating activity in the ~1.4 MDa complex (Cain *et al.*, 2000) suggests that this complex is incorrectly formed and supports the hypothesis that the correctly formed complex is the ~700 kDa complex observed in apoptotic cells. Another possibility is the presence of an inhibitory protein within the ~1.4 MDa complex, but to date only NAC has been reported to associate with this complex and enhance the activity of the complex (Chu *et al.*, 2001). As FLAG-tagged APAF1 undergoes this cleavage event mediated by caspases upon induction of apoptosis it is likely that it is also associated with the incorrectly formed complex. This hypothesis is further supported by the association of T7-caspase-9 and FLAG-APAF1 in un-activated 293 cell lysates and the fact this association is detected in a complex of ~700 kDa or larger in control cells. Unfortunately, this meant that FLAG-APAF1 is not suitable for use as a tool in the purification of the apoptosome and is also not suited for experiments aimed at identifying novel components of the ~700 kDa apoptosome. It may still be of use in investigating possible regulatory proteins by determining if they are able to prevent the association between caspase-9 and FLAG-APAF1 in control cells especially if this allowed FLAG-APAF1 to form an active ~700 kDa apoptosome. By combining the predicted accessibility of various enzymatic cleavage sites, such as trypsin cleavage sites, using various programmes available via the internet, and the structural data available for APAF1 it should be possible to determine the accuracy of the hypothetical models of the CED-4

and WD40 regions. This should then allow one to map sites of interaction within the protein by a method similar in principle to that of the RNase protection assay as various cleavage sites will be concealed by interactions with the protein. This would then allow a comparison between the cleavage products produced from APAF1 with and without associated proteins. The size of the fragments missing in the sample with associated proteins can then be used to predict the region involved in the interaction.

Data in this thesis also demonstrates that caspase-9 associates with APAF1 via a CARD / CARD interaction as previously reported (Li *et al.*, 1997; Srinivasula *et al.*, 1998; Zou *et al.*, 1999) and that this interaction is enhanced by the presence of the CED-4 region of APAF1. This could be either due to a CED-4-induced change in the structure of the APAF1-CARD or an interaction between the CED-4 region of APAF1 and caspase-9. The CED-4 region is unlikely to cause a change in the structure of the CARD as the structure of the CARD has been solved both alone and in complex with the CARD of caspase-9 (Chou *et al.*, 1998; Day *et al.*, 1999; Qin *et al.*, 1999; Vaughn *et al.*, 1999; Zhou *et al.*, 1999b). These studies revealed that this binding is extremely tight and that it does not change significantly upon binding of the CARD of caspase-9. An interaction between CED-4 and the protease domain of CED-3 has been previously described (Chaudhary *et al.*, 1998) and a similar interaction may occur between the CED-4 region of APAF1 and the protease domain of caspase-9. The residues involved in the interaction between CED-4 and CED-3 are between the Walkers A and B boxes, which are homologous to the same region in APAF1. This would however require caspase-9 to bind in parallel to APAF1 and would be opposed to the current model of anti-parallel binding (Figure 7.2). This interaction could be further investigated by using deletion mutants to obtain binding constants for caspase-9 with the CARD as opposed to the CARD / CED-4 region of APAF1. This interaction could also be mapped using trypsin digestion as in the anti-parallel binding model the

trypsin cleavage sites in caspase-9 would be exposed in all but the CARD domain, whereas in the parallel binding model binding to APAF1 would protect these sites. Parallel binding of caspase-9 to APAF1 would allow APAF1 to assume the role of one half of the heterotetramer

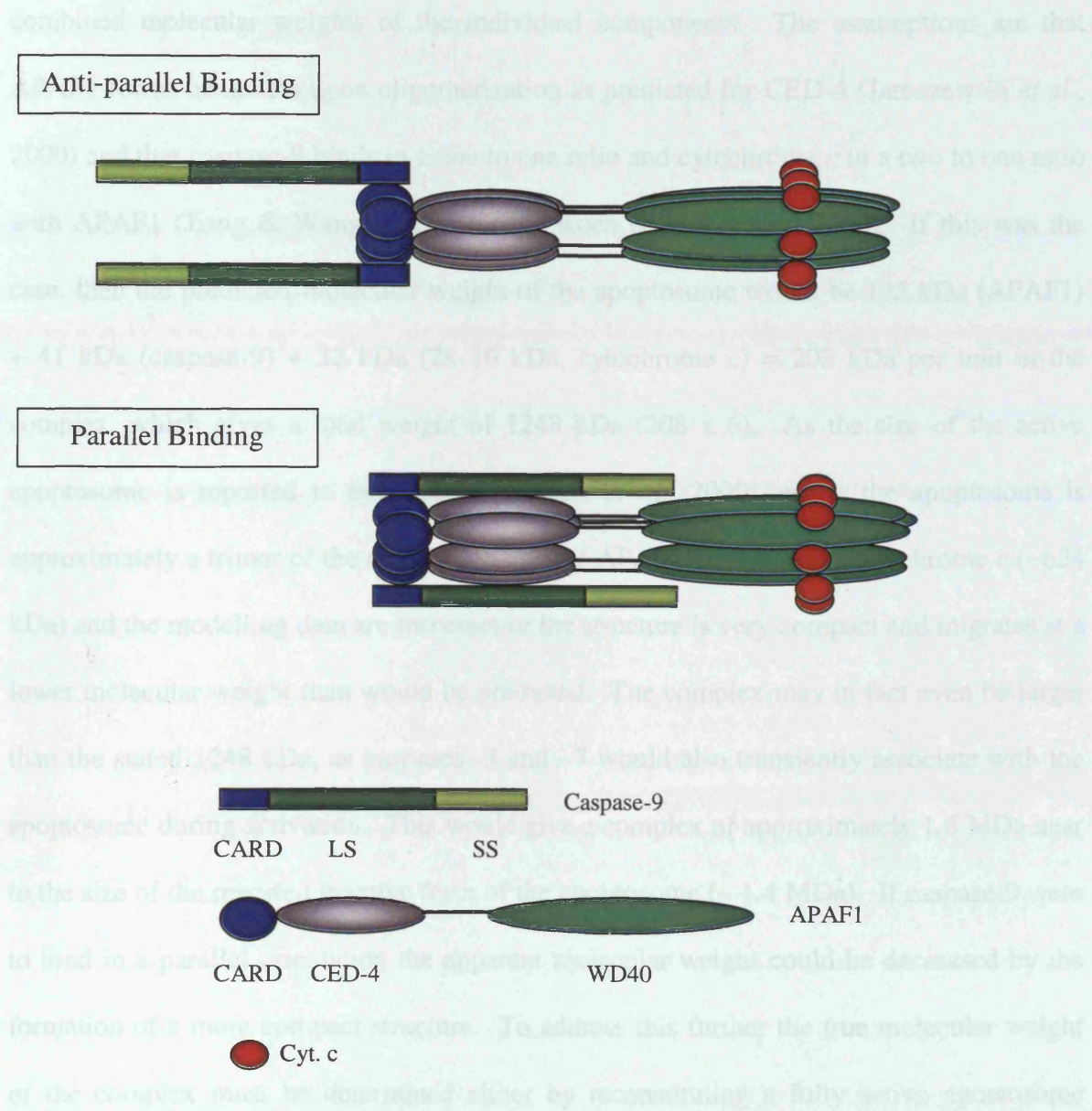


**Figure 7.2 Opposing models for the binding of caspase-9 to APAF1**

Binding of caspase-9 to APAF1 can occur in two orientations either parallel (N-termini together and C-termini together) or anti-parallel (N-termini together C-termini at opposite ends). Parallel binding would allow interaction between the CED-4 region of APAF1 (grey) and the large (LS) and small (SS) subunits of caspase-9.

a conformation that active caspases normally assume. This is consistent with the hypothesis that the complex of caspase-9 and APAF1 forms a holoenzyme and that caspase-9 requires APAF1 binding for activity (Rodriguez & Lazebnik, 1999). This may also help explain the discrepancy between the observed size of the apoptosome and the combined molecular weights of the individual components. The assumptions are that APAF1 forms hexamers upon oligomerization as predicted for CED-4 (Jaroszewski *et al.*, 2000) and that caspase-9 binds in a one to one ratio and cytochrome *c* in a two to one ratio with APAF1 (Jiang & Wang, 2000; Purring-Koch & McLendon, 2000). If this was the case, then the predicted molecular weight of the apoptosome would be 135 kDa (APAF1) + 41 kDa (caspase-9) + 32 kDa (2x 16 kDa, cytochrome *c*) = 208 kDa per unit in the complex, which gives a total weight of 1248 kDa (208 x 6). As the size of the active apoptosome is reported to be ~700 kDa (Cain *et al.*, 2000), either the apoptosome is approximately a trimer of the active “subunit” of APAF1 / caspase-9 / cytochrome *c* (~624 kDa) and the modelling data are incorrect or the structure is very compact and migrates at a lower molecular weight than would be predicted. The complex may in fact even be larger than the stated 1248 kDa, as caspases -3 and -7 would also transiently associate with the apoptosome during activation. This would give a complex of approximately 1.6 MDa near to the size of the reported inactive form of the apoptosome (~ 1.4 MDa). If caspase-9 were to bind in a parallel orientation the apparent molecular weight could be decreased by the formation of a more compact structure. To address this further the true molecular weight of the complex must be determined either by reconstituting a fully active apoptosome using recombinant components and determining their stoichiometry or by identifying each of the components and their relative amounts in a “pure” apoptosome isolated from cells undergoing apoptosis.

### 7.1.2 Smac and Smac $\beta$

Smac and its murine homologue DIABLO were initially identified based on their ability to bind IAP family members and suppress their inhibitory action on caspases (Du *et al.*, 2000; Verhagen *et al.*, 2000). Smac is targeted to the mitochondria by a classical mitochondrial targeting signal sequence within its N-terminus and is only released from mitochondria upon exposure of the cell to an apoptotic stimulus. Once released Smac binds to IAP family members, in particular XIAP, thereby displacing them from active caspases (such as caspase-9) that have initially been activated following a simultaneous release of cytochrome *c* from the mitochondria (Ekert *et al.*, 2001). Further analysis has shown that this effect of Smac is due to competition for a similar XIAP binding motif present in auto-activated caspase-9 but absent in caspase-3-activated caspase-9 (Srinivasula *et al.*, 2001). Data presented in this thesis demonstrates the existence of a second splice form of Smac, Smac  $\beta$  that is localised to the cell cortex and lacks an IAP binding site following proteolytic maturation. Smac  $\beta$  and Smac deletion mutants, lacking the N-terminal IAP binding motif, retain their pro-apoptotic activity demonstrating that Smac can act independently of IAPs to induce apoptosis. The data also demonstrate that Smac has a far greater affinity for XIAP over c-IAP-1 and c-IAP-2 in a cellular lysate indicating that the anti-IAP role of Smac is restricted to XIAP and the pathways XIAP is involved in. Smac is proposed to be a mammalian homologue of the Reaper, Hid and Grim proteins found in *Drosophila* based upon a shared N-terminal IAP binding motif (Silke *et al.*, 2000). Reaper can however act independently of IAPs to induce apoptosis via its interaction with the *Drosophila* protein Scythe (Thress *et al.*, 1998). This binding of Reaper to Scythe causes the release of a sequestered cytochrome *c* releasing activity from Scythe and results in apoptosis (Thress *et al.*, 1999a). Scythe has also been shown to inhibit HSP70 protein folding activity and Reaper can in turn inhibit this function of

Scythe (Thress *et al.*, 2001). Therefore, as Smac possesses an IAP-independent pro-apoptotic activity it is likely to function in a manner similar to Reaper by either causing the release of a cytochrome *c* releasing activity from a human homologue of Scythe or by indirect regulation of HSP70 function. If Smac were to modulate the function of HSP70 it could indirectly affect the function of the apoptosome as HSP70 has been shown to inhibit both caspase-9 recruitment and activation in the apoptosome (Beere *et al.*, 2000; Saleh *et al.*, 2000). Smac has been shown to act independently of APAF1 and can be released independently of cytochrome *c* to activate caspase-9 (Chauhan *et al.*, 2001), suggesting separate release mechanisms for Smac and cytochrome *c*. In order to independently release Smac and retain cytochrome *c* the proteins must be in a different location within the mitochondria as Smac is approximately 10 kDa larger than cytochrome *c* and exists as a dimer (Chai *et al.*, 2000; Du *et al.*, 2000). Therefore the opening of a pore large enough to allow the transit of Smac would also be permeable to cytochrome *c*. As Smac possesses a classical mitochondrial targeting signal sequence it would be predicted to be targeted to the mitochondrial matrix and remain there whereas cytochrome *c* is known to be located in the intermembrane space. This would allow a pore that breached both membranes to selectively release Smac. Recently another mitochondrial protein, HtrA2 has been identified as a pro-apoptotic protein. HtrA2 is a serine protease and is also able to bind IAPs in a manner similar to Smac and is able to induce apoptosis via both its serine protease activity and its IAP binding ability (Hegde *et al.*, 2002; Martins *et al.*, 2002; Suzuki *et al.*, 2001a; Verhagen *et al.*, 2002). As the structure of Smac has already been solved (Chai *et al.*, 2000; Liu *et al.*, 2000; Wu *et al.*, 2000) it will now be interesting to develop a structural picture of the homology between Smac and HtrA2 in order to determine whether they share any other domains and bind the BIR domains of XIAP in the same manner. HtrA2, like Smac, contains a classical mitochondrial-targeting signal

sequence and therefore may reside in the same sub-mitochondrial compartment. Thus, by comparing the release dynamics of these two proteins it would be possible to determine whether they were released via the same mechanism. As Reaper is transcriptionally regulated by p53 there have been suggestions that Smac may also be regulated in the same manner (Du *et al.*, 2000) allowing transcriptional regulation of both Smac and APAF1 (Kannan *et al.*, 2001; Moroni *et al.*, 2001; Soengas *et al.*, 1999) by a single regulatory protein. Therefore it will be of interest to determine whether HtrA2 may also be regulated in a similar manner. It may also be of interest to determine if these two proteins are translationally regulated by mechanisms such as the regulation of APAF1 by an internal ribosome entry site (Coldwell *et al.*, 2000) or whether this type of regulation is limited to cytosolic proteins.

## **7.2 CONCLUDING REMARKS**

In conclusion the data presented in this thesis has revealed the existence of multiple forms of APAF1 which may act in parallel pathways during apoptosis and methods by which the structure and regulation of APAF1 may be further investigated. This data has also revealed the existence of an IAP-independent mechanism by which Smac can induce apoptosis, probably through a mammalian homologue of Scythe.

**APPENDIX 1: ACCESSION NUMBERS OF DNA SEQUENCES**

**APPENDIX 1: Accession numbers of DNA sequences used in this study**

All DNA sequences used in this thesis were deposited in GenBank and the accession numbers are given below.

Name	Accession number
APAF1	AF013263
APAF1WD13	AF134397
APAF1LWD13	AF149794
APAF1S	AJ243107
Exon 1	AF098868
Exon 1	AF098869
Exon 2	AF098870
Exons 2 and 3	AF098871
Exon 4	AF098873
Exon 4	AF098874
Exon 5	AF098875
Exon 5	AF098876
Exon 6	AF098877
Exons 6 and 7	AF098878
Exon 8	AF098880
Exon 8	AF098881
Exon 9	AF098882
Exon 9	AF098883
Exon 10	AF098884
Exon 10	AF098885
Exon 11	AF098886
Exon 11	AF098887
Exon 12	AF098888
Exon 12	AF098889
Exon 13	AF098890
Exon 13	AF098891
Exon 14	AF098892
Exon 14	AF098893
Exon 15	AF098894
Exon 15	AF098895
Exon 16	AF098896
Exon 16	AF098897
Exon 17	AF098898
Exon 17	AF098899
Exon 17A	AF117658
Exon 17A	AF117659
Exon 18	AF098900
Exon 18	AF098901
Exon 19	AF098902
Exon 19	AF098903
Exon 20	AF098904

Exon 20	AF098905
Exon 21	AF098906
Exon 21	AF098907
Exons 22 and 23	AF098908
Exon 23	AF098909
Exon 24	AF098910
Exon 24	AF098911
Exon 25	AF098912
Exon 25	AF098913
Exon 26	AF098914
Exon 17 / Intron boundary	AJ133645
Intron / Exon 18 boundary	AJ133644
Exon 18 / Intron boundary	AJ133643
Chromosome 12	NT_009681
SMAC	AF262240
SMAC $\beta$	AF298770
SMAC gene	See chromosome 12

The sequences AJ133643, AJ133644, and AJ133645 were submitted to GenBank as part of this project.

**APPENDIX 2: PRIMERS USED IN THIS STUDY**

**APPENDIX 2: Primers used in this study**

All primers used were synthesized by PNAOL, University of Leicester.

Name	Sequence (5' to 3')	T <sub>m</sub> (°C)	Use
CED3 US	GCTTGCGGCCGCGATGCAAAAGCTCGAAATTGT	58	C, R
CED3 DS	GCTCGAGCTCAACAGGAATGCCATCATGGAG	62	C, R
CED4 US	CGGGGCGGCCGCTCTCCATGATGGCATTCTGTG	66	C, R
CED4 DS	GCTCGAGCTCTCCATTCCGATCACAGAATAAAAG	60	C, R
WD US	CGGGGCGGCCGCTCTTTTATTCTGTGATCGGAATG	60	C, R
WD DS	GCTCGAGCTCGTTCAACTACATTAATGCTTAAC	60	C, R
WDRT US	GACTGGGGAAGTAGTACACACC	68	R
WDRT DS	CCATCAGGAGAAAACATCACAC	64	R
3UTR US	CTCAGCACTTTTGGGAGGCC	64	P, S
3UTR DS	GGAGGCTGGGTGACTGACC	64	P, S
EXON3A IN	GATTCAGTTAGTGGAATAACTTCG	66	R
EXON3A OUT	CTTCTTCCAGTGTAAGGACAGTC	68	R
EXON18 IN	GATGGTGCTGTGATGGCCCG	66	R
EXON18 OUT	GTCTGTATTCCACAAAAGATTTA	62	R
EXON25 IN	CACAACGGCTGTGTGCGCTG	66	R
EXON25 OUT	CTGCAAAGATCTGGAATGTCTC	62	R
GENO US	CAGTGGAGCTAGCACTCACATTC	70	P, S
GENO DS	CATGGACCCGTGAACAAAGGTC	68	P, S
SMAC US	GCGGATCCATGGCGGCTCTGAAGAGTTGG	66	C, R
SMAC DS	GCAAGCTTCCAATCCTCACGCAGGTAGGC	64	C, R
SMAC $\beta$ US	GCGGATCCATGAAATCTGACTTCTACTTCCAG	66	C, R
SMACD55 US	GCGGATCCATGGCGGTTTCTATTGCACAG	56	C
SMACD60 US	GCGGATCCATGCAGAAATCAGAGCCTCATTCC	62	C
SMACD75 US	GCGGATCCATGAGAGCAGTGTCTTTGGTAACAG	64	C

Primers were used for cloning (C), RT-PCR (R), PCR analysis (P), or sequencing (S).

**APPENDIX 3: PUBLICATIONS ARISING FROM THIS WORK**



# Caspase-3 cleaves Apaf-1 into an ~30 kDa fragment that associates with an inappropriately oligomerized and biologically inactive ~1.4 MDa apoptosome complex

SB Bratton<sup>1</sup>, G Walker<sup>1</sup>, DL Roberts<sup>1</sup>, K Cain<sup>1</sup> and GM Cohen<sup>\*1</sup>

<sup>1</sup> MRC Toxicology Unit, Hodgkin Building, University of Leicester, P.O. Box 138, Lancaster Road, Leicester LE1 9HN, UK

\* Corresponding author: GM Cohen, MRC Toxicology Unit, Hodgkin Building, University of Leicester, P.O. Box 138, Lancaster Road, Leicester LE1 9HN, UK. Tel: 44-116-252-5601; Fax: 44-116-252-5616; E-mail: gmc2@le.ac.uk

Received 8.11.00; revised 4.12.00; accepted 14.12.00  
Edited by G Melino

## Abstract

Cytochrome *c* and dATP/ATP induce oligomerization of Apaf-1 into two distinct apoptosome complexes: an ~700 kDa complex, which recruits and activates caspases-9, -3 and -7, and an ~1.4 MDa complex, which recruits and processes caspase-9, but does not efficiently activate effector caspases. While searching for potential inhibitors of the ~1.4 MDa apoptosome complex, we observed an ~30 kDa Apaf-1 immunoreactive fragment that was associated exclusively with the inactive complex. We subsequently determined that caspase-3 cleaved Apaf-1 within its CED-4 domain (SVTD<sup>271</sup>↓S) in both dATP-activated lysates and apoptotic cells to form a prominent ~30 kDa (p30) N-terminal fragment. Purified recombinant Apaf-1 p30 fragment weakly inhibited dATP-dependent activation of caspase-3 *in vitro*. However, more importantly, prevention of endogenous formation of the p30 fragment did not stimulate latent effector caspase processing activity in the large complex. Similarly, the possibility that XIAP, an inhibitor of apoptosis protein (IAP), was responsible for the inactivity of the ~1.4 MDa complex was excluded as immunodepletion of this caspase inhibitor failed to relieve the inhibition. However, selective proteolytic digestion of the ~1.4 MDa and ~700 kDa complexes showed that Apaf-1 was present in conformationally distinct forms in these two complexes. Therefore, the inability of the ~1.4 MDa apoptosome complex to process effector caspases most likely results from inappropriately folded or oligomerized Apaf-1. *Cell Death and Differentiation* (2001) 8, 425–433.

**Keywords:** Apaf-1; apoptosome; effector caspases

**Abbreviations:** CARD, caspase recruitment domain; Z-VAD.FMK, benzyloxycarbonyl-Val-Ala-Asp-(OMe) fluoromethyl ketone; DEVD.CHO, acetyl-Asp-Glu-Val-Asp aldehyde; HEK 293 cells, human embryonic kidney cells

## Introduction

Apoptosis is an evolutionarily conserved, biochemically and morphologically distinct form of cell death, characterized by an ordered dismantling of the cell. In most cases, a highly selective class of cysteine proteases, known as caspases, carry out this process. Caspases are often categorized based on their function within the cell, the length of their prodomains and their apparent substrate specificity (reviewed in<sup>1–3</sup>). Initiator caspases, such as caspases-8 and -9, contain long prodomains and are involved in transducing receptor-mediated and stress-induced death signals, respectively.<sup>3,4</sup> They activate effector caspases, such as caspase-3 and -7, which contain short prodomains and are responsible for cleavage of many cellular proteins during the execution phase of apoptosis (reviewed in<sup>3,5</sup>).

In stress-induced apoptosis, unknown cellular signals initiate the release of mitochondrial cytochrome *c*, which interacts with Apaf-1.<sup>6,7</sup> Apaf-1 is composed of three domains: an N-terminal caspase-recruitment domain (CARD), a CED-4 domain that contains Walker's A and B boxes, and a series of C-terminal WD repeats (WDR).<sup>7</sup> After associating with cytochrome *c*, Apaf-1 binds to dATP/ATP, undergoes a conformational change and self-oligomerizes via its CED-4 domains.<sup>8–10</sup> This process simultaneously exposes the CARD in Apaf-1, allowing it to recruit and facilitate processing of procaspase-9.<sup>9–11</sup> This complex of cytochrome *c*, Apaf-1 and caspase-9 is commonly referred to as the 'apoptosome'. Interestingly, Apaf-1 proteins that lack WDR appear to spontaneously oligomerize in the absence of cytochrome *c* and activate caspase-9, but do not activate caspase-3. Thus, the WDR appear to negatively regulate Apaf-1 oligomerization and may be required for recruitment and activation of effector caspases.<sup>8,10,12</sup> The precise binding site for cytochrome *c* on Apaf-1 has not been identified, but an interaction between cytochrome *c* and the WDR in Apaf-1 may induce a conformational change in Apaf-1 that exposes its CED-4 domain. In fact, WDR proteins are likely to form  $\beta$ -propeller structures, with the outer surfaces serving as stable platforms through which multiple proteins may sequentially and/or simultaneously interact to form complexes.<sup>13</sup>

The apoptosome is a very large caspase-activating complex, containing multiple copies of Apaf-1 and caspase-9. Reconstitution experiments with recombinant proteins indicate the apoptosome is ~1.4 MDa in size, whereas those conducted in native cell lysates suggest it is ~700 kDa.<sup>14–16</sup> However, we have recently described the formation of both these complexes in dATP-activated lysates. Significantly, however, only the ~700 kDa complex was biologically active as assessed by its ability to process and activate effector caspases.<sup>17</sup> In the present study, we wished to determine why the ~1.4 MDa Apaf-1

containing apoptosome complex was biologically inactive. We now report that in apoptotic cells and dATP-activated cell lysates, Apaf-1 is cleaved by caspase-3 to yield an ~30 kDa N-terminal fragment. This p30 fragment selectively associates with the ~1.4 MDa apoptosome complex, and addition of the purified recombinant protein to whole lysates inhibits dATP-activation of caspase-3. However, the p30 fragment is not responsible for the inactivity of the ~1.4 MDa complex. Therefore, the physiological function of the p30 fragment during apoptosis is currently unknown. We also exclude a potential role for the endogenous caspase inhibitor, XIAP, in inhibiting the effector caspase processing activity of the ~1.4 MDa complex. Instead, the conformational state of Apaf-1 within the ~1.4 MDa and ~700 kDa complexes appears to be significantly different. Therefore, the inactive ~1.4 MDa complex is likely formed as a result of inappropriate Apaf-1 oligomerization.

## Results

### An ~30 kDa protein selectively associates with the ~1.4 MDa apoptosome complex

We recently described the formation of two Apaf-1 complexes in dATP-activated THP.1 lysates: a biologically active ~700 kDa complex and an inactive ~1.4 MDa complex.<sup>17</sup> In the current studies, in control lysates, Apaf-1 and procaspase-9 eluted off the Superose-6 column in fractions 18–24 ( $M_r$  ~158,000) and 18–26 ( $M_r$  ~60,000), respectively (Figure 1A). Following dATP activation of the lysate for 1 h, Apaf-1 oligomerized into ~1.4 MDa and ~700 kDa apoptosome complexes (Figure 1B, fractions 6–8 and fractions 10–16, respectively). Procaspase-9 was processed to its catalytically active large subunits and was associated with both the ~1.4 MDa and ~700 kDa apoptosome complexes or was present as the free enzyme (Figure 1B). All DEVDase activity eluted in fractions 21–28 ( $M_r$  ~60,000) (Figure 1C), along with fully processed caspase-3 (data not shown). When both the ~1.4 MDa and ~700 kDa complexes were assayed for their ability to process and activate exogenously added effector caspases, only the ~700 kDa complex produced significant DEVDase activity (Figure 1C). These results were essentially identical to those previously reported.<sup>17</sup> However, upon dATP activation we also observed the formation of an Apaf-1 immunoreactive ~30 kDa protein, which was selectively associated with the inactive ~1.4 MDa complex (Figure 1B, fractions 6–7). Consequently, we hypothesized that this ~30 kDa protein (p30) may be a caspase-mediated cleavage product of Apaf-1 and may act as an inhibitor of the ~1.4 MDa complex.

### Effector caspases cleave Apaf-1 into an ~30 kDa fragment in dATP-activated lysates and apoptotic cells

In order to test the hypothesis that Apaf-1 was cleaved by caspases and to determine if the cleavage was cell-type specific, lysates from both THP.1 and HEK 293 cells were activated with dATP in the presence or absence of caspase inhibitors. The p30 fragment was observed 15 min after

activation and was inhibited by both DEVD.CHO and Z-VAD.FMK, indicating that cleavage of Apaf-1 was caspase-dependent (Figure 1D,E). In addition, the p30 fragment was observed in THP.1 cells treated with either TPCK (75  $\mu$ M), etoposide (10  $\mu$ M), or Ara-C (20  $\mu$ M), and the amount of the p30 formed was consistent with the degree of apoptosis (Figure 1F).

### Recombinant caspases-3 and -7 cleave purified Apaf-1 at SVTD<sup>260/271</sup>↓S

Since DEVD.CHO potently inhibits the effector caspases-3 and -7, as well as the initiator caspase-8,<sup>18</sup> we next incubated purified unactivated Apaf-1 with either recombinant caspases-3, -7 or -8. Both caspases-3 and -7 processed Apaf-1 in a concentration-dependent manner into several identifiable fragments, the most prominent of which was the p30 fragment previously observed in dATP-activated cell lysates (Figure 2A,B). Of note, ~5–10 nM concentrations of active caspases-3 and -7 were sufficient to process Apaf-1 and were below the concentration of active caspase-3 observed in dATP-activated THP.1 lysates. At the same concentrations, caspase-8 demonstrated no ability to process Apaf-1 (Figure 2C). Moreover, a role for caspase-6 was excluded because it did not process purified Apaf-1, and the caspase-6 selective inhibitor, VEID.CHO, did not inhibit Apaf-1 cleavage in THP.1 lysates (data not shown). The p30 fragment was confirmed to be an N-terminal fragment of Apaf-1 because Flag-Apaf-1 expressed in HEK 293 produced a Flag-p30 fragment following incubation with active recombinant caspase-3 (Figure 2D). Since the p30 fragment was derived from the N-terminus of Apaf-1, we estimated the probable caspase cleavage site motif to be SVTD<sup>260</sup>↓S in Apaf-1/Apaf-1L or SVTD<sup>271</sup>↓S in Apaf-1XL, which contains an additional eleven amino acids between the CARD and CED-4 domains (Figure 2E). To confirm this cleavage site, we utilized a truncated form of Apaf-1 (residues 1–530; ~62 kDa) which could be more easily mutated and *in vitro* transcribed/translated. Caspase-3 cleaved wild-type [<sup>35</sup>S]Apaf-530 into two fragments, one corresponding to the first 260 amino acids (p30 fragment) and the other corresponding to the remainder of the molecule, including the C-terminal His6 tag (Figure 2E, lanes 2–4). The latter fragment appeared to undergo a second cleavage event to form a slightly smaller C-terminal fragment (Figure 2E, asterisk, lanes 3–4). In contrast, the mutated [<sup>35</sup>S]Apaf-530 (D260A) was not cleaved at all by caspase-3 (Figure 2E, lanes 5–8). Thus, caspase-3 cleaves Apaf-1 within its CED-4 domain (SVTD↓S), downstream of the Walker's B box (Figure 2E).

### Recombinant p30 weakly inhibits dATP-activation of caspase-3

In order to determine the biological effects of the p30 fragment, we cloned, expressed and purified the protein for subsequent studies. We initially verified that recombinant p30 could associate with the ~1.4 MDa complex when added to lysate that was subsequently dATP-activated (data not shown). Next, we assessed the ability of purified Apaf-1L and p30 to activate caspase-9 in a pure recombinant system using *in vitro* transcribed/translated [<sup>35</sup>S]procaspase-9, cytochrome *c* and dATP. Interestingly, while recombinant

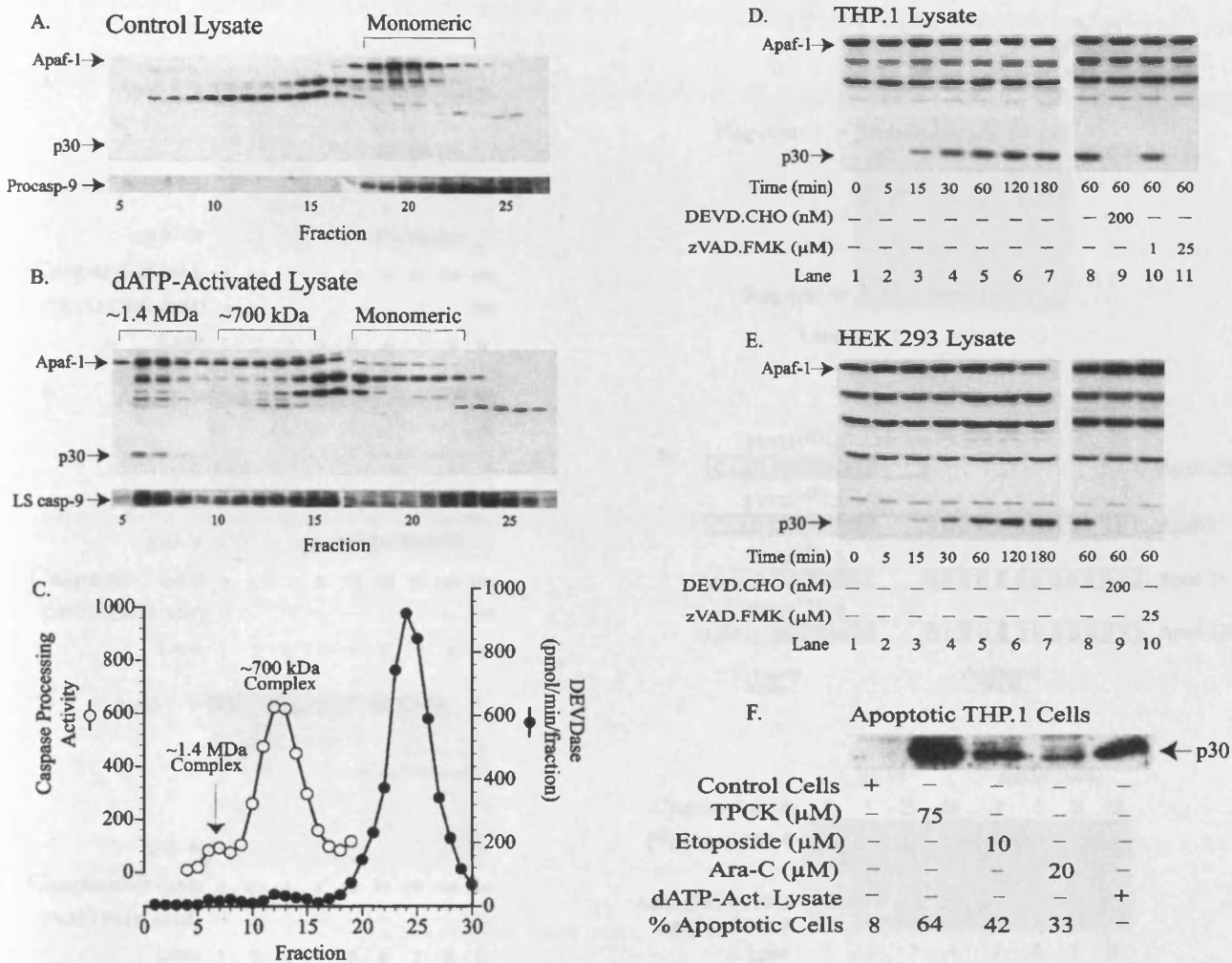


**Figure 1** An ~30 kDa protein selectively associates with the inactive ~1.4 MDa apoptosome complex. (A) Control THP.1 lysate (10 mg/ml) and (B) lysate activated with dATP/MgCl<sub>2</sub> (2 mM) for 1 h at 37°C were loaded onto a Superose 6 HR 10/30 column. The ~1.4 MDa (fractions 6–8) and ~700 kDa (fractions 11–16) apoptosome complexes were separated as described in Materials and Methods. A portion of each column fraction was mixed with 10× SDS loading buffer and analyzed by SDS-PAGE/immunoblotting for Apaf-1 or caspase-9. Caspase-9 was detected either as its unprocessed zymogen (Procasp-9) or as its processed large subunits together with the prodomain (LS casp-9). (C) Column fractions from dATP-activated lysates were assayed for DEVDase activity (●). The ~1.4 MDa and ~700 kDa apoptosome complexes were also examined for their ability to process and activate exogenously added effector caspases (○). (D) THP.1 or (E) HEK 293 dATP-activated cell lysates were preincubated on ice with either DEVD.CHO or Z-VAD.FMK for 1 h prior to dATP activation. All incubations were quenched with the addition of 2× SDS gel loading buffer, and 25 μg of lysate was subsequently subjected to SDS-PAGE. An Apaf-1 antibody raised against amino acids 10–254 (CARD/CED-4 region) was then utilized for immunoblotting. (F) Lysates obtained from THP.1 cells treated with various apoptotic stimuli were immunoblotted for the presence of the p30 Apaf-1 fragment. Apoptosis was assessed by externalization of phosphatidylserine

Apaf-1L readily activated caspase-9 (Figure 3A, lanes 1–4), the recombinant p30 was incapable of activating caspase-9 (Figure 3A, lanes 5–7). Since the p30 fragment would be expected to bind procaspase-9 through a CARD-CARD interaction similar to Apaf-1L, we hypothesized that the p30 fragment might behave as a competitive inhibitor of caspase-9 activation. Indeed, addition of purified p30 to THP.1 lysates slightly inhibited dATP-mediated activation of caspase-3 by caspase-9, as demonstrated by inhibition of caspase-3 processing and decreased DEVDase activity (Figure 3B). Thus, the Apaf-1 p30 fragment appeared to compete weakly with endogenous full-length Apaf-1 for procaspase-9 and

consequently decreased the number of available active Apaf-1/caspase-9 complexes. However, as the concentrations of p30 required to inhibit caspase activation were far above those generated endogenously, the physiological significance of this result is presently unclear.

#### Immunodepletion of caspase-3 prevents association of the ~30 kDa fragment with the ~1.4 MDa complex

Caspases-3 and -7 are frequently viewed as redundant caspases because they often cleave the same substrates *in*

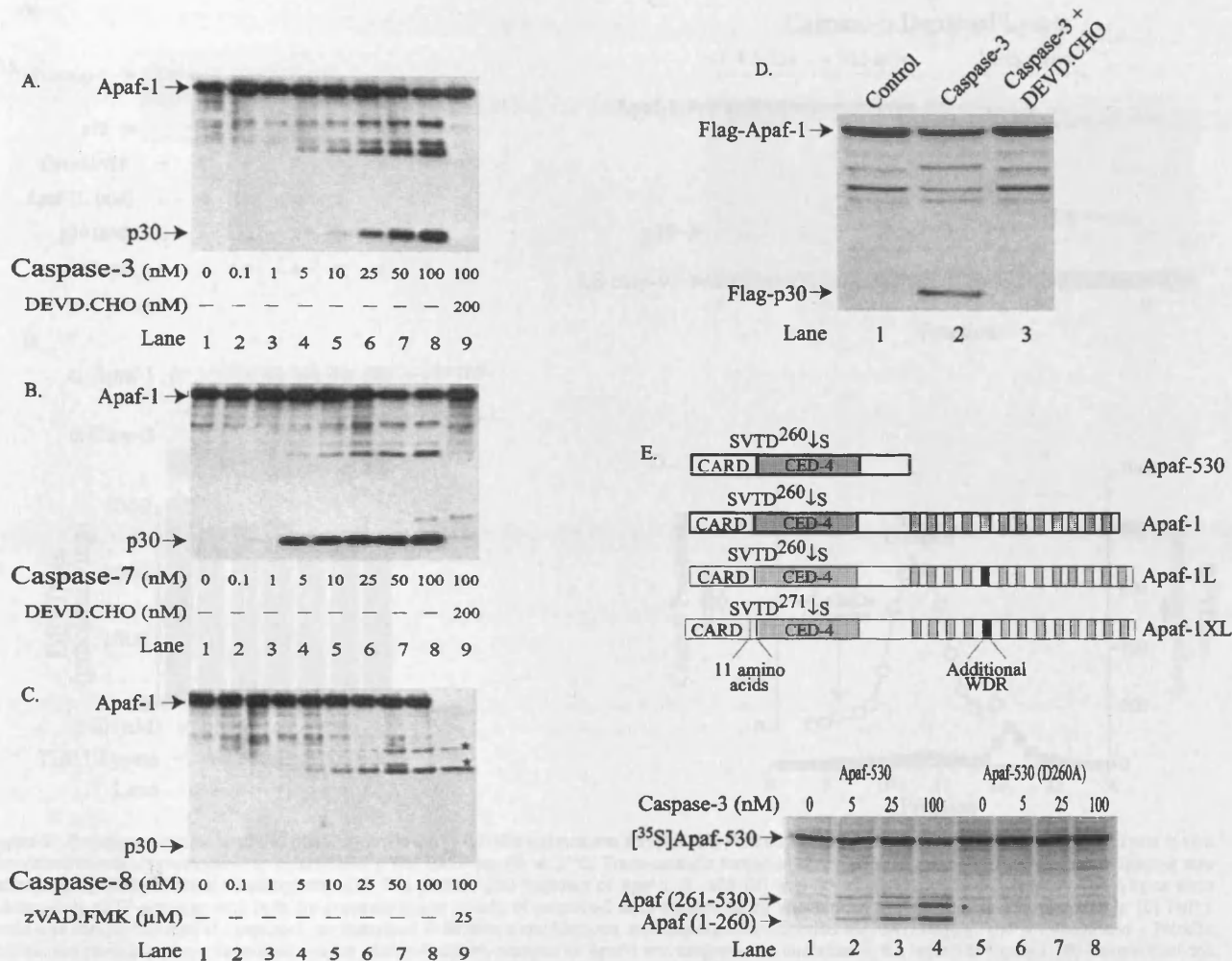


**Figure 2** Apaf-1 is cleaved by caspase-3 at SVTD<sup>260/271</sup>↓S. (A–C) Recombinant caspases-3, -7 and -8 (0.1–100 nM) were incubated with purified full-length Apaf-1 (~200 ng) for 1 h at 37°C and Western blotted for Apaf-1 fragments. Non-specific immunoreactive bands are denoted by an (\*), including two minor contaminants present in the caspase-8 preparation. (D) Lysates from HEK 293 cells expressing NH<sub>2</sub>-terminal Flag-Apaf-1 were incubated with active caspase-3 (100 nM) for 1 h at 37°C. Afterwards, Flag-Apaf-1 fragments were separated by SDS–PAGE and immunoblotted using an anti-Flag antibody. (E) Wild-type, truncated Apaf-530 and the site-directed mutant Apaf-530 (D260A) were incubated with active caspase-3 and analyzed by SDS–PAGE/autoradiography. The schematic represents truncated Apaf-530, various splice forms of Apaf-1, and the location of the caspase-3 cleavage site in each protein. In both Apaf-1L and Apaf-1XL, an additional WDR is shown in black, and in Apaf-1XL, the additional eleven amino acids between the CARD and CED-4 domains is shown in white

*vitro*. However, a number of studies suggest these caspases may play distinct roles in dATP-activated cell lysates and apoptotic cells.<sup>15,19,20</sup> Consequently, in order to determine the contribution of caspase-3 in producing the Apaf-1 p30 fragment and to assess the effects of blocking its formation on apoptosome function, we immunodepleted caspase-3 from lysates prior to dATP activation. Following dATP activation and separation by gel filtration, caspase-3 depleted lysate exhibited a >95% loss in DEVDase activity (Figure 3D). The remaining DEVDase activity co-eluted with processed caspase-7 in fractions 19–23 (Figure 3D and data not shown). Importantly, the p30 fragment was no longer associated with the ~1.4 MDa apoptosome complex (Figures 3C and 1B, compare fractions 6–7). In contrast, immunodepletion of caspase-7 did not significantly inhibit the

association of the p30 fragment with the ~1.4 MDa apoptosome complex (data not shown). This appeared somewhat surprising given that recombinant caspase-7 was slightly more effective than caspase-3 at processing purified Apaf-1 *in vitro* (Figure 2A,B). However, caspase-7 is present at significantly lower concentrations than caspase-3 in our THP.1 cell lysates. Therefore, immunodepletion of caspase-3, but not caspase-7, effectively inhibited formation and association of the p30 fragment with the ~1.4 MDa apoptosome complex. However, the ~1.4 MDa apoptosome complex was still inactive when assayed for its ability to process effector caspases and generate DEVDase activity (Figure 3D, fractions 6–8). In contrast, the ~700 kDa complex displayed its normal capacity to process effector caspases (Figure 3D, fractions 10–16). Thus, caspase-3 appeared primarily



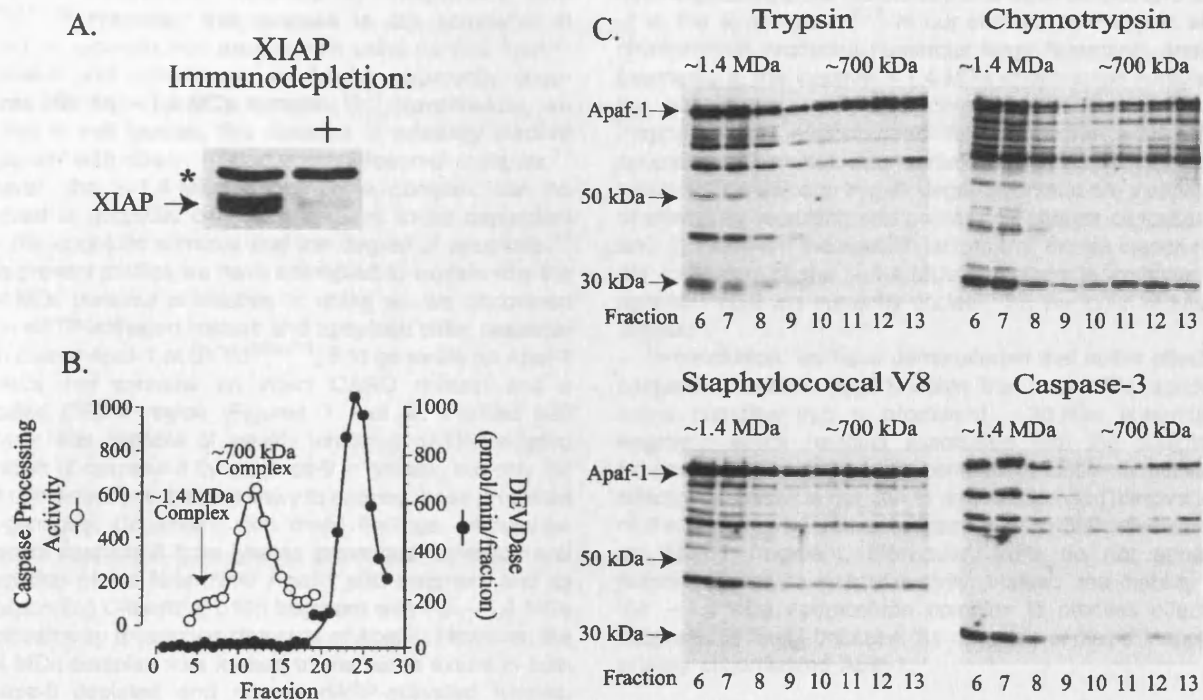


**Figure 4** Inappropriately oligomerized Apaf-1, and not XIAP, is responsible for the lack of effector caspase processing activity in the ~1.4 MDa apoptosome complex. (A) XIAP was immunodepleted from THP.1 lysates, as described in Materials and Methods, and immunoblotted to confirm its absence. A non-specific band (\*) present in both the naïve and immunodepleted lysates confirms equal protein loading. (B) XIAP immunodepleted lysate was dATP-activated and separated by gel filtration as previously described. Column fractions were assayed for DEVDase activity (●) and the ~1.4 MDa and ~700 kDa apoptosome complexes were examined for their ability to process and activate exogenously added effector caspases (○). (C) Column fractions (30  $\mu$ l), obtained from caspase-3 immunodepleted lysates activated with dATP (Figure 3C), were exposed to sequencing grade trypsin, chymotrypsin or staphylococcal V8 (1 ng/ $\mu$ l) for 15 min or to recombinant caspase-3 (100 nM) for 2 h. The reactions were quenched with 2 $\times$  SDS loading buffer, and the samples were separated by SDS-PAGE and immunoblotted for Apaf-1 fragments

size of the active ~700 kDa apoptosome complex, (iii) not directly inactivated by caspase-3 or the endogenously derived p30 fragment, and (iv) not inactivated by the presence of IAPs, we hypothesized that the ~1.4 MDa apoptosome complex might simply be inappropriately formed. We speculated that Apaf-1 might be present in a conformational state that prevents normal recruitment/processing of effector caspases. Therefore, we isolated both ~700 kDa and ~1.4 MDa apoptosome complexes from dATP-activated caspase-3 immunodepleted lysates and subjected them to partial proteolysis with trypsin, chymotrypsin or staphylococcal V8 protease. Apaf-1 in the ~1.4 MDa complex was generally more susceptible to proteolytic cleavage by all of the proteases compared to Apaf-1 in the ~700 kDa complex (Figure 4C). In addition, the pattern of protein fragments was strikingly different. Trypsin produced at least three low molecular weight fragments (<50 kDa) from the ~1.4 MDa complex that were not detected following proteolysis of the ~700 kDa complex, and both trypsin and chymotrypsin produced numerous larger molecular weight fragments (~65–125 kDa) that were primarily generated from the larger complex.

The apparent sensitivity of the ~1.4 MDa complex to proteolytic cleavage led to us to question if this complex might likewise demonstrate greater sensitivity to caspase-3 mediated cleavage. Indeed, Apaf-1 within the ~1.4 MDa

complex (Figure 4C, fractions 6–8) was clearly more susceptible to cleavage by caspase-3 than Apaf-1 within the ~700 kDa complex (Figure 4C, fractions 11–13). These data were compatible with the hypothesis that the ~700 kDa apoptosome complex initially activated caspase-3, which in turn cleaved Apaf-1 within the ~1.4 MDa apoptosome complex to form the ~30 kDa fragment. Caspase-3 was capable of cleaving purified monomeric Apaf-1 into the ~30 kDa fragment (Figure 2A) and recombinant p30 associated with the ~1.4 MDa complex when added to dATP-activated lysates (data not shown). Thus, it appears that both monomeric and inappropriately oligomerized Apaf-1 are sensitive to cleavage by caspase-3 and that in either case the resulting Apaf-1 p30 fragment associates with the ~1.4 MDa apoptosome complex. However, since the vast majority of Apaf-1 undergoes oligomerization in dATP-activated lysates prior to activation of effector caspases,<sup>17</sup> it appears more likely that caspase-3 targets the inappropriately oligomerized Apaf-1 in the ~1.4 MDa complex rather than unactivated Apaf-1.

## Discussion

Cytochrome *c*/dATP-dependent oligomerization of Apaf-1 is required for formation of a functional apoptosome that

processes caspase-9, followed by caspases-3 and -7.<sup>9,10,14–16</sup> However, this process is still somewhat ill defined. In reconstitution experiments using purified Apaf-1, caspase-9 and cytochrome *c*, Apaf-1 apparently oligomerizes into an ~1.4 MDa complex.<sup>14,16</sup> Nevertheless, we find that in cell lysates, this complex is relatively inactive compared with the ~700 kDa apoptosome complex.<sup>17</sup> However, the ~1.4 MDa apoptosome complex can be observed in apoptotic cells and appears to be dependent upon the apoptotic stimulus and the degree of apoptosis.<sup>17</sup> In the present studies we have attempted to explain why the ~1.4 MDa complex is inactive. In doing so, we discovered that in dATP-activated lysates and apoptotic cells, caspase-3 can cleave Apaf-1 at SVTD<sup>260/271</sup>↓S to generate an Apaf-1 fragment that contains an intact CARD domain and a truncated CED-4 region (Figures 1 and 2). Purified p30 fragment was capable of weakly inhibiting dATP-mediated activation of caspase-3 by caspase-9 in lysates, but only did so at concentrations that are likely to exceed those produced endogenously. Consistent with these findings, immunodepletion of caspase-3 from lysates prevented formation and association of the N-terminal Apaf-1 p30 fragment and its corresponding C-terminal p105 fragment with the ~1.4 MDa apoptosome by preventing cleavage of Apaf-1. However, the ~1.4 MDa complex was formed to the same extent in both caspase-3 depleted and normal dATP-activated lysates, indicating that the p30 fragment did not 'convert' an active ~700 kDa apoptosome complex into an inactive ~1.4 MDa apoptosome complex. In addition, the ~1.4 MDa apoptosome complexes remained incapable of activating effector caspases, even in the absence of any Apaf-1 p30 fragment (Figure 3). Thus, although the biological consequences of Apaf-1 cleavage remain unknown, neither cleavage of Apaf-1 nor the resulting p30 fragment were responsible for producing or inhibiting the ~1.4 MDa complex.

Interestingly, processed caspase-9 was associated with the inactive ~1.4 MDa apoptosome complex, implying that the large complex might be capable of promoting trans-activation of procaspase-9 or alternatively, might simply recruit processed caspase-9 released from the active ~700 kDa apoptosome complex. If the former were in fact true, then the presence of a caspase-9 inhibitor, for example a member of the inhibitor of apoptosis (IAP) family of proteins such as XIAP,<sup>21,22</sup> might explain the inability of the ~1.4 MDa complex to activate effector caspases. However, XIAP was not responsible for the inactivity of the ~1.4 MDa complex as its removal did not restore the activity of the large complex (Figure 4). Rather, partial proteolysis of both the ~700 kDa and ~1.4 MDa complexes revealed markedly different proteolytic digestion profiles and suggested that the ~1.4 MDa apoptosome complex was inappropriately formed (Figure 4). Indeed, all of the proteases tested, including caspase-3, appeared to cleave Apaf-1 in the ~1.4 MDa complex far more efficiently than in the ~700 kDa complex. It is interesting to note that the WD repeats present in Gβ-subunits form β-propeller structures, which are very resistant to trypsin, unless they are misfolded or disturbed by particular amino acid substitutions.<sup>25</sup> Apaf-1 contains a large C-terminal WD40 repeat region, which has been suggested to form β-propellers and which has recently

been implicated in the recruitment of effector caspases-3 and -7 to the apoptosome.<sup>7,12</sup> In our studies, both trypsin and chymotrypsin produced numerous large N-terminal Apaf-1 fragments in the inactive ~1.4 MDa apoptosome complex, but not in the ~700 kDa complex (Figure 4). Thus, inappropriately oligomerized Apaf-1 in the ~1.4 MDa apoptosome complex may contain misfolded WD repeats, which are sensitive to trypsin degradation and are incapable of effectively recruiting and processing effector caspases-3 and -7. However, the specific factors that dictate inappropriate formation of the ~1.4 MDa apoptosome complex in apoptotic cells are currently unclear, but the focus of future research.

In conclusion, we have demonstrated that active effector caspase-3 cleaves Apaf-1 within the ~1.4 MDa apoptosome complex into a prominent ~30 kDa N-terminal fragment, which remains associated with the complex. However, the inability of this complex to efficiently activate effector caspases is not due to degradation and inactivation of the complex by active caspase-3 or to the presence of an Apaf-1 fragment. Moreover, IAPs do not appear responsible for its lack of activity. Instead, the inability of the ~1.4 MDa apoptosome complex to process effector caspases is likely because the complex contains inappropriately oligomerized Apaf-1.

## Materials and Methods

### Preparation and activation of cell lysates/apoptotic cells

Human monocytic THP.1 cells and human embryonic kidney (HEK) 293 cells were grown in RPMI 1640 and DMEM, respectively, supplemented with 10% heat inactivated FBS in 5% CO<sub>2</sub> at 37°C. Cell lysates were prepared as previously described.<sup>15</sup> *In vitro* activation of caspases was initiated by incubating lysates (10 mg/ml) with dATP/MgCl<sub>2</sub> (2 mM) for various times at 37°C. Exogenous cytochrome *c* was not required as it was released from mitochondria during lysate preparation. In some experiments, THP.1 cells were treated with either *N*-tosyl-*L*-phenylalanyl chloromethyl ketone (TPCK; 75 μM), etoposide (10 μM), or 1-β-D-arabinofuranosylcytosine hydrochloride (Ara-C; 20 μM) for varying times, and apoptosis was assessed by phosphatidylserine exposure as previously described.<sup>26</sup>

### Caspase cleavage of endogenous and recombinant Apaf-1

THP.1 and HEK293 lysates (25 μg protein) were activated with dATP in the presence or absence of the caspase inhibitors, benzyloxycarbonyl-Val-Ala-Asp(OMe) fluoromethyl-ketone (Z-VAD.FMK) or Ac-Asp-Glu-Val-Asp aldehyde (DEVD.CHO). Z-VAD.FMK inhibits all known caspases, whereas DEVD.CHO is more selective for caspases-3, -7 and -8.<sup>18</sup> Purified recombinant unactivated Apaf-1 (~200 ng) was incubated with active caspases-3, -6, -7 or -8 for 1 h at 37°C. All protein samples were mixed with 2 × SDS loading buffer, separated by SDS-PAGE, and immunoblotted for Apaf-1 cleavage products using an antibody generously provided by Dr. Xiaodong Wang (University of Texas Southwestern Medical Center, Dallas, TX, USA). This antibody was raised against the N-terminus of Apaf-1 (amino acids 10–254).<sup>7</sup>

### Apaf-1 mutagenesis/deletions

The caspase cleavage site in Apaf-1 was determined using a truncated form of Apaf-1 (pET28a-Apaf-530; generously provided by Dr. Emad S. Alnemri).<sup>10</sup> Asp-260 was mutated to an Ala using Stratagene's Quik-Change kit with the following primers (mutation underlined) (5'→CAAGAGTGTTACAGCTTCAGTAATGG→3'; 5'→CCATTACTGAAGCTGTAACACTCTTG→3') and confirmed by DNA sequencing. The wild-type Apaf-530 and Apaf-530 (D<sup>260</sup>→A) plasmids were transcribed/translated using the T7 TNT system (Promega), and the <sup>35</sup>S-labeled proteins were incubated with recombinant caspase-3 for 2 h and analyzed by SDS-PAGE/autoradiography. This mutation corresponds to D<sup>271</sup>→A in Apaf-1XL/Apaf-1WD13,<sup>12,16</sup> which contains an additional 11 amino acids between the CARD and CED-4 domains. While conducting these studies, Apaf-1XL was shown to be the primary form of Apaf-1 present in cells.<sup>27</sup> Consequently, we PCR amplified the sequence corresponding to the N-terminal cleavage product of Apaf-1XL (residues 1–271), using an Apaf-1XL construct (kindly provided by Dr. Gabriel Nuñez) as a template and the following primers which contained the necessary restriction sites (5'→CGGGATCCATGGATGCAAAAGCTCGAAATTG→3' and 5'→GGGGT-ACCAGCTGTAACACTCTTGTCTCTGGTTG→3'). The PCR product was cloned into pTriEX-1 (Novagen) at the *Bam*HI/*Kpn*I sites and incorporated C-terminal HSV and His-6 tags. In addition, the D<sup>271</sup>→A mutation was also included in the fragment to ensure that the HSV and His-6 tags would not be removed by caspase-3 during dATP activation experiments.

### Expression and purification of human recombinant Apaf-1 (and its p30 cleavage fragment) and caspases

Sf-9 insect cells were infected with high titer baculoviral stocks encoding full-length Apaf-1.<sup>16</sup> Cells were harvested 48 h later and His-tagged Apaf-1 was purified on a Ni<sup>2+</sup> column essentially as previously described.<sup>16</sup> Similarly, the p30 Apaf-1 fragment was bacterially expressed, isolated on Ni<sup>2+</sup> beads, and further purified by DEAE-chromatography. Active caspases-3, -6, -7 and -8 were expressed, purified and active site titrated as previously described.<sup>28,29</sup>

### Analysis of apoptosome complexes/immunodepletion of caspase-3 and XIAP

Control and dATP-activated lysates were fractionated by size-exclusion chromatography, using an FPLC protein purification system with a Superose 6 HR 10/30 column (Amersham Pharmacia Biotech, Herts, UK). Apoptosome complexes (~700 kDa and ~1.4 MDa) were eluted using column buffer supplemented with 50 mM NaCl, assayed for their ability to process exogenously added caspases-9, -3 and -7, and immunoblotted for Apaf-1 and caspase-9 (D.R. Green, La Jolla Institute for Allergy and Immunology, San Diego, CA, USA) as previously described.<sup>17</sup> In some experiments, lysates were immunodepleted of caspase-3 or XIAP prior to dATP-activation. Briefly, protein G sepharose beads (500 µl of 50% slurry; Amersham Pharmacia Biotech, Herts, UK) were blocked with 3% BSA, preincubated for 2 h with anti-caspase-3 or XIAP antibodies (1:50; Transduction Laboratories/Pharmingen, San Diego, CA, USA) and thoroughly washed to remove unbound antibody. Lysates (15 mg/ml) were then incubated with antibody coated beads for 2 h. Partially immunodepleted supernatants were removed by centrifugation and subjected to a second round of immunodepletion in order to completely deplete caspase-3 or XIAP.

### Partial proteolysis of ~1.4 MDa and ~700 kDa apoptosome complexes

Following dATP activation of caspase-3 immunodepleted lysates, apoptosome complexes were isolated by gel filtration as described above. A portion of each column fraction (30 µl) was incubated with either 100 nM caspase-3 for 2 h or 1 ng/ml of sequencing grade trypsin, chymotrypsin or staphylococcal V8 protease (Boehringer Mannheim, Lewes, UK) for 15 min at 37°C. Reactions were terminated with an equal volume of 2 × SDS loading buffer and analyzed for Apaf-1 cleavage products.

### Acknowledgements

The authors thank Dr. Xiaodong Wang (University of Texas Southwestern Medical Center, Dallas, TX) for the baculoviral Apaf-1 stock and anti-Apaf-1 antibody, Dr. Emad S. Alnemri for the Apaf-1-530 construct, Dr. Douglas R. Green (La Jolla Institute for Allergy and Immunology, San Diego, CA) for anti-caspase-9 antibody, and Dr. D.W. Nicholson (Merck Frosst, Canada) for anti-caspase-3 antibody. The authors also thank X-M Sun, C Langlais and D Brown for their technical expertise and helpful discussions during the preparation of this manuscript.

### References

- Cohen GM (1997) Caspases: the executioners of apoptosis. *Biochem. J.* 326: 1–16
- Bratton SB, MacFarlane M, Cain K and Cohen GM (2000) Protein complexes activate distinct caspase cascades in death receptor and stress-induced apoptosis. *Exp. Cell Res.* 256: 27–33
- Eamshaw WC, Martins LM and Kaufmann SH (1999) Mammalian caspases: structure, activation, substrates, and functions during apoptosis. *Annu. Rev. Biochem.* 68: 383–424
- Sun XM, MacFarlane M, Zhuang J, Wolf BB, Green DR and Cohen GM (1999) Distinct caspase cascades are initiated in receptor-mediated and chemical-induced apoptosis. *J. Biol. Chem.* 274: 5053–5060
- Nicholson DW (1999) Caspase structure, proteolytic substrates, and function during apoptotic cell death. *Cell Death Differ.* 6: 1028–1042
- Green DR and Reed JC (1998) Mitochondria and apoptosis. *Science* 281: 1309–1312
- Zou H, Henzel WJ, Liu X, Lutschg A and Wang X (1997) Apaf-1, a human protein homologous to *C. elegans* CED-4, participates in cytochrome c-dependent activation of caspase-3. *Cell* 90: 405–413
- Hu Y, Ding L, Spencer DM and Nunez G (1998) WD-40 repeat region regulates Apaf-1 self-association and procaspase-9 activation. *J. Biol. Chem.* 273: 33489–33494
- Li P, Nijhawan D, Budihardjo I, Srinivasula SM, Ahmad M, Alnemri ES and Wang X (1997) Cytochrome c and dATP-dependent formation of Apaf-1/caspase-9 complex initiates an apoptotic protease cascade. *Cell* 91: 479–489
- Srinivasula SM, Ahmad M, Fernandes-Alnemri T and Alnemri ES (1998) Autoactivation of procaspase-9 by Apaf-1-mediated oligomerization. *Mol. Cell* 1: 949–957
- Qin H, Srinivasula SM, Wu G, Fernandes-Alnemri T, Alnemri ES and Shi Y (1999) Structural basis of procaspase-9 recruitment by the apoptotic protease-activating factor 1. *Nature* 399: 549–557
- Hu Y, Benedict MA, Ding L and Nunez G (1999) Role of cytochrome c and dATP/ATP hydrolysis in Apaf-1-mediated caspase-9 activation and apoptosis. *EMBO J.* 18: 3586–3595
- Smith TF, Gaitatzes C, Saxena K and Neer EJ (1999) The WD repeat: a common architecture for diverse functions. *Trends Biochem. Sci.* 24: 181–185
- Saleh A, Srinivasula SM, Acharya S, Fishel R and Alnemri ES (1999) Cytochrome c and dATP-mediated oligomerization of Apaf-1 is a prerequisite for procaspase-9 activation. *J. Biol. Chem.* 274: 17941–17945



15. Cain K, Brown DG, Langlais C and Cohen GM (1999) Caspase activation involves the formation of the aposome, a large (~700 kDa) caspase-activating complex. *J. Biol. Chem.* 274: 22686–22692
16. Zou H, Li Y, Liu X and Wang X (1999) An APAF-1.cytochrome c multimeric complex is a functional apoptosome that activates procaspase-9. *J. Biol. Chem.* 274: 11549–11556
17. Cain K, Bratton SB, Langlais C, Walker G, Brown DG, Sun XM and Cohen GM (2000) Apaf-1 oligomerizes into biologically active ~700 kDa and inactive ~1.4 MDa apoptosome complexes. *J. Biol. Chem.* 275: 6067–6070
18. Garcia-Calvo M, Peterson EP, Leiting B, Ruel R, Nicholson DW and Thornberry NA (1998) Inhibition of human caspases by peptide-based and macromolecular inhibitors. *J. Biol. Chem.* 273: 32608–32613
19. Chandler JM, Cohen GM and MacFarlane M (1998) Different subcellular distribution of caspase-3 and caspase-7 following Fas-induced apoptosis in mouse liver. *J. Biol. Chem.* 273: 10815–10818
20. Germain M, Affar EB, D'Amours D, Dixit VM, Salvesen GS and Poirier GG (1999) Cleavage of automodified poly(ADP-ribose)polymerase during apoptosis. Evidence for involvement of caspase-7. *J. Biol. Chem.* 274: 28379–28384
21. Deveraux QL, Takahashi R, Salvesen GS and Reed JC (1997) X-linked IAP is a direct inhibitor of cell-death proteases. *Nature* 388: 300–304
22. Deveraux QL, Roy N, Stennicke HR, Van Arsedale T, Zhou Q, Srinivasula SM, Alnemri ES, Salvesen GS and Reed JC (1998) IAPs block apoptotic events induced by caspase-8 and cytochrome c by direct inhibition of distinct caspases. *EMBO J.* 17: 2215–2223
23. Du C, Fang M, Li Y, Li L and Wang X (2000) Smac, a mitochondrial protein that promotes cytochrome c-dependent caspase activation by eliminating IAP inhibition. *Cell* 102: 33–42
24. Verhagen AM, Ekert PG, Pakusch M, Silke J, Connolly LM, Reid GE, Moritz RL, Simpson RJ and Vaux DL (2000) Identification of DIABLO, a mammalian protein that promotes apoptosis by binding to and antagonizing IAP proteins. *Cell* 102: 43–53
25. Garcia-Higuera I, Gaitatzes C, Smith TF and Neer EJ (1998) Folding a WD repeat propeller. Role of highly conserved aspartic acid residues in the G protein beta subunit and Sec13. *J. Biol. Chem.* 273: 9041–9049
26. Zhuang J, Ren Y, Snowden RT, Zhu H, Gogvadze V, Savill JS and Cohen GM (1998) Dissociation of phagocyte recognition of cells undergoing apoptosis from other features of the apoptotic program. *J. Biol. Chem.* 273: 15628–15632
27. Benedict MA, Hu Y, Inohara N and Nunez G (2000) Expression and functional analysis of Apaf-1 isoforms. Extra WD-40 repeat is required for cytochrome c binding and regulated activation of procaspase-9. *J. Biol. Chem.* 275: 8461–8468
28. Srinivasula SM, Ahmad M, Fernandes-Alnemri T, Litwack G and Alnemri ES (1996) Molecular ordering of the Fas-apoptotic pathway: the Fas/APO-1 protease Mch5 is a CrmA-inhibitable protease that activates multiple Ced-3/ICE-like cysteine proteases. *Proc. Natl. Acad. Sci. USA* 93: 14486–14491
29. Garcia-Calvo M, Peterson EP, Rasper DM, Vaillancourt JP, Zamboni R, Nicholson DW and Thornberry NA (1999) Purification and catalytic properties of human caspase family members. *Cell Death Differ.* 6: 362–369

# The Inhibitor of Apoptosis Protein-binding Domain of Smac Is Not Essential for its Proapoptotic Activity

Darren L. Roberts, Wendy Merrison, Marion MacFarlane, and Gerald M. Cohen

Medical Research Council Toxicology Unit, University of Leicester, Leicester LE1 9HN, United Kingdom

**Abstract.** Smac/DIABLO, a recently identified inhibitor of apoptosis protein (IAP)-binding protein, is released from the mitochondria during apoptosis and reportedly potentiates apoptosis by relieving the inhibition of IAPs on caspases. We now describe the molecular characterization of Smac  $\beta$ , an alternatively spliced form of Smac, which lacks the mitochondrial-targeting sequence found in Smac and has a cortical distribution in both human embryonic kidney 293 and breast epithelial tumor MCF-7 cells. Smac  $\beta$ , which binds IAPs *in vitro*, does not bind IAPs in intact cells due to cellular processing and removal of its NH<sub>2</sub>-terminal IAP-binding domain. Despite its inability to interact with IAPs in cells, processed Smac

$\beta$  is proapoptotic, as demonstrated by its ability to potentiate apoptosis induced by both death receptor and chemical stimuli. Furthermore, expression of a NH<sub>2</sub>-terminally truncated Smac mutant ( $\Delta$ 75), which lacks the entire IAP-interacting domain, potentiates apoptosis to the same extent as Smac and Smac  $\beta$ . Our data support the hypothesis that the main proapoptotic function of Smac and Smac  $\beta$  is due to a mechanism other than IAP binding.

**Key words:** TRAIL • XIAP • alternative splicing • MCF-7 cells • mitochondria

## Introduction

Apoptosis is an essential mechanism of cell death required for the correct development and homeostasis of multicellular organisms. Two major apoptotic pathways have been identified: (a) triggering of cell surface death receptors of the tumor necrosis factor (TNF)<sup>1</sup> receptor superfamily, including TNF $\alpha$ , CD95 (Fas/Apo-1), and TNF-related apoptosis-inducing ligand (TRAIL), where caspase-8 is activated following its recruitment to a trimerized receptor–ligand complex via adaptor molecules (for reviews see Ashkenazi and Dixit, 1999; Bratton et al., 2000), and (b) stress-induced apoptosis, caused by chemicals and growth factor deprivation, which results in perturbation of mitochondria and the ensuing release of proteins, such as cytochrome *c*, from the intermitochondrial membrane space (Green and Reed, 1998; Bratton et al., 2000). Released cytochrome *c* binds to the human CED4 homologue Apaf-1 (Zou et al., 1997), which in the presence of dATP, results in the recruitment

and activation of caspase-9 (Li et al., 1997; Cain et al., 1999; Zou et al., 1999). The release of cytochrome *c* from the mitochondria is also regulated partly by Bcl-2 family members with antiapoptotic and proapoptotic members inhibiting or promoting the release, respectively (Kluck et al., 1997; Yang et al., 1997; Li et al., 1998; Luo et al., 1998). The activated initiator caspases-8 and -9 then activate the effector caspases-3, -6, and -7, which are responsible for the cleavage of important cellular substrates, resulting in the classical biochemical and morphological changes associated with the apoptotic phenotype (Cohen, 1997; Earnshaw et al., 1999).

Caspase activity is also regulated by the inhibitor of apoptosis proteins (IAPs), which are found in a range of organisms and are characterized by one or more baculovirus IAP repeats, which are responsible for their antiapoptotic activity (for reviews see Deveraux et al., 1997; Deveraux and Reed, 1999). One major function of IAPs, particularly c-IAP-1 and -2 and X-linked IAP (XIAP), is their propensity to bind to and inhibit key initiator and effector caspases including caspases-9, -3, and -7 (Deveraux et al., 1997; Deveraux and Reed, 1999).

Recently, a novel protein, Smac, and its murine homologue, DIABLO, were described, which promoted caspase activation by eliminating IAP inhibition of caspases (Du et

Address correspondence to M. MacFarlane, MRC Toxicology Unit, Hodgkin Bldg., University of Leicester, PO Box 138, Lancaster Road, Leicester LE1 9HN, UK. Tel.: 44-116-252-5553. Fax: 44-116-252-5616. E-mail: mm21@le.ac.uk

<sup>1</sup>Abbreviations used in this paper: HSV, herpes simplex virus; IAP, inhibitor of apoptosis protein; MG132, carbobenzoxy-leuciny-leuciny-leucinal; TNF, tumor necrosis factor; TRAIL, TNF-related apoptosis-inducing ligand; XIAP, X-linked IAP.

al., 2000; Verhagen et al., 2000). Smac is synthesized as a 239-amino acid precursor protein, with the NH<sub>2</sub>-terminal 55 amino acids serving as a mitochondrial-targeting signal. In response to apoptotic stimuli, mature Smac is released into the cytoplasm. In vitro, mature Smac binds all known human IAP family members and relieves their inhibition of caspases. Recently, this interaction has been mapped to the NH<sub>2</sub>-terminal 20 amino acids of the mature Smac protein, and removal of this region completely blocks its ability to bind XIAP (Chai et al., 2000; Srinivasula et al., 2000). Because Smac acts to prevent IAP activity, it is proposed to be a human equivalent of the *Drosophila* proteins Reaper, Grim, and Hid (Du et al., 2000; Verhagen et al., 2000).

In this study, we describe Smac  $\beta$ , an alternatively spliced form of Smac, which lacks the mitochondrial-targeting sequence and has a cortical as opposed to a mitochondrial subcellular distribution. Both Smac  $\beta$  and truncated forms of Smac that lack the IAP interacting domain, markedly potentiate apoptosis induced by diverse apoptotic stimuli. These data demonstrate that the main proapoptotic function of Smac and Smac  $\beta$  is not mediated through an interaction with the IAPs.

## Materials and Methods

### Materials

Medium and serum were purchased from Life Technologies. c-IAP-1 and -2 polyclonal antibodies were from R&D Systems, and XIAP and herpes simplex virus (HSV) monoclonal antibodies were from BD Transduction Labs and Novagen, respectively. The HRP-conjugated secondary antibodies, goat anti-rabbit and goat anti-mouse, were from Dako and Sigma-Aldrich, respectively. Anti-mouse Alexa 488 and MitoTracker™ red CMXRos were from Molecular Probes. Carbobenzoxyl-leuciny-leuciny-leucinal (MG132) was obtained from Calbiochem. TRAIL was produced as described previously (MacFarlane et al., 1997a). Unless stated otherwise, all other chemicals were from Sigma-Aldrich.

### Generation of Constructs

All Smac and Smac  $\beta$  constructs were generated by PCR amplification and cloned into the expression vector pTriEx-1 (Novagen). Total RNA was isolated using TriReagent and reverse transcribed using Expand™ reverse transcriptase (Roche Diagnostics) before amplification of full-length Smac and Smac  $\beta$  cDNA using *Pfu* DNA polymerase (Stratagene). Deletion mutants were generated in the same manner, and all constructs were verified by DNA sequencing.

### Cell Culture, Transfection, and Induction of Cell Death

Human embryonic kidney 293 cells were obtained from the European Collection of Animal Cell Cultures and grown in high glucose DME supplemented with 10% FBS. MCF-7-Fas (MCF-7) human breast epithelial cells (from Dr. M. Jaattela, Danish Cancer Society Research Center, Copenhagen, Denmark) were grown in RPMI 1640 supplemented with 10% FBS and 2 mM Glutamax™. Both cell lines were cultured in an atmosphere of 5% CO<sub>2</sub> in air at 37°C and maintained by routine passage every 3–4 d. Cells were transiently transfected using Fugene 6™ (Roche Biochemicals) and 0.5–4  $\mu$ g DNA, where indicated in the presence of pRSC *lacZ* (MacFarlane et al., 1997a). After 24 h, cells were either harvested or exposed to an apoptotic stimulus. Apoptosis was induced by treatment for 6 h with either etoposide, MG132, TNF (in the presence or absence of cycloheximide), or TRAIL. The extent of apoptosis was assessed by counting the percentage of apoptotic blue- ( $\beta$ -galactosidase-expressing) transfected cells.

### Immunofluorescence Microscopy

Cells were grown on coverslips and 24 h after transfection, stained with MitoTracker™ (100 nM) for 15 min at 37°C before fixation in 3.8% form-

aldehyde for 20 min at room temperature. Cells were rinsed three times in PBS, permeabilized with 0.1% Triton X-100 in PBS and blocked overnight in 3% BSA in PBS at 4°C. Cells were incubated with HSV antibody (1:25,000 in 3% BSA) for 3 h at room temperature and then incubated with anti-mouse Alexa 488 (1:300) for 45 min at room temperature. The cells were then washed and nuclei were stained with Hoechst 33258 (0.25  $\mu$ g/ml) for 20 min before mounting onto glass slides using Vectashield® (Vector Laboratories). Optical sections were taken using argon-krypton, UV lasers, and a Leica TCS-4D confocal imaging system.

### Production of Recombinant Proteins

Recombinant proteins were produced in *Escherichia coli* BL21(DE3) as described previously (Zou et al., 1997) and retained on beads. The purified proteins were stored in aliquots at 4°C, and their identity was confirmed by Western blotting using anti-HSV monoclonal antibody.

### Production of <sup>35</sup>S-labeled Proteins and In Vitro Interaction Assay

<sup>35</sup>S-labeled proteins were produced using the TNT®-coupled reticulocyte lysate system (Promega). The constructs used were pcDNA3 human MIHB (c-IAP-1), human MIHC (c-IAP-2), and pSP72 XIAP (gifts from Dr. D. Vaux, The Walter and Eliza Hall Institute, Melbourne, Australia). For the in vitro interaction assay, 10  $\mu$ l of Ni-NTA agarose beads (QIAGEN) or beads bound to recombinant protein were added to 5  $\mu$ l of TNT mix, and the final volume was adjusted to 100  $\mu$ l with buffer A (50 mM Tris, 150 mM NaCl, 0.1% IGEPAL CA-630, pH 7.6), before incubation for 1 h at room temperature. The beads were then pelleted, washed in buffer A, and resuspended in SDS-PAGE sample buffer before resolving on a 13% SDS-polyacrylamide gel. As a marker, 1  $\mu$ l of the TNT reaction was run alongside the beads. The gel was then dried and visualized by autoradiography.

### Immunoprecipitation Studies

Cells were harvested 24 h after transfection, and immunoprecipitation of XIAP was carried out as described previously (Srinivasula et al., 1997). To precipitate Smac and Smac  $\beta$  via the His<sub>6</sub> tag, lysates were prepared and incubated overnight with Ni-NTA agarose beads at 4°C and then washed and prepared for SDS-PAGE.

### Gel Electrophoresis and Western Blotting

Equal amounts of lysate were diluted in SDS-PAGE sample buffer and separated on 13% (HSV) or 10% (XIAP and c-IAP-1 and -2) polyacrylamide gels followed by electrophoretic transfer onto polyvinylidene difluoride membrane (Bio-Rad Laboratories). Immunodetection was carried out as described previously (MacFarlane et al., 1997b) using ECL detection (Amersham-Pharmacia Biotech).

## Results and Discussion

### Identification of Smac $\beta$

The protein sequence of Smac was used to search the human ESTs deposited in GenBank using the programme TBLASTN. This search revealed several ESTs, which corresponded to the previously reported Smac and some that contained an alternative prosequence (for example, sequence data available from GenBank/EMBL/DDBJ under accession number AA156765) or other sequence differences. A search of the nonredundant database resulted in the identification of Smac  $\beta$ , a form of Smac, with an alternative NH<sub>2</sub> terminus (sequence data available from GenBank/EMBL/DDBJ under accession number AK001399). Translation of this sequence revealed an ORF of 186 amino acids that was identical to the reported Smac molecule in all but the prosequence (Fig. 1, A and B) with an in-frame stop codon upstream of the initiator methionine, indicating a full-length reading frame (data not

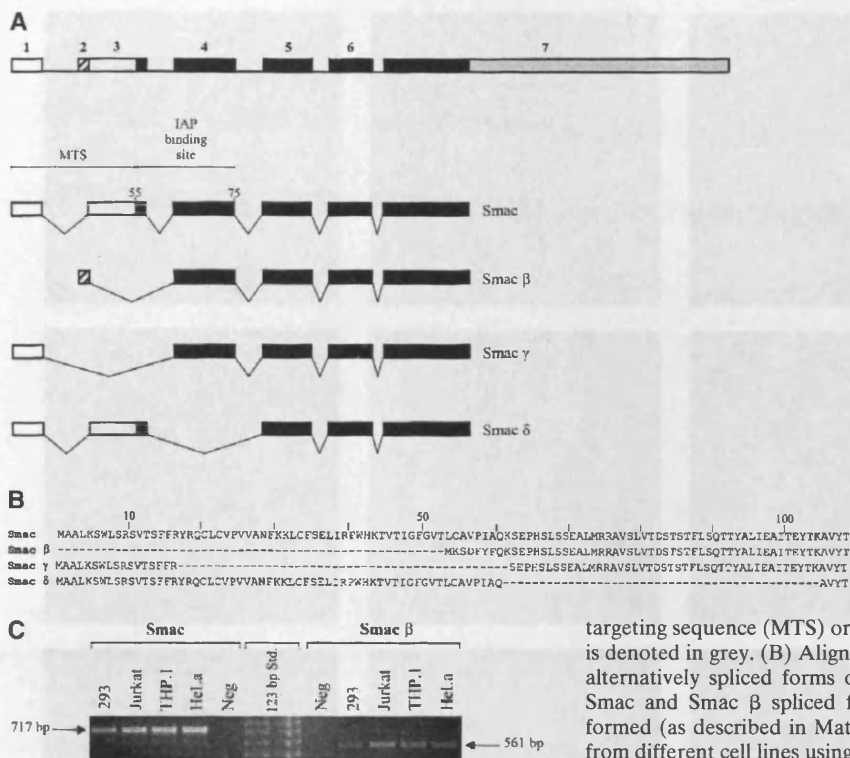


**Figure 1.** Smac exists as several differentially spliced forms. (A) Schematic representation of the *Smac* gene (exons 1–7) and spliced forms encoding changes in either the mitochondrial-targeting sequence (MTS) or the IAP-binding site. The noncoding region is denoted in grey. (B) Alignment of the first 109 amino acids of the four alternatively spliced forms of Smac. (C) To confirm expression of the Smac and Smac  $\beta$  spliced forms, reverse transcriptase–PCR was performed (as described in Materials and Methods) on total RNA isolated from different cell lines using primers specific for either Smac or Smac  $\beta$ .

shown). Primers were designed to amplify either Smac or Smac  $\beta$  cDNA and were used in reverse transcriptase–PCR using total RNA isolated from various cell lines as a template. The mRNA for both Smac and Smac  $\beta$  was detected in all the cell lines examined and showed similar expression levels (Fig. 1 C). To confirm that the Smac  $\beta$  mRNA was in fact a spliced form of Smac, both the protein and cDNA sequence of Smac were used to search the HTGS section of GenBank. These searches revealed a genomic sequence (sequence data available from GenBank/EMBL/DDBJ under accession number NT\_009438) that contained regions of identity to Smac and Smac  $\beta$  sequences, indicative of the exon structure of the gene. The genomic sequence was composed of sequence from the q arm of chromosome 12, mapping the *Smac* gene close to the *APAF1* gene (Kim et al., 1999). From the genomic sequence, it was deduced that the *Smac* gene is composed of seven exons (Fig. 1 A), with the prosequence of Smac encoded by exons 1 and 3, and the prosequence of Smac  $\beta$  encoded by exon 2.

Like many other genes encoding proteins involved in apoptosis, the *Smac* gene may produce several alternatively spliced forms (Fig. 1 A). As database searching revealed at least three other putative short splice forms of Smac, we have designated these Smac  $\beta$ ,  $\gamma$ , and  $\delta$ . Smac  $\beta$  is identical to the recently described Smac-S (Srinivasula et al., 2000). Smac  $\gamma$  (sequence data available from GenBank/EMBL/DDBJ under accession number BE383154) should have a similar cellular distribution to Smac  $\beta$ , due to the loss of amino acids 18–62 in the mitochondrial-targeting sequence (exon 3) and may bind IAPs only weakly. Smac  $\delta$  (sequence data available from GenBank/EMBL/

DDBJ under accession number AW247557) should be targeted to the mitochondria due to the presence of an intact targeting sequence (amino acids 1–55) and may bind to the baculoviral IAP repeat-3 domain of XIAP as amino acids 56–61 are retained. However, Smac  $\delta$  lacks amino acids 62–105 due to differential splicing of exon 4 (Fig. 1 B), probably weakening its binding to XIAP (Chai et al., 2000; Srinivasula et al., 2000).

#### *Smac $\beta$ Localizes to the Cell Cortex*

Smac and Smac  $\beta$  were overexpressed in 293 and MCF-7 cells, and their subcellular localization was determined by confocal microscopy using an anti-HSV tag antibody (Fig. 2). Smac colocalized with MitoTracker<sup>TM</sup>, indicating a mitochondrial distribution (Fig. 2, A–C). Thus, overexpressed Smac showed the same cellular localization as endogenous Smac (Du et al., 2000). In contrast, Smac  $\beta$  showed a distinct cortical distribution with no mitochondrial localization evident (Fig. 2, E–G and I–K). The subcellular localization of Smac  $\beta$  was confirmed by fractionation of transfected cells (data not shown). To determine the effects of both death receptor and chemically mediated apoptosis on the distribution of Smac and Smac  $\beta$ , cells were exposed to either TRAIL or etoposide, a DNA topoisomerase II inhibitor. TRAIL causes a rapid induction of apoptosis in MCF-7 cells, with caspase-8 as the apical caspase (MacFarlane et al., 2000). Both apoptotic stimuli induced the release of Smac from the mitochondria (Fig. 2 D; data not shown) in agreement with previous reports (Du et al., 2000; Verhagen et al., 2000). In some apoptotic cells, Smac redistributed to the cell periphery and displayed a similar distribution to Smac  $\beta$ . No major

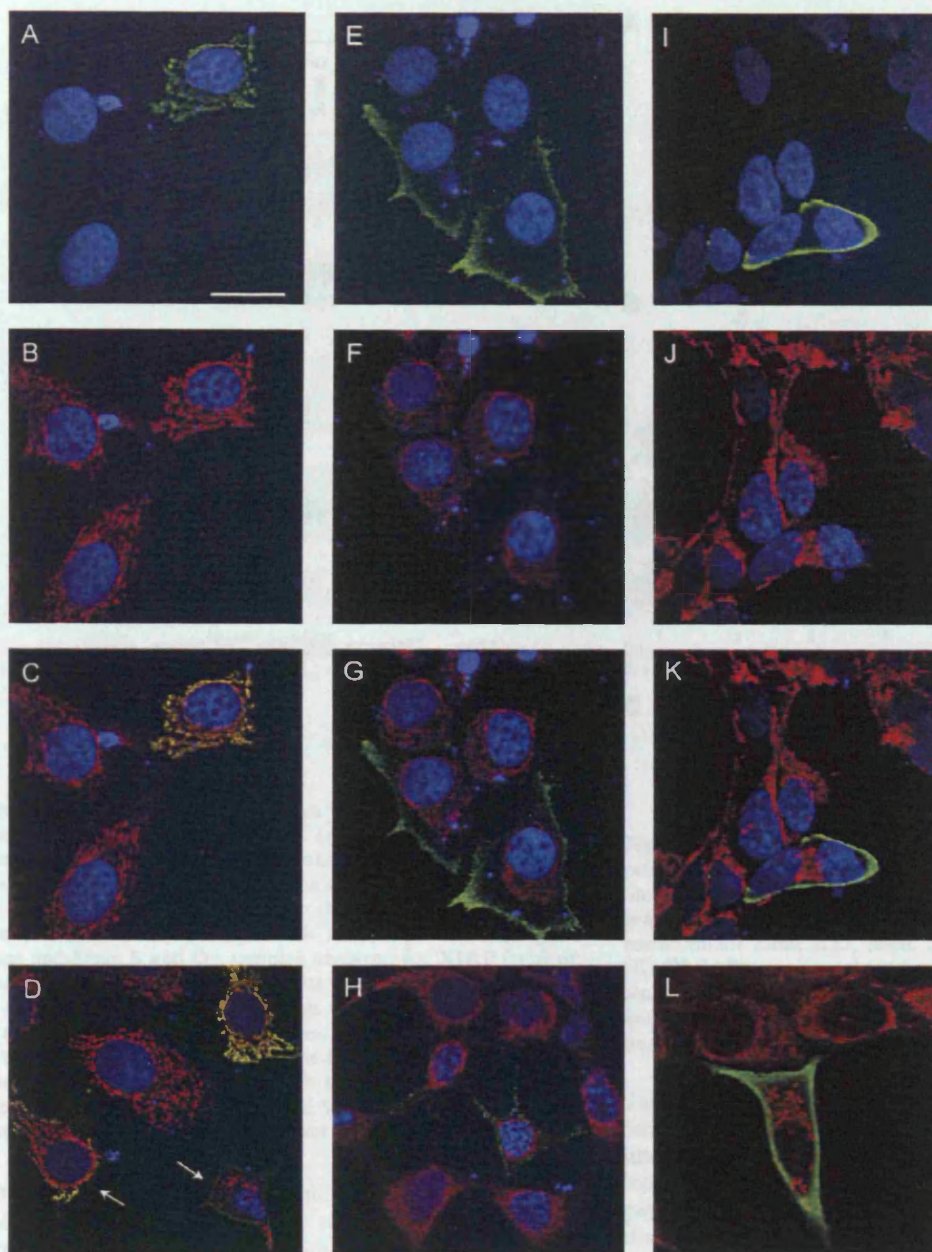


**Figure 2.** Smac and Smac  $\beta$  exhibit a different subcellular distribution. MCF-7 (A–H) and 293 (I–K) cells were transiently transfected with either Smac (A–D) or Smac  $\beta$  (E–K) and after 24 h were fixed and stained for immunofluorescence microscopy as described in Materials and Methods. Transfected cells were stained green (Alexa 488). Mitochondria were labeled with MitoTracker™ red CMXRos (B–D, F–H, and J–L). Cell nuclei were labeled with Hoechst 33258 (A–K). Smac but not Smac  $\beta$  colocalized with mitochondria (compare C with G and K). TRAIL treatment resulted in loss of Smac from mitochondria of cells undergoing apoptosis (indicated by the arrows in D) and a more punctate distribution of Smac  $\beta$  (H). MCF-7 cells transfected with Smac  $\Delta$ 60 showed a cortical distribution (L). Bar, 10  $\mu$ m.

changes in the distribution of Smac  $\beta$  were observed in apoptotic cells, but it appeared more punctate and accumulated closer to the cell periphery (Fig. 2 H; data not shown). Thus, in contrast to Smac, Smac  $\beta$  showed a different distribution, and its cellular compartmentalization did not significantly change upon induction of apoptosis.

#### **Smac $\beta$ Does Not Interact with IAP Family Members**

To test whether Smac  $\beta$  also interacted with IAPs, lysates were prepared from transfected 293 cells. Immunoprecipitation of endogenous XIAP demonstrated a strong interaction with Smac but little or no interaction with Smac  $\beta$  (Fig. 3 A, top, lanes 5 and 6), although XIAP was completely depleted from the lysates (Fig. 3 A, top, lanes 1–3). Similarly, immunoprecipitation of Smac/Smac  $\beta$ , which completely removed Smac/Smac  $\beta$  (Fig. 3 B, middle, lanes

2 and 3), confirmed that XIAP interacted with Smac but not Smac  $\beta$  (Fig. 3 B, top, lanes 5 and 6). As Smac  $\beta$  was distributed to the cell periphery, it raised the possibility that it bound specifically with c-IAP-1 or -2 rather than with XIAP. Reprobing the blots revealed no interaction of Smac or Smac  $\beta$  with endogenous c-IAP-1 or -2 (Fig. 3 B, bottom, lanes 5 and 6). Taken together, these data strongly suggest that the *in vivo* interaction of Smac with endogenous XIAP is much stronger than with c-IAP-1 or -2 and that Smac  $\beta$  in cells does not interact with endogenous XIAP or c-IAP-1 or -2.

#### **NH<sub>2</sub>-terminal Processing of Smac $\beta$ in Cells Prevents Its Interaction with XIAP**

The NH<sub>2</sub>-terminal 55-amino acid residues of Smac are removed upon mitochondrial import, yielding mature  $\sim$ 21-

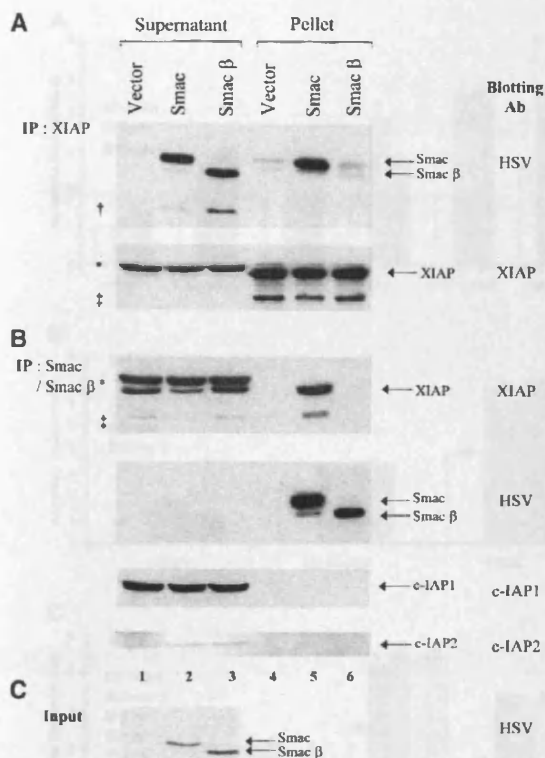


**Figure 3.** Smac but not Smac  $\beta$  can bind XIAP. Lysates were prepared from transfected 293 cells. (A) Endogenous XIAP was immunoprecipitated, and the supernatant and pellet were examined either for Smac or Smac  $\beta$  using the HSV antibody (top) or for XIAP using the XIAP antibody (bottom). (B) Lysates were also incubated with Ni-NTA beads to precipitate His<sub>6</sub>-tagged Smac and Smac  $\beta$  and the samples analyzed for XIAP (top) or Smac and Smac  $\beta$  (middle). The blots were reprobed for c-IAP-1 or -2 (bottom). (C) Expression levels of Smac and Smac  $\beta$  were measured in the transfected cell lysates. Nonspecific bands detected by the anti-XIAP antibody (\*) and the heavy chain of the antibody used for immunoprecipitation (‡) are indicated. Occasionally, an alternative start site in the Smac and Smac  $\beta$  constructs gave rise to a smaller product (†), which did not interact with IAPs.

kD Smac. Since Smac  $\beta$  has no mitochondrial targeting sequence, its predicted molecular weight is  $\sim$ 21.2 kD. Although transiently expressed Smac and Smac  $\beta$  should comigrate on SDS-PAGE since they are similarly tagged, Smac  $\beta$  appeared to be processed intracellularly as it consistently migrated below mature Smac (Fig. 4 A, compare lanes 2 and 3). To further examine this possibility, the migration of transiently transfected Smac and Smac  $\beta$  was compared with partially purified recombinant mature Smac ( $\Delta$ 55), Smac  $\beta$ , or Smac  $\Delta$ 75 (Fig. 4 A). Transiently expressed Smac  $\beta$  migrated below both recombinant Smac  $\Delta$ 55 and Smac  $\beta$  but similarly to Smac  $\Delta$ 75. These results further supported the hypothesis that Smac  $\beta$  was processed intracellularly. This processing must have occurred at the amino terminus, since the protein retained the COOH-terminal HSV and His<sub>6</sub> tags, and Smac  $\beta$  appeared to be processed  $\sim$ 20 amino acids from its NH<sub>2</sub> terminus. Initial experiments to identify this cleavage site were unsuccessful because Smac  $\beta$  isolated from cells was NH<sub>2</sub>-terminally blocked. Because this NH<sub>2</sub>-terminal processing would be predicted to remove the IAP binding domain of

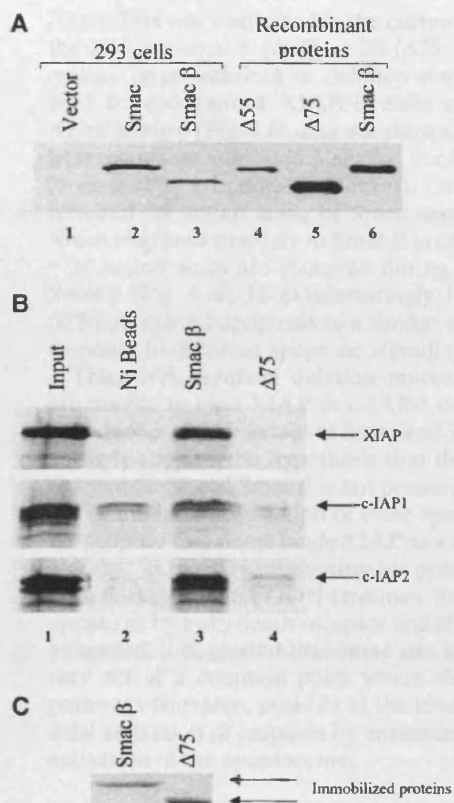


**Figure 4.** Smac  $\beta$  cannot bind XIAP in vivo due to NH<sub>2</sub>-terminal processing. (A) 293 cells were transfected with empty vector, Smac, or Smac  $\beta$  and harvested at 24 h (lanes 1–3), and the migration on SDS gels of Smac and Smac  $\beta$  was compared with recombinant Smac  $\Delta$ 55, Smac  $\Delta$ 75, and Smac  $\beta$  (lanes 4–6). (B) <sup>35</sup>S IAPs were incubated with beads alone, recombinant Smac  $\beta$ , or Smac  $\Delta$ 75 bound to Ni-NTA beads, washed, and analyzed by autoradiography. (C) Input control showing the beads bound to Smac  $\beta$  and Smac  $\Delta$ 75.

Smac  $\beta$ , we assessed the ability of full-length recombinant Smac  $\beta$  and Smac  $\Delta$ 75 to interact with IAPs in an in vitro interaction assay. Recombinant Smac  $\beta$  but not Smac  $\Delta$ 75 interacted with XIAP and c-IAP-1 and -2 (Fig. 4 B, compare lanes 3 and 4). Taken together, these data suggest that the NH<sub>2</sub> terminus of Smac  $\beta$  is removed by cellular processing, therefore explaining its inability to interact with XIAP in intact cells (Fig. 3, A and B, top, lane 6).

#### Smac $\beta$ Potentiates Apoptosis

Processed Smac  $\beta$  may act as a dominant negative inhibitor of apoptosis, since it did not interact with IAPs in intact cells. To test this hypothesis, cells were cotransfected with constructs for full-length Smac or Smac  $\beta$  together with the reporter construct pRSC *lacZ* and then treated with different apoptotic stimuli, including death receptor stimuli (TRAIL and TNF) and etoposide and the proteasome inhibitor, MG132. In 293 cells, both Smac and Smac  $\beta$  potentiated apoptosis induced by all five apoptotic stimuli (Fig. 5 A). Similar potentiation was also observed in MCF-7 cells (Fig. 5 B). As Smac  $\beta$  is NH<sub>2</sub>-terminally processed to a form, which is unable to interact with IAPs, we propose that the domain(s) for the proapoptotic function of Smac  $\beta$  resides in the remaining COOH-terminal frag-

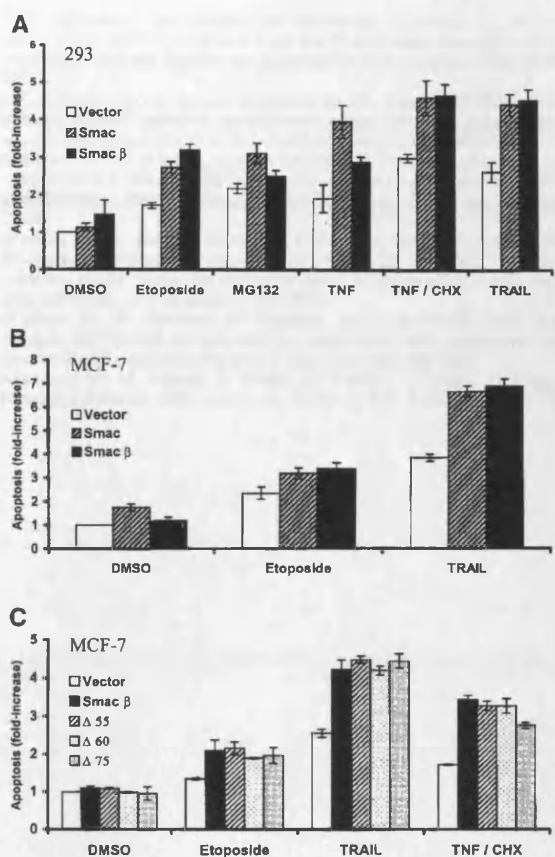


**Figure 5.** NH<sub>2</sub>-terminal truncations of Smac, lacking the IAP-binding domain, potentiate apoptosis. (A) 293 and (B and C) MCF-7 cells were cotransfected with either empty vector, Smac, Smac  $\beta$ , or NH<sub>2</sub>-terminal deletions of Smac together with pRSC *lacZ*. Similar levels of transfected proteins were expressed (data not shown). After 24 h, cells were treated for 6 h with DMSO (vehicle control), etoposide (10  $\mu$ M), MG132 (0.1  $\mu$ M), TRAIL (0.25  $\mu$ g/ml in MCF-7 or 1  $\mu$ g/ml in 293 cells), or TNF (10 ng/ml) in the presence or absence of cycloheximide (1  $\mu$ M). Cells were then fixed and stained with X-gal. Apoptosis was assessed by morphological analysis and expressed as a percentage of transfected (blue) cells. The extent of apoptosis represents the fold increase over DMSO-treated cells transfected with empty vector. The bars represent the mean  $\pm$  standard error of three independent experiments performed in triplicate. In all of the experiments, the potentiation of apoptosis by Smac, Smac  $\beta$ , and the deletion mutants was significantly different ( $P < 0.05$ ) from the vector controls as assessed by single factor ANOVA.

ment and is independent of IAP interaction. However, it was formally possible that the NH<sub>2</sub>-terminal peptide released, following processing of Smac  $\beta$ , bound to cellular IAPs, and therefore relieved caspase inhibition when exposed to an apoptotic stimulus. To examine this possibility, NH<sub>2</sub>-terminal deletion mutants of Smac, which lacked the IAP interacting domain, were prepared.

#### NH<sub>2</sub>-terminal Truncations of Smac, Lacking IAP Binding, Potentiate Apoptosis

The IAP-binding domain of Smac resides in the NH<sub>2</sub>-terminal amino acids (Chai et al., 2000; Srinivasula et al.,

2000). This was confirmed in the current study; removal of the NH<sub>2</sub>-terminal 5 ( $\Delta 60$ ) or 20 ( $\Delta 75$ ) amino acids from mature Smac resulted in deletion mutants that did not bind to endogenous XIAP in cells or to recombinant XIAP in vitro (Fig. 4 B; data not shown). Both of these deletion mutants exhibited a similar cortical distribution to Smac  $\beta$  (Fig. 2 L; data not shown). Deletion of the NH<sub>2</sub>-terminal 75 amino acids of Smac resulted in a protein, which migrated similarly to Smac  $\beta$  in cells, suggesting that  $\sim 22$  amino acids are removed during the maturation of Smac  $\beta$  (Fig. 4 A). Most interestingly, both Smac  $\Delta 60$  and  $\Delta 75$  potentiated apoptosis to a similar extent as Smac  $\beta$  in response to different apoptotic stimuli (Fig. 5 C).

Thus, NH<sub>2</sub>-terminal deletion mutants of Smac, which are unable to bind XIAP or c-IAP-1 or -2, potentiate apoptosis to a similar extent as Smac and Smac  $\beta$ . These data strongly support the hypothesis that the proapoptotic activity of Smac and Smac  $\beta$  is not primarily mediated via relief of the inhibitory action of these specific IAPs. Rather, we propose that Smac binds XIAP as a secondary function and that its primary mechanism for promoting apoptosis is via a domain in the COOH terminus. Because induction of apoptosis by both death receptor and chemical stimuli was enhanced, it suggested that Smac and its deletion mutants may act at a common point where these two apoptotic pathways converge, possibly at the level of postmitochondrial activation of caspases by enhancing the formation or activation of the apoptosome.

We thank our colleagues Drs. K. Cain and S. Bratton for helpful comments and discussion.

Submitted: 14 December 2000

Revised: 1 February 2001

Accepted: 2 February 2001

#### References

- Ashkenazi, A., and V.M. Dixit. 1999. Apoptosis control by death and decoy receptors. *Curr. Opin. Cell Biol.* 11:255–260.
- Bratton, S.B., M. MacFarlane, K. Cain, and G.M. Cohen. 2000. Protein complexes activate distinct caspase cascades in death receptor and stress-induced apoptosis. *Exp. Cell Res.* 256:27–33.
- Cain, K., D.G. Brown, C. Langlais, and G.M. Cohen. 1999. Caspase activation involves the formation of the apoptosome, a large ( $\sim 700$  kDa) caspase-activating complex. *J. Biol. Chem.* 274:22686–22692.
- Chai, J., C. Du, J.W. Wu, S. Kyin, X. Wang, and Y. Shi. 2000. Structural and biochemical basis of apoptotic activation by Smac/DIABLO. *Nature.* 406:855–862.
- Cohen, G.M. 1997. Caspases: the executioners of apoptosis. *Biochem. J.* 326:1–16.
- Deveraux, Q.L., and J.C. Reed. 1999. IAP family proteins—suppressors of apoptosis. *Genes Dev.* 13:239–252.
- Deveraux, Q.L., R. Takahashi, G.S. Salvesen, and J.C. Reed. 1997. X-linked IAP is a direct inhibitor of cell-death proteases. *Nature.* 388:300–304.
- Du, C., M. Fang, Y. Li, L. Li, and X. Wang. 2000. Smac, a mitochondrial protein that promotes cytochrome c-dependent caspase activation by eliminating IAP inhibition. *Cell.* 102:33–42.
- Earnshaw, W.C., L.M. Martins, and S.H. Kaufmann. 1999. Mammalian caspases: structure, activation, substrates, and functions during apoptosis. *Annu. Rev. Biochem.* 68:383–424.
- Green, D.R., and J.C. Reed. 1998. Mitochondria and apoptosis. *Science.* 281:1309–1312.
- Kim, H., Y.K. Jung, Y.K. Kwon, and S.H. Park. 1999. Assignment of apoptotic protease activating factor-1 gene (APAF1) to human chromosome band 12q23 by fluorescence in situ hybridization. *Cytogenet. Cell Genet.* 87:252–253.
- Kluck, R.M., E. Bossy-Wetzel, D.R. Green, and D.D. Newmeyer. 1997. The release of cytochrome c from mitochondria: a primary site for Bcl-2 regulation of apoptosis. *Science.* 275:1132–1136.
- Li, H., H. Zhu, C.-J. Xu, and J. Yuan. 1998. Cleavage of BID by caspase-8 mediates the mitochondrial damage in the Fas pathway of apoptosis. *Cell.* 94:491–501.

- Li, P., D. Nijhawan, I. Budihardjo, S.M. Srinivasula, M. Ahmad, E.S. Alnemri, and X. Wang. 1997. Cytochrome c and dATP-dependent formation of Apaf-1/caspase-9 complex initiates an apoptotic protease cascade. *Cell*. 91:479-489.
- Luo, X., I. Budihardjo, H. Zou, C. Slaughter, and X. Wang. 1998. Bid, a Bcl2 interacting protein, mediates cytochrome c release from mitochondria in response to activation of cell surface death receptors. *Cell*. 94:481-490.
- MacFarlane, M., M. Ahmad, S.M. Srinivasula, T. Fernandes-Alnemri, G.M. Cohen, and E.S. Alnemri. 1997a. Identification and molecular cloning of two novel receptors for the cytotoxic ligand TRAIL. *J. Biol. Chem.* 272:25417-25420.
- MacFarlane, M., K. Cain, X.-M. Sun, E.S. Alnemri, and G.M. Cohen. 1997b. Processing/activation of at least four interleukin-1 $\beta$  converting enzyme-like proteases occurs during the execution phase of apoptosis in human monocytic tumor cells. *J. Cell Biol.* 137:469-479.
- MacFarlane, M., W. Merrison, D. Dinsdale, and G.M. Cohen. 2000. Active caspases and cleaved cytokeratins are sequestered into cytoplasmic inclusions in TRAIL-induced apoptosis. *J. Cell Biol.* 148:1239-1254.
- Srinivasula, S.M., M. Ahmad, S. Otilie, F. Bultrich, S. Banks, Y. Wang, T. Fernandes-Alnemri, C.M. Croce, G. Litwack, K.J. Tomaselli, et al. 1997. FLAME-1, a novel FADD-like anti-apoptotic molecule that regulates Fas/TNFR1-induced apoptosis. *J. Biol. Chem.* 272:18542-18545.
- Srinivasula, S.M., P. Datta, X.-J. Fan, T. Fernandes-Alnemri, Z. Huang, and E.S. Alnemri. 2000. Molecular determinants of the caspase-promoting activity of Smac/DIABLO and its role in the death receptor pathway. *J. Biol. Chem.* 275:36152-36157.
- Verhagen, A.M., P.G. Ekert, M. Pakusch, J. Silke, L.M. Connolly, G.E. Reid, R.L. Moritz, R.J. Simpson, and D.L. Vaux. 2000. Identification of DIABLO, a mammalian protein that promotes apoptosis by binding to and antagonizing IAP proteins. *Cell*. 102:43-53.
- Yang, J., X. Liu, K. Bhalla, C.N. Kim, A.M. Ibrado, J. Cai, T.I. Peng, D.P. Jones, and X. Wang. 1997. Prevention of apoptosis by Bcl-2: release of cytochrome c from mitochondria blocked. *Science*. 275:1129-1132.
- Zou, H., W.J. Henzel, X. Liu, A. Lutschg, and X. Wang. 1997. Apaf-1, a human protein homologous to *C. elegans* CED-4, participates in cytochrome c-dependent activation of caspase-3. *Cell*. 90:405-413.
- Zou, H., Y. Li, X. Liu, and X. Wang. 1999. An APAF-1/cytochrome c multimeric complex is a functional apoptosome that activates procaspase-9. *J. Biol. Chem.* 274:11549-11556.

**BIBLIOGRAPHY**

- Adrain, C., Slee, E.A., Harte, M.T. & Martin, S.J. (1999). *J. Biol. Chem.*, **274**, 20855-20860.
- Bala, S., Oliver, H., Renault, B., Montgomery, K., Dutta, S., Rao, P., Houldsworth, J., Kucherlapati, R., Wang, X., Chaganti, R.S. & Murty, V.V. (2000). *Genes Chromosomes Cancer*, **28**, 258-268.
- Basanez, G., Zhang, J., Chau, B.N., Makshev, G.I., Frolov, V.A., Brandt, T.A., Burch, J., Hardwick, J.M. & Zimmerberg, J. (2001). *J. Biol. Chem.*, **276**, 31083-31091.
- Beere, H.M., Wolf, B.B., Cain, K., Mosser, D.D., Mahboubi, A., Kuwana, T., Taylor, P., Morimoto, R.I., Cohen, G.M. & Green, D.R. (2000). *Nat. Cell Biol.*, **2**, 469-475.
- Benedict, M.A., Hu, Y., Inohara, N. & Nunez, G. (2000). *J. Biol. Chem.*, **275**, 8461-8468.
- Bertin, J., Nir, W.-J., Fischer, C.M., Tayber, O.V., Errada, P.R., Grant, J.R., Keilty, J.J., Gosselin, M.L., Robison, K.E., Wong, G.H.W., Glucksmann, M.A. & DiStefano, P.S. (1999). *J. Biol. Chem.*, **274**, 12955-12958.
- Bodmer, J.L., Holler, N., Reynard, S., Vinciguerra, P., Schneider, P., Juo, P., Blenis, J. & Tschopp, J. (2000). *Nat. Cell Biol.*, **2**, 241-243.
- Boldin, M.P., Goncharov, T.M., Goltsev, Y.V. & Wallach, D. (1996). *Cell*, **85**, 803-815.
- Bossy-Wetzell, E. & Green, D.R. (1999). *Mutat. Res.*, **434**, 243-251.
- Boya, P., Roques, B. & Kroemer, G. (2001). *EMBO J.*, **20**, 4325-4331.
- Bratton, S.B., MacFarlane, M., Cain, K. & Cohen, G.M. (2000). *Exp. Cell Res.*, **256**, 27-33.
- Bratton, S.B., Walker, G., Roberts, D.L., Cain, K. & Cohen, G.M. (2001). *Cell Death Differ.*, **8**, 425-433.

- Bratton, S.B., Walker, G., Srinivasula, S.M., Sun, X.M., Butterworth, M., Alnemri, E.S. & Cohen, G.M. (2001). *EMBO J.*, **20**, 998-1009.
- Breitschopf, K., Haendeler, J., Malchow, P., Zeiher, A.M. & Dimmeler, S. (2000). *Mol. Cell. Biol.*, **20**, 1886-1896.
- Bruey, J.M., Ducasse, C., Bonniaud, P., Ravagnan, L., Susin, S.A., Diaz-Latoud, C., Gurbuxani, S., Arrigo, A.P., Kroemer, G., Solary, E. & Garrido, C. (2000). *Nat. Cell Biol.*, **2**, 645-652.
- Budihardjo, I., Oliver, H., Lutter, M., Luo, X. & Wang, X. (1999). *Annu. Rev. Cell Dev. Biol.*, **15**, 269-290.
- Burgess, D.H., Svensson, M., Dandrea, T., Gronlund, K., Hammarquist, F., Orrenius, S. & Cotgreave, I.A. (1999). *Cell Death Differ.*, **6**, 256-261.
- Cain, K., Bratton, S.B., Langlais, C., Walker, G., Brown, D.G., Sun, X.-M. & Cohen, G.M. (2000). *J. Biol. Chem.*, **275**, 6067-6070.
- Cain, K., Brown, D.G., Langlais, C. & Cohen, G.M. (1999). *J. Biol. Chem.*, **274**, 22686-22692.
- Cardozo, T.J. & Abagyan, R. (1998). *J. Mol. Model.*, **4**, 83-93.
- Cecconi, F., Alvarez-Bolado, G., Meyer, B.I., Roth, K.A. & Gruss, P. (1998). *Cell*, **94**, 727-737.
- Chai, J., Du, C., Wu, J.W., Kyin, S., Wang, X. & Shi, Y. (2000). *Nature*, **406**, 855-862.
- Chan, S.L., Yee, K.S., Tan, K.M. & Yu, V.C. (2000). *J. Biol. Chem.*, **275**, 17925-17928.
- Chaudhary, D., O'Rourke, K., Chinnaiyan, A.M. & Dixit, V.M. (1998). *J. Biol. Chem.*, **273**, 17708-17712.
- Chauhan, D., Hideshima, T., Rosen, S., Reed, J.C., Kharbanda, S. & Anderson, K.C. (2001). *J. Biol. Chem.*, **276**, 24453-24456.

- Chen, F., Hersh, B.M., Conradt, B., Zhou, Z., Riemer, D., Gruenbaum, Y. & Horvitz, H.R. (2000a). *Science*, **287**, 1485-1489.
- Chen, Q., Gong, B. & Almasan, A. (2000b). *Cell Death Differ.*, **7**, 227-233.
- Chen, Z., Naito, M., Hori, S., Mashima, T., Yamori, T. & Tsuruo, T. (1999). *Biochem. Biophys. Res. Commun.*, **264**, 847-854.
- Chinnaiyan, A.M., Tepper, C.G., Seldin, M.F., O'Rourke, K., Kischkel, F.C., Hellbardt, S., Krammer, P.H., Peter, M.E. & Dixit, V.M. (1996). *J. Biol. Chem.*, **271**, 4961-4965.
- Chipuk, J.E., Bhat, M., Hsing, A.Y., Ma, J. & Danielpour, D. (2001). *J. Biol. Chem.*, **276**, 26614-26621.
- Cho, J.H. (2001). *Inflamm. Bowel Dis.*, **7**, 271-275.
- Chou, J.J., Matsuo, H., Duan, H. & Wagner, G. (1998). *Cell*, **94**, 171-180.
- Chu, Z.L., McKinsey, T.A., Liu, L., Gentry, J.J., Malim, M.H. & Ballard, D.W. (1997). *Proc. Natl. Acad. Sci. U S A*, **94**, 10057-10062.
- Chu, Z.-L., Pio, F., Xie, Z., Welsh, K., Krajewska, M., Krajewski, S., Godzik, A. & Reed, J.C. (2001). *J. Biol. Chem.*, **276**, 9239-16398.
- Clem, R.J., Cheng, E.H., Karp, C.L., Kirsch, D.G., Ueno, K., Takahashi, A., Kastan, M.B., Griffin, D.E., Earnshaw, W.C., Veluona, M.A. & Hardwick, J.M. (1998). *Proc. Natl. Acad. Sci. U S A*, **95**, 554-559.
- Clem, R.J., Sheu, T.-T., Richter, B.W.M., He, W.-W., Thornberry, N.A., Duckett, C.S. & Hardwick, J.M. (2001). *J. Biol. Chem.*, **276**, 7602-7608.
- Cohen, G.M. (1997). *Biochem. J.*, **326**, 1-16.
- Coldwell, M.J., Mitchell, S.A., Stoneley, M., MacFarlane, M. & Willis, A.E. (2000). *Oncogene*, **19**, 899-905.
- Concannon, C.G., Orrenius, S. & Samali, A. (2001). *Gene Expr.*, **9**, 195-201.
- Conus, S., Rosse, T. & Borner, C. (2000). *Cell Death Differ.*, **7**, 947-954.

- Cosulich, S.C., Savory, P.J. & Clarke, P.R. (1999). *Curr. Biol.*, **9**, 147-150.
- Crompton, M. (1999). *Biochem. J.*, **341**, 233-249.
- Crompton, M. (2000). *Curr. Opin. Cell Biol.*, **12**, 414 - 419.
- Damiano, J.S., Stehlik, C., Pio, F., Godzik, A. & Reed, J.C. (2001). *Genomics*, **75**, 77-83.
- Day, C.L., Dupont, C., Lackmann, M., Vaux, D.L. & Hinds, M.G. (1999). *Cell Death Differ.*, **6**, 1125-1132.
- del Peso, L., Gonzalez, V.M., Inohara, N., Ellis, R.E. & Nunez, G. (2000). *J. Biol. Chem.*, **275**, 27205-27211.
- Deng, X., Xiao, L., Lang, W., Gao, F., Ruvolo, P. & May, W.S., Jr. (2001). *J. Biol. Chem.*, **276**, 23681-23688.
- Deveraux, Q.L., Leo, E., Stennicke, H.R., Welsh, K., Salvesen, G.S. & Reed, J.C. (1999a). *EMBO J.*, **18**, 5242-5251.
- Deveraux, Q.L. & Reed, J.C. (1999). *Genes Dev.*, **13**, 239-252.
- Deveraux, Q.L., Roy, N., Stennicke, H.R., Van Arsdale, T., Zhou, Q., Srinivasula, S.M., Alnemri, E.S., Salvesen, G.S. & Reed, J.C. (1998). *EMBO J.*, **17**, 2215-2223.
- Deveraux, Q.L., Stennicke, H.R., Salvesen, G.S. & Reed, J.C. (1999b). *J. Clin. Immunol.*, **19**, 388-398.
- Deveraux, Q.L., Takahashi, R., Salvesen, G.S. & Reed, J.C. (1997). *Nature*, **388**, 300-304.
- Dey, R. & Moraes, C.T. (2000). *J. Biol. Chem.*, **275**, 7087-7094.
- Du, C., Fang, M., Li, Y., Li, L. & Wang, X. (2000). *Cell*, **102**, 33-42.
- Duan, H., Orth, K., Chinnaiyan, A.M., Poirier, G.G., Froelich, C.J., He, W.-W. & Dixit, V.M. (1996). *J. Biol. Chem.*, **271**, 16720-16724.
- Duckett, C.S., Li, F., Wang, Y., Tomaselli, K.J., Thompson, C.B. & Armstrong, R.C. (1998). *Mol. Cell Biol.*, **18**, 608-615.
- Eiben, L.J. & Duckett, C.S. (1998). *Results Probl. Cell Differ.*, **24**, 91-104.

- Ekert, P.G., Silke, J., Hawkins, C.J., Verhagen, A.M. & Vaux, D.L. (2001). *J. Cell Biol.*, **152**, 483-490.
- Eskes, R., Antonsson, B., Osen-Sand, A., Montessuit, S., Richter, C., Sadoul, R., Mazzei, G., Nichols, A. & Martinou, J.C. (1998). *J. Cell Biol.*, **143**, 217-224.
- Eskes, R., Desagher, S., Antonsson, B. & Martinou, J.C. (2000). *Mol. Cell Biol.*, **20**, 929-935.
- Esposti, M.D., Erler, J.T., Hickman, J.A. & Dive, C. (2001). *Mol. Cell Biol.*, **21**, 7268-7276.
- Fairbrother, W.J., Gordon, N.C., Humke, E.W., O'Rourke, K.M., Starovasnik, M.A., Yin, J.P. & Dixit, V.M. (2001). *Protein Sci.*, **10**, 1911-1918.
- Fang, G., Chang, B.S., Kim, C.N., Perkins, C., Thompson, C.B. & Bhalla, K.N. (1998). *Cancer Res.*, **58**, 3202-3208.
- Fernandes-Alnemri, T., Litwack, G. & Alnemri, E. (1994). *J. Biol. Chem.*, **269**, 30761-30764.
- Fernandes-Alnemri, T., Litwack, G. & Alnemri, E.S. (1995). *Cancer Res.*, **55**, 2737-2742.
- Finucane, D.M., Bossy-Wetzel, E., Waterhouse, N.J., Cotter, T.G. & Green, D.R. (1999). *J. Biol. Chem.*, **274**, 2225-2233.
- Fu, W.N., Kelsey, S.M., Newland, A.C. & Jia, L. (2001). *Biochem. Biophys. Res. Commun.*, **282**, 268-272.
- Furukawa, Y., Iwase, S., Kikuchi, J., Terui, Y., Nakamura, M., Yamada, H., Kano, Y. & Matsuda, M. (2000). *J. Biol. Chem.*, **275**, 21661-21667.
- Garcia-Higuera, I., Fenoglio, J., Li, Y., Lewis, C., Panchenko, M.P., Reiner, O., Smith, T.F. & Neer, E.J. (1996). *Biochemistry*, **35**, 13985-13994.

- Geddes, B.J., Wang, L., Huang, W.J., Lavellee, M., Manji, G.A., Brown, M., Jurman, M., Cao, J., Morgenstern, J., Merriam, S., Glucksmann, M.A., DiStefano, P.S. & Bertin, J. (2001). *Biochem. Biophys. Res. Commun.*, **284**, 77-82.
- Goyal, L., McCall, K., Agapite, J., Hartwig, E. & Steller, H. (2000). *EMBO J.*, **19**, 589-597.
- Granville, D.J., Cassidy, B.A., Ruehlmann, D.O., Choy, J.C., Brenner, C., Kroemer, G., van Breemen, C., Margaron, P., Hunt, D.W. & McManus, B.M. (2001). *Am. J. Pathol.*, **159**, 305-311.
- Gross, A., McDonnell, J.M. & Korsmeyer, S.J. (1999). *Genes Dev.*, **13**, 1899-1911.
- Hacker, G., Hawkins, C.J., Smith, K.G. & Vaux, D.L. (1996). *Behring Inst. Mitt.*, 118-126.
- Hahn, C., Hirsch, B., Jahnke, D., Durkop, H. & Stein, H. (1999). *Biochem. Biophys. Res. Commun.*, **261**, 746-749.
- Hakem, R., Hakem, A., Duncan, G.S., Henderson, J.T., Woo, M., Soengas, M.S., Elia, A., de la Pompa, J.L., Kagi, D., Khoo, W., Potter, J., Yoshida, R., Kaufman, S.A., Lowe, S.W., Penninger, J.M. & Mak, T.W. (1998). *Cell*, **94**, 339-352.
- Hampe, J., Cuthbert, A., Croucher, P.J., Mirza, M.M., Mascheretti, S., Fisher, S., Frenzel, H., King, K., Hasselmeyer, A., MacPherson, A.J., Bridger, S., van Deventer, S., Forbes, A., Nikolaus, S., Lennard-Jones, J.E., Foelsch, U.R., Krawczak, M., Lewis, C., Schreiber, S. & Mathew, C.G. (2001). *Lancet*, **357**, 1925-1928.
- Harper, N., Farrow, S.N., Kaptein, A., Cohen, G.M. & MacFarlane, M. (2001). *J. Biol. Chem.*, **276**, 34743-34752.
- Harris, M.H. & Thompson, C.B. (2000). *Cell Death Differ.*, **7**, 1182-1191.
- Harvey, A.J., Bidwai, A.P. & Miller, L.K. (1997). *Mol. Cell Biol.*, **17**, 2835-2843.
- Hauser, H.P., Bardroff, M., Pyrowolakis, G. & Jentsch, S. (1998). *J. Cell Biol.*, **141**, 1415-1422.

- Hausmann, G., O'Reilly, L.A., van Driel, R., Beaumont, J.G., Strasser, A., Adams, J.M. & Huang, D.C.S. (2000). *J. Cell Biol.*, **149**, 623-612.
- Hay, B.A. (2000). *Cell Death Differ.*, **7**, 1045-1056.
- Hegde, R., Srinivasula, S.M., Zhang, Z., Wassell, R., Mukattash, R., Cilenti, L., DuBois, G., Lazebnik, Y., Zervos, A.S., Fernandes-Alnemri, T. & Alnemri, E.S. (2002). *J. Biol. Chem.*, **277**, 432-438.
- Herr, I., Wilhelm, D., Bohler, T., Angel, P. & Debatin, K.M. (1999a). *Int. J. Cancer*, **80**, 417-424.
- Herr, I., Wilhelm, D., Meyer, E., Jeremias, I., Angel, P. & Debatin, K.M. (1999b). *Cell Death Differ.*, **6**, 130-135.
- Hlaing, T., Guo, R.-F., Dilley, K.A., Loussia, J.M., Morrish, T.A., Shi, M.M., Vincenz, C. & Ward, P.A. (2001). *J. Biol. Chem.*, **276**, 9320-9328.
- Honarpour, N., Du, C., Richardson, J.A., Hammer, R.E., Wang, X. & Herz, J. (2000). *Dev. Biol.*, **218**, 248-258.
- Hu, W.H., Johnson, H. & Shu, H.B. (1999a). *J. Biol. Chem.*, **274**, 30603-30610.
- Hu, Y., Benedict, M.A., Ding, L. & Nunez, G. (1999b). *EMBO J.*, **18**, 3586-3595.
- Hu, Y., Benedict, M.A., Wu, D., Inohara, N. & Nunez, G. (1998a). *Proc. Natl. Acad. Sci. U S A*, **95**, 4386-4391.
- Hu, Y., Ding, L., Spencer, D.M. & Nunez, G. (1998b). *J. Biol. Chem.*, **273**, 33489-33494.
- Huang, D.C., Cory, S. & Strasser, A. (1997a). *Oncogene*, **14**, 405-414.
- Huang, D.C., O'Reilly, L.A., Strasser, A. & Cory, S. (1997b). *EMBO J.*, **16**, 4628-4638.
- Huang, H.-k., Joazeiro, C.A.P., Bonfoco, E., Kamada, S., Levenson, J.D. & Hunter, T. (2000). *J. Biol. Chem.*, **275**, 26661-26664.
- Hugot, J.P., Chamaillard, M., Zouali, H., Lesage, S., Cezard, J.P., Belaiche, J., Almer, S., Tysk, C., O'Morain, C.A., Gassull, M., Binder, V., Finkel, Y., Cortot, A.,

- Modigliani, R., Laurent-Puig, P., Gower-Rousseau, C., Macry, J., Colombel, J.F., Sahbatou, M. & Thomas, G. (2001). *Nature*, **411**, 599-603.
- Inohara, N., Koseki, T., del Peso, L., Hu, Y., Yee, C., Chen, S., Carrio, R., Merino, J., Liu, D., Ni, J. & Nunez, G. (1999). *J. Biol. Chem.*, **274**, 14560-14567.
- Inohara, N. & Nunez, G. (2000). *Cell Death Differ.*, **7**, 509-510.
- Inohara, N. & Nunez, G. (2001). *Oncogene*, **20**, 6473-6481.
- Inohara, N., Ogura, Y., Chen, F.F., Muto, A. & Nunez, G. (2001). *J. Biol. Chem.*, **276**, 2551-2554.
- Ioannou, P.A. & de Jong, P.J. (1996). *Current Protocols in Human Genetics, Vol. Unit 5.15*. Dracopoli *et al.* (ed.). John Wiley and Sons: New York.
- Jacotot, E., Ferri, K.F., El Hamel, C., Brenner, C., Druillennec, S., Hoebeke, J., Rustin, P., Metivier, D., Lenoir, C., Geuskens, M., Vieira, H.L., Loeffler, M., Belzacq, A.S., Briand, J.P., Zamzami, N., Edelman, L., Xie, Z.H., Reed, J.C., Roques, B.P. & Kroemer, G. (2001). *J. Exp. Med.*, **193**, 509-519.
- Jaroszewski, L., Rychlewski, L., Reed, J.C. & Godzik, A. (2000). *Proteins*, **39**, 197-203.
- Jiang, X. & Wang, X. (2000). *J. Biol. Chem.*, **275**, 31199-31203.
- Johnson, D.E., Gastman, B.R., Wieckowski, E., Wang, G.Q., Amoscato, A., Delach, S.M. & Rabinowich, H. (2000). *Cancer Res.*, **60**, 1818-1823.
- Joza, N., Susin, S.A., Daugas, E., Stanford, W.L., Cho, S.K., Li, C.Y., Sasaki, T., Elia, A.J., Cheng, H.Y., Ravagnan, L., Ferri, K.F., Zamzami, N., Wakeham, A., Hakem, R., Yoshida, H., Kong, Y.Y., Mak, T.W., Zuniga-Pflucker, J.C., Kroemer, G. & Penninger, J.M. (2001). *Nature*, **410**, 549-554.
- Kannan, K., Kaminski, N., Rechavi, G., Jakob-Hirsch, J., Amariglio, N. & Givol, D. (2001). *Oncogene*, **20**, 3449-3455.

- Kim, C.N., Wang, X., Huang, Y., Ibrado, A.M., Liu, L., Fang, G. & Bhalla, K. (1997). *Cancer Res.*, **57**, 3115-3120.
- Kim, H., Jung, Y.K., Kwon, Y.K. & Park, S.H. (1999). *Cytogenet. Cell Genet.*, **87**, 252-253.
- Kischkel, F.C., Hellbardt, S., Behrmann, I., Germer, M., Pawlita, M., Krammer, P.H. & Peter, M.E. (1995). *EMBO J.*, **14**, 5579-5588.
- Kluck, R.M., Esposti, M.D., Perkins, G., Renken, C., Kuwana, T., Bossy-Wetzell, E., Goldberg, M., Allen, T., Barber, M.J., Green, D.R. & Newmeyer, D.D. (1999). *J. Cell Biol.*, **147**, 809-822.
- Krammer, P.H. (1998). *Toxicol. Lett.*, **102-103**, 131-137.
- Krammer, P.H. (1999). *Adv. Immunol.*, **71**, 163-210.
- Krueger, A., Schmitz, I., Baumann, S., Krammer, P.H. & Kirchhoff, S. (2001). *J. Biol. Chem.*, **276**, 20633-21409.
- Kuang, A.A., Diehl, G.E., Zhang, J. & Winoto, A. (2000). *J. Biol. Chem.*, **275**, 25065-25068.
- Kuida, K., Haydar, T.F., Kuan, C.Y., Gu, Y., Taya, C., Karasuyama, H., Su, M.S., Rakic, P. & Flavell, R.A. (1998). *Cell*, **94**, 325-337.
- Kuida, K., Lippke, J.A., Ku, G., Harding, M.W., Livingston, D.J., Su, M.S. & Flavell, R.A. (1995). *Science*, **267**, 2000-2003.
- Kuida, K., Zheng, T.S., Na, S., Kuan, C., Yang, D., Karasuyama, H., Rakic, P. & Flavell, R.A. (1996). *Nature*, **384**, 368-372.
- Lauber, K., Appel, H.A.E., Schlosser, S.F., Gregor, M., Schulze-Osthoff, K. & Wesselborg, S. (2001). *J. Biol. Chem.*, **276**, 29772-29781.
- Li, C.-Y., Lee, J.-S., Ko, Y.-G., Kim, J.-I. & Seo, J.-S. (2000). *J. Biol. Chem.*, **275**, 25665-25671.

- Li, F., Ambrosini, G., Chu, E.Y., Plescia, J., Tognin, S., Marchisio, P.C. & Altieri, D.C. (1998). *Nature*, **396**, 580-584.
- Li, L.Y., Luo, X. & Wang, X. (2001). *Nature*, **412**, 95-99.
- Li, P., Nijhawan, D., Budihardjo, I., Srinivasula, S.M., Ahmad, M., Alnemri, E.S. & Wang, X. (1997). *Cell*, **91**, 479-489.
- Lin, Y., Devin, A., Cook, A., Keane, M.M., Kelliher, M., Lipkowitz, S. & Liu, Z. (2000). *Mol. Cell. Biol.*, **20**, 6638-6645.
- Lisi, S., Mazzon, I. & White, K. (2000). *Genetics*, **154**, 669-678.
- Liston, P., Roy, N., Tamai, K., Lefebvre, C., Baird, S., Cherton-Horvat, G., Farahani, R., McLean, M., Ikeda, J.E., MacKenzie, A. & Korneluk, R.G. (1996). *Nature*, **379**, 349-353.
- Liu, X., Kim, C.N., Yang, J., Jemmerson, R. & Wang, X. (1996). *Cell*, **86**, 147-157.
- Liu, Z., Sun, C., Olejniczak, E.T., Meadows, R.P., Betz, S.F., Oost, T., Herrmann, J., Wu, J.C. & Fesik, S.W. (2000). *Nature*, **408**, 1004-1008.
- Lorenzo, H.K., Susin, S.A., Penninger, J. & Kroemer, G. (1999). *Cell Death Differ.*, **6**, 516-524.
- Luo, X., Budihardjo, I., Zou, H., Slaughter, C. & Wang, X. (1998). *Cell*, **94**, 481-490.
- MacFarlane, M., Cain, K., Sun, X.M., Alnemri, E.S. & Cohen, G.M. (1997). *J. Cell Biol.*, **137**, 469-479.
- Mancini, M., Machamer, C.E., Roy, S., Nicholson, D.W., Thornberry, N.A., Casciola-Rosen, L.A. & Rosen, A. (2000). *J. Cell Biol.*, **149**, 603-612.
- Martins, L.M., Iaccarino, I., Tenev, T., Gschmeissner, S., Totty, N.F., Lemoine, N.R., Savopoulos, J., Gray, C.W., Creasy, C.L., Dingwall, C. & Downward, J. (2002). *J. Biol. Chem.*, **277**, 439-444.

- Marzo, I., Brenner, C., Zamzami, N., Jurgensmeier, J.M., Susin, S.A., Vieira, H.L., Prevost, M.C., Xie, Z., Matsuyama, S., Reed, J.C. & Kroemer, G. (1998a). *Science*, **281**, 2027-2031.
- Marzo, I., Brenner, C., Zamzami, N., Susin, S.A., Beutner, G., Brdiczka, D., Remy, R., Xie, Z.H., Reed, J.C. & Kroemer, G. (1998b). *J. Exp. Med.*, **187**, 1261-1271.
- McCarthy, J.V. & Dixit, V.M. (1998). *J. Biol. Chem.*, **273**, 24009-24015.
- Medema, J.P., Scaffidi, C., Kischkel, F.C., Shevchenko, A., Mann, M., Krammer, P.H. & Peter, M.E. (1997). *EMBO J.*, **16**, 2794-2804.
- Miceli-Richard, C., Lesage, S., Rybojad, M., Prieur, A.M., Manouvrier-Hanu, S., Hafner, R., Chamaillard, M., Zouali, H., Thomas, G. & Hugot, J.P. (2001). *Nat. Genet.*, **29**, 19-20.
- Moriishi, K., Huang, D.C., Cory, S. & Adams, J.M. (1999). *Proc. Natl. Acad. Sci. U S A*, **96**, 9683-9688.
- Moroni, M.C., Hickman, E.S., Denchi, E.L., Caprara, G., Colli, E., Cecconi, F., Muller, H. & Helin, K. (2001). *Nat. Cell Biol.*, **3**, 552-558.
- Muhlenbeck, F., Haas, E., Schwenzler, R., Schubert, G., Grell, M., Smith, C., Scheurich, P. & Wajant, H. (1998). *J. Biol. Chem.*, **273**, 33091-33098.
- Muhlenbeck, F., Schneider, P., Bodmer, J.L., Schwenzler, R., Hausser, A., Schubert, G., Scheurich, P., Moosmayer, D., Tschopp, J. & Wajant, H. (2000). *J. Biol. Chem.*, **275**, 32208-32213.
- Nakamura, K., Bossy-Wetzler, E., Burns, K., Fadel, M.P., Lozyk, M., Goping, I.S., Opas, M., Bleackley, R.C., Green, D.R. & Michalak, M. (2000). *J. Cell Biol.*, **150**, 731-740.
- Newmeyer, D.D., Bossy-Wetzler, E., Kluck, R.M., Wolf, B.B., Beere, H.M. & Green, D.R. (2000). *Cell Death Differ.*, **7**, 402-407.

- O'Connor, D.S., Grossman, D., Plescia, J., Li, F., Zhang, H., Villa, A., Tognin, S., Marchisio, P.C. & Altieri, D.C. (2000). *Proc. Natl. Acad. Sci. U S A*, **97**, 13103-13107.
- Ogura, Y., Bonen, D.K., Inohara, N., Nicolae, D.L., Chen, F.F., Ramos, R., Britton, H., Moran, T., Karaliuskas, R., Duerr, R.H., Achkar, J.P., Brant, S.R., Bayless, T.M., Kirschner, B.S., Hanauer, S.B., Nunez, G. & Cho, J.H. (2001a). *Nature*, **411**, 603-606.
- Ogura, Y., Inohara, N., Benito, A., Chen, F.F., Yamaoka, S. & Nunez, G. (2001b). *J. Biol. Chem.*, **276**, 4812-4818.
- O'Reilly, L.A., Huang, D.C. & Strasser, A. (1996). *EMBO J.*, **15**, 6979-6990.
- Orth, K., O'Rourke, K., Salvesen, G.S. & Dixit, V.M. (1996). *J. Biol. Chem.*, **271**, 20977-20980.
- Pan, G., O'Rourke, K. & Dixit, V.M. (1998). *J. Biol. Chem.*, **273**, 5841-5845.
- Pandey, P., Farber, R., Nakazawa, A., Kumar, S., Bharti, A., Nalin, C., Weichselbaum, R., Kufe, D. & Kharbanda, S. (2000a). *Oncogene*, **19**, 1975-1981.
- Pandey, P., Saleh, A., Nakazawa, A., Kumar, S., Srinivasula, S.M., Kumar, V., Weichselbaum, R., Nalin, C., Alnemri, E.S., Kufe, D. & Kharbanda, S. (2000b). *EMBO J.*, **19**, 4310-4322.
- Parrish, J., Li, L., Klotz, K., Ledwich, D., Wang, X. & Xue, D. (2001). *Nature*, **412**, 90-94.
- Pawlowski, J. & Kraft, A.S. (2000). *Proc. Natl. Acad. Sci. U S A*, **97**, 529-531.
- Perkins, C., Kim, C.N., Fang, G. & Bhalla, K.N. (1998). *Cancer Res.*, **58**, 4561-4566.
- Poyet, J.-L., Srinivasula, S.M., Tnani, M., Razmara, M., Fernandes-Alnemri, T. & Alnemri, E.S. (2001). *J. Biol. Chem.*, **276**, 28309-28313.
- Purring-Koch, C. & McLendon, G. (2000). *Proc. Natl. Acad. Sci. U S A*, **97**, 11928-11931.

- Qin, H., Srinivasula, S.M., Wu, G., Fernandes-Alnemri, T., Alnemri, E.S. & Shi, Y. (1999). *Nature*, **399**, 549-557.
- Rao, R.V., Hermel, E., Castro-Obregon, S., del Rio, G., Ellerby, L.M., Ellerby, H.M. & Bredesen, D.E. (2001). *J. Biol. Chem.*, **276**, 33869-33874.
- Reed, J.C., Jurgensmeier, J.M. & Matsuyama, S. (1998). *Biochim. Biophys. Acta.*, **1366**, 127-137.
- Reimertz, C., Kogel, D., Lankiewicz, S., Poppe, M. & Prehn, J.H. (2001). *J. Neurochem.*, **78**, 1256-1266.
- Richter, B.W., Mir, S.S., Eiben, L.J., Lewis, J., Reffey, S.B., Frattini, A., Tian, L., Frank, S., Youle, R.J., Nelson, D.L., Notarangelo, L.D., Vezzoni, P., Fearnhead, H.O. & Duckett, C.S. (2001). *Mol. Cell. Biol.*, **21**, 4292-4301.
- Riedl, S.J., Renatus, M., Schwarzenbacher, R., Zhou, Q., Sun, C., Fesik, S.W., Liddington, R.C. & Salvesen, G.S. (2001). *Cell*, **104**, 791-800.
- Roberts, D.L., Merrison, W., MacFarlane, M. & Cohen, G.M. (2001). *J. Cell Biol.*, **153**, 221-228.
- Robertson, G.S., Crocker, S.J., Nicholson, D.W. & Schulz, J.B. (2000). *Brain Pathol.*, **10**, 283-292.
- Robles, R., Tao, X.J., Trbovich, A.M., Maravel, D.V., Nahum, R., Perez, G.I., Tilly, K.I. & Tilly, J.L. (1999). *Endocrinology*, **140**, 2641-2644.
- Rodriguez, A., Oliver, H., Zou, H., Chen, P., Wang, X. & Abrams, J.M. (1999a). *Nat. Cell Biol.*, **1**, 272-279.
- Rodriguez, A., Oliver, H., Zou, H., Chen, P., Wang, X. & Abrams, J.M. (1999b). *Nat. Cell Biol.*, **1**, 272-279.
- Rodriguez, J. & Lazebnik, Y. (1999). *Genes Dev.*, **13**, 3179-3184.

- Rothe, M., Pan, M.G., Henzel, W.J., Ayres, T.M. & Goeddel, D.V. (1995). *Cell*, **83**, 1243-1252.
- Roy, N., Deveraux, Q.L., Takahashi, R., Salvesen, G.S. & Reed, J.C. (1997). *EMBO J.*, **16**, 6914-6925.
- Ruiz-Vela, A., Albar, J.P. & Martinez, C.A. (2001). *FEBS Lett.*, **501**, 79-83.
- Saleh, A., Srinivasula, S.M., Acharya, S., Fishel, R. & Alnemri, E.S. (1999). *J. Biol. Chem.*, **274**, 17941-17945.
- Saleh, A., Srinivasula, S.M., Balkir, L., Robbins, P.D. & Alnemri, E.S. (2000). *Nat. Cell Biol.*, **2**, 476-483.
- Salvesen, G.S. & Dixit, V.M. (1999). *Proc. Natl. Acad. Sci. U S A*, **96**, 10964-10967.
- Scaffidi, C., Fulda, S., Srinivasan, A., Friesen, C., Li, F., Tomaselli, K.J., Debatin, K.M., Krammer, P.H. & Peter, M.E. (1998). *EMBO J.*, **17**, 1675-1687.
- Scaffidi, C., Kirchhoff, S., Krammer, P.H. & Peter, M.E. (1999a). *Curr. Opin. Immunol.*, **11**, 277-285.
- Scaffidi, C., Krammer, P.H. & Peter, M.E. (1999b). *Methods*, **17**, 287-291.
- Scaffidi, C., Medema, J.P., Krammer, P.H. & Peter, M.E. (1997). *J. Biol. Chem.*, **272**, 26953-26958.
- Scaffidi, C., Schmitz, I., Krammer, P.H. & Peter, M.E. (1999c). *J. Biol. Chem.*, **274**, 1541-1548.
- Scaffidi, C., Schmitz, I., Zha, J., Korsmeyer, S.J., Krammer, P.H. & Peter, M.E. (1999d). *J. Biol. Chem.*, **274**, 22532-22538.
- Schneider, P., Thome, M., Burns, K., Bodmer, J.L., Hofmann, K., Kataoka, T., Holler, N. & Tschopp, J. (1997). *Immunity*, **7**, 831-836.
- Schneider, P. & Tschopp, J. (2000). *Pharm. Acta. Helv.*, **74**, 281-286.

- Schulze-Osthoff, K., Ferrari, D., Los, M., Wesselborg, S. & Peter, M.E. (1998). *Eur. J. Biochem.*, **254**, 439-459.
- Seol, D.W. & Billiar, T.R. (1999). *J. Biol. Chem.*, **274**, 2072-2076.
- Shaham, S. (1998). *J. Biol. Chem.*, **273**, 35109-35117.
- Shaham, S. & Horvitz, H.R. (1996). *Cell*, **86**, 201-208.
- Shimizu, S., Konishi, A., Kodama, T. & Tsujimoto, Y. (2000a). *Proc. Natl. Acad. Sci. U S A*, **97**, 3100-3105.
- Shimizu, S., Narita, M. & Tsujimoto, Y. (1999). *Nature*, **399**, 483-487.
- Shimizu, S., Shinohara, Y. & Tsujimoto, Y. (2000b). *Oncogene*, **19**, 4309-4318.
- Shimizu, S. & Tsujimoto, Y. (2000). *Proc. Natl. Acad. Sci. U S A*, **97**, 577-582.
- Shinoura, N., Sakurai, S., Asai, A., Kirino, T. & Hamada, H. (2000). *Biochem. Biophys. Res. Commun.*, **272**, 667-673.
- Silke, J., Ekert, P.G., Day, C.L., Hawkins, C.J., Baca, M., Chew, J., Pakusch, M., Verhagen, A.M. & Vaux, D.L. (2001). *EMBO J.*, **20**, 3114-3123.
- Silke, J. & Vaux, D.L. (2001). *J. Cell Sci.*, **114**, 1821-1827.
- Silke, J., Verhagen, A.M., Ekert, P.G. & Vaux, D.L. (2000). *Cell Death Differ.*, **7**, 1275.
- Smith, T.F., Gaitatzes, C., Saxena, K. & Neer, E.J. (1999). *Trends Biochem. Sci.*, **24**, 181-185.
- Soengas, M.S., Alarcon, R.M., Yoshida, H., Giaccia, A.J., Hakem, R., Mak, T.W. & Lowe, S.W. (1999). *Science*, **284**, 156-159.
- Song, Z., Guan, B., Bergman, A., Nicholson, D.W., Thornberry, N.A., Peterson, E.P. & Steller, H. (2000). *Mol. Cell. Biol.*, **20**, 2907-2914.
- Sprick, M.R., Weigand, M.A., Rieser, E., Rauch, C.T., Juo, P., Blenis, J., Krammer, P.H. & Walczak, H. (2000). *Immunity*, **12**, 599-609.

- Srinivasula, S.M., Ahmad, M., Fernandes-Alnemri, T. & Alnemri, E.S. (1998). *Mol. Cell*, **1**, 949-957.
- Srinivasula, S.M., Ahmad, M., Guo, Y., Zhan, Y., Lazebnik, Y., Fernandes-Alnemri, T. & Alnemri, E.S. (1999). *Cancer Res.*, **59**, 999-1002.
- Srinivasula, S.M., Datta, P., Fan, X.-J., Fernandes-Alnemri, T., Huang, Z. & Alnemri, E.S. (2000). *J. Biol. Chem.*, **275**, 36152-36157.
- Srinivasula, S.M., Fernandes-Alnemri, T., Zangrilli, J., Robertson, N., Armstrong, R.C., Wang, L., Trapani, J.A., Tomaselli, K.J., Litwack, G. & Alnemri, E.S. (1996). *J. Biol. Chem.*, **271**, 27099-27106.
- Srinivasula, S.M., Hegde, R., Saleh, A., Datta, P., Shiozaki, E., Chai, J., Lee, R.A., Robbins, P.D., Fernandes-Alnemri, T., Shi, Y. & Alnemri, E.S. (2001). *Nature*, **410**, 112-116.
- Steller, H. (2000). *Nat. Cell Biol.*, **2**, E100-102.
- Strasser, A., Harris, A.W., Huang, D.C., Krammer, P.H. & Cory, S. (1995). *EMBO J.*, **14**, 6136-6147.
- Susin, S.A., Zamzami, N., Castedo, M., Hirsch, T., Marchetti, P., Macho, A., Daugas, E., Geuskens, M. & Kroemer, G. (1996). *J. Exp. Med.*, **184**, 1331-1341.
- Suzuki, Y., Imai, Y., Nakayama, H., Takahashi, K., Takio, K. & Takahashi, R. (2001a). *Mol. Cell*, **8**, 613-621.
- Suzuki, Y., Nakabayashi, Y., Nakata, K., Reed, J.C. & Takahashi, R. (2001b). *J. Biol. Chem.*, **276**, 27058-27063.
- Suzuki, Y., Nakabayashi, Y. & Takahashi, R. (2001c). *Proc. Natl. Acad. Sci. U S A*, **98**, 8662-8667.
- Takeuchi, M., Rothe, M. & Goeddel, D.V. (1996). *J. Biol. Chem.*, **271**, 19935-19942.

- Tamm, I., Wang, Y., Sausville, E., Scudiero, D.A., Vigna, N., Oltersdorf, T. & Reed, J.C. (1998). *Cancer Res.*, **58**, 5315-5320.
- Tan, K.M., Chan, S.L., Tan, K.O. & Yu, V.C. (2001). *J. Biol. Chem.*, **276**, 44193-44202.
- Thome, M., Schneider, P., Hofmann, K., Fickenscher, H., Meinl, E., Neipel, F., Mattmann, C., Burns, K., Bodmer, J.L., Schroter, M., Scaffidi, C., Krammer, P.H., Peter, M.E. & Tschopp, J. (1997). *Nature*, **386**, 517-521.
- Thornberry, N.A., Chapman, K.T. & Nicholson, D.W. (2000). *Methods Enzymol.*, **322**, 100-110.
- Thress, K., Evans, E.K. & Kornbluth, S. (1999a). *EMBO J*, **18**, 5486-5493.
- Thress, K., Henzel, W., Shillinglaw, W. & Kornbluth, S. (1998). *EMBO J.*, **17**, 6135-6143.
- Thress, K., Kornbluth, S. & Smith, J.J. (1999b). *J. Bioenerg. Biomembr.*, **31**, 321-326.
- Thress, K., Song, J., Morimoto, R.I. & Kornbluth, S. (2001). *EMBO J.*, **20**, 1033-1041.
- Tsujimoto, Y. & Shimizu, S. (2000). *Cell Death Differ.*, **7**, 1174-1181.
- van der Biezen, E.A. & Jones, J.D. (1998). *Curr. Biol.*, **8**, R226-227.
- Vander Heiden, M.G., Li, X.X., Gottlieb, E., Hill, R.B., Thompson, C.B. & Colombini, M. (2001). *J. Biol. Chem.*, **276**, 19414-19419.
- Vaughn, D.E., Rodriguez, J., Lazebnik, Y. & Joshua-Tor, L. (1999). *J. Mol. Biol.*, **293**, 439-447.
- Verhagen, A.M., Ekert, P.G., Pakusch, M., Silke, J., Connolly, L.M., Reid, G.E., Moritz, R.L., Simpson, R.J. & Vaux, D.L. (2000). *Cell*, **102**, 43-53.
- Verhagen, A.M., Silke, J., Ekert, P.G., Pakusch, M., Kaufmann, H., Connolly, L.M., Day, C.L., Tikoo, A., Burke, R., Wrobel, C., Moritz, R.L., Simpson, R.J. & Vaux, D.L. (2002). *J. Biol. Chem.*, **277**, 445-454.
- Vucic, D., Kaiser, W.J., Harvey, A.J. & Miller, L.K. (1997). *Proc. Natl. Acad. Sci. U S A*, **94**, 10183-10188.

- Vucic, D., Kaiser, W.J. & Miller, L.K. (1998). *Mol. Cell. Biol.*, **18**, 3300-3309.
- Wajant, H., Johannes, F.J., Haas, E., Siemienski, K., Schwenzer, R., Schubert, G., Weiss, T., Grell, M. & Scheurich, P. (1998). *Curr. Biol.*, **8**, 113-116.
- Walczak, H. & Krammer, P.H. (2000). *Exp. Cell Res.*, **256**, 58-66.
- Walke, D.W. & Morgan, J.I. (2000). *Brain Res.*, **886**, 73-81.
- Wallach, D., Varfolomeev, E.E., Malinin, N.L., Goltsev, Y.V., Kovalenko, A.V. & Boldin, M.P. (1999). *Annu. Rev. Immunol.*, **17**, 331-367.
- Wang, C.Y., Mayo, M.W., Korneluk, R.G., Goeddel, D.V. & Baldwin, A.S., Jr. (1998). *Science*, **281**, 1680-1683.
- Ware, C.F., VanArsdale, S. & VanArsdale, T.L. (1996). *J. Cell. Biochem.*, **60**, 47-55.
- Wing, J.P., Zhou, L., Schwartz, L.M. & Nambu, J.R. (1998). *Cell Death Differ.*, **5**, 930-939.
- Wolf, B.B., Schuler, M., Li, W., Eggers-Sedlet, B., Lee, W., Taylor, P., Fitzgerald, P., Mills, G.B. & Green, D.R. (2001). *J. Biol. Chem.*, **276**, 34244-34251.
- Wu, D., Chen, P.J., Chen, S., Hu, Y., Nunez, G. & Ellis, R.E. (1999). *Development*, **126**, 2021-2031.
- Wu, G., Chai, J., Suber, T.L., Wu, J.W., Du, C., Wang, X. & Shi, Y. (2000). *Nature*, **408**, 1008-1012.
- Xue, D., Shaham, S. & Horvitz, H.R. (1996). *Genes Dev.*, **10**, 1073-1083.
- Yamada, H., Tada-Oikawa, S., Uchida, A. & Kawanishi, S. (1999). *Biochem. Biophys. Res. Commun.*, **265**, 130-133.
- Yamamoto, H., Gil, J., Schwartz, S., Jr. & Perucho, M. (2000). *Cell Death Differ.*, **7**, 238-239.
- Yang, J., Liu, X., Bhalla, K., Kim, C.N., Ibrado, A.M., Cai, J., Peng, T.I., Jones, D.P. & Wang, X. (1997). *Science*, **275**, 1129-1132.

- Yang, Y., Fang, S., Jensen, J.P., Weissman, A.M. & Ashwell, J.D. (2000). *Science*, **288**, 874-877.
- Yoneda, T., Imaizumi, K., Oono, K., Yui, D., Gomi, F., Katayama, T. & Tohyama, M. (2001). *J. Biol. Chem.*, **276**, 13935-13941.
- Yoshida, H., Kong, Y.Y., Yoshida, R., Elia, A.J., Hakem, A., Hakem, R., Penninger, J.M. & Mak, T.W. (1998). *Cell*, **94**, 739-750.
- Zamzami, N., Brenner, C., Marzo, I., Susin, S.A. & Kroemer, G. (1998). *Oncogene*, **16**, 2265-2282.
- Zhou, L., Schnitzler, A., Agapite, J., Schwartz, L.M., Steller, H. & Nambu, J.R. (1997). *Proc. Natl. Acad. Sci. U S A*, **94**, 5131-5136.
- Zhou, L., Song, Z., Tittel, J. & Steller, H. (1999a). *Mol. Cell*, **4**, 745-755.
- Zhou, P., Chou, J., Olea, R.S., Yuan, J. & Wagner, G. (1999b). *Proc. Natl. Acad. Sci. U S A*, **96**, 11265-11270.
- Zhou, Q., Krebs, J.F., Snipas, S.J., Price, A., Alnemri, E.S., Tomaselli, K.J. & Salvesen, G.S. (1998). *Biochemistry*, **37**, 10757-10765.
- Zou, H., Henzel, W.J., Liu, X., Lutschg, A. & Wang, X. (1997). *Cell*, **90**, 405-413.
- Zou, H., Li, Y., Liu, X. & Wang, X. (1999). *J. Biol. Chem.*, **274**, 11549-11556.